The effects of processing on performance and utility in plant fibre-based composites

By:

Stella Manoli

Submitted to The University of Sheffield in partial fulfilment for the degree of Doctor of Philosophy

The University of Sheffield

Faculty of Engineering

Mechanical Engineering

October 2018

LIST OF CONTENTS

LIST OF TABLES

LIST OF FIGURES

LIST OF EQUATIONS

LIST OF ABBREVIATIONS

MP	Minimally processed
I	Industrial
MPN	Minimally processed nettle
MPF	Minimally processed flax
IN	Industrial nettle
IF	Industrial flax
LCA	Life Cycle Assessment
LCI	Life Cycle Inventory
LCIA	Life Cycle Impact Assessment
SCEnAT	Supply Chain Environmental Analysis Tool
MPa	Megapascal
GPa	Gigapascal
DSC	Dynamic Scanning Calorimetry
DMA	Dynamic Modulus Analysis
T_g	Glass tradition temperature
T_m	Melting temperature
T_c	Crystallisation temperature
ΔH_m	Melting enthalpy
L_c	Critical length
GWP	Global warming potential
AP	Acidification Potential
EP	Eutrophication Potential
HTP	Human Toxicity Potential
ATP	Aquatic Toxicity Potential
ODP	Ozone Depletion Potential
POCP	Photochemical Oxidants Creation Potential
CO_2	Carbon Dioxide

PLA	Polylactic acid
PC	Polycarbonates
ABS	Acrylonitrile Butadiene Styrene,
PET	Polyethylene Terephthalate
LDPE	Low-Density Polyethylene
PP	Polypropylene
PVC	Polyvinyl Chloride
PE	Polyethylene
PET	Polyethylene terephthalate
PA	Polyamide
PTT	Polytrimethylene Terephthalate
PHA	Polyhydroxyalkanoates
PBS	Polybutylene Succinate
PBAT	Polybutylene Adipate Terephthalate
PCL	Polycaprolactone,
MFA	Microfibril Angle
SEM	Scanning Electron Microscopes
ISO	International Standards Organisation
AM	Additive Manufacture
FDM	Fused deposition modelling
RH	Relative Humidity
FTIR	Fourier Transform Infrared Spectroscopy

ABSTRACT

The global concern about the growing consumption of non-recycled plastics has led material scientists to explore alternative materials for the development of environmentally friendly products that can be recycled or re-used. Natural fibres and biodegradable polymers are renewable materials that can be used for composite manufacturing. In this study flax and nettle fibre-reinforced Floreon composites were made using traditional and new developed techniques. Flax and nettle fibres of two different preparation processes were used as reinforcing materials. The physical, mechanical, and thermal properties of industrially and minimally processed flax and nettle fibres were studied, showing a clear species and preparation-based differences on the fibres' properties.

Flax and nettle single fibres were prepared properly and blended with Floreon using extrusion. Flax and nettle fibre-reinforced Floreon composites were then made by injection moulding. The relationship between the fibre type, content, and processing parameters was investigated. It was found that composites consisting of minimally processed fibres had increased mechanical properties compared to composites made by the respective industrially processed fibres. The appropriate processing parameters for composites were established for the different fibre types.

The physical and mechanical properties of 3D printed flax and nettle fibre-reinforced Floreon composites using fused deposition modelling were also investigated. The 3D printed composites showed greater tensile and flexural strength results compared to the injection moulded composites. The effects of fibre type, content, printing parameters such as nozzle temperature, fill density, layer height thickness and pattern orientation were experimentally studied. It was found that with increasing flax and nettle fibre content, the mechanical properties of composites produced increased.

The environmental sustainability of flax and nettle fibres, Floreon, and composites produced were analysed using life cycle assessment methodology. The environmental analysis was used to evaluate the emissions of each raw material used, the energy and materials requirements during composite manufacturing.

ACKNOWLEDGEMENTS

I would like to thank my supervisors, Professor Patrick Fairclough and Dr. Chris Holland for accepting my as a PhD student. I sincerely thank you for your supervision, continuous guidance and encouragement through the period of this research. I am very grateful to Patrick who provided me with accurate advice. Also I am thankful to Chris for the inspiring discussions. This study would not have been possible without your help.

Many thanks to Wendy Birtwistle and Ying Lan Ang for the constant laboratory work support, valuable discussions, advices and cooperation during performing this project.

I also wish to express my appreciation to all staff and my colleagues for their help and encouragement and to the Natural Materials Group for helping me with the technical procedures during my study.

Finally, I would like to thank my parents and brother who were the first who believed in me. I am also grateful to my other family members who have supported me along the way. Special thanks goes to Charalambos Rossides, for the moral support, the long conversations and because you are always beside me.

1 INTRODUCTION

1.1 Research background

Composites are materials composed of at least two physically separated parts, usually a reinforcing material surrounded by a continuous matrix. Each individual constituent of a composite contributes towards the physical, mechanical, and thermal properties of the final material. Composites often display properties that are greater than the sum of their individual parts [1], [2]. Furthermore, composite properties are influenced by each component's structure, amount, and manufacture [2]. From an industrial perspective, the matrix normally provides the shape, surface, durability, and environmental tolerance in the composite material, and the reinforcing materials are responsible for a composite's strength and stiffness [3]. Common reinforcing materials are fibres and particles, and they typically present larger values for breaking strength compared to a continuous matrix [4], [5].

While composites are commonly used in various industries, they exist in nature where they are used to create structural materials. In fact, nature may indeed serve as an important resource for industrial composite materials and provide inspiration for future composite development, as shall be explored in this thesis.

Over the past ten years there has been a rising global concern surrounding the release of environmentally detrimental substances (emissions) arising from manufacturing processes [6]. Such emissions adversely affect the environment leading to concerning complications (impacts) such as small or large scale pollution, global warming, etc. [7]–[9]. Recent attempts to reduce the life cycle environmental impact and/or to reduce the required raw material for the manufacturing of a product led to the development of recycling techniques [10], [11]. Recycling refers to a product's decomposition to its constitutive materials when it reaches its end of life so that they can be reused for the manufacturing of a new product. When the recycling process yields lower emissions than the alternative case of manufacturing the product from scratch, recycling is more environmentally friendly [14]. This has in turn led governments to enact laws to stimulate the production of environmentally friendly materials, with the ability to be recycled by end of life treatments [12], [13]. This has been particularly challenging for the composites industry, where the products are usually microscopic combinations of different materials, making them hard to recycle. Therefore, research is gaining momentum in areas of alternative sources of

materials to minimise the environmental impacts related to composite production [14].

Bio-composite is a material composed of two or more separate materials, one of which naturally derived [5]. Natural fibres (flax, hemp, jute, sisal, wood fibres) and polymers from renewable resources are used to manufacture bio-composites. Bio-composites present lower environmental emissions compared to composites composed of synthetic fibres such as glass fibres, and are perceived to be sustainable [5], [15]. To date, bio-composites have found applications in various industries from automotive to packaging and offer a useful alternative to non-biodegradable and non-recyclable products [16].

Natural fibres extracted from plants and trees are widely used as reinforcing materials as they present several advantages over synthetic fibres, such as lower density and cost, but with comparable mechanical properties to synthetic fibres such as E-glass [17]. However, studies have shown that the properties of natural fibres are heavily influenced by the preparation and processing methods [18].

For matrix production in bio-composites, polylactic acid (PLA) is a thermoplastic that is rapidly becoming the polymer of choice. PLA can be produced from natural resources such as corn starch and sugarcane and is biodegradable and recyclable with reuse potential, leading to the development of commercial products such as Floreon* [19]–[22]. Life-cycle assessment (LCA), a technique by which the environmental impact of a material or process is assessed, has identified PLA as a polymer with one of the lowest total carbon dioxide (CO_2 eq/kg) emissions during its life cycle [23].

Once the individual components for bio-composite production have been identified, the impact of processing needs to be addressed for a successful product. Typically, chopped natural fibres are mixed with a polymer using extrusion compounding. Shaping techniques such as injection and compression moulding, and more recently 3D printing, can be used for the production of samples for further mechanical testing to better understand how processing affects performance [5], [24], [25].

1.2 Research objectives

This research has a goal to develop a natural fibre-reinforced composite with low environmental emissions created using materials from renewable resources.

*Floreon is a trademark of Floreon-Transforming Packaging Limited

Specific objectives were:

1) Investigate the properties of industrially and minimally processed flax and nettle fibres and evaluate the effects of the fibre preparation process on the fibres' mechanical and sustainable properties.
2) Relate processing to performance during the manufacturing of natural fibre-reinforced Floreon composites using traditional techniques, such as extrusion and injection moulding, as well as new technologies, such as additive manufacture.
3) Evaluate the environmental impacts of flax and nettle fibres, Floreon, and composites produced from them.

The experimental and analytical work during this project was divided into three main phases:

Part A: Fibres

Flax and nettle fibres were evaluated according to their physical and mechanical properties. Single fibres directly extracted from flax and nettle stems (referred to as minimally processed flax and nettle fibres in the following chapters) were compared to commonly processed flax and nettle fibres (referred to as industrially processed flax and nettle fibres) using tensile testing across a range of hydration states.

Part B: Composites

Composites consisting of minimally or industrially processed flax and nettle fibres and Floreon were created using extrusion and injection moulding and by 3D printing. Composites were tested under tension and by three-point bending in order to evaluate their mechanical properties. To determine the effects of processing on these composites, different processing parameters such as moulding and nozzle temperature, pressure, architecture, and time were evaluated. These results were then assessed within the context of fibre/polymer concentration, fibre type, manufacturing, and applied processing parameters.

Part C: Environmental analysis

LCA was finally used to evaluate the environmental impacts of the proposed fibres, Floreon, composites, and manufacturing in terms of CO_2 eq/kg emissions. To achieve this, a supply chain was created based on input data, including the amount of energy, water, soil, and fertilisers required for fibre production. The LCA of Floreon was performed according to its biodegradability and potential to be recycled at its end of life. Finally, the sustainability of the composite manufacturing

(extrusion, injection moulding, and 3D printing) was evaluated in terms of the required amount of energy and material waste.

1.3 Chapter overview

To achieve the overall objectives of this thesis, in addition to the three main parts listed above; the work was divided into the following chapters:

- Chapter 1 presents a general introduction to natural fibres and composites. The aim and objectives of this research are described in this chapter, along with the structure of the thesis.
- Chapter 2 presents a literature review and the current state of the art in the field of natural fibres and fibre-reinforced composites. Information on manufacturing procedures and mechanical properties of fibre-reinforced composites relevant to this project are presented.
- Chapter 3 concerns the study of flax and nettle fibres. The research methodology used for evaluation of the physical and mechanical properties of flax and nettle fibres is described and subsequent results are presented in this chapter.
- Chapter 4 focuses on injection-moulded, fibre-reinforced composites. The research methodology, material selection, manufacturing, and results from property evaluation methods for minimally and industrially processed flax and nettle fibre-reinforced Floreon composites are discussed.
- Chapter 5 presents work on injection-moulded bio-composites. The physical, mechanical, and thermal properties of minimally and industrially processed flax and nettle fibre-reinforced Floreon composites are analysed and results considered within the context of the wider literature.
- Chapter 6 focuses on 3D-printed bio-composites. Samples of 3D-printed minimally and industrially processed flax and nettle fibre-reinforced Floreon composites are produced and then compared to results from the traditional shaping technologies used in chapter 5.
- Chapter 7 complements the previous chapters by performing an environmental analysis of flax and nettle fibres, Floreon, and the composites produced as part of this thesis. The environmental impacts and the total CO_2 emissions of the individual raw materials and composites obtained from LCA are presented and discussed within the context of the wider literature.

- Chapter 8 summarises the results obtained from the fibres and composite investigation research and concludes this thesis with conclusions and proposals for future work.

2 LITERATURE REVIEW

2.1 Introduction

Composite materials have a wide range of applications, from automotive and aerospace industries to construction and home utilities. Composite materials can be made through diverse manufacturing methods using different types of materials. Concerns about the sustainability of materials produced have been raised due to environmental impacts, emissions, and possible end-of-life treatment options. Therefore, because of the urgent need for the manufacture of environmentally friendly material, material researchers have turned their interest to materials that are extracted from renewable resources for the production of natural composites with high mechanical properties and low environmental emissions.

This research focuses on the manufacture of natural composites with individual materials extracted from natural resources. This chapter presents an overview and literature review of plant fibres, polymers, and manufacture of composite materials.

2.2 Plant fibres

The renewable, biodegradable, and sustainable character of wood and nonwood fibres, in combination with its mechanical properties—in some cases comparable to synthetic fibres—have led to interest by material researchers in evaluating and using plant fibres in different applications [5], [26], [27]. In recent years, interest in the use of plant fibres has increased due to their many advantages [16]. Plant fibres are widely used as reinforcing materials in the manufacture of composites, contributing to the production of materials with biodegradable characteristics [26], [28], [29].

2.2.1 Ligno-cellulosic fibres

Plant fibres are mainly consisting of cellulose, hemicellulose and lignin [30]. Ligno-cellulose fibres can be found in abundance in nature, coming from different sources such as annual crops, agricultural waste, and wood resources and are classified according to their origin [15], [28], [31]. Ligno-cellosic fibres can be derived from wood and nonwood resources. Nonwood fibres have subcategories depending on which part of the plant are extracted, as shown in Figure 2.1 [31], [32].

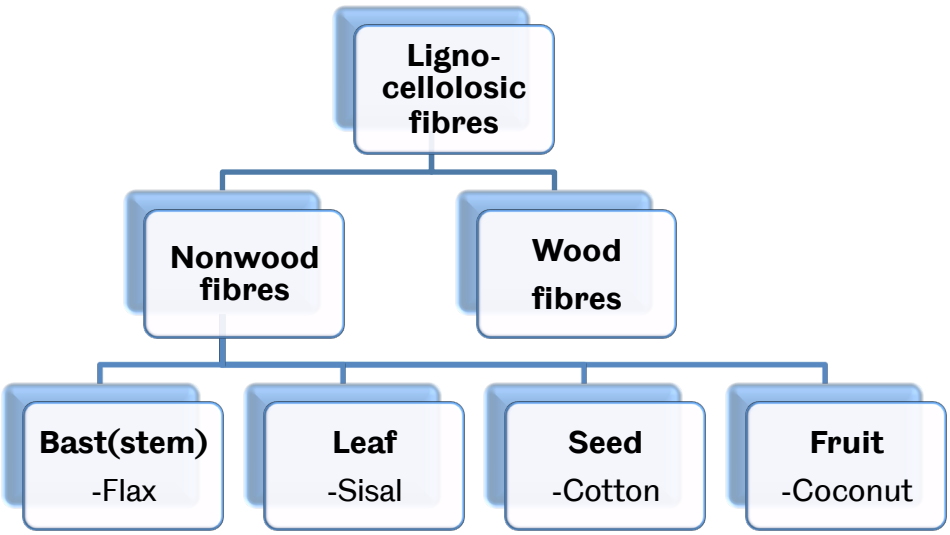

Figure 2.1 Overview of common ligno-cellulosic fibre resources (adapted from [31]).

Fibres extracted from wood resources are characterised as short fibres, with a length between 1–5 mm and a high void content (20-56% by volume) [33]. Although wood fibres have poor mechanical properties compared to nonwood and synthetic fibres due to their low density, low cost and low energy demand during manufacture are used in the furniture and construction industries. They are also used as reinforcing materials when combined with thermoplastic matrices for composite manufacture [25], [27].

Nonwood fibres are long (5–50 mm), have greater mechanical properties than wood fibres, and are used to produce composites for a variety of applications, from aerospace and automotive industries to materials for home utilities [27], [34]. Nonwood fibres, especially stem fibres, of flax, jute, and hemp are used as reinforcing materials, in composites mixed with thermoplastic or thermoset matrices. The reinforcing stem fibres provide the strength and stiffness to the fibre-reinforced composite [27], [35].

2.2.2 Ligno-cellulose fibre chemistry

A description about the chemistry of the three most important constituents, cellulose, hemicellulose and lignin, of wood and nonwood fibres, are presents in this section [36].

Cellulose $(C_6H_{10}O_5)_n$ is one of the most abundant compounds in nature and is found in the plant cell walls [37]. Cellulose is a polysaccharide consisting of ß(1-4) D glucose monomer units [38]. Glucose units are joined forming a lineal flat molecule that includes networks of hydrogen bonds [39], [40]. The hydroxyl groups from one

chain of the glucose forms hydrogen bonds with oxygen atoms from the same or the next chain, which are holding the chain steady and forming microfibrils [38]. Cellulose microfibril is a linear homopolysaccharide and is composed of amorphous cellulose regions with no oriented cellulose chains (see Figure 2.2) [41].

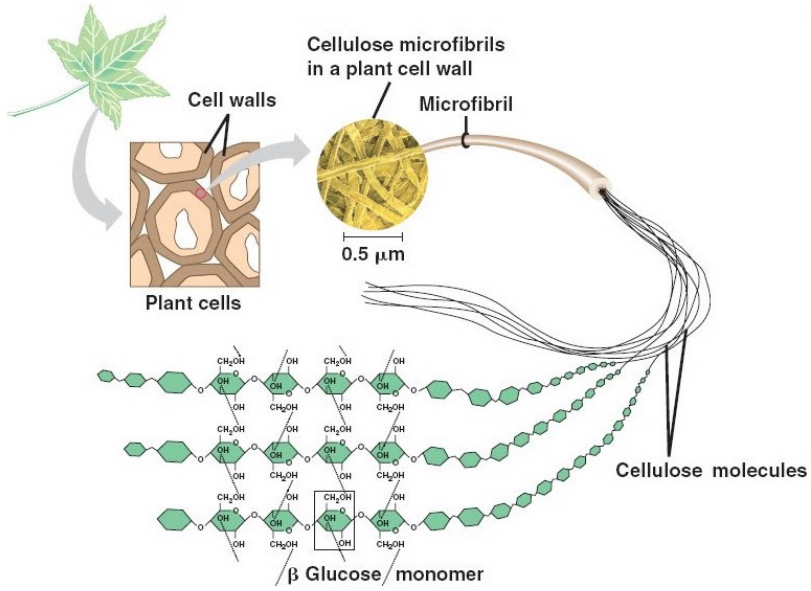

Figure 2.2 Structure of cellulose microfibrils. Copyright © 2008 Pearson Education, Inc., publishing as Pearson Benjamin Cummings.

Cellulose is an insoluble molecule and its highly affected by materials containing hydroxyls, especially water [42]. Based on the hydroxyl functional groups, cellulose is very reactive with water, interacting with two possible ways [32]. The first way is to bind the water with the hydrogen bonds and the second way is to accumulate the unbounded water between the microfibrils [42].

Cellulose fibres are a group of microfibrils formed during biosynthesis [41]. Cellulose microfibrils are embedded in a lignin-hemicellulose matrix wrapped helically around the cell wall at a specific angle with respect to the fibre angle, known as the microfibril angle (MFA), as seen in Figure 2.2 [38]. The MFA has a direct relation to the plant fibre mechanical properties. Fibres with lower MFA have higher tensile modulus and strength and smaller failure strain. As MFA increases, the elastic range of fibres is decrease and there is a reduction on the tensile strength and Young's modulus [43].

Hemicellulose is a polysaccharide found in most plants' cell walls and consists of shorter chains compared to cellulose [36]. Hemicellulose is made up of several monomers: xylose, galactose, mannose, rhamnose, and arabinose and is linked and bonded with pectin, in which cellulose microfibrils are embedded, to form cross-

linked fibres [36]. Hemicelluloses consist of glucose and several other water-soluble sugars produced during photosynthesis, unlike cellulose, which is made only from glucose. Hemicellulose cross-links with either cellulose or lignin as a result the strengthening of plants' cell wall [44]. Comparing cellulose with hemicellulose, cellulose is a crystalline, strong polymer in contrast to hemicellulose, which is an amorphous polymer of lower strength [30], [36]. The main difference among the two is the role of each polysaccharide in the plant cell wall, with cellulose to be the main structural component of the primary cell wall of plants and to be present along with cellulose to strength the cell wall. Hemicelluloses are insoluble in water but soluble in alkaline solutions [44].

Lignin consists of aliphatic and aromatic constituents and is found between the cellulose, hemicellulose, and pectin components in the plant cell walls, acting as a supporting mechanism [45]. Lignin fills the spaces in the plant cell wall between cellulose, hemicellulose, and pectin components and it has a crucial part in channelling water in plant stems [44].

Pectin can be found in the primary cell wall and can be found in abundant in the non-woody parts of the plants. Removing the pectins from a fibre bundles resulting to the separation of the bundles into the elementary fibres [44]. The difference in the chemical structure of the above mentioned cellulose, hemicellulose, lignin and pectin are presented in Figure 2.3.

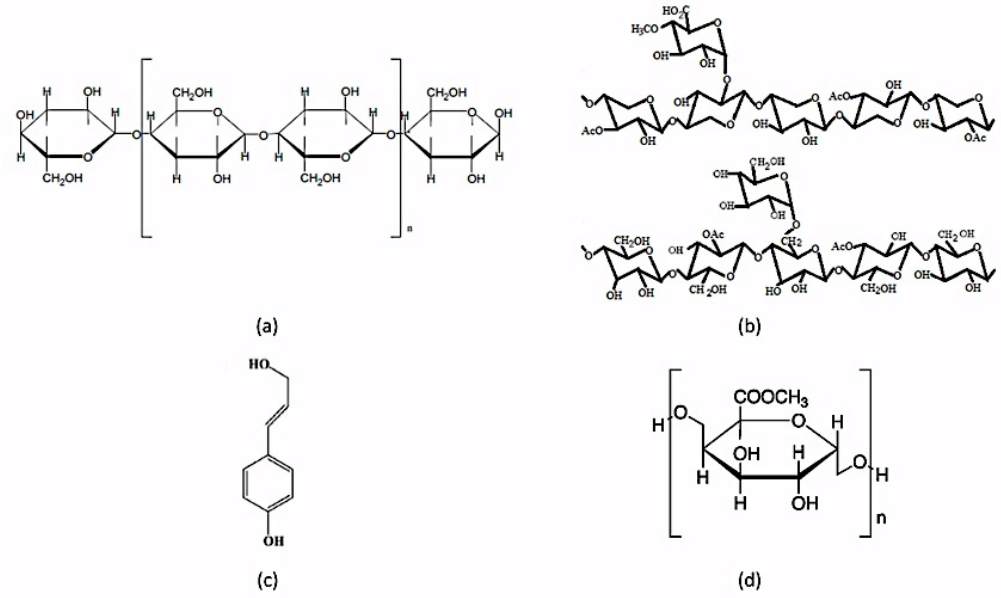

Figure 2.3 Chemical structure of a) cellulose, b) hemicellulose, c) lignin and d) pectin. Reprinted from 'Factors that affect the mechanical properties of kenaf fiber reinforced polymer: A review', Xiaowei Zhou *et al.* © 2016 Xiaowei Zhou *et al.*

Cellulose and hemicellulose components are mainly responsible for the mechanical properties of plant fibres [46]. Cellulose acts as a reinforcement between the fibres, while hemicellulose and pectin bond the fibres within the plant cell walls [31]. The lignin and wax (waxy esters, long-chain fatty acids, and alcohols) components provide the fibre stiffness and protect the plant from oxidative degradation [36]. The hydrogen atoms included in the hydroxyl groups of cellulose and hemicellulose are responsible for the hydrophilic and moisture absorption character of cellulosic fibres (described in the next sections) [47]. The physical properties of fibres are affected by the degree of polymerisation, cellulose content, microfibril orientation, and crystallinity [46].

Fibres that are extracted from different parts of the plant, as seen in Figure 2.1, have different concentrations of the aforementioned chemical components and are presented in Table 2.1 [48].

Table 2.1 Chemical compositions of plant fibres (taken from references [49]–[53]**).**

Component (%)	Softwood	Flax	Hemp	Sisal	Ramie
Cellulose	44-50	45-76	60-77	53-66	68-76
Hemicellulose	20-30	13-22	10	12	13
Lignin	20-35	0.6-13	5-13	10-14	0-1
Pectin	-	0.9-5	2.9	1	0.3-2
Waxes	-	0.2-1.7	0.9	0.5	0.3
Microfibril angle (degree)	30-60	5-10	4	20-25	7.5
Crystallinity	60-70	90-100	94	71	72

Fibres with higher cellulose concentrations, such as the stem fibres flax and hemp, present higher mechanical properties over cellulosic fibres with lower cellulose concentrations [37]. The properties of cellulosic fibres are affected not only by the fibre chemical composition but also by the fibre morphology, internal fibre structure, plant species, age, geographic location, climate, and fibre preparation methods (described in the next sections) [28], [32], [54].

2.2.3 Plant fibre morphology and structure

The main body of a vascular plant consists of the dermal, ground, and vascular tissue systems [55]. A vascular plant refers to land plants that have lignified tissues for conducting water throughout the plant [55]. The dermal tissue system is the

outer layer of the vascular plant and consists of the epidermis and periderms tissues [56]. The epidermis and periderms tissues are responsible for protection and plant support. The ground tissue system is located within the dermal tissue and consists of all tissues apart from the dermal and vascular tissue system [55]. The main functions of the ground tissue system are photosynthesis, food storage, and plant support. Ligno-cellulosic fibres are a part of the ground tissue system (as part of the sclerenchyma cells) and their function is purely mechanical [56]. The vascular tissue system is consisted of the xylem and phloem tissues, which are responsible for food and water transportation [55].

Stem fibres (derived of nonwood fibres see Figure 2,1) are located in the outer surface of the vascular plant stem in the form of fibre bundles, which consist of single elementary fibres [52]. Ligno-cellulosic fibres are characterised as a composite material themselves due to their complex structure [31]. Generally, a lingo-cellulose fibre bundle has diameter between 50–100 μm. As these fibre bundles are used for textile and technical applications, they are therefore also called technical fibres [43], [57]. Each c fibre bundle is consisted of single elementary fibres 10-20 μm in diameter, as seen in Figure 2.4 [58].

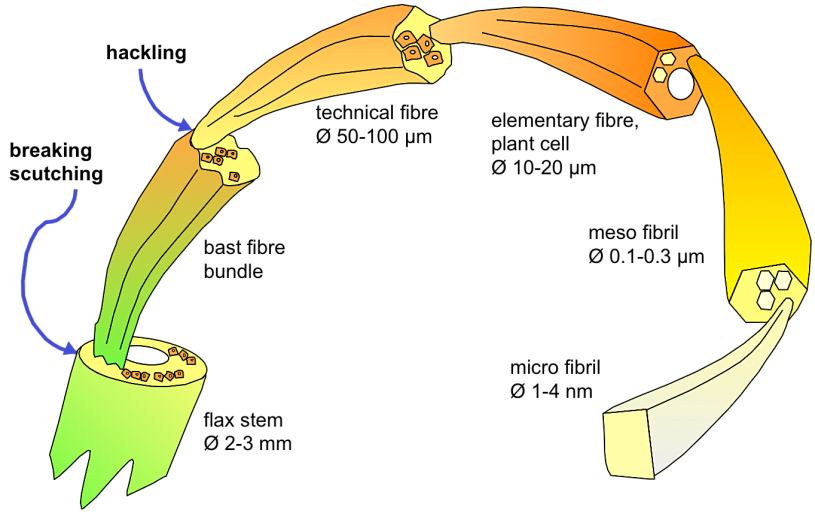

Figure 2.4 Hierarchy of flax fibre; from flax stem to fibre microfibril [58]**. The fibre bundles and single fibres are obtained after a series of preparation processing steps. The diameter and length of each fibre is affected from the plant species, climate and crop growth and preparations processing methods** [18], [59]**. Reprinted from 'The potential of flax fibres as reinforcement for composite materials', Harriëtte Bos, PhD Thesis Technical University of Eindhoven, 2004 © 2004 Harriëtte L.Bos.**

At a macroscopic level, a plant stem bundle contains between 10 to 40 fibres which that are linked together mainly by pectins. Looking these single elementary fibres at a microscopic level are composed of layers with different thickness, chemical

composition and structure (Figure 2.4) [60]. Single elementary fibres are composed of a cell wall formed by microfibril groups bonded with pectin and lignin [30]. The single fibre cell wall splits in three layers starting from the lumen, to the secondary cell wall up to the primary cell wall, as shown in Figure 2.4 [55]. The primary cell wall is thin and flexible, and formed during the growing period of the plant [26]. A thicker wall, the secondary cell wall is located within the primary cell wall and provides protection, rigidity, and flexibility to the fibre due to the presence of lignin. The secondary cell wall consists of three layers (S1, S2, and S3, as shown in Figure 2.5) of different microfibril orientations [30]. Each of the three layers is composed of cellulose microfibrils in parallel direction between each other as a result forming a microfibrilar angle with the fibre direction. The secondary cell wall has the minimum MFA [60]. The microfibril is composed of cellulose chains, which are embedded in an amorphous matrix mainly made of pectins and hemicelluloses [60]. Cellulose, hemicellulose, and lignin polysaccharides are found in both primary and secondary cell walls, while pectin is found only in the primary cell wall, as presented in Figure 2.5 [36].

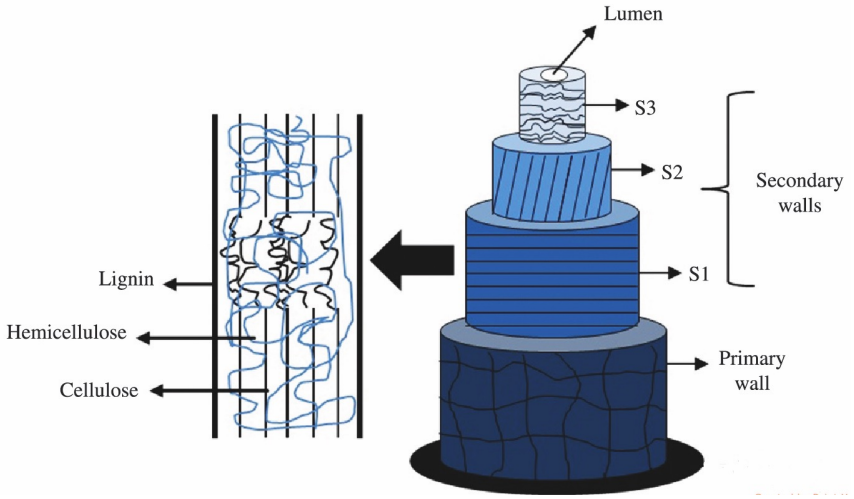

Figure 2.5 Schematic representation of a single fibre morphology [30]. Lumen is the core (empty space) of the single fibre, covered by the multilayer structures of the secondary cell wall (S1, S2, S3) [30].[36]. The primary wall is the outer layer of a single fibre and has the highest concentration of lignin (up to 70%) compared to the secondary walls. in the S1 layer the concentration of lignin is up to 45% [32]. The S2 and S3 secondary wall layers have higher concentrations of cellulose (45-50%) and hemicellulose (35-40%) compared to the respective concentrations in the primary cell wall (15% and 15-20%) [32]. Reprinted from Vegetal fibers in polymeric composites: a review by SEÇÃO TÉCNICA, 2015 © 2015 Paulo Henrique Fernandes Pereira *et al.*

2.2.4 Processing methods: from plants to industrial fibres

Specific preparation processes are needed to produce the appropriate fibre forms from the respective plants. The process is determined by the fibre source and the intended applications [28]. Fibres can be in a form of a yarn, short chopped fibres and woven fabric [61]. Specifically the fibre bundles (section 2.2.2) require a series of processing preparation steps in order to be used in composite applications [62].

The preparation process of stem fibres starts with the rippling procedure, in which the plant seeds are removed [31]. The retting process follows, which separates the fibre bundles from the stem and disconnect the fibres from woody tissue (xylem) of the fibre crops [59]. During the retting process, the pectinous materials that bond the fibres are removed [59]. Retting can be performed by different treatments, such as biological or chemical [31]. Biological treatments include water or dew retting processes [62]. In the water retting process, the stems are immersed in either cold or warm water and bacteria separate the fibre bundles from xylem [31], [59]. During dew retting, the sun and fungi act as the separation mechanism [63]. Chemical retting is faster than other retting processes. The stems are immersed in a solution of sodium hydroxide and pectinolytic enzymes [59]. Subsequently, the process of decortication take places, where the non-fibrous materials are removed mechanically from the stems [64]. After retting, the next step is hackling, in which the short fibres are removed and the remaining long fibres are unravelled by carding [31]. In order to decrease the mass per unit length of fibres, the remaining unravelled fibres are processed through gilling making them suitable for spinning [65]. The last preparation process step is spinning, where the fibres are spun and twisted to produce yarn [31].

Surface treatment of cellulose fibres is a common procedure during the preparation process and is used to improve the surface appearance and texture of the fibres [66]. Surface treatment is achieved through a range of treatments [67]. Acetylation method is chemically modifying the lignocellulose fibres by using acetic anhydride. Anhydride attached to the –OH groups, realising an acetic molecule which subsequently reacted with the free water within the fibre producing acetic acid [5], [25]. Scouring is used to remove natural fats, waxes, and proteins from cellulose fibres by using aqueous and/or alkali remonving the hydrophilic components of the fibre [68], [69]. For the fibre surface modification and improvement of fibre mechanical properties such as fibre strength and resistance, mercerisation is applied by using solutions of caustic alkali [70]. Mercerizing gives ligno-cellulosic fibres increased tensile strength, greater absorptive properties,

and, usually, a high degree of lustre [70]. Bleaching is used for decolourisation and improving whiteness [66].

Although these preparation processes are necessary for the modification of cellulosic fibres into suitable forms, they can affect the fibres' mechanical and physical properties [71]. The (industrial) mechanical processing damages the fibres by increasing their flexibility and reducing the fibres' tensile strength and stiffness [71]. Additionally, the industrial fibre processing requires a high-energy input and results in a large environmental footprint. The surface treatment of fibres also influences the biodegradable and sustainable character of fibres, as described in the next sections [50], [72].

2.2.4.1 Microstructure of ligno-cellulosic fibres

The effect of industrial preparation processes on the ligno-cellulosic fibre structure has been studied by analysing the fibre surface and its structure using optical and electron microscopes [73]. During the preparation process of fibre bundles, and during the plant growing period, areas of dislocations are formed, affecting the mechanical properties of the industrial processed fibres [74]. These regions can be found perpendicular to the fibre axis and disrupt the cellulose microfibrils in the cell wall [75]. Preparation processes such as decortication and spinning (described in section 2.2.3) expose the fibres to stretching, bending, and compression. As a result, defects along the fibre bundles are created [76]. Higher numbers and larger sizes of defects along the fibre axis significantly affect the fibre's tensile strength (the resistance of fibres to breaking under tension) and Young's modulus (the fibre's stiffness) [77].

2.2.5 Mechanical properties of single fibres

Frequently, cellulose fibres are used as reinforcing materials in composite structures to enhance the mechanical properties of the final sample compared to the properties of the polymers [1], [25]. Cellulose fibres are preferred over synthetic fibres due to a combination of degradable characteristics, lower density values, and in some cases such as with flax fibres, the comparable mechanical properties with synthetic (e.g., E-glass) fibres [1], [26], [63]. Additionally, cellulose fibres as lightweight materials reduce the final weight of the composite produced compared to composites with industrial reinforced fibres, leading to a positive impact on the environment due to the lower energy requirements (less energy is needed to modify and process lighter fibres than heavier) for the production and recycling of the product [78].

For the calculation of tensile strength, tensile strain at failure, and Young's modulus, single fibres are subjected to tensile tests [79], [80]. During tensile testing, the fibre is slowly stretched in an axial direction until fracture occurs [81]. Tensile strength describes the resistance of the fibre to overcome failure under an applied stretching force. Tensile strain at failure describes the elongation of the fibre until fracture occurs [81]. Young's modulus or elastic modulus is a measurement of the fibre's stiffness, describing the resistance over the change in fibre length and is calculated as the ratio of tensile stress to strain [82]. During tensile test, a typical output is a stress-strain diagram as shown in Figure 2.6. Tensile stress is calculated as the ratio of the applied load over the cross section area of the sample.

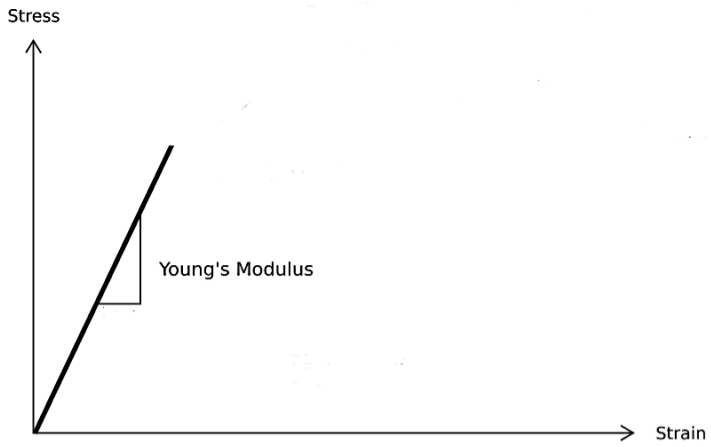

Figure 2.6 Typical stress-strain diagram. The stress is increasing proportional to strain and Young's modulus is calculated from the slope.

The mechanical properties of fibres are affected by and determined from various parameters, as described in sections 2.2.1–2.2.3 [18], [83]. The chemical composition, preparation process, and void concentration are some of the main factors affecting the fibre's tensile properties [48], [84], [85]. Stem fibres, due to their higher concentrations of cellulose, (Table 2.1) have higher tensile strength and Young's modulus values, as displayed in Table 2.2 [28], [37]. Flax fibres have greater mechanical properties due to their long elementary fibres, smaller MFA orientation, and higher cellulose concentration, approaching the tensile strength results of E-glass fibres [86].

Table 2.2 Mechanical properties of ligno-cellulosic and synthetic fibres (taken from references [16], [49], [58], [87]–[89]).

Fibre type	Density (g/cm^{-3})	Tensile strength (MPa)	Strain at failure (%)	Young's modulus (GPa)
Stem Fibres				
Flax	1.54	345-2000	2-3	27-85
Ramie	1.5-1.56	400-1000	3-4	27-128
Nettle	1.51	560-1600	2.1-2.5	24-87
Hemp	1.47	368-800	1-6	17-70
Leaf fibres				
Sisal	1.45-1.5	350-700	2-3	9-22
Seed fibres				
Cotton	1.5-1.6	287-597	6-9	5.5-12.6
Fruit fibres				
Coconut	1.15	131-175	10-15	4-6
Synthetic fibres				
Carbon	1.8	4000	1.3-1.7	230
E-glass	2.5	2000-3500	1.8-3.2	70

2.2.6 Thermal stability of ligno-cellulosic fibres

In order to be used successfully as reinforcements in composite applications, lingo-cellulosic fibres have to overcome the problem of thermal degradation [90], [91]. For composite manufacture, the lingo-cellulosic fibres are mixed with thermoforming polymers in procedures that require elevated processing temperatures due to the polymer's melting temperature [92]. The chemical components of ligno-cellulosic fibres, as presented in section 2.2.1 (cellulose, hemicellulose and lignin), are sensitive to temperatures above 150 °C and thermal degradation may occur. Most cellulosic fibres start to show significant degradation at 240 °C [93], [94]. Specifically, lignin starts to degrade at temperatures around 145 °C, hemicellulose between 200–260 °C, and cellulose at 260–350 °C [90], [95], [96]. Lignin above that temperature starts to flow affecting therefore the fibres and composites properties [90]. Plant fibres with higher lignin concentrations have lower heat resistance compared to fibres with higher cellulose content due to the lower glass transition temperature of lignin [29]. The thermal degradation of plant

fibres cause the desorption of water molecules and a reduction in the fibre's mechanical properties [93], [97]. To improve thermal stability, cellulose fibres undergo chemical treatments to remove proportions of hemicellulose and lignin components [72].

2.2.7 Moisture absorption of ligno-cellulosic fibres

The numerous hydroxyl bonds in the molecular chain of cellulose, hemicellulose and lignin makes the ligno-cellulosic fibres hydrophilic materials [40], [98]. Wood and nonwood based fibres increases in volume during absorption in their try to include as much as possible water molecules. The swelling caused an expansion of the lignin-hemicellulose matrix in which the microfibrils are embedded (section 2.2.2). At the moisture equilibrium phase (EMC) (the moisture level at which there isn't any gain nor loss of moisture), the flux of the water molecules existing in the cell wall and the flux of the water molecules entering the cell wall are in balance (dynamic equilibrium). Although not all of the –OH components of the polysaccharides are accessible to the water molecules [99].

The absorption of moisture at the EMC of the lingo-cellulose fibres from a lower to higher relative humidity level is always lower from moisture desorption from high to lower relative humidity levels. By determining the EMC of lingo-cellulose fibres at different levels of relative humidity at constant temperature the sorption isotherm is obtained. The sorption isotherm indicates the corresponding water content as a constant temperature for each humidity level [100]. This phenomenon is described by hysteresis as seen in Figure 2.7 [99].

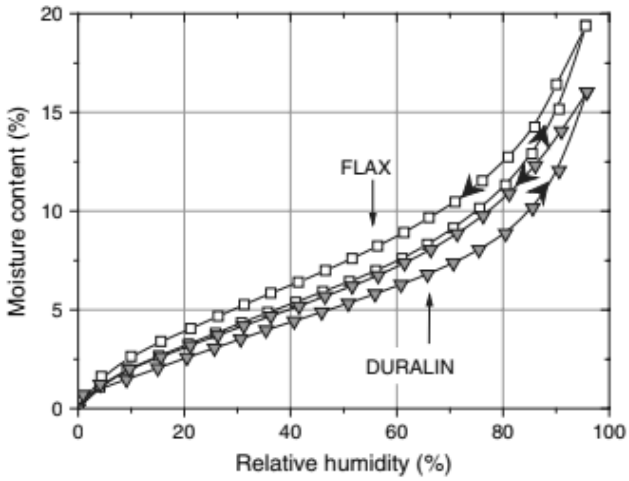

Figure 2.7 Water vapour sorption behaviour of flax and hygrothermally modified flax (Duralin) fibres. Reprinted from Natural fibre reinforced composites opportunities and challenges by Callum Hill and Mark Hughes, 2010 © 2010 Csllum Hill and Mark Hughes.

Hill and Hughes studied the effect of moisture absorption on flax and hygrothermally modified flax (Duralin) fibres presenting the sorption behaviour and the effects of thermal modification on the fibres with respect to different humidity levels. It was shown from the hysteresis (Figure 2.7) that the thermal modified flax fibres (Duralin) had reduced moisture susceptibility [101].

According to literature, cotton fibres have EMC values of 8–25%, flax fibres 10–12%, hemp 10–12% and ramie (Asian nettle fibres) 12–17% [102]. The degree of moisture absorption depends on the humidity level and exposure time [103]. The differences in the moisture EMC values are strongly connected with the cell wall lignin content of the fibres [101].

During the investigation of the hydrophilic character of lingo-cellulose fibres, the dynamic vapour sorption (DVS) technique was used. DVS presents with high accuracy the sorption kinetics behaviour and sorption isotherms [100]. Rautkari *et al.* studied the accessibility of hardwood species by analysing the deuterium exchange in the DVS apparatus by using D_2O water [100], It was found that as the vapour pressure increased the moisture content of lingo-cellulose fibres was increase, while as the vapour pressure decreased the moisture content decrease. The increase of the moisture content approached a constant value with is the EMC of fibres [104].

The moisture absorption caused dimensional instability, increased weight, and a reduction in the fibre's mechanical properties [105]. The dimensional instability of fibres leads to a reduction in mechanical properties of the composites in which fibres are used. As a consequence, at high moisture levels, the fibre/matrix adhesion is weak and the fibre-reinforced composite fails at lower values of applied force [106]. With a weak fibre/matrix adhesion, the fibres are not able to transfer the stress to the surrounding matrix, causing premature fibre failure and void formation [107].

2.3 Composite materials

In the field of composites, numerous combinations of materials and techniques have been studied. However, natural fibres and newly developed polymers have not yet been fully studied and therefore the evaluation of the manufacture of natural fibre-reinforced composites seems timely. However, it must be pointed out that bioderived adhesives (manufactured from renewable feedstock) have been developed and used over a century. For example, soybean flour and soybean protein adhesives are used for the wood composites applications due to strong adhesion properties, fast and simple preparation methods [108]. In wood bonding,

casein glues are used due to their high moisture resistance and aging characteristics [109].

The following sections present and describe a comprehensive literature review about the types, manufacturing, and evaluation processes of composites. Particular emphasis is given to fibre-reinforced composites because of this project's interest.

A composite is defined as a material formed from at least two individual materials with different physical and mechanical properties [1]. The ideal combination of the individual materials (type of materials and concentration) and applied processing parameters led to the manufacture of composites with improved physical and mechanical properties [2], [110].

2.3.1 Classification of composites

Composites can be characterised based on the use of reinforcing or non-reinforcing phase and on the matrix phase [111]. In the reinforcing phase, the raw materials are mainly fibres and/or particles that are embedded in the matrix [110]. In the non-reinforcing phase, the matrix is holding the fibres together or the efficient transfer of load between them [33]. In general, the matrix is a softer, continuous component, while the reinforcing materials are stiffer and stronger components [1]. The selection of the reinforcing and matrix materials mainly determines the applications of the composite. Composites can be used in aerospace, marine, and automotive industries as well in construction, homes, and sport equipment due to the wide range of applicable materials [3] [112].

2.3.1.1 Classification based on the matrix material

Composites are characterised as metal matrix, ceramic matrix and polymer matrix composites based on the material used as a matrix [61]. In the polymer matrix composite category two types of polymers, thermoplastic and thermosetting, can be used [68], [113].

Thermoplastic polymers are characterised by reversible chemical change during the solidification process [113]. At high temperatures, a thermoplastic polymer can melt to a viscous liquid phase and return back to solid after cooling [61].

Polypropylene (PP), polyethylene (PE), PLA, and aliphatic polyester are some of the most widely known thermoplastic polymers used in composite applications [114]. Thermoplastic polymers can be mixed with a variety of reinforcing materials by using different manufacturing processes [114]. Composites consisting of thermoplastic polymers are mainly manufactured through compression and

injection moulding, due to the ability of this technique to develop high temperatures within short periods [113]. However, weak interfacial bonding between thermoplastic polymers with reinforcing materials has been reported due to the high viscosity of the polymer [61], [115].

Thermosetting polymers undergo an irreversible chemical change during the solidification process [116]. Thermosetting polymers change from liquid to solid after curing [110]. Thermosetting polymers are generally stronger than thermoplastic polymers due to the stronger bonds in the polymers' network and are preferred for high-temperature applications [116]. Thermosetting polymers such as epoxy, unsaturated polyester, and vinyl ester are used for the fabrication of composites for structural applications due to their good penetration into the fibre bundles [116]. In recent years, the use of thermosetting polymers has been under scrutiny because of the polymers' non-recyclability, long biodegradation period, and non-reusability [117].

2.3.1.2 Classification based on the reinforcing material

Based on the selected reinforcing materials, the composites are divided into three categories: particle-reinforced composites, structural composites, and fibre-reinforced composites [61].

In the case of particle-reinforced composites, the reinforcing particles are added to the binding matrix and carry the major portion of the load [110]. Particle-reinforced composites are classified in two categories according to the particle's size, dispersion-strengthened and large-particle composites [110]. Dispersion-strengthened composites contain particles between 10–100 nm. In these composites, the matrix carries the main portion of the applied load and the particles prevent dislocation movement, limiting the plastic deformation [118]. Large-particle composites contain particles larger than 100 nm, which prevent movement of the matrix under an applied force [119]. The most common large-particle composite is concrete, which is widely used in construction applications [110].

Structural composites are also called sandwich-structure composites because of the fabrication method. Structural composites made by attaching at least two thin and very stiff layers onto a thick and lightweight core [110]. A common type of structural composite is laminar composite. Its properties depend on the constituents, geometrical design, and fibre direction within the composite [120]. Different layers of materials can be used, making a hybrid material [120].

Fibre-reinforced composites are used in applications that required high strength per unit weight [110]. The reinforcing fibres are usually blended with ductile matrix materials, such as metals and polymers, and are the primary load-bearing components [121]. The properties of the reinforcing fibres such as the tensile strength and Young's modulus affect the final composite's properties [121]. Composites can be made using either synthetic or natural (cellulose) fibres and through numerous manufacturing processes [121]. An extensive discussion of fibre-reinforced composites follows in the next sections.

Due to the wide range of available and applicable reinforcing and binding materials, the material selection for the design and manufacture of composite is a complicated procedure. For that reason, Michael Ashby of Cambridge University created data plots known as Ashby plots that summarise and compare the mechanical, physical, and thermal properties of potential materials [122], [123]. Figure 2.8 presents an Ashby plot that compares the mechanical properties of different types of polymers, fibres, and composites.

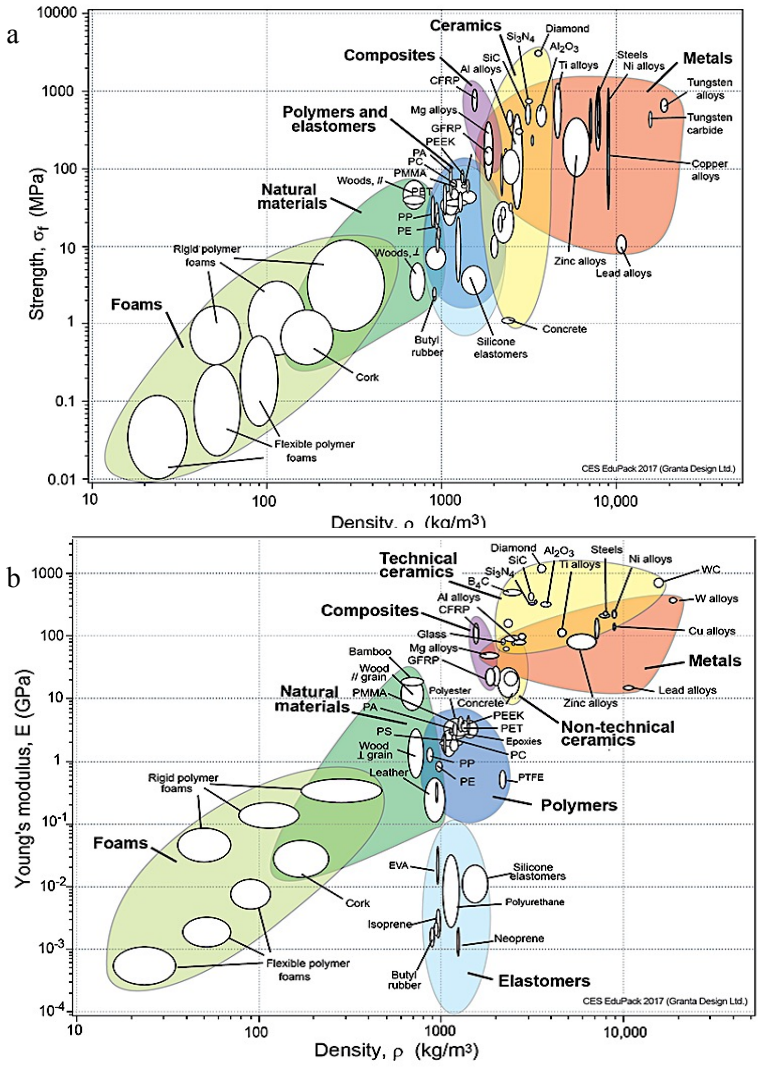

Figure 2.8 Ashby plots summarizing the a) tensile strength and b) Young's modulus of different types of materials (i.e. polymers, metals, ceramics and composites) [123]**. Reprinted from Strength vs Density and Young's Modulus vs Density Charts, by Material Family Chart. Chart created using CES EduPack 2018, Granta Design Ltd.**

2.3.2 Composites manufacturing

Extrusion can be used with thermoplastic and thermosetting polymers for mixing with synthetic and natural fibres [124]. The extrusion temperature and pressure are determined by the thermal properties of the polymer and fibre [124], [125]. Extrusion is used to manufacture materials such as pipes, fencing, window frames, plastic films, and wire insulation [24]. Generally, the extrusion process precedes injection moulding in a material's preparation [124], [125]. The working operation of an extruder is presented in Figure 2.9.

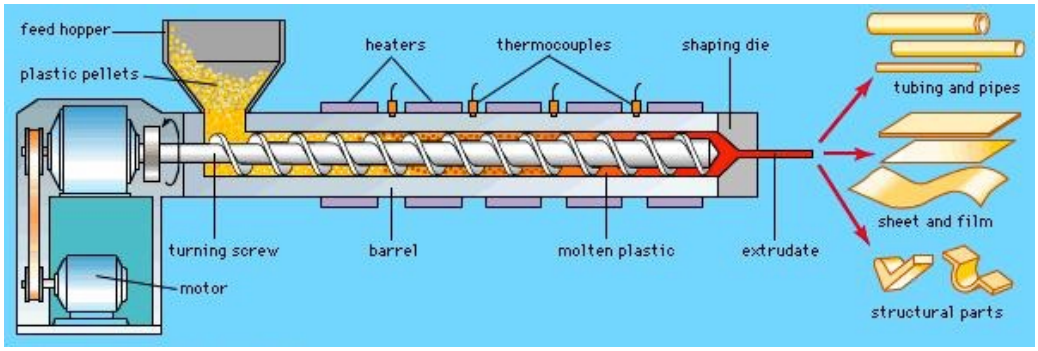

Figure 2.9 An extruder consists of a feed hopper including a set of mixing screws linked with an attached die [126]**. The materials are placed in the feed hoper where are mixed through the extrusion screws. The granules are pushed in the transition zone in which the polymer melts and blends with the fibres** [126]**. The transition zone has different temperature zones that are set up according to the thermal properties of the materials** [125]**. At the end of the transition zone, the blended polymer with fibres result in a continuous homogeneous filament, shaped according to the dimension of the die** [126]**. The filament is immersed in water to cool down and solidify, and it can be turn into pellets, powder and liquid form** [124]**. Reprinted, "By courtesy of Encyclopaedia Britannica, Inc., copyright 1997; used with permission."**

Extruders can be consisted by one or more screws. A twin screw extruder is more flexible and consistent compared to the one screw extruder and is able to ensure transporting, compressing, mixing, shearing, heating and cooling with high level of flexibility. In twin screw extrusion processing, a variety of raw materials can be used as solids (powders, granulates, flours), and liquids. Extruded products are plastics compounds, chemically modified polymers, textured food and feed products [124], [125]..

Injection moulding was introduced in 1872 and can be used for a variety of materials such as metals and glasses. It is highly preferred for thermoplastic and thermosetting polymers [127]. Injection moulding is used for the production of wire spools, bottles, packaging, and automotive parts and generally for the production of parts requiring the use of a mould [128].

The injection moulder consists of a heating barrel and a mould cavity as it can be seen in Figure 2.10 [127]. Typical moulds are made from hardened steel, aluminium, and copper alloys [128]. The polymer is melted in the heating barrel and flows into the cavity under high pressure. The materials cool down and solidify in the mould cavity [5].

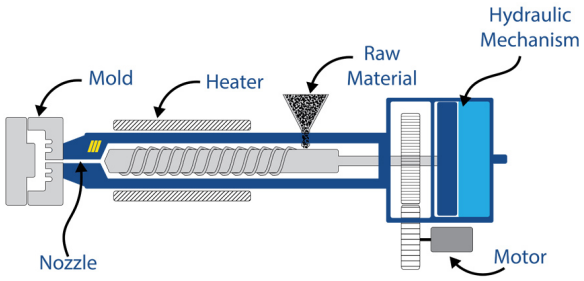

Figure 2.10 A standard injection moulder is consisted by a heater and a mould cavity. A plastic injection moulding can be used for the production of both thermoplastic and thermosetting plastic materials. Reprinted," How hydraulics is used in injection moulding machines by Walker Gross © http://www.rg-group.com/blogs/how-hydraulics-is-used-in-injection-moulding-machines/

Common problem during the injection moulding process include a so-called blister that occurs during the cooling period of the output material [129]. A blister is trapped gas at the surface of the material, causing problems with the homogeneity and stability of the produced product [129]. Blisters may occur from insufficient cooling times, mould temperature, and applied moulding pressures [130].

Compression moulding was first developed for the construction of more complex structures and high volume materials, with applications in the automobile industry [131]. A compression moulder only requires a mould cavity and electric heaters to control the temperature [131].

To begin the process, the mould is sealed and preheated according to the melting temperature of the materials [132]. The materials in the form of pellets, filaments, or sheets are placed on the preheated mould. The melted material retains the shape of the mould after hydraulic pressure is applied [131]. The specimen is left to cool and solidify either in atmospheric conditions or a water bath. For easier ejection of the finished specimen out of the mould cavity, there is frequently an ejector pin in the bottom part of the mould [131].

For the fibre-reinforced composite manufacture, a combination of film stacking and compression moulding is commonly used [133]. Thermoplastic polymers in a form of pellets are turned into thin films by heating and compression. The fibres are stacked between the films [132], [133]. The fibres can be in the form of fibre mats, woven fibres, or individual unidirectional fibre bundles [134]. The final film stack is heated in a hydraulic press until the polymer melts and covers the fibre

layers. The composite is cooled to room temperature under constant pressure [132], [134].

Fibre-reinforced composites composed of thermoplastic polymers require high pressures and temperatures over a short period of time [113]. The processing parameters depend on the type and properties of the polymer and reinforcements [135]. The selected processing temperature is dictated by the polymer's melting temperature and the fibre's degradation temperature [77], [136]. The processing pressure needs to be sufficiently high to avoid any problems such as voids that can be created during the manufacturing process [77].

2.3.3 Mechanical properties of composites

The mechanical properties of composites are measured by their tensile, flexural, impact, and fracture toughness properties [88], [116]. The final mechanical properties of a fibre-reinforced composite are controlled by the mechanical properties of the reinforcing fibres (section 2.2.4) and polymer matrix [25], [137]. During composite manufacturing, the mechanical properties of the composite may be altered by the fibre/polymer content, fibre/polymer adhesion, fibre orientation, and the void content in the composite structure [2], [61], [88], [138]. The selected manufacturing processes also significantly affect the composite's mechanical properties [139].

2.3.3.1 Role of fibre orientation and volumetric composition

The fibre orientation is critical in determining the composite properties and has been widely studied. Madsen *et al*. found that by using highly aligned fibres, the fibre volume fraction could be increased compared with composites consisting of randomly oriented fibres [140]. Composites with high fibre volume also tend to have lower void content, resulting in higher mechanical properties [140]. Miao *et al.* studied the fibre direction in relation to the mechanical properties of the composites, showing that non-woven mats with a specific fibre orientation have higher mechanical properties than non-woven mats with fully random fibre orientations [141]. Composites made with aligned non-woven mats showed a lower stiffness than composites with a unidirectional woven fabric [141].

Madsen *et al*. evaluated the volumetric composition of the composites by creating a model that modified the rule of mixtures by including the porosity and evaluating its effects on the composite stiffness and density [140]. Similar modifications to the rule of mixtures model were made by Lamy and Baley, including definitions of the

optimum fibre diameter in order to achieve the correct stiffness of fibre-reinforced composites [142].

2.3.3.2 Role of fibre/matrix adhesion and voids formation

In the sections above, the fibre/matrix adhesion and void formations were discussed. Due to the importance of these aspects in a composite's mechanical properties, there are numerous related studies.

Graupner *et al.* studied the fibre/matrix adhesion during mechanical testing [143]. They found that weak bonding between the reinforcing fibres and polymer matrix causes issues with the load transfer during mechanical testing, leading to a reduction in the composite's tensile and flexural properties [143].

The formation of voids in a composite structure is the result of different parameters [144]. The processing parameters during the composite manufacture process, such as the extrusion and moulding pressure, temperature, and time, can affect the void content in a composite structure [77], [144]. The formation of voids in a composite affects the mechanical and physical properties of composites (density and weight) and the efficient product life [85], [144]. The microstructure of fibres and composites can be analysed using non-invasive, X-ray transmission techniques such as micro-computed tomography (micro-CT) and scanning electron microscopes (SEM) [77].

Freiman *et al.* described the failure of composites in terms of the strength variability with respect to void size [145]. It was observed that large variations in void size caused larger variations in the composite's tensile strength [145]. Little *et al.* and Li *et al.* studied the correlation between the fibre and void content, observing higher void concentrations at higher fibre contents [77], [144].

In the case of cellulosic fibres (section 2.2.1), the fibres enclosed natural voids in their structure due to lumen [146]. Also, due to the fibres' hydrophilic character (section 2.2.6), fibres absorbed high rates of moisture and thus increased the formation of voids in the composite's structure. Higher fibre content may result in larger void concentrations [85], [106]. It was found that composites with up to 50% fibre content in a thermoplastic polymer led to weak interfacial adhesion between the fibres and matrix, and the formation of voids was up to 30% of the total structure of the specimen [147].

Weak interfacial fibre/matrix adhesion can be caused by void formation, moisture absorption, and insufficient polymer content to bond the reinforcing fibres [25], [143], [148]. It was reported that the formation of voids increases the composite's

porosity and functions as a crack-prone position that is more likely to absorb moisture [77].

2.3.3.3 Mechanical testing

For the characterisation of the composites' mechanical properties, four tests are commonly used: tensile, flexural, impact, and compression test. These tests provide an overview of the most significant features (i.e., tensile and flexural strength, Young's modulus, and energy absorbance) of the produced composites, which are based on the International Organization for Standardization (ISO).

The **tensile test** determines the tensile strength, Young's modulus, and elongation at the breaking point for a composite. During the tensile test, composites are stretched in the axial direction and the tensile stress is transferred from the matrix to the fibre. Fibre-reinforced composites have three types of failures: the matrix fails before the fibres, the matrix starts to undergo cracking, or the failure of the matrix and fibres occur at the same time [149]. According to the British standard BS EN ISO 527 the test specimen is extended along its major longitudinal axis at a constant speed until the specimen fractures. The thickness of injection moulding test specimens should be within 5 mm. Thicker specimens may fail at the gripping area prior the specimen reach the tensile strength of the material, while thinner specimens will be affected by the stress caused along the grips. The use of end taps helps to reduce the stress from the grips to the specimen and carry the load to the specimen in a uniform way [150], [151].

The composite may break immediately, (i.e., at low strains) in the case of a brittle matrix or it can show surface fractures before complete failure. The appearance of cracks on the matrix surface tends to allow higher strain and improved toughness around the breaking point [149], [152].

In the case of the matrix failure, a transverse crack is transmitted through the matrix and, due to the poor bonding with the fibres, the load cannot be properly transferred to the fibres [153]. Ideally, in a good fibre-matrix adhesion, even if the matrix is cracked and the strain increases in the cracking area, the load can still be transferred to the fibres [149]. Usually during an instantaneous matrix/fibre failure, the failure initiates at the edge of the composite [149].

The flexural properties of composites are measured by bending tests. A bending force is applied to the composite to identify the composite's stiffness and resistance to deformation. In a fibre-reinforced composite, the applied bending force is transferred from the matrix to the reinforcing fibres. Bending tests define the flexural stress strain, and the flexural modulus of the composite [154].

According to British Standard BS EN ISO 14125:1998, 'the flexural modulus is defined as the ratio of the stress difference divided by the corresponding strain difference in the initial linear portion of the stress–strain curve' [155]. During bending tests, three flexural failures cases commonly occur: failure at the centre point of the composite, cracking near the support span, and composite's delamination near the support span [154]. It has been observed that the flexural strength is usually greater than the corresponding tensile strength, due to the combination of the compression and tensile stresses in which the composite is forced during the bending tests [154]. During bending tests, the greatest tensile stresses act only in on the composite's surface layer, which is much smaller compared to the total composite volume tested during tensile tests [111].

The flexural properties of composites can be determined by three-point and four-point bending tests. During three-point bending tests, a rectangular cross section of the sample is bent from above while the sample is supported on two span points over the sample's length. In the case of four-point bending tests, the sample is bent in two symmetrical points across its length. Because of the double load in four-point bending tests, the bending load is constant and thus causes lower stresses in the tested samples in contrast to the three-point bending, in which the sample is directly under the central load [111]. The symmetrical bending of four-point bending test is more intense on brittle materials in which the calculated flexural strength is related to the number and severity of the cracks [154], [156].

Impact tests characterise the capability of composites to resist damage under a rapidly applied load and are expressed in terms of energy. The impact strength of a composite is defined as the ratio of the energy required for breaking the composite divided by its thickness and is measured by using Charpy and Izod impact tests [157]. Quantitative and qualitative results can be obtained. The quantitative results are used to measure the toughness of the composite, and the qualitative results are used to determine the ductility of composite [139], [157]. Using impact tests, three possible outcomes may occur: the tested sample has a linear-elastic load over time fracture reaction; brittle and fast fracture occurs after yielding; and fully ductile fracture occurs. The difficulty of a successful impact test is to avoid the formation of cracks of different angles, lengths, and shapes by using hand-held razor blades, which are necessarily used to make the required notched samples [158], [159]. Kuppusamy and Tomlison developed a new methodology for pre-crack growing without using a blade, creating natural cracks and reducing the risks of potential pre-crack formations [159].

Compression tests determine the behaviour of a composite under a compressive load. The tested sample is loaded along its length and becomes shorter and flatter in the direction of the applied load and expands perpendicular to the applied load [114]. With composites, the sample commonly fractures and powders. The failure can occur catastrophically, with a sudden fracture propagating through the sample, or more gradually with a series of small compressive failures. During the compression test, values such as the maximum load to compress and deform the specimen are recorded. From compression test, the compressive and yield strength, elastic limit, and the elastic modulus are measured. The compression failures of a composite may occur in different ways, such as an elastic or plastic micro-buckling failure, fibre-crushing buckling fibres, or matrix splitting parallel to the fibre axis [160].

2.3.3.4 Composite's failure mechanism

Generally, a fibre-reinforced composite material during mechanical testing, as presented in section 2.3.3.3, is facing three main types of failure—fibre failure, matrix cracking, and composite delamination, as seen in Figure 2.11 [61], [149].

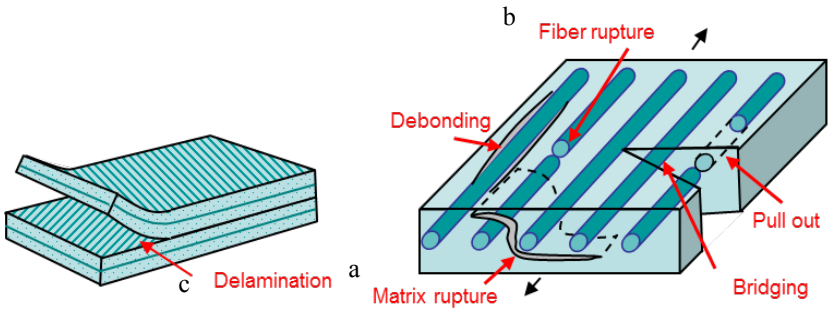

Figure 2.11 Composites failure mechanism: a) matrix fracture, b) fibre fracture and c) delamination of a fibre-reinforced composite. Reprinted from Brittle and Ductile Materials by Tom Irvine © www.vibrationdata.wordpress.com

During mechanical tests, the weaker material (usually the matrix) will break first and the applied load will be completely transferred and carried by the second composite component (Figure 2.10a) [107]. If the stronger material withstands the additional load, the fractures will occur in the brittle material [107], [161].

In the case of fibre fracture (Figure 2.10b), two possible failure mechanisms occur according to the matrix behaviour [162]. During the fibre's failure, a single fracture appears on the fibre structure, and if the matrix cannot withstand the additional load, the composite fails at the point of the weakest region [162]. In the second

case, the matrix can withstand the extra load and small segments will appear along the broken fibres, until the matrix reaches its failure strain [162].

In matrix cracking, the polymer matrix is the brittle material, with the reinforcing fibres able to withstand high strain-to failure values. The matrix fails below the applied load and cracks appear at the polymer surface [153].

The third type of composite failure mechanism is fibre/matrix delamination (Figure 2.10c), which is widely observed in fibre-reinforced composites and is caused by high interlaminar stresses. Delamination occurs when pre-existing matrix and fibre failures lead to the final sample failure [154]. The fibre/matrix delamination is affected by the fibre length and orientation in the composite [143], [163].

To prevent fibre/matrix delamination, the critical fibre length (L_c) is required, which determines the minimum useful fibre length (L_f) in a short fibre-reinforced composite and can be determined with a fibre pull-out test [143], [154]. If the fibre's length is smaller than the fibre critical length ($L_f < L_c$), the maximum load is never achieved because the fibres are too short for the stress to be transferred [164]. If the fibre length is larger than the fibre critical length ($L_f > L_c$), the fibres mainly carry the applied load and, ideally, continuous fibres transfer the load to the matrix before their failure [165]. For a successful load transfer from the fibres to the matrix before fibre failure, the fibres' length should be equal to the critical fibre length [164].

According to observations during mechanical testing, the failure of composites can also arise from the testing machines [120]. Staab proved that premature composite failure in tensile experiments can be due to the concentrations of high stresses in the gripping area of the testing machine [120]. This premature failure of composites can be avoided by using end tabs on the gripping area to protect the test specimen from the high stress concentrations [120], [166].

2.3.4 Thermal properties of composites

For an in-depth analysis of composite properties, the thermal properties must be included. The thermal properties of fibre-reinforced composites are affected by the thermal properties of the individual raw materials [158]. The thermal properties of polymers dominate the thermal properties of the whole composite [167]. In some cases, the reinforced fibres can alter the thermal properties of a composite, such as the glass transition, melting temperature and the level of composite and polymer crystallisation [168].

For the investigation of the thermal properties, techniques such as differential scanning calorimetry (DSC) and dynamic mechanical analysis (DMA) are used [169], [170]. DSC is used for the determination of the polymer's crystallisation and for the identification of the glass transition (T_g), melting temperatures (T_m), and crystallisation temperature (T_c) [168], [171]. The glass transition temperature describes the temperature region where the polymer transforms from a solid glass material to a rubber material. Melting temperature, also called crystalline melting temperature, describes the transition from a crystalline or semi-crystalline phase to a viscous liquid amorphous phase of the polymer. The crystallisation temperature is the point when the viscous liquid transforms to a solid and can be easily found from the DSC heat flow curve as the point with a large exothermic transition, as Figure 2.11 shows. Heat flow describes the required heat to raise the temperature of the sample, as energy flows from one substance to another.

To be practically observed, the T_c must be above the T_g of the polymer. Due to the effects of chain re-organisation kinetics in polymer systems, the T_c occurs at a lower temperature than the T_m [167], [172]. The outcomes of DSC experiments are shown in the form of heat flux curves due to temperature or exposure time, as seen in Figure 2.12. From the heat flux curves, the polymer's enthalpy (H) can be calculated as the total of heat content of the polymer.

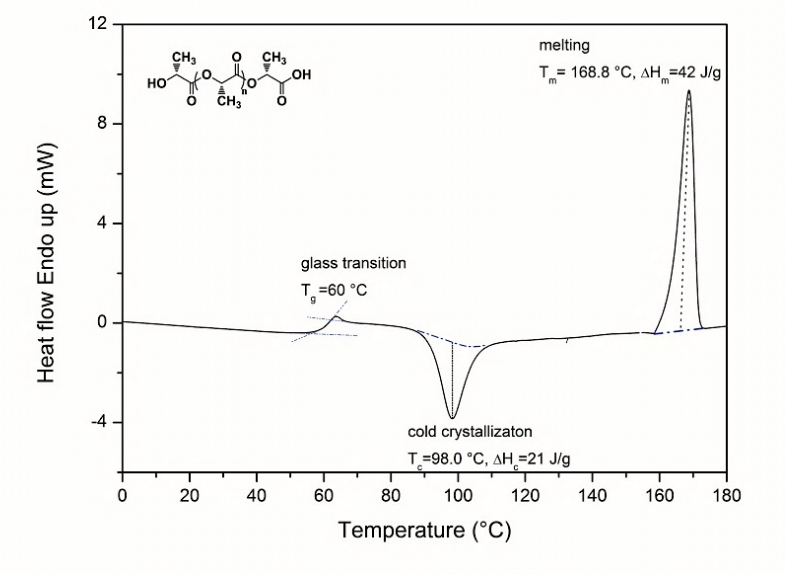

Figure 2.12 DSC curve of PLA heated from 0-180 °C. The glass transition and melting temperature are measured as the first two peaks at 60 °C and 168.8 °C during the heating cycle [173]**. The term cold crystallisation is used to describe an exothermic process, in which the heating sample was rapidly cooled without sufficient time to crystallise. Reprinted from Application of Differential Scanning Calorimetry to the Characterization of Biopolymers by Adriana Gregorova, 2012 © 2012 Adriana Gregorova.**

DMA is used to study the viscoelastic behaviour of polymers by applying stress and measuring the caused strain on the material and determined the complex modulus. The T_g of the polymer and composite can be determined [174]. DMA can be also be used to measure the effect of humidity on the mechanical properties of the composites by actively control both the temperature and relative humidity [175].

2.4 Biodegradable composites

Over the last decade, there have been numerous new regulations in many countries related to environmental protection [12], [13]. Carbon dioxide emissions, global climate change, and the increase of 'disposable' materials leading to oceanic pollution and increased landfill use all sound the alarm to address these problems with immediate action. The European Union has specific regulations on waste management, with a particular focus on landfills (based on Articles 11 and 191–193 of the treaty on the functioning of the European Union) [13]. LCA is currently an option for the manufacturing companies, with increasing applications from both manufacturing companies and their material supplies [13].

Materials manufacturers and the composite industry have expressed their interest in alternative sources of environmentally friendly, recyclable, and biodegradable materials for the production of 'green' products from natural resources known as bio-composites [5], [26], [176]. The term 'green' material is used to characterise materials with a lower environmental impact, highlighting the natural origin of the materials [26]. Beyond the efforts for environmental sensitisation, the phenomenon of 'greenwashing' exists. 'Greenwash' is cleverly used to mislead the public that the product and the policies used in manufacturing processes are environmentally friendly. EU legislations now force the 'green' manufacturing companies to prove that the overall environmental impacts are lower than 'non-green' products (materials that are completely industrially manufactured) [177].

In the field of natural fibre and natural-based composites, greenwashing is used to camouflage preparation and manufacturing processes that require high amounts of non-renewable energy and chemicals and produce high material waste, leading to increased environmental impacts [178]. The evaluation of the sustainability of the material based on EU legislations is through the LCA, which has been standardised by the ISO since 1997 [179]. A materials is characterised as sustainable when all possible choices during manufacturing, use and disposal methods have been made such as the total impacts on the environment is minimised [179], [180].

2.4.1 Classification of biodegradable composites

Statistics for 2013 showed that the annual world production of plastics amounts to 245 million tonnes and increases each year by 6%, from which a tiny portion is recycled and/or reused [181]. The high volume of plastic disposals led material researchers to develop sustainable polymers known as bioplastics [16], [176]. Bioplastics can be formed from plant starches, cellulose, animals, and vegeTable oils, avoiding the use of fossil fuels, gases, and oils [176]. Some bioplastics as PLA and PHA (polyhydroxyalkanoates) are characterised as biodegradable materials because they can be decomposed by bacteria or other living organisms [71], [176]. However, this is not the case for all bio-sourced polymers. Despite the fact other polymers as PE (polyethylene) can be produced from renewable resources are not biodegradable [181]. A composite is called bio-composites when is consisted by i) natural fibres and natural based polymer or ii) natural fibres and fossil based polymer [5]. A bio-composites is biodegradable if it has the ability to undergo a natural decomposition process. The property of biodegradation is independent from the origin of the material but is related to its chemical structure [26]. A separation of polymers based on their biodegradable properties can be seen in Figure 2.13.

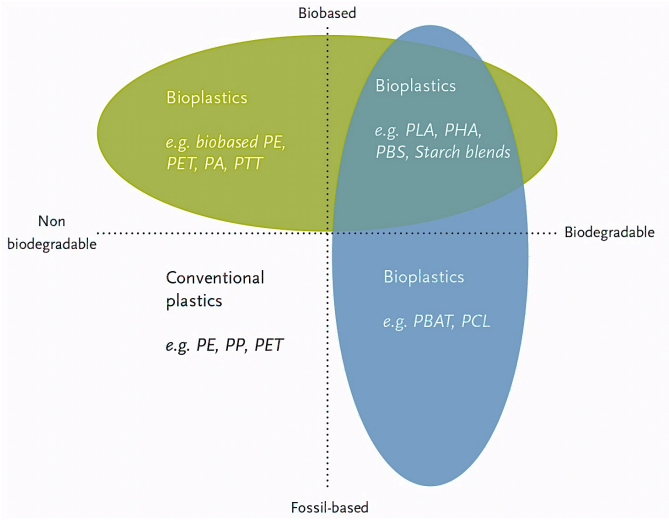

Figure 2.13 Bio-based and biodegradable polymers [181]**. Biodegradable bio-composites are consisting of natural based polymers such as PLA, thermoplastic starch, cellulose and PHAc, and petroleum based polymers such as aliphatic polyester, polyvinyl alcohol and poly(ester amide)** [16]**. Each of the acronyms are as followings PE= Polyethylene, PET= Polyethylene terephthalate, PA= Polyamide, PTT= Polytrimethylene terephthalate, PLA= Polylactic acid, PHA= Polyhydroxyalkanoates,PBS= Polybutylene succinate ,PBAT=Polybutylene adipate terephthalate ,PCL= Polycaprolactone, PP= Polypropylene. Reprinted from © European Bioplastics www.european-bioplastics.org.**

2.4.1.1 Classification of bio-composites based on the reinforcing fibres

Using natural fibres in composite applications can contribute to the reduction of agricultural waste, reducing the amount of seeds, leaves, stalks, and roots in landfill [182]. Ligno-cellulosic fibres such as flax, jute, and hemp have been used as a source of raw materials to make ropes and clothes since antiquity [34], [57]. In the U.S.A. approximately 11.9 million tons of textile waste was generated in 2017. The 4.7 wt% of the textile waste was the total municipal solid waste (MSW), and only 15.9% was reuses and recycled. About 54% of the MSW was landfilled, 13% incinerated in waste-to-energy facilities, and 33% recovered for recycling or composting [183], [184]. In UK, is estimated that 350,000 tonnes of textiles goes to landfill annually at a staggering value of £140 million [14], [26].

Today, flax, hemp, jute, and sisal are used as reinforcement materials in fibre-reinforced composites for applications in the automotive industry, building, and as alternative packaging options [25].

In this study, it was of particular interest to use fibres from plants grown in the United Kingdom as reinforcing materials. The researcher has environmental concerns about the increased use of industrially manufactured materials with increased environmental emissions. Therefore, the researcher has a keen interest in using materials from natural resources as plants for the construction of new materials, as in the case of this project, composite materials reinforced with natural fibres. The selection of nettle fibres was based on the fact that nettles have been used extensively in previous years (more details follow in the section below), but not as reinforcing materials for composite applications. On the other hand, flax fibres have been extensively tested and have been selected as a benchmark. A literature review of these fibres follows.

Linum usitatissimum, also known as common flax, is a member of *Linaceae* family [185]. Countries of central Europe such as France, Germany, Holland, Italy, and Belgium are some of the most flax-growing countries, with approximately 5 million hectares of flax cultivation in total [31]. Flax production in the United Kingdom (mainly in Northern Ireland, Scotland, and England) is ranked eighth in the world's production, with an annual flax harvest of 71,000 kg, according to the latest survey in 2016 [186].

Flax fibres are documented as one of the oldest textile fibres. In Egypt, in 5000 BC, flax yarns and fabrics were used to wrap mummies [185]. The first application of flax as reinforcement material was during World War II as a linen fabric in phenol resin for the construction of aircraft [185]. Today, flax fibres are used as

reinforcement materials in composites for structural applications such as turbine blades, bridges, helicopters, and airplanes [28].

Flax fibres are extracted from the bast (or stem) of the plant, similar to hemp, jute and nettle fibres [86]. Over the years, many studies have been undertaken to determination flax fibre physical and mechanical properties [17], [63], [142].

The structure of a flax plant from the stem to microfibrils is shown in Figure 2.14. Analysing the physical properties of flax fibres, Baley referred to the shape of single flax fibres as hexagonal or pentagonal [17]. The non-uniform geometry of flax fibres causes problems in the calculation of its cross-section area [142]. Charlet *et al.* focused on the calculation of the diameter of single fibres flax extracted from different locations of the stem [60]. Single fibres from the top, middle, and bottom part of the same flax stem were examined. The highest fibre diameter was found in fibres extracted from the bottom part of the stem, with average values of 25–30 μm, and fibres from the top part of the stem had significantly smaller dimensions, averaging 14.8 μm [60]. The diameter of flax fibre bundles and single fibres depends on the thickness and length of the flax stem and the age of the plant [31].

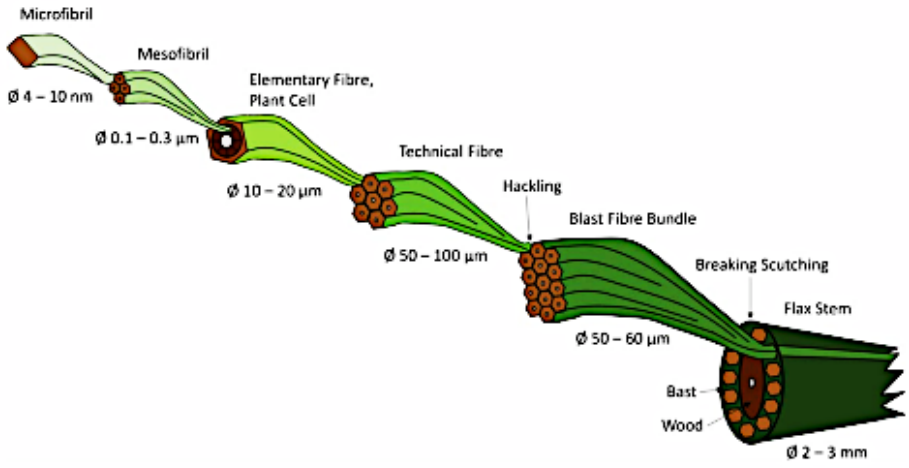

Figure 2.14 From flax stem to flax microfibril [187]**. The diameter of flax stem is between 2-3 mm with the fibre bundles located in the outer surface of the stem** [65]**. Approximately 20-50 fibre bundles are located in the perimeter of the stem with diameter between 50-100 μm and length between 60-140 cm** [188]**. The fibre bundles are consisted of thinner single/elementary fibres of diameter 10-20 μm and length of 20-50 mm** [188]**. The number of single fibres was estimated between 10-40 with different dimensions** [65]**. Elementary fibres are consisted with microfibrils of diameter between 4-10 nm** [65]**. Reprinted from Re-Emerging Field of Lignocellulosic Fiber – Polymer Composites and Ionizing Radiation Technology in their Formulation by Olgun Güven, Sergio N. Monteiro, Esperidiana A. B. Moura & Jaroslaw W. Drelich, 2016, Polymer Reviews, 56:4, 702-736, DOI: 10.1080/15583724.2016.1176037 by permission of Taylor & Francis Ltd.**

Flax fibre is one of the strongest and commonly used plant fibre, with a tensile strength of 2000 MPa, (average tenacity between 50–58 cN/tex for flax yarn), Young's modulus of 85 GPa, and strain at failure between 1.8–2.2% [63], [142].

The thermal properties of flax fibres have been studied, with Van de Velde and Kiekens reporting that thermal degradation of flax fibres occurs at 200 °C, with insignificant changes in the fibre structure in the first few minutes of exposure to high temperatures [97]. Mieck *et al.* reported that flax fibres start to degrade at 240 °C after four minutes of exposure [157]. Flax fibres have a high moisture absorption rate, at approximately 12% [103].

The perennial stinging nettle (*Urtica dioica L.*) from the family of *Urticaceae* can be found on rough sites, at the edges of forests, and in wooded areas mainly in Europe, Asia and North America [87]. Nettle fibres are from the stem of the plant and have similar morphological and chemical characteristic as flax fibres [87]. Nettle fibres can produce finer and silkier fabrics than flax fibres due to their white colour and smooth touch [187], [189]. From the environmental perspective, nettle fibres are characterised as greener than other stem fibres because nettle plants require lower water consumption and almost zero use of fertilisers and pesticides due to the stronger resistance of nettle plants to parasites [190].

The use of nettle fibres dates to the Neolithic period, with archaeological findings showing the use of nettles for string and cloth [187]. During the First World War, due to a lack of cotton, Germany used nettles to make military uniforms [187]. Recently, in 2004, the Department for Environment, Food and Rural Affairs (DEFRA) funded the project 'Sustainable Technology in Nettle Growing' (STING) at Leicester's De Montfort University which produced a thread from nettle plants that was stronger and finer than that of other plants such as hemp [191].

Despite the fact that a large number of stem fibres are already considered as reinforcing material for composites, the use of nettle fibres is limited due to the difficulty of the fibre extraction [27], [68]. Virgilio studied the properties of nettle fibres and recorded an elongation at the breaking point of 2.3–2.5%, tensile strength of 1600 MPa (average tenacity of about 30-35 cN/tex), and Young's modulus of 87 GPa [87]. It should be mentioned that the mechanical properties of nettle fibres (as in all cellulose fibres) are highly affected by the extraction and processing processes [190]. The wider literature reported that the mechanical properties of thermoplastic polymers were improved with the addition of nettle fibres as reinforcing materials [192].

2.4.1.2 Classification of bio-composites based on the matrices

Biodegradable polymers used as binding matrices are also described with the term bioplastics [20]. European Bioplastics reports that the productions of bioplastics reached only 1% of the total 300 million tonnes of plastic produced annually, while the global production of bioplastics is predicted to grow 50% by 2021 [181].

Polylactic acid (PLA), also known as polylactide, is characterised as a biodegradable, 'environmentally friendly', and fully degradable polymer made entirely from renewable resources such as corn starch and sugarcane [22], [168], [193]. Wallace Carothers developed PLA in 1932, and during recent years, up to 25 companies produce it. The desire for greener materials has led PLA to one of the highest consumption levels compared to other types of bioplastics as biobased Polyethylene terephthalate (PET), Polyhydroxyalkanoate (PHA), Polybutylene terephthalate (PBT) and Polybutylene succinate (PBS) [16], [26]. The largest production was recorded in the US, with a capacity of 140,000 tonnes per year [181].

PLA $(C_3H_4O_2)_n$ is a thermoplastic polymer within the aliphatic polyesters family [92]. The chemical structure of PLA can be seen in Figure 2.15.

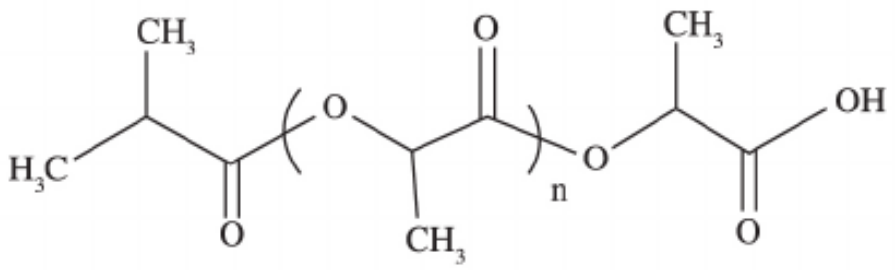

Figure 2.15 Chemical structure of PLA

The formation of PLA is based on the fermentation plant starch such as corn and sugarcane. PLA is formed in two steps. Firstly, corn or corn starch is converted to corn sugar (dextrose, or D-glucose) [194], [195]. The starch is removed from the corn kernel by wet milling and the remaining starches are treated with acid and/or enzymes to hydrolyse dextrose from starch [195]. Secondly, dextrose is turned to lactic acid monomers through glycolysis [194], [195].

Lactic acid and the lactide (cyclic di-ester) monomers are used for the formation of PLA by polymerisation in three forms of L-lactide, D-lactide, and meso-lactide [195]. The final properties of PLA, such as the molecular weight, crystallinity, and mechanical and thermal properties are affected by the proportions of the different

lactides [22]. L- and D-lactide affect the melting point, while higher portions of L-lactide increases the percentage of crystallinity in PLA [22].

The tensile strength of a semi-crystalline PLA is in the range of 50–70 MPa, Young's modulus of 3–4 GPa, tensile stain between 2–10%, flexural strength between 50–120 MPa, and flexural modulus of 3.5–5 GPa [22]. PLA richer in L/D-lactic acid monomers has a lower tensile strength of 40–53 MPa [22].

Comparing PLA with other types of thermoplastics such as cellulose acetate (CA) and polypropylene, PLA appears to have higher mechanical properties. CA and PLA polymers have the same density of 1.3 g/cm^3, although CA has a lower flexural modulus of 1.7–2.1 GPa but higher elongation in the range of 25–30% [196]. In the case of PP, the flexural modulus and flexural strength are lower, with a flexural modulus of 1.3 GPa and flexural strength of 31 MPa [196]. The mechanical properties of different thermoplastics are presented in Table 2.3, from which can be seen that PLA is one of the stiffer thermoplastics.

Table 2.3 Mechanical properties of different thermoplastic polymer [21], [26], [71], [110], [181], [197], [198].

Polymer	Tensile strength (MPa)	Young's modulus (GPa)	Flexural strength (MPa)	Flexural modulus (GPa)
PLA	50-70	3-4	60-80	4
ABS	41-46	2.3	58-61	2.2-3
CA	37.6	1.26	40-55	1.7-2.1
HDPE	36-38	1-1.5	40	0.9-1.3
PP	35-37	1.6-1.7	30-33	1.3
PET	84-88	26-27	125	3-3.3

Kowalczyk *et al.* studied the thermal properties of PLA, indicating a melting point between 130–230 °C and T_g between 50–70 °C according to the concentration of L- and D-lactic acid monomers [199]. Based on PLA's molecular weight, the crystallisation temperature of amorphous PLA is within the range of 110–130 °C [199]. Běhálek *et al.* studied the crystallisation and melting behaviour of PLA, analysing the DSC heating curves and observing a double melting point of PLA. A similar phenomenon has been observed in other polymers such as PE, PP, and PET as a result of multiple crystal forms, different crystal orientations, size, and crystal morphologies during heating experiments [168]. In the case of PLA, a cold

crystallisation appears at 10 °C because of the fusion of crystals with lower thermal stability [168]. The existence of crystals with higher thermal stability leads to the recrystallisation of the polymer, providing high melting temperatures during the crystallisation (as seen in Figure 2.8) [22], [168].

PLA is one of the most widespread biopolymer due to it sustainable and biodegradable characteristics [200]. The sustainable and lower CO_2 emissions of PLA due to its natural origin is purported to reduce the environmental impacts compared to industrially manufactured polymers, with only 0.5 kg of CO_2 emission per 1 kg of the polymer [193]. The calculations of CO_2 emissions included the cultivation of corn starch and/or the conversion of corn starch into PLA. A comparison of the CO_2 emissions of PLA and other polymers can be seen Figure 2.16.

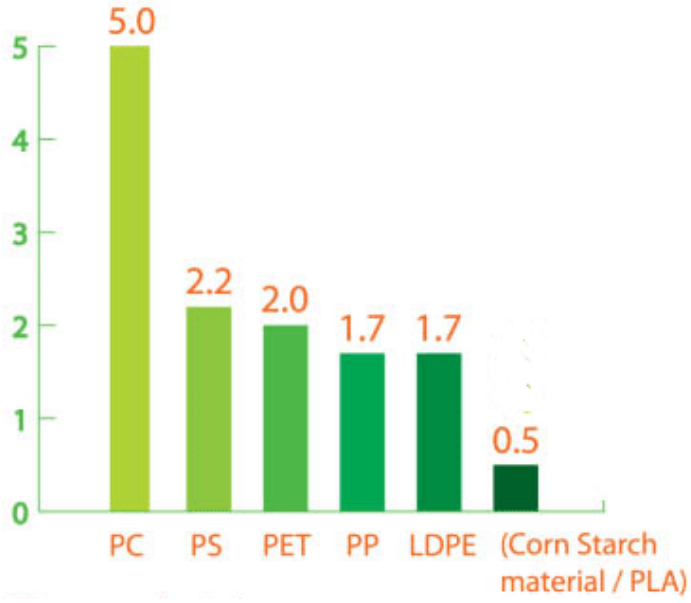

Figure 2.16 Carbon dioxide emission (kg CO_2/ kg of polymer) of different types of polymers. PLA has the lowest CO_2 emission among other polymers due to its renewable origin [21]**. Each of the acronyms are as following; PC= Polycarbonates, PS=Polystyrene, PET= Polyethylene terephthalate, PP= Polypropylene, LDPE= Low-density polyethylene and PLA= Polylactic acid. Reprinted from Plastic Europe, Association of plastics manufacturers © www.plasticseurope.org**

As part of the environmental analysis, the end-of-life options are evaluated [201]. PLA and PLA-based products have a wide range of end-of-life scenarios, such as mechanical recycling, organic recycling including microorganism decomposition, reuse opportunities, and composting [21], [22], [195].

The degradation of PLA in a completely natural environment can take from six months up to two years, depending on the environmental conditions such as temperature and humidity. In contrast, the degradation process of PP is between 500 and 1,000 years [22]. The industrial degradation process for PLA can take three to four weeks, according to the type of microorganisms present [202]. PLA can be degraded by hydrolysis at temperatures above 200 °C, by lactide reformation, and by oxidation [202]. Boonmee *et al.* studied the effects of degradation on the physical properties of PLA and indicated a weight decrease with increasing burying time. Furthermore the colour of PLA was changed from the clear colour to opaque white and fragmentations occurred after 15 days of burying [203].

PLA has applications in various fields from packaging and home utilities products, sport equipment to medical implants [200]. Due to its transparency and decomposition, PLA is used in a variety of packaging materials such as recyclable cups, food packaging, disposable Tableware, and grocery bags [193]. Furthermore PLA can be used in sportswear due to its breathability and soft feel, and in sport equipment because it is washable [204]. PLA is used for building and construction applications as insulation foams, carpets, and furniture due to its heat resistance at 110 °C [200]. Additionally, PLA is used as medical implants in the form of anchors, screws, plates, and pins due to the fact that is able to degrade into innocuous lactic acid that the body can discard [200]. On the other hand PLA has a low glass transition temperature (50–70 °C), which caused problems to applications dealing with heat. To enhance the mechanical resistance of PLA at high temperatures, PLA is blended with polymers with higher glass transition temperatures for example PLA/PC blend in the presence of a catalyst consisting of triacetine and tetrabutylammonium tetra-phenylborate (TBATPB) [205], [206].

A new entry in the bioplastic family is that of Floreon. **Floreon** is a blend based on PLA completely made from renewable resources [19]. Floreon is manufactured by Floreon-Transforming Packaging Limited, in close collaboration with the University of Sheffield and approved by the EN13432 standard [19].

Floreon was made with the prospect of preserving the sustainable origin and recyclability of PLA, while improving its mechanical and chemical properties. For this reason Floreon was chosen as the binding matrix in the current project. Floreon is 71–98% polylactide resin, 1–9% 2-oxepanone (caprolactone) homopolymer, and 1–20% aliphatic polymer, produced by compounding. During compounding, PLA pellets are melted in a blending process with colours and/or pigments for the final formation of Floreon [19].

Comparing Floreon with PLA, Floreon has been characterised as four times tougher than a standard PLA with fewer breaks and fractures during the manufacturing and testing [19]. The calculated (maximum) tensile strength of Floreon is up to 1.6 GPa and elongation at break (fracture strain) of 14%, according to ISO 527-2 [19], [150]. Compared with PET, Floreon has a 15% higher tensile strength, 30% higher Young's modulus, and 85% improved toughness [19].

Floreon has higher thermal properties compared to PLA, with its melting temperature and crystallisation temperature 210 °C and 85 °C respectively [19], [207]. Floreon's glass transition temperatures is at 65 °C. Floreon can be used in extrusion procedures with melting temperatures of 170–180 °C, but no higher than 220 °C as the decomposition temperature of Floreon is 250 °C [19]. After crystallisation, to avoid moisture absorption, it is recommended to dry Floreon at 65–90 °C [19].

Floreon can be used in compounding, film extrusion, injection moulding, extrusion, and thermoforming manufacture processes. Currently, there have been developed eight different grades of Floreon, called FL100 to FL800, which are suitable for different applications and processes [19]. Floreon can be used in 3D printing and is more efficient in 3D and lithographic printing applications over PLA due to its ultraviolet light degradation resistance [19].

2.4.1.3 Mechanical properties of PLA fibre-reinforced bio-composites

The mechanical properties of PLA-based fibre-reinforced composites are found to be comparable with E-glass fibre-reinforced PLA composite, as presented in Table 2.4 [2], [188], [208].

Table 2.4 Tensile properties of PLA-based fibre-reinforced composites.

PLA-based composites	Fibre content (wt%)	Tensile strength (MPa)	Young's modulus (GPa)	Reference
Flax/PLA	30	100	8	[2]
Hemp/PLA	47	55	9	[2]
Jute/PLA	44	42	8.5	[209]
Nettle/PLA	40	40-52	4.8	[192]
Ramie/PLA	30	40	1.3	[210]
Kenaf/PLA	40	88	8	[2]
E-glass/PLA	30	80	6.7	[211]

It was reported that the tensile properties of bio-composites were highly affected by the fibre type, content, and applied processing parameters during composite manufacturing, as described in section 2.3.3 [2], [147], [192]. Fischer *et al*. studied the properties of nettle fibre/PLA composites and reported the highest tensile strength of 59 MPa at 30 wt%, while at 20 wt% and 40 wt%, the composites had reduced results [192].

Alimuzzaman investigated the influence of moulding parameters during the extrusion procedure of flax/PLA composites of 40 wt% flax fibre content, reporting that the maximum tensile strength was obtained at 180 °C moulding temperature and a five minute moulding time [147]. Gassan and Bledzki showed that the tensile strength of flax fibres exposed at 210 °C decreased by approximately 50% [93]. Comparing the mechanical properties of composites of PLA and PP; the mechanical properties of flax fibre/PLA composite were about 50% higher with respect to the corresponding properties of flax fibres/PP composite, because of a better fibre/matrix adhesion [92].

PLA natural fibre-reinforced composites absorb moisture from the surrounding environment due to the high amount of hydroxyl groups included in the cellulose, hemicellulose and lignin components of ligno-cellulose fibres (sections 2.2.2&2.2.6) [103]. There are three mechanism of absorption: i) diffusion, ii) capillary and iii) transport of water molecules [212]. Diffusion occurs inside the microgaps between the chains of the polymer, while capillary between the gaps at the fibre/matrix interface. The poor wettability between the reinforcing fibres and the binding matrix makes the capillary mechanism stronger[161], [213]. PLA absorbs moisture up to 5 wt% and is more intense in the flax/PLA composites, up to 12 wt% [161].

2.5 Alternative composite manufacturing

New investigations have been also made in the manufacturing field, with additive manufacturing (AM) methods gaining ground in composite manufacturing, as opposed to 'traditional' composite manufacturing (section 2.3). AM aims to manufacture materials with improved physical, mechanical, and thermal properties, as well to promote the sustainability of the specimens produced [214], [215].

2.5.1 Additive layer manufacture methods

AM is a rapidly growing technology in material manufacturing industries [216]. AM uses layer-by-layer building methods with 3D printers [217]. Stereolithography, multi-jet modelling, selective laser melting, laser sintering, and fused deposition

modelling (FDM) are the most well-known AM techniques [218], [219]. Depending on the AM technique selected, different types of materials can be used. Thermoplastic polymers such as acrylonitrile butadiene styrene (ABS), PC, and PLA in the form of continuous filaments are used with FDM [220].

AM is used in automotive and aerospace applications, medical implants, and even household products [216], [221]. The biomedical field uses FDM technique for tissue engineering applications to produce biodegradable scaffolds, bionic ears, aortic valves, and liver tissue constructs [222]. The field of electronics also uses 3D printing in the production of electronic, capacitive, and piezoresistive sensors through FDM [223].

2.5.1.1 3D FDM printer

The term 3D printing is used for the production of three-dimensional parts with complex shapes and structures [221]. Even the simplest 3D FDM printer consists of multiple components [219]. The extrusion and nozzle of a 3D FDM printer can move in the X, Y, and Z axis along the flat print bed, as seen in Figure 2.17 [219]. The print bed is a horizontal layer of either glass or aluminium for uniform heat distribution and it is heated to a certain temperature according to the material type [219]. The raw material is placed and melted in the extruder tool head (according to the material's melting temperature), which includes temperature sensors, a heating coil, and a motor to push the material into the nozzle. The melted material is extruded from the printer's nozzle [217], [219].

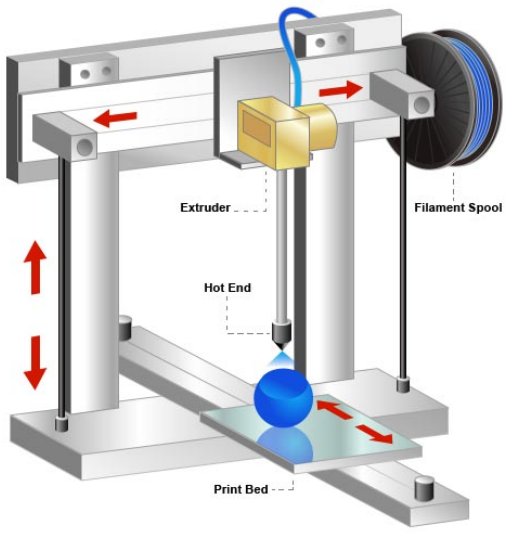

Figure 2.17 3D printer's components. Generally, a 3D printer has three key parts: the extruder tool head (including thermocouples and a motor), the nozzle and print bed [219]**. Reprinted from Anatomy of a 3D printed © 3D printer power, http://3dprinterpower.com/3d-printer-anatomy/**

2.5.2 3D FDM printed composites

FDM is preferred for the production of fibre-reinforced composites consisting of thermoplastic polymers with natural or synthetic reinforcing fibres due to the ability to incorporate filaments in the 3D printers [224], [225], [226]. Printing parameters such as the nozzle temperature, printing pattern orientation, layer height thickness, and fill density affect the mechanical properties of the polymers and composites used [223], [226], [227]. Table 2.5 summarises the mechanical properties of 3D printed ABS and PLA samples according to different values of layer height thickness and pattern orientation [227].

Table 2.5 Tensile properties of FDM 3D printed ABS and PLA samples according to different printing parameters. The samples were 3D printed with fill density of 100% [227].

	ABS		PLA	
Printing parameters	**Tensile strength (MPa)**	**Young's modulus (GPa)**	**Tensile strength (MPa)**	**Young's modulus (GPa)**
Layer height thickness: 0.4mm	28.2	1.875	54.9	3.286
0.3mm	27.6	1.736	48.5	3.334
0.2mm	29.7	1.839	60.4	3.480
Pattern orientation: 0°/90°	27.7	1.867	54.9	3.336
-45°/45°	29.5	1.739	52.3	3.384

Depending on the printing angles and patterns, as seen in Figure 2.18, the mechanical properties can be changed [228]. Tymrak observed a slightly improvement on the tensile properties of 3D printed PLA samples with printing pattern orientations of 0°/90° instead of -45°/45° [227]. In the case of 3D printed ABS samples, the samples with printing pattern orientations of -45°/45° were the strongest, probably due to performing of the tests at a higher strain rate [227].

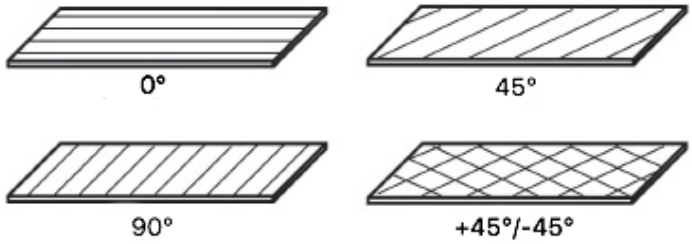

Figure 2.18 Printing pattern orientations [229]**. The printing orientation is determined by the direction of the nozzle during the 3D printing process** [229]**. Reprinted from Anisotropic mechanical properties of ABS parts fabricated by Fused Deposition Modelling by Constance Ziemian, Mala Sharma and Sophia Ziemian 2012, © 2012 Ziemian, Sharma, Ziemian.**

The fill density value depends on the intended application and typically ranges from 40–100% [223]. Samples 3D printed with higher fill density values, between 80–100%, have higher material and time consumption and a more condensed structure, as seen in Figure 2.19 [223], [229]. Depending on the density values, different mechanical properties have been observed, as presented in Table 2.6 [229].

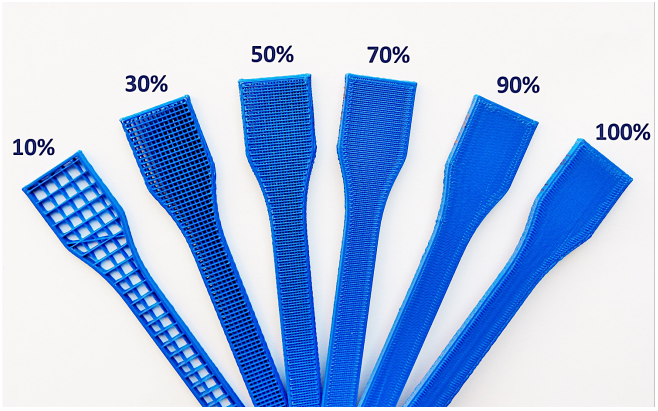

Figure 2.19 Inner structures of 3D printed samples according to the different values of fill density [229]**. Samples that are 3D printed with fill density of 100% are heavier due to the larger material consumption** [223]**. Reprinted from "What is the influence of infill %, layer height and infill pattern on my 3D prints?" © 3D Matter powered by Standardizing Distributed 3D Manufacturing, http://my3dmatter.com/**

Table 2.6 Tensile strength of PLA due to different values of fill density [229]**. PLA samples were 3D printed with layer height thickness of 0.2 mm and linear infill pattern** [229]**.**

Fill Density (%)	Tensile strength (MPa)
100%	46
80%	35
60%	26
40%	17
20%	13

The 3D printed wood fibre-reinforced PLA composites, (20 wt% wood fibre content) have been studied [230]. Duigou *et al.* reported a strong correlation between the printing orientation and the composite's tensile properties. The wood fibre composites printed with a rectilinear fill pattern orientation had an elastic linear behaviour until the breaking point during the tensile test. The highest tensile strength of 30 MPa was obtained at a pattern orientation of 0°, while the tensile strength at a 90° pattern orientation was 20 MPa [230]. For Young's modulus, composites printed at a 0° pattern orientation had up to 4 GPa, compared to 3.6 GPa for composites with a 90° pattern orientation [230].

2.5.2.1 3D printing sustainability

AM is also evaluated in terms of sustainability. The ability to choose printing parameters with 3D printing assists in the manufacture of materials with a minimum required material consumption [215].

The sustainability of the 3D printing process was evaluated in terms of energy consumption [215]. Kreiger and Pearce investigated the energy consumption of 3D printing (through LCA) by using distributed manufacturing of PLA samples [231]. Samples of 3D printed PLA with a fill density of 100% consumed up to 8.23 MJ compared to the injection-moulded PLA samples that consumed up to 7.09 MJ [231]. Reducing the fill density by 25% reduced the consumed energy to 4.22 MJ [231].

However, the environmental analysis of 3D printing is in early stages and needs to be improved in order to produce results that may be compared with other production processes.

2.6 Life Cycle Assessment (LCA)

Life cycle assessment (LCA) is the most widespread technique for the evaluation of the environmental impacts generated by the material production [12]. LCA is a cradle-to-grave assessment that represents the entire life cycle of the product starting from the raw materials extraction and acquisition, thought the manufacture process, the use, recycling and end-of-life options of the product [232], [233]. A cradle-to-grave analysis related with material's production includes a full life cycle assessment from material extraction ('cradle') up to the use, disposal and end-of-life option of the material ('grave'). Cradle-to-cradle is part of the cradle-to-grave assessment, with the difference that it only refers to products that are recycled [234].

LCA can be used for the identification of the product's emissions related to different manufacture and recycling processes and linked them with the potentially affected environmental categories [233], [235]. LCA studies focus on the detection of harmful emissions based on the selected manufacturing procedures, type and amount of raw materials [233].

A comprehensive cradle-to-grave LCA study includes five main phases [236]:

I. Goal
II. Scope
III. Life cycle inventory analysis (LCI)
IV. Life cycle impact assessment (LCIA)
V. Interpretation.

The first phase, the goal, determines the decision framework and study applications [235]. The second phase, the scope determines the studied system, the functional unit, the environmental impacts, and the assumptions related with the data collected, methods used and the interpretation approaches [235]. During the third step, the input data, which are related with the amount and type of materials used, energy and water consumptions and output emissions during the different procedures, are collected [236]. During the LCIA step, the analysis of the data collected with respect to the environmental impacts took place [236]. In the final step of the interpretation, the identification of significant environmental emissions and carbon footprint are reported [237]. LCA is operated according to ISO: 14040 and ISO: 14044 international standards and the input and output data are analysed with environmental analysis software as descripted in Table 2.7 [233], [236].

Table 2.7 Description of LCA methodology based on the software selection [238]–[240].

Methods	Description
SimaPro	It can be used for: • Carbon footprint calculation • Environmental product declaration (EPD) • Environmental impact of products • Environmental reporting (GRI)
ECO calculator	Widely used in Switzerland, Germany and UK. It can be used for: • Determination of the effects of emissions on the ecosystem • Deterioration of human health
Swedish CPM	Includes a database with environmental data related with the environmental impacts and emissions

SimaPro software includes large databases for a variety of materials and applied processes [238]. Similarly there are many European and worldwide databases as ECO calculator software; which includes input data collected from European resources as the Swedish centre for environmental assessment of product and material systems database, the Japanese environmental management association for industry, the US national renewable energy laboratory, the Swiss Ecoinvent, and the European reference life cycle database [238]–[240].

2.6.1 LCA for natural fibres

LCA for natural fibres focuses on the fibre extraction and preparation steps, analysing the chemicals, energy, and water consumption during the plant growing and extraction processes [10], [26], [241]. The environmental impacts of plant fibres such as flax, hemp, sisal, and jute have been studied using LCA methodology [209], [242], [243]. Environmental studies for nettle fibres have not yet been released due to lack of input data [13], [244].

Environmental categories such as the greenhouse effect and soil acidification are differently affected based on the selected extraction and fibre manufactured methods [241]. The greenhouse effect is associated with increased CO_2, methane

(CH_4), and nitrous oxide (N_2O) emissions, leading to climate change [245]. The rapid increase of CO_2 emissions is attributed to fossil fuel consumption, land use, and solid waste disposal. CH_4 and N_2O emissions are mainly from agricultural operations and from the waste produced [10], [245].

Agricultural operations affect the soil pH levels, causing acidification of the soil. Acidic soils limit the availability of nutrients and affect plant growth. The use of ammonium- and nitrogen-based fertilisers during agricultural operations gradually decrease the soil pH [246]. Fertilisers and pesticides can be transported to soil, water, and air either from rainwater or from natural processes such as animal feed [247]. Fertilisers rich in nitrogen and phosphorus are the dominant source of nutrient pollution, causing eutrophication that subsequently causes structural changes to the ecosystem [248].

Measurements of CO_2 emissions are calculated based on the greenhouse gas protocol (GHG) [245]. Zampori *et al.* investigated the environmental emissions of hemp fibres used as thermal insulator materials [245], [249]. The CO_2 emissions were calculated according to ISO 14067 and PAS (Publicly Available Specification) 2050 standards as the total carbon emissions embedded in the product, including carbon dioxide emissions during production and decomposition processes [7], [237]. The total CO_2 emissions for the production of 1 tonne of hemp fibres during the fibre cultivation and extraction process are up to 200 kg (CO_2 eq./t) [249]. Andrew Norton studied among other parameters the CO_2 emissions of hemp fibres, cultivated and prepared in the UK. Hemp crops requires nitrogen, phosphorus and potassium fertilisers on average 100 kg/ha of nitrogen, 30 kg/ha of phosphorus and 30 kg/ha of potassium highlighting that soils with different pH levels require different amounts of fertilisers [250].

Similarly, Althaus *et al.* reported CO_2 emissions up to 560 kg (CO_2 eq./t) for jute fibres [251]. Sisal fibres produced CO_2 emissions at the same level as jute fibres, at 590 kg (CO_2 eq./t), while flax fibres had lower CO_2 emissions, up to 250 kg (CO_2 eq./t) [8], [243]. The environmental emissions calculations are based on data collected from fibre cultivation, including soil preparation, use of fertilisers and pesticides, and fibre preparation processes such as scutching and retting, in relation to the material, energy and fossil consumption [10], [235], [251]. For comparison purposes, the CO_2 emissions of glass fibres are up to 2,630 kg (CO_2 eq./t), according to Kellenberger *et al.* [252].

The emissions of agriculture operations represent 10–12% of the total anthropogenic greenhouse gas emissions [253]. Specifically, agricultural procedures contribute up to 60% of global N_2O emissions [254]. According to the

Centre for Sustainable Crop Management, flax plant cultivation in the UK consumes up to 50 kg/ha of nitrogen-based fertilisers (N), 60 kg/ha of phosphorus-based fertilisers (P) as P_2O_3, and 60 kg/ha of potassium based fertilisers (K) as K_2O [255]. P-fertilisers are responsible increase the water pollution by 80%, while N- and P-fertilisers increase the terrestrial acidification by 60.9%, freshwater eutrophication by 37%, and the marine eutrophication by 77% [8].

Flax fibres are one of the most widely used reinforcing materials and have been extensively tested for environmental impacts [8], [241], [242]. LCA studies have focused on environmental emissions for the different extraction and preparation steps, including input data for each process [236]–[238]. There is a particular interest in the LCA for flax fibres, as flax fibres were used as reinforcing materials in the present project and have been similarly examined with LCA methodologies.

In the UK, flax plant cultivation involves the preparation of the soil, including ploughing and seed harrowing [8], [256]. Different types of fertilisers are used as part of the soil fertilisation and plant protection [8], [257]. P-, K- and N-based fertilisers are used during soil preparation and for flax plant protection [241]. The use of fertilisers and pesticides during flax cultivation has impacts on environmental categories such as climate change, human toxicity, fossil depletion, and photochemical oxidant formation [8]. The amount of fertiliser and energy consumption required for the production of 1 tonne of flax fibres is presented in Table 2.8.

Table 2.8 Chemical and energy requirements for the production of 1 tonne flax yarn [242], [255], [258].

Type of chemicals	**Amount (kg/tonne)**	**Energy consumption (GJ/tonne)**
Lime	2445	3.53
Ammonium nitrate	445	29.37
Triple superphosphate	238	3.33
Potassium chloride	368	3.31
Pesticides	9.4	2.26

Another factor that affects the amount of chemicals used is the depth of the soil where the seeds are planted. It has been reported that flax seeds planted deeper required lower amounts of N fertilisers but higher amounts of S fertilisers as shown in Table 2.9 [258].

Table 2.9 Fertilisers (kg/ha) requirements for flax fibres cultivation according to different soil depths. The reported value of P fertilisers for 0-15 cm soil depth was at 16 (kg/ha) and soil pH 8 [258].

Soil Depth (cm)	Nitrogen (NO_3)	Sulphur (SO_4)
0-15	15	3
15-30	10	3
30-60	10	7

2.6.2 LCA for polymers

LCAs related to polymers are investigating the energy consumption during the manufacture process, the recycling abilities of the products produced and the performance of different types of polymers according to their environmental impacts [193], [259]. Polymers are evaluated according to the material, energy, and cost efficiency, use of renewable resources and biodegradability [20], [260], [261]. Environmental categories such as acidification, eco-toxicity, global warming, and ozone depletion are mainly considered, as seen in Figure 2.20 [20].

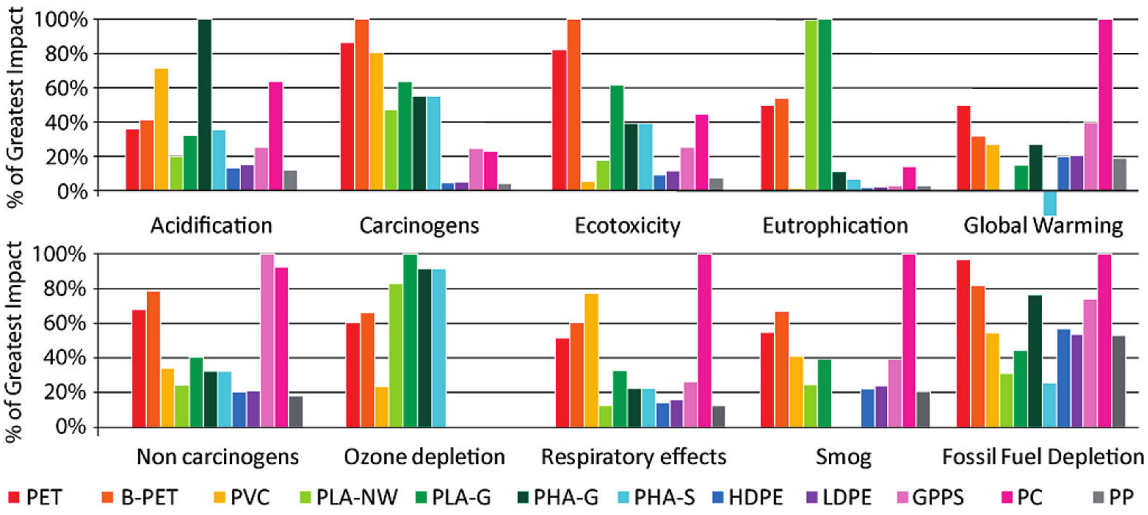

Figure 2.20 Life cycle assessment results of different polymers according to the environmental impacts [20]**. The mentioned polymers are PET= polyethylene terephthalate, B-PET= recycled polyethylene terephthalate, PVC= polyvinyl chloride, PLA-NW= polylactic acid by NatureWorks LLC, PLA-G= polylactic acid of general process, PHA-G= polyhydroxyalkanoate from corn grain, PHA-S=polylactic acid from corn stover, HDPE= high-density polyethylene, LDPE= low-density polyethylene,, GPPS= polystyrene (general purpose), PC= polycarbonates, PP= polypropylene. Reprinted with permissions form Sustainability metrics: Life cycle assessment and green design in polymers by Michelangelo D. Tabone, James J. Gregg, Eric J. Beckman and Amy E. Landis, 2010 © 2010, American Chemical Society.**

In terms of the environmental emissions, petroleum-based polymers such as PET and PC have been identified as having the highest impacts in eco-toxicity and carcinogenic environmental categories due to the required industrial polymerisation processes [20]. In comparison, PLA as a biodegradable polymer has a lower eco-toxicity compared to other biodegradable and petroleum-based polymers [20]. Although PLA is a natural-based polymer, it has higher impacts on acidification and eutrophication as a result of the required phosphorous and nitrogen fertilisers during agricultural operations [201].

Analysing the energy requirements during manufacturing, PLA requires a lower energy consumption of 55 MJ/kg, compared to PP and PET, with energy consumptions of 77 and 76 MJ/kg respectively [262]. According to Gruber, the CO_2 emissions of PLA are 1820 kg (CO_2 eq./t), while the CO_2 emissions of PP and PET are 1,852 and 4,143 kg (CO_2 eq./t) respectively [262].

Recycling methods have a great influence on total energy consumption and CO_2 emissions [201]. Recycling mechanisms such as mechanical recycling, pyrolysis, and recycling through chemical treatment are mainly used for polymers [263]. Pyrolysis is considered a sustainable, profiTable recycle solution for plastics. It is used on a large scale due to the small amount of water and applied chemicals required, leading to lower CO_2 emissions [264].

Despite the environmental regulations for environmental studies, conducting LCA studies is a time consuming and complicated procedure [12], [265]. The lack of input data in combination with the numerous manufactured, recycled, and end-of-life treatments of the products leads to qualitative LCA studies that are focused only on specific farms or manufacturing routes. As such, LCA can be used as an identification factor but no general comparisons can be made [265].

2.7 Summary

The increased demand and consumption of polymers led to the development of materials with improved physical and mechanical properties, extended life periods, and reduced manufacture costs [12], [181]. In the past years, due to government legislations, materials manufacturing industries turned their interest to the manufacture of environmentally friendly materials, investigating alternative and renewable resources [12], [13], [201]. The materials produced are evaluated and characterised by using LCA in terms of the material, energy, and water consumption during the manufacture and end-of-treatment processes, while the environmental emissions are calculated, highlighting potential hotspot emissions [9], [232], [266]. Although LCA methodology is widely used, its implementation is

complicated due to the lack of information (i.e., input and output data from the material manufacture companies) and thus the current literature needs improvement and further analysis [10], [265].

In the effort to produce materials with improved properties (physical, mechanical, and thermal), researchers have focused on the manufacture of composite materials incorporating at least two individual raw materials [61], [267]. The fibre-reinforced composite category has been widely investigated due to the range of applicable materials, manufacturing processes, and applications [238].

The need for sustainable composites led to the investigation of polymers from renewable resources [16]. A new entry in the category of biodegradable and sustainable polymers is Floreon, a polymer from renewable resources with mechanical properties comparable to PLA [19]. Although Floreon is a promising material, its use as a binding matrix in composite applications is still in the early stages [19].

In the manufacture of bio-composites, natural fibres are used as reinforcements [25], [26], [92]. Natural fibres are used due to their biodegradable character, lower density compared to industrial fibres (e.g., carbon and E-glass fibres), and comparable mechanical properties in the case of flax fibres and E-glass fibres [102], [268]. Cellulosic fibres such as flax, hemp, sisal, and jute have been widely studied and their mechanical, physical, and thermal properties analysed. Although nettle fibre has similar morphological and chemical structure as flax fibre, it has not been fully studied or considered as reinforcement for composites. Beyond the determination of the mechanical and physical properties of natural fibres, environmental studies have been performed to investigate the environmental impacts and CO_2 emissions produced during the cultivation and preparation process of natural fibres [242], [269].

Based on the aforementioned considerations, this project focuses on developing natural fibre-reinforced composites from renewable and biodegradable resources. The reinforcing fibres and binding matrix were selected based on the material‘s natural origin and due to the researcher's interest in expanding the field of composites with materials that have not yet been fully tested. In the next chapters, the research methodology, results, and conclusions from the manufacture and characterisation of natural fibre-reinforced composites are presented.

3 FLAX AND NETTLE FIBRES

Physical, mechanical, and chemical analysis of minimally and industrially processed flax and nettle fibres

3.1 Introduction

Flax and nettle fibres are used as reinforcing materials to provide strength and stiffness to composites. Industrially and minimally processed flax and nettle fibres were tested to determine the fibres' mechanical and physical properties and to investigate potential differences in the fibres' properties based on the preparation processes.

This chapter provides information on the reinforcing fibres and the testing and preparation methods for the evaluation of the fibres' physical, mechanical, and thermal properties prior to their application in composite manufacturing.

3.2 Research methodology

Fibre-reinforced composites are comprised of reinforcing fibres and the binding matrix. The physical and mechanical properties of fibre-reinforced composites are mainly dependent on the properties of the individual components [121]. Therefore, as a first step, the physical, mechanical and thermal properties of the reinforced flax and nettle fibres were identified and analysed.

3.2.1 Material selection

For this work, flax and nettle fibres were selected for reinforcing materials. Flax fibre is classified as a bast or stem fibre, with higher mechanical properties (section 2.2.5, Table 2.2) than other stem fibres. In particular, flax has a tensile strength up to 2000 MPa, a maximum Young's modulus of 85 GPa, and a low density of 1.54 g/cm^3 [17], [58], [88]. Extensive research of its physical and mechanical properties show that flax fibres are suitable materials to be used as a reinforcements [63], [112]. Nettle fibres are included in the same bast fibre category. Currently, research on the mechanical and physical properties of nettle fibres is limited due to the lengthy preparation required for its fibres [189], [192]. The average tensile properties of nettle fibres are; Young's modulus of 87 GPa, tensile strength up to 1594 MPa, strain at failure to 2.11% and density at 1.5 g/cm^3 [270].

3.2.2 Material testing

The physical and mechanical properties of nettle and flax reinforcing fibres were examined and evaluated before their mixture with a polymer matrix. Of special interest was the comparison between industrially processed flax and nettle fibres with the corresponding minimally processed flax and nettle fibres. Industrially fibres are commonly in a form of a yarn, indicating that the fibres have been under industrial preparation procedures to induce flexibility within the fibres. This is primarily driven by weaving applications. The term minimally processed refers to fibres extracted from stems without any processes to induce flexibility in the fibres.

The physical parameters of fibres such as fibre diameter and critical fibre length were determined. The fibre diameter is an important parameter for the cross-section area calculations required for calculations of the fibre's mechanical properties. The critical fibre length is determined by the fibre strength and the matrix/fibre adhesion and as such, is crucial for composite manufacturing. Due to the non-uniform structure of the fibres, the length, thickness, and cross-section area of flax and nettle fibres had a large distribution, especially in the case of minimally processed fibres.

The mechanical properties of the fibres—tensile strength (stress at which the fibres fails), tensile strain at failure, and Young's modulus—were determined. The Young's modulus, tensile strength and tensile stain at failure are extracted from the stress-strain curves (chapter 2, section 2.2.5). Industrially and minimally processed flax and nettle fibres were tested as fibre yarns and single fibres by tensile tests. For the determination of the tensile properties of fibres, values of the cross-section area, the maximum force at failure, and tensile strain at failure of fibres were first determined.

3.3 Fibre preparation process

3.3.1 Industrially processed flax and nettle fibres

The industrial flax and nettle fibres were obtained from WildFibres (www.wildfibres.co.uk) [†]. Flax and nettle plants were harvested from UK farms (the exact location of the farms is not available) prepared, and delivered as yarns (Figure 3.1). The industrial single fibres were extracted by hand from the

[†] There is no reference to flax and nettle fibre's mechanical properties from Wildfibres.

respective yarns and for better visibility, placed under a Leica DM LM optical microscope.

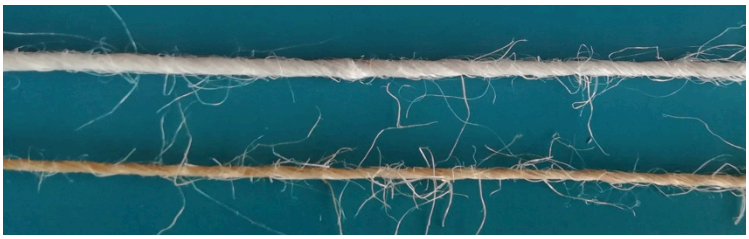

Figure 3.1 The nettle (top) and flax (bottom) yarns were tensile tested without any additional processing and preparation steps. The industrially processed nettle and flax single fibres can be seen unravelled lengthwise the yarns.

3.3.2 Minimally processed flax fibres

The minimally processed flax fibres were extracted from the flax stems, as can be seen in Figure 3.2. The flax stems were harvested from farms in Sussex and delivered unprocessed, dry, and without leaves.

Flax stems had an average length of 0.55 ± 0.15 m and an average diameter of 5.0 ± 0.3 mm. The flax single fibres were extracted manually using a pair of tongs, from the outer layer of the stem (Figure 3.2b), under a Leica DM LM optical microscope.

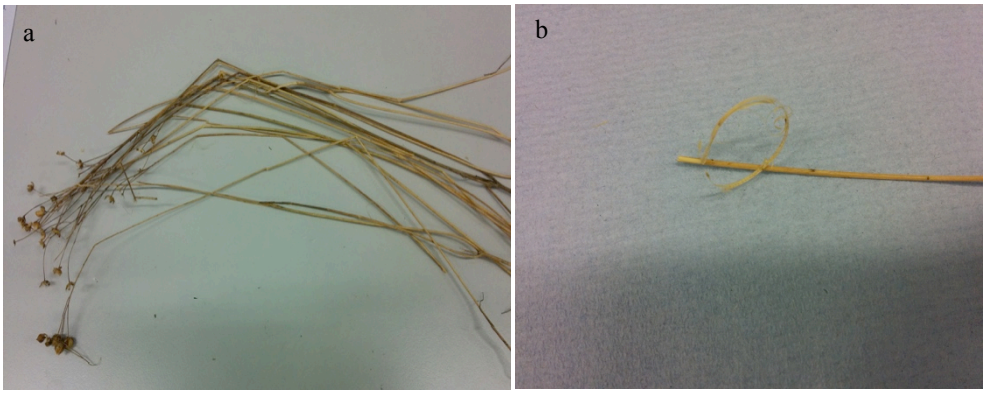

Figure 3.2 Flax stems a) Dry flax stems as harvested from farms in Sussex, b) outer layer of flax stem. The minimally processed flax single fibres are located within the outer layer of the stem and were carefully by hand extracted.

3.3.3 Minimally processed nettle fibres

The nettle plants were harvested from gardens and parks in Sheffield in April to September, 2015–2017. The length and diameter of nettle stems varied according to the harvest month and year. Nettle stems had an average length of 0.4 ± 0.2 m and an average diameter of 6 ± 2 mm during the early growing months (April–

June). From June to September, nettle plants were up to 1.5 ± 0.1 m in height and had a diameter of 20.0 ± 0.1 mm.

The average length and diameter of nettle plants related to the harvested period are summarised in Table 3.1. The diameter of nettle plants was measured and calculated as an average value along the stem length at the top, middle, and bottom.

Table 3.1 Average length and diameter of nettle stem according to the harvested periods. The length of nettle plants was measured with a tape and the diameter with an electronic micrometre. The measurement's uncertainty (±) was according to the instrument's accuracy.

Harvested period	Length (±0.1 m)	Diameter (±0.1 mm)
April-May	0.45	4.0 (top) 5.5 (middle) 7.0 (bottom)
June-July	0.75	6.5 (top) 9.0 (middle) 12.0 (bottom)
August-September	1.25	11 (top) 14.5 (middle) 17.5 (bottom)

3.3.4 Extraction process of minimally processed nettle fibres

The extraction process for minimally processed nettle fibres consisted of four main preparation steps. Throughout the extraction process, gloves were worn to avoid possible skin irritation.

1) Removal of the leaves from the nettle stem by a knife (the leaves were cut from the plant nodes, where the leaves were growing).

2) Following this, the stems were immersed in tap water to remove the stinging layer from the surface of the nettle stem (Figure 3.3a). The immersion period depended on the size of the stems. The stems were left in water for 7–10 days, changing the water regularly. At this point, the stems were soft enough that the stinging layer was easily removed by slightly rubbing the surface of the stem.

3) Subsequently, the clean stems were left to dry under atmospheric conditions at T=23 ± 2 °C and 50 ± 5% relative humidity (RH) for 10 days (Figure 3.3b). The stems were then ready for the fibre extraction process (Figure 3.3c).

4) To extract the minimally processed nettle fibres, firstly the stem's wooden core was removed by pressing the stem to split it in half. Secondly, the outer skin layer in which the fibres were embedded (similar to minimally processed flax fibres, Figure 3.2b) was gently pulled from the stalk.

Figure 3.3 Preparation and extraction process of minimally processed nettle single fibre including; a) the immersion of nettle stems without leaves in tap water, b) the removal of the stinging layer from the stems and stems' drying in atmospheric conditions (T= 23±2 °C and 50±5% RH), c) dried nettle stems ready for the fibre extraction. Nettle stems were placed under Leica DM LM optical microscope for better visibility.

3.3.5 Single fibre preparation process

Industrially and minimally processed flax and nettle fibres were prepared as single fibres prior to mechanical testing. Single fibres were glued on a cardholder, as illustrated in Figure 3.4. The cardholder was designed with CorelDraw software as a .cdr file. An Epilog 40W laser cutter was used to cut the cardholders on white cardstock. At the top and bottom part of the cardholder, three dots were printed in a straight line as a guideline for gluing the single fibre.

All the cardholders had identical dimensions (height of 1.9 cm, width of 1.5 cm) and the length of each single fibre attached on the cardholder was 5 mm. An ethyl-2-cyanoacrylate ('Super Glue') was used to glue the fibres onto the cardholder. The edges of the glued fibres (Figure 3.4, points a and b) were secured with two additional square cards to protect the fibres from potential damage caused by the clamps of the tensile tester machine.

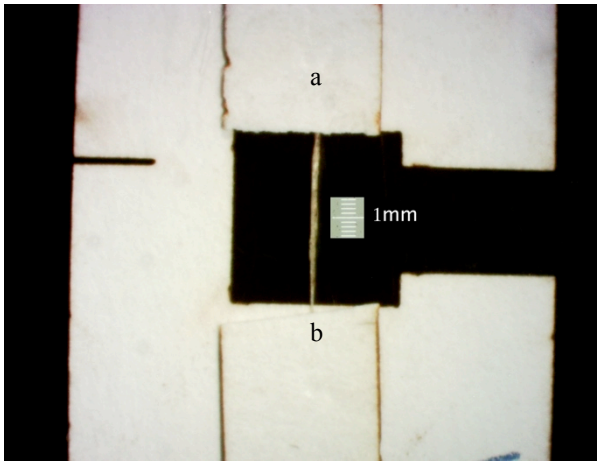

Figure 3.4 Flax single fibre attached on a handmade cardholder. The cardholder holds the fibres in a straight line and protects the fibre's edges from potential damage (points a and b) and helps to avoid incorrect measurements during the mechanical testing, such as higher tensile strain than the actual value. The picture was captured with a Leica DM LM optical microscope with 5x lens magnification using the micro-eyesee software[‡].

To obtain reliable and reproducible results from the mechanical tests, special emphasis was given to the single fibre's preparation procedure. The prepared single fibres were examined under a Leica DM LM optical microscope. The key points were to ensure that it was a single fibre, the fibre was attached in a straight line, and that the fibre gauge length was cleaned of glue.

3.3.6 Fibre storage

Particular attention was given to the storage of fibres to avoid as much as possible any caused dimension instability from moisture absorption (see chapter 2, section 2.2.6). After the preparation process, minimally and industrially processed fibres were oven dried at 100 ± 1 °C for 24 hours before their application in the composite manufacturing. At this point the moisture levels were much lower compared to the fibres stored under atmospheric conditions, although the exact moisture content was not measured (see detailed description in section 3.5.4).

3.4 Characterisation equipment and procedures

Firstly, the physical properties of industrially and minimally processed flax and nettle fibres were investigated, followed by the characterisation of their mechanical properties. An analysis of the techniques, equipment, and procedures used is described in the following sections.

[‡] https://www.dinolite.us/products/eyepiece-cameras/

3.4.1 Physical properties

3.4.1.1 Diameter and length

For flax and nettle yarns, the diameter and length were measured with an electronic digital micrometre with 0.001 mm accuracy. For the calculation of the mean value of the yarn's diameter and length, 50 individual flax and nettle yarns were measured respectively.

For a single fibre's diameter and length, a Leica DM LM optical microscope and a Jeol JSM-6010la analytical SEM were used, as shown in Figures 3.5-3.7 in accordance with BS ISO 11567: 1995 standards [271]. Before the measurements a microscope calibration slide with minimum division of 0.01 mm was used.

Images from different parts along the flax and nettle single fibre's length were captured and analysed with the use of ImageJ software. For the calculation of the mean value of the industrially and minimally processed flax and nettle single fibre diameters and lengths, 100 individual single fibres were tested. Each single fibre was measured once, with three measurements' along the fibre's length (top, middle and bottom part of the fibre), with the middle and bottom part having larger diameters compared to the top part.

The calculation of the fibre's diameter was a crucial parameter used for the determination of a fibre's cross-section area, which was later used for the tensile strength and Young's modulus calculations. The diameter of the fibres was also used for the fibre volume fraction measurement to determine the fibre/polymer content in the composite.

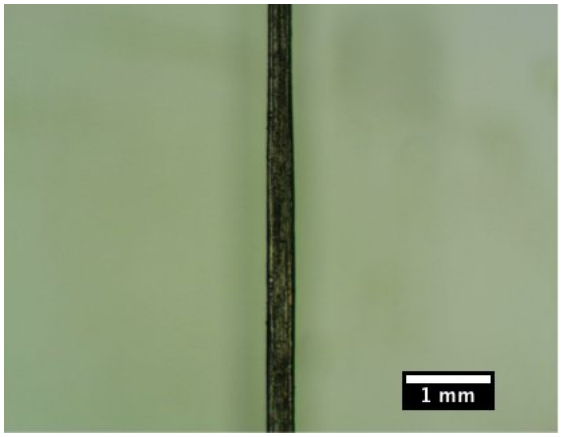

Figure 3.5 Minimally processed nettle single fibre under Leica DM LM optical microscope with 5x lens magnification. The fibre's diameter was calculated as a mean value of three measurements along the fibre's length. The scale bar was added during the analysis with ImageJ software.

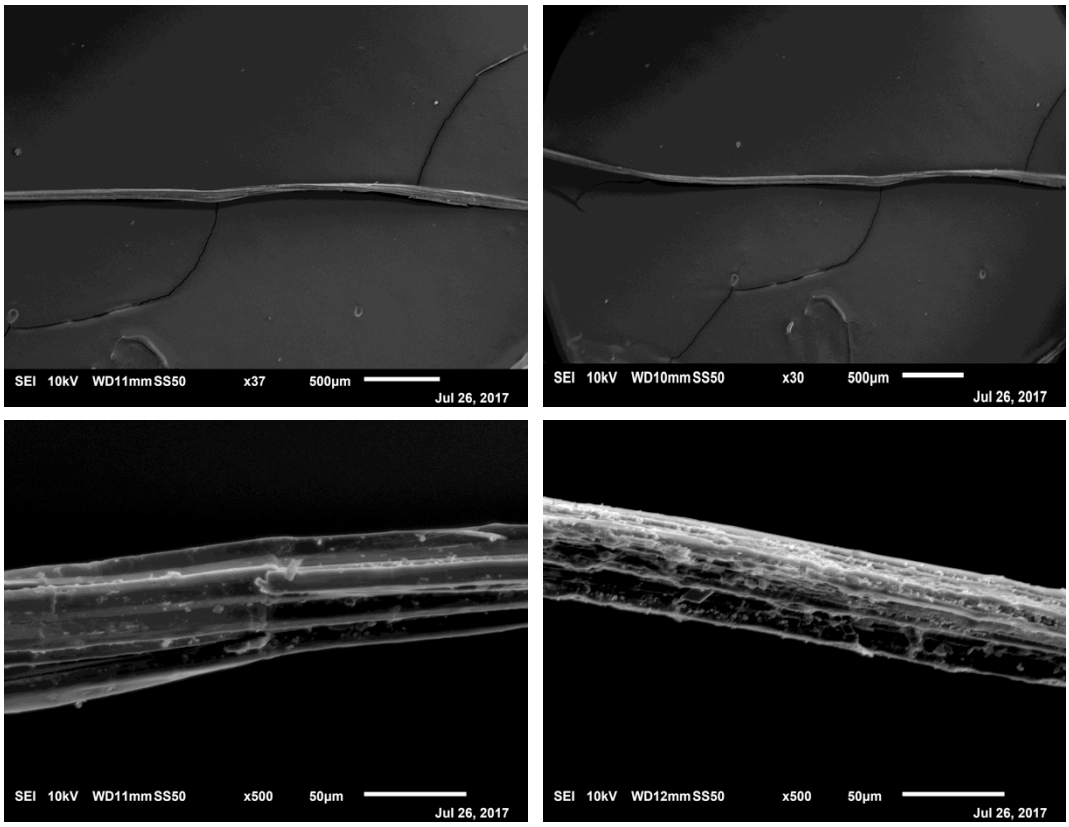

Figure 3.6 SEM micrograph of the diameter of minimally processed nettle fibres.

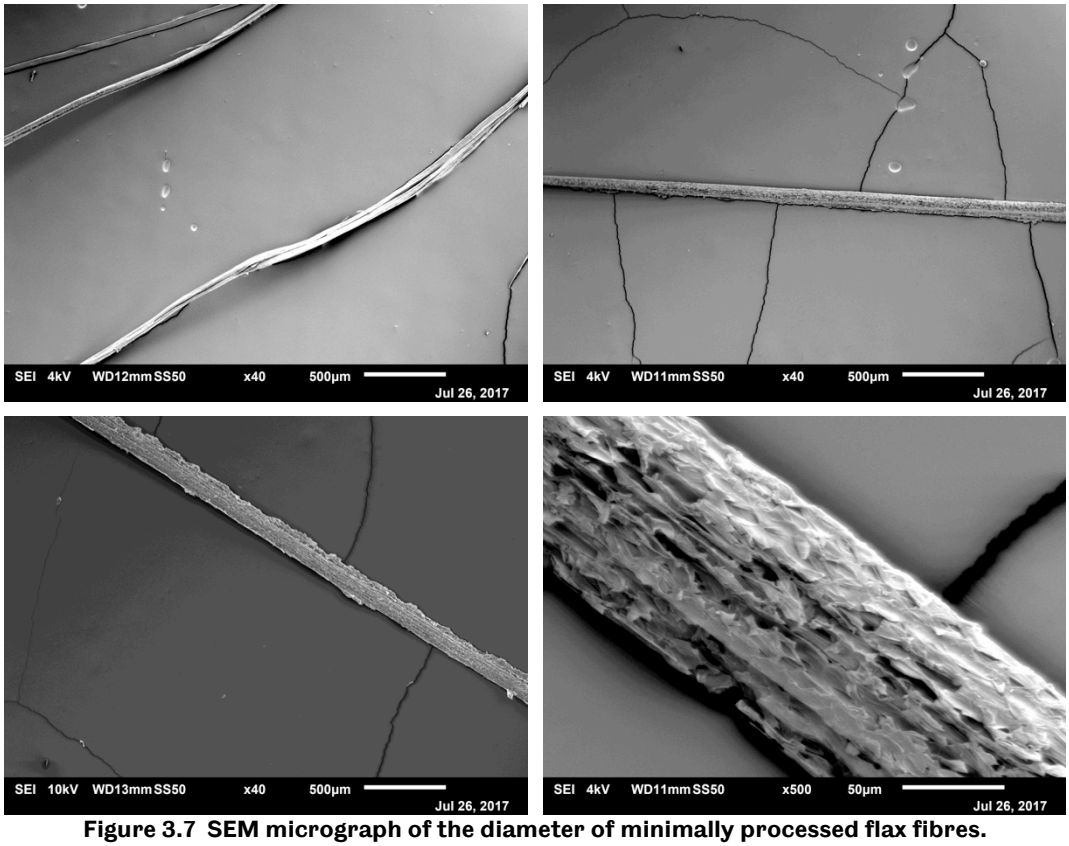

Figure 3.7 SEM micrograph of the diameter of minimally processed flax fibres.

3.4.1.2 Cross-section area

For the determination of flax and nettle fibre cross sections, single fibres and yarns were prepared according to ISO 7211-3:1984 and BS ISO 11567: 1995 standard methods [271], [272]. Flax and nettle yarns were placed within plastic PP tubes (1 mm diameter) and filled with glue. The prepared samples were left to dry for 24 hours in atmospheric conditions at T=23 $\pm$ 2 °C and 50 $\pm$ 5% RH and analysed under a Leica DM LM optical microscope. Figure 3.8a shows the prepared industrial flax yarn for the cross-section area calculation captured with the optical microscope with 5x lens magnification. To increase the results precision, fibres from different locations across the stem's length were selected and prepared.

The captured images of fibre were uploaded and analysed with ImageJ software, presented in Figure 3.8b-d. During the analyses the point of interest was coloured in a grey scale (Figure 3.8b) and unnecessary information was removed (Figure 3.8c). The point of interest was marked then with a yellow line, as seen in Figure 3.8d, and the cross-section area of the marked area calculated. The increased cross-section area precision of flax and nettle fibres led to more precise calculations of the tensile strength and Young's modulus of the fibres.

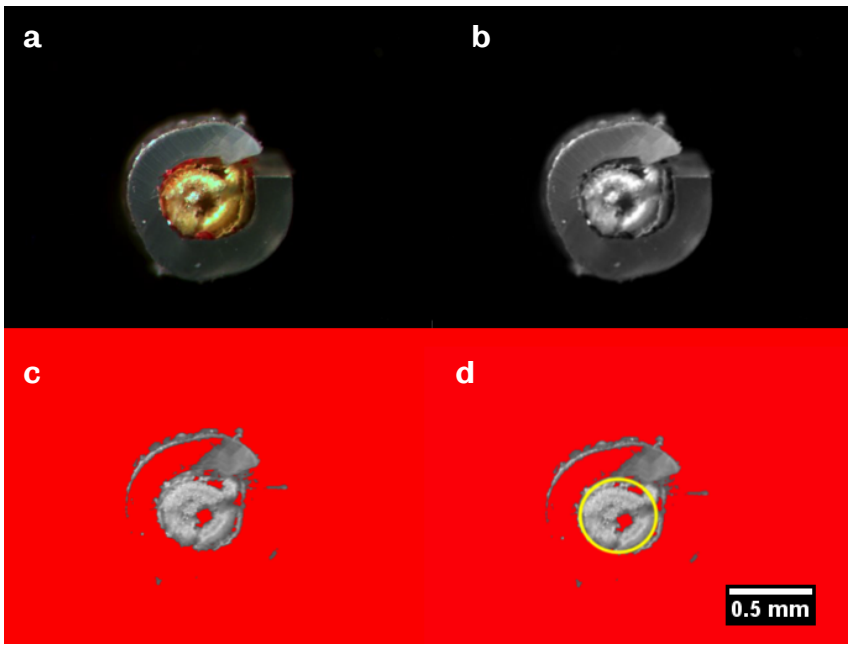

Figure 3.8 Flax yarns prepared for the cross-section area calculations. During the preparation, a) red dye was used to distinguish the yarn from the surrounding glue, b-d) cross-section area calculation steps through ImageJ software[§].

[§] https://imagej.net/ImageJ

According to the literature, the true cross-section area can be measured by the aspect ratio of fibres, based on a fitted ellipsoidal cross-sectional area between the major and the minor axis [273]. Aslan showed that the calculated cross-section area of flax fibres using the circular assumption was 39% higher as compared to the precise delimitation of the cross-sectional area [86].

3.4.2 Mechanical properties

Following the determination of the physical properties of the fibres, the mechanical properties of flax and nettle fibres were calculated. Yarns and single fibres were tensile tested and the results are presented in the following sections. Single fibres were tested for the evaluation of the mechanical properties at a micro scale level due to their non-uniform fibre structure.

The tensile tests of yarns and single fibres were performed under constant temperature and humidity at T= 23 $\pm$ 2 °C and 55 $\pm$ 5% RH, which were controlled by the laboratory environmental control system. All fibres were oven dried at 100 °C for 24 hours before the tensile testing (section 3.3.6). The drying conditions were selected based on the desorption tests of fibres (section 3.5.4). The moisture content of fibres at 55 % RH lever was between 5-6 % for flax and 6-7% for nettles (section 3.5.3).

3.4.2.1 Tensile test-yarns

The tensile test for industrial flax and nettle yarns was carried out using a TA500 tensile testing machine with load cell of 500 N and head speed of 1 mm/minute according ISO 6939:1988 standards, as shown in Figure 3.9 [274]. The fibre grips were designed in such a way that the tested fibres were wrapped around the grips and secured at the end.

Figure 3.9 Industrial flax yarn prepared for tensile test. The gauge length of each yarn was measured with an electronic digital micrometer between the testing grips.

3.4.2.2 Tensile test-single fibres

The tensile test of single industrial and minimally processed flax and nettle fibres was carried out using a Zwick Roell ZTN 0.5 tensile testing machine with load cell of 0.5 kN and head speed of 5 mm/minute in accordance with the BS ISO 11566: 1996 standard method [80]. Single fibres were attached on a cardholder (Figure 3.4), as described in section 3.3.5, with constant gauge length of 5 mm, as depicted in Figure 3.10. The square cards on the edge of the fibre (Figure 3.4) were used as end-tab materials preventing slippage of the fibres during the tensile test. Furthermore, two cameras with magnification of 3x and 10x were attached to the Zwick Roell ZTN 0.5 tensile tester for video recording during the tensile test. The recorded videos allowed visual verification of the point and time of the fibre failure.

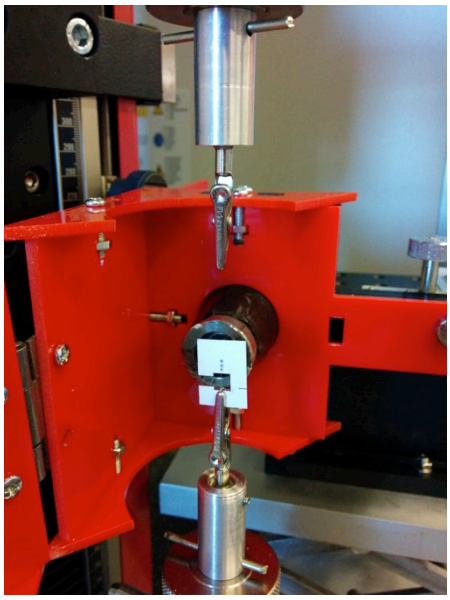

Figure 3.10 Minimally processed nettle single fibre prepared for tensile test.

During the tensile tests, values for the loading force and elongation of the tested fibre were recorded. The tensile stress of single fibre and yarns was calculated using Equation 3.1.

$$\sigma_f = \frac{F_f}{A_f} \qquad \textbf{Equation 3.1}$$

where,

σ_f is the tensile stress (MPa);

F_f is the maximum tensile force (N);

A_f is the cross-section area of fibre (mm^2).

The tensile strain of single and yarns was calculated using Equation 3.2.

$$\varepsilon_f = \frac{\Delta L_f}{L_f} \cdot 100 \qquad \textbf{Equation 3.2}$$

where,

ε_f is the tensile strain;

l_f is the fibre gauge length (mm);

Δl_f is the difference in the fibre gauge length between the initial and final fibre length after the tensile test (mm).

The gauge length between the testing grips of single fibre and yarns was measured before each measurement. The difference between the initial and the final length of single fibre and yarn was calculated from the corresponding software used during the tensile tests. The same approach was followed for all tested fibres for consistency in the measurements.

The Young's modulus of single fibre and yarns was calculated using Equation 3.3.The Young' modulus can be calculated from the slope of a stress-strain curve as shown in Figure 2.5.

$$E_f = \frac{\sigma_f}{\varepsilon_f} \qquad \textbf{Equation 3.3}$$

where,

E_f is Young's modulus (GPa);

σ_f is the tensile strength (MPa);

ε_f is the tensile strain.

3.4.3 Moisture absorption and desorption tests of flax and nettle fibres

Moisture absorption and desorption tests were conducted under different humidity conditions to investigate potential effects on the physical and mechanical properties of the fibres. The moisture absorption test followed the BS ISO 18457:2016 standard test methods [180]. Minimally and industrially processed flax and nettle fibres were placed in a humidity chamber with controlled humidity levels and exposed to 40%, 60%, and 80% RH levels for 24 hours. It was observed that the weight of the tested fibres after the first 40 minutes of exposure did not increase or decrease (equilibrium moisture content). The tests were held for up to 24 hours to detect possible alterations in the fibre structure. The temperature in the humidity chamber was set up at T= 25 $\pm$ 2 °C. Five fibres from each fibre type were tested at each RH level.

During the water desorption test, minimally and industrially processed flax and nettle fibres were oven dried at 40 °C, 60 °C, 80 °C, and 100 °C for 24 hours to determine the fibre weight loss. Five samples from each fibre type were tested in each drying temperature. Initially, the weight of each fibre was measured with a Semi-Micro Analytical Balance GR-200 with a 0.001 mg accuracy and the fibre's radius was measured with a Leica DM LM optical microscope. After exposure to different RH levels and oven drying, the flax and nettle fibres were tensile tested.

The percentage of weight increase or decrease due to moisture absorption and desorption test was calculated using Equation 3.4.

$$\Delta M(t) = \frac{m_2 - m_1}{m_1} \cdot 100\% \qquad \textbf{Equation 3.4}$$

where,

ΔM(t) is the percentage by mass of moisture absorption (%);

m_2 is the mass of fibres after the exposure to RH (mg);

m_1 is the initial mass of fibres (mg).

The difference in the radius of fibres was calculated using Equation 3.5.

$$\Delta R(\%) = \frac{R_f - R_i}{R_i} \cdot 100\% \qquad \textbf{Equation 3.5}$$

where,

ΔR is the increase in the fibre radius (%);

R_f is the fibre radius after the exposure to RH (μm);

R_i is the initial fibre radius (μm).

The residual mechanical properties were calculated using Equation 3.6.

$$\textbf{Residual mechanical property (\%)} = \frac{P_d}{P_i} \cdot 100\% \qquad \textbf{Equation 3.6}$$

where,

P_d is the tensile properties of fibres after the test;

P_i is the initial tensile properties of fibres.

3.4.4 Statistical analysis

The non-uniform structure of flax and nettle fibres and the large deviations in the physical and mechanical properties of fibres raised the question of how many fibres should be tested in order to deliver comprehensive, meaningful results.

To identify the required number of tests and to reduce the margin of error, analysis of variance (ANOVA) statistical test was used [275].

The total number of the tested fibres was calculated using Equation 3.7.

$$a = \frac{Z_{score} \bullet SD}{\sqrt{N}}$$ **Equation 3.7**

where,

Z_{score} depends on the selected confidence level and it is described as:

- Z_{score}= 1.645 with 90% confidence level;
- Z_{score}= 1.960 at 95% confidence level;
- Z_{score}= 2.576 at 99% confidence level.

SD is the standard deviation;

a is the margin of error;

N is sample size.

In most cases, the likelihood of a result being within the margin of error is at a 95% confidence level and thus this value was established. ANOVA, single factor tests were also performed for the evaluation of the statistical significance of the results as presented in the following chapters.

3.4.5 Surface morphology testing

To analyse the microstructure of fibres, a Jeol JSM-6010la analytical SEM was used to examine the surface and structure of industrially and minimally processed fibres. The fibres were placed on metal stubs with carbon tape and gold coated with an Agar Manual Sputter Coater, as shown in Figure 3.11a-b. The thin layer of gold turns fibres into conductive materials. Jeol JSM-6010la microscope set between 4–11 kV voltages depending on the quality of the pictures taken. For each fibre, SEM pictures were taken with different magnification starting at 50, 100, and 1,000x.

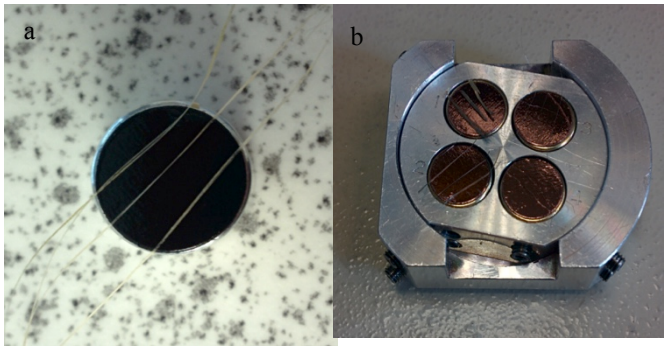

Figure 3.11 Surface morphology testing, a) minimally processed nettle single fibres on SEM stub b) gold coated flax and nettle fibres on SEM stubs.

3.4.6 Chemical structure of fibres

Fourier-transform infrared spectroscopy (FTIR) was used to determine any differences in the chemical structure of minimally and industrially processed flax and nettle fibres. A Nicolet 380 spectrometer (Thermo Scientific, Madison, USA) with an attached attenuated total reflection device (Golden Gate, 45° single-bounce diamond anvil, Specac, UK) was used to implement FTIR. Minimally and industrially processed flax and nettle fibres were placed on the reflector device and scanned between 500–4,000 cm^{-1} by 32 scans at 4 cm^{-1} resolution.

3.5 Results and discussion

3.5.1 Physical properties

3.5.1.1 Flax and nettle single fibres evaluation

Table 3.2 summarises flax and nettles single fibre physical properties. For the calculation of the fibre cross-section area, the assumptions of a uniform diameter along the fibre's length and a cylindrical shape of the fibre were adopted.

Table 3.2 Physical properties of flax and nettle single fibres. For the calculations of fibre's average diameter and cross-section area, 100 fibres from each fibre category were used based on the statistical analysis (section 3.4.4). The errors of the diameter, radius and cross-section area represent ±1SD (samples tested for every set of error bars n=25).

Fibres n=100	**Average Diameter (μm)**	**Average Radius (μm)**	**Average Cross-section area x10^{-3} (mm^2)**
Flax (I)*	52 ± 7	26 ± 4	2.13 ± 0.46
Flax (MP)	52.5 ± 10	26.2 ± 6	2.15 ±0.34
Nettle (I)	49 ± 5	24.5 ± 3	1.88 ±0.55
Nettle (MP)	60 ± 11	30 ± 6	2.80 ±0.28

* The notation (I) referred to the industrially processed fibres and (MP) to the minimally processed fibres.

It was observed that, in the case of MP flax and nettle fibres, the calculated diameter had a larger deviation compared to IF and IN fibres. The diameter of the extracted fibres was strongly connected to the total length and diameter of the source plant (section 3.3.3, Table 3.1). Thus, MP fibres extracted from the top part of stem had a smaller diameter, while the fibres extracted closer to the roots of the plant had larger diameters (Table 3.1).

3.5.1.2 Flax and nettle yarns evaluation

Table 3.3 summarises the length, diameter, radius, and cross-section area of flax and nettle fibre yarns. Only industrial fibres were tested due to the difficulty in extracting a continuous fibre from flax and nettle plant stems. It was observed that the industrial flax and nettle yarns had a more uniform shape with a cross-section area closer to a cylindrical shape. For the calculation of the yarn's diameter and length, 50 yarns were tested.

Table 3.3 Physical properties of IF and IN yarns. For the calculations of yarns', diameter and cross-section area, 50 fibres from each fibre category were used based on the statistical analysis (section 3.4.4). The same fibre yarns were further used for tensile testing. The errors represent ±1SD (samples tested for every set of error bars n=15).

Fibre yarns n=50	**Average Length ±0.5 (mm)**	**Average Diameter (mm)**	**Average Radius (mm)**	**Average Cross-section area (mm^2)**
Flax (I)	82.5	0.43 ± 0.06	0.21 ± 0.04	0.145 ± 0.010
Nettle (I)	80	0.47 ± 0.08	0.24 ± 0.06	0.175 ± 0.009

The cross-section area for both single fibre and yarns is related to the radius of each fibre and hence to the initial dimensions of the fibres. Based on this, the calculation is made separately for each fibre and cannot be compared with previous studies.

The diameter of flax and nettle fibres in the wider literature and in this study is presented within a range of results, due to the large deviations in plant diameter and length [276] Based on the literature, the average diameter of nettle and flax single fibres were 20 μm and 23 μm respectively [190].

3.5.2 Mechanical properties

3.5.2.1 Tensile test- yarns

Following the evaluation of physical properties, the tensile properties were evaluated and calculated according to Equations 3.1–3.3 for 50 yarns from each fibre category. During the tensile tests, the industrial flax and nettle yarns had a linear stress–strain relationship. The linear stress–strain relationship of IN and IF yarns was the result of an elastic deformation of fibres caused by the orientation of cellulose microfibrils during the tensile tests [137]. The highest reached point of stress (Figure 3.12, point a) was used as the tensile strength. Tensile strength

represents the resistance of yarns to the maximum stress at the time of failure. The linear part of the curve (slope) was used for the calculation of Yong's modulus. Figure 3.12 presents the average value of tensile stress over strain for a total of 50 IN and IF yarns.

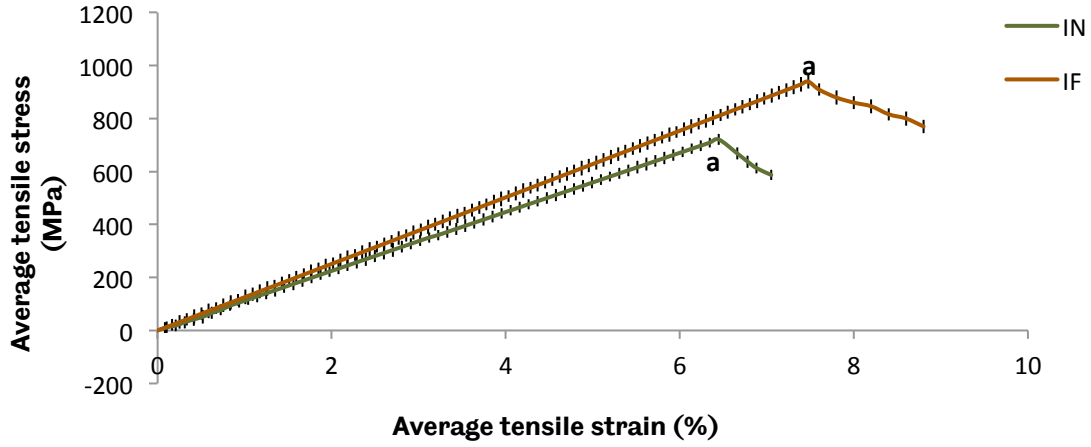

Figure 3.12 Stress-strain curves of 50 tested (based on the statistical analysis, section 3.4.4) IN and IF yarns. The curves present the average values of tensile stress up to the maximum stress values (tensile strength), from which Young's modulus was calculated.

Table 3.4 summarises the tensile properties of IF and IN yarns, with the highest tensile strength and Young's modulus observed in the case of IF yarns.

Table 3.4 Tensile properties of IF and IN yarns. The average tensile properties were calculated as the arithmetic mean, of 50 fibres from each fibre category. The errors represent ±1SD (samples tested for every set of error bars n=15).

Yarns n=50	Tensile strength (MPa)	Average Tensile strength (MPa)	Elongation at break (%)	Average Elongation at break (%)	Young's modulus (GPa)	Average Young's modulus (GPa)
Flax	601-1282	941±25	5-10	7.5±0.2	58-117	87±9
Nettle	457-968	713±23	4-9	6.5±0.2	67-109	88±8

The tensile properties are highly dependent on the diameter and therefore the cross-section area of the tested fibres. Due to variation in the measured diameter of fibres (Table 3.3), the tensile results also varied. Comparing the tensile properties of flax and nettle yarns with industrially fibre bundles as carbon a huge different is observed. Carbon fibre bundles have tensile strength up to 4.1 GPa and Young's modulus at 228 GPa. The high strength and stiffness of carbon fibres are due to it structure which is consisting of carbon atoms bonded together forming a long chain [277].

The tensile properties of flax and nettle yarns are presented within a range of results, covering the lowest and highest tensile strength and Young's modulus. Figure 3.13 shows the distribution (number of samples) of IF and IN yarns according to the tensile strength. As can be seen from Figure 3.13, the largest concentration of IF and IN yarns was between 600–800 MPa.

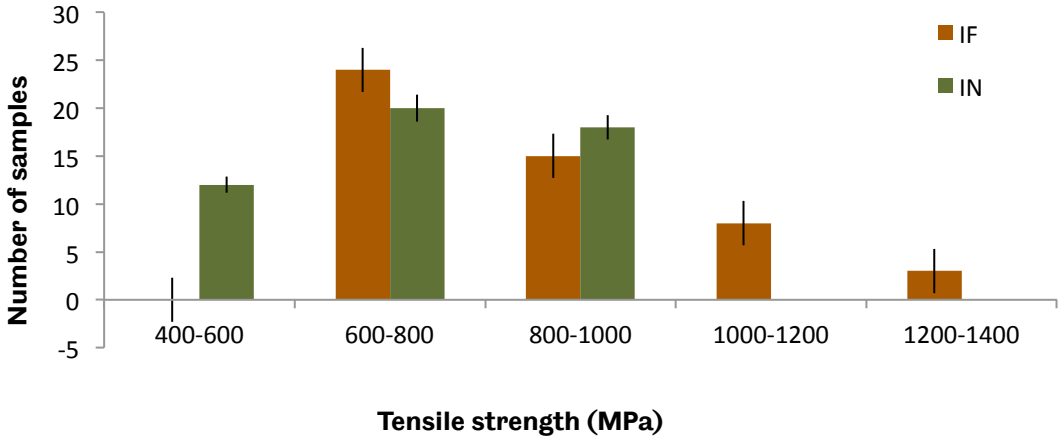

Figure 3.13 Tensile strength of IF and IN yarns for 50 tested fibres from each fibre category. The notation (IF) is referred to the use of industrial flax (solid brown bars) and (IN) to the corresponding nettle yarns (solid green bars).

3.5.2.2 Tensile test-single fibres

The tensile stress, strain, and Young's modulus results for minimally and industrially processed flax and nettle single fibres were calculated according to Equations 3.1–3.3 for 100 single fibres from each fibre category. Figure 3.14 shows the average tensile stress over strain for MPF, MPN, IF and IN single fibres. The tensile stress–strain curves for all tested single fibres show a linear stress–strain relationship until the point of failure. Young modulus's was calculated at the slope of the linear stress-strain part. The highest recorded value of stress (Figure 3.14, point a) for each fibre is the tensile strength, which is presented in Table 3.5

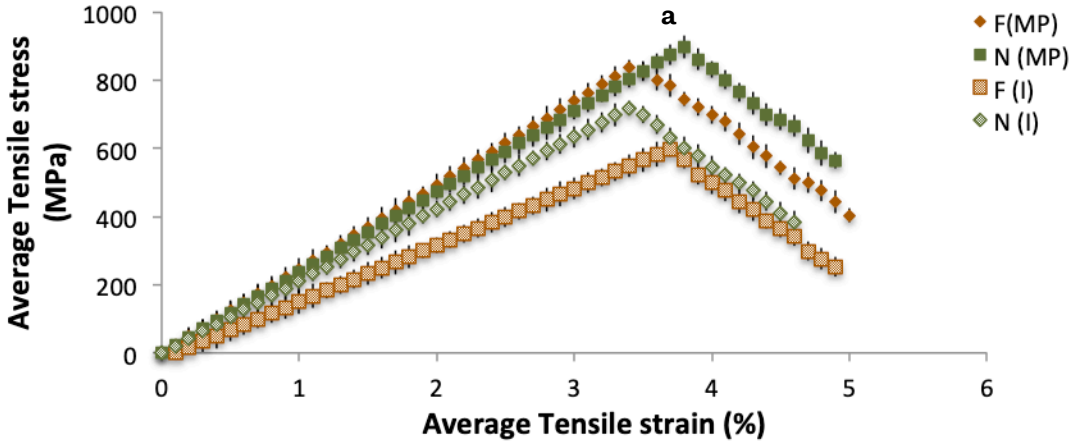

Figure 3.14 Tensile stress-strain curves of MPF, MPN, IF and IN single fibres for 100 fibres from each fibre type. The notation N (MP) and F (MP) are referred to the use of minimally processed nettle (green squares) and flax fibres (brown rhombus) respectively. The notation N (I) and F (I) are referred to the use of Industrially processed nettle (green dashed rhombus) and flax fibres (brown dashed squares) respectively. Point a presents the tensile strength. The error bars represent ±1SD (samples tested for every set of error bars n=25).

The tensile properties of single fibres from all fibre types and preparation processes were calculated and are presented in Table 3.5. The highest tensile strength results were observed in the case of MP fibres. MPN single fibres had a maximum reached tensile strength of 1415 ± 15 MPa, followed by MPF single fibre at 1294 ± 23 MPa. MP fibres had higher tensile stress, strength and Young modulus's values compared to the corresponding IN fibres. The higher obtained tensile properties of MP fibres indicated that the different extraction and preparation processes have an influence on the fibres' properties.

Table 3.5 Tensile properties of flax and nettle single fibres. The tensile properties are presented within a range of results covering the lowest and highest obtained values for 100 fibres from each fibre type. The average tensile properties were calculated as the arithmetic mean. The error bars represent ±1SD (samples tested for every set of error bars n=25).

Single fibres n=100	Tensile strength (MPa)	Average Tensile strength (MPa)	Elongation at break (%)	Average Elongation at break (%)	Young's modulus (GPa)	Average Young's modulus (GPa)
Flax(I)	329-869	599±37	2.2-5.0	3.6±0.2	11-34	22±2
Nettle(I)	301-1138	719±35	2.0-5.0	3.5±0.2	10-37	23±3
Flax(MP)	379-1294	837±31	1.9-5.0	3.4±0.3	14-36	25±4
Nettle (MP)	382-1415	898±33	3.0-4.7	3.8±0.2	10-47	28±3

Of great interest was the calculation and comparison of the tensile properties of the minimally processed flax and nettle fibres with the corresponding industrially processed fibres, to investigate whether and why there are differences. The tensile properties were reduced in the case of IF and IN fibres (Table 3.5), possibly because of the fibre processing procedure [62]. As described in chapter 2 (section 2.2.3), the fibres are processed into yarns by retting and spinning (Figure 3.1). Zeng *et al.* reported a reduction in the tensile properties of flax fibres due to different levels of retting, which is in agreement with the aforementioned results (Table 3.5) for the MPF and IF fibres [18]. In contrast, the MP fibres that were extracted by hand from the respective stems, avoiding any other preparation steps (section 3.3.4), had higher tensile strength and Young's modulus results.

Comparing the tensile properties of single and yarns it was observed that nettle and flax single fibres had lower Young modulus's results. Single fibres had lower tensile strength and strain values compare to the respective yarns. A possible explanation for the higher Young modulus' of yarns is the present of waxes added during the manufacturing process that enhanced the strength of flax and nettle yarns.

The tensile properties of flax and nettle fibres show a large deviation across different studies. Zafeiropoulos reported tensile strength between 650–2000 MPa and tensile strain of 2.5% for flax fibres [83]. Charlet *et al.* reported tensile strength of flax fibres between 400–1500 MPa and Young's modulus of 70 GPa [60]. In the case of nettle fibres, the average Young's modulus was up to 87 GPa, tensile strength was 1594 MPa, and tensile strain at failure up to 2.11% [270].

The Young's modulus of plant fibres is directly connected with the molecular structure of the plant. The secondary wall structure (chapter 2, Figure 2.5) provides high axial stiffness to the plant fibres. The microfibril angle and cellulose content influence the stiffness of the fibres in such a way the plants with higher cellulose contents have higher Young's modulus (stiffness) results [36], [37]. Flax and nettle fibres have approximately the same consecration in cellulose (chapter 2, Table 2.1) and thus the Young's modulus results are within the same range. The formation of voids in the fibre structure has a significant role in the reduction of the tensile stress and strength [85]. As it can be seen in the followed section (section 3.5.6, Figure 3.25) flax and nettle fibres include voids and this is an identification factor why the tensile strength from one fibre to another varies.

The results obtained from the tensile tests fall into the range of results reported from previous studies. The differences lie in the fact that the mechanical properties of fibres are affected mainly by the fibre preparation process and

chemical treatment and to a lesser degree by the country of origin of the plant. The results obtained from the physical and mechanical analysis of nettle and flax fibres have shown a clear species-based difference on the fibres' properties. Nettle fibres had higher tensile strength and Young's modulus results compared to flax fibres. It was found that the preparation process clearly effects the fibres' properties, with the MPN fibres displaying greater properties compared to the IN fibres. From the results obtained from the physical and mechanical analysis of flax and nettle fibres, nettle plants should be consider in the future as an additional source of fibres. The limitations of the time-consuming nettle fibre extraction process can be solved if mechanisms specially designed for fibre extraction processes are developed.

3.5.3 Statistical analysis

All tested single fibres have been statistically analysed to identify if there are statistically significant differences between the calculated tensile strength and Young's modulus. Table 3.6 shows between which comparisons there are statistically significant differences of the calculated tensile strength and Young's modulus for MPN, MPF, IN and IF single fibres.

Table 3.6 Statistical test for the identification of statistically significant difference. Anova-single factor tests was applied for the calculation of p-value for the tensile strength of MPN, MPF, IN and IF single fibres. P- values smaller than 0.005 (yellow highlighted) are presenting statistically significant differences between the tested fibres, while P-values higher than 0.005 (red highlighted) represent not statistically significant differences between the tested fibres.

P-values for tensile strength	**MPN**	**MPF**	**IN**	**IF**
MPN	-	-	-	-
MPF	5.03E-14	-	-	-
IN	4.12E-14	6.12E-14	-	-
IF	4.33E-14	7.02E-14	0.0057	-
P-values for Young's modulus	**MPN**	**MPF**	**IN**	**IF**
MPN	-	-	-	-
MPF	4.12E-13	-	-	-
IN	5.16E-13	4.74E-13	-	-
IF	6.23E-13	2.02E-13	0.0079	-

Based on the p-value calculations the difference between the tensile strength and Young's modulus of MPN and MPF fibres is statistically significant. Also the difference between the tensile strength and Young's modulus between the MPN and IN, MPF and IF single fibres are statistically significant. Unlikely, the tensile strength and Young's modulus results for IN and IF fibres are not statistically significant.

3.5.4 Moisture absorption tests

Industrial and minimally processed flax and nettle fibres were exposed at 40,60, and 80% RH levels for 24 hours respectively, to evaluate the effect of moisture absorption on flax and nettles fibres' physical and mechanical properties. 100% RH could not be achieved due to the inability of the used humidity chamber to reach values above 80%. The moisture absorption (weight increase) and changes in fibre radius were calculated using Equations 3.4 and 3.5. Figure 3.15 shows the moisture absorption (wt%) of MPF, MPN, IF, and IN fibres as a percentage against the different humidity levels. Since the fibres were not tested at 100% RH, it cannot be claimed that the fibres reached EMC. As Figure 3.15 shows, moisture absorption increased at higher levels of humidity, as expected.

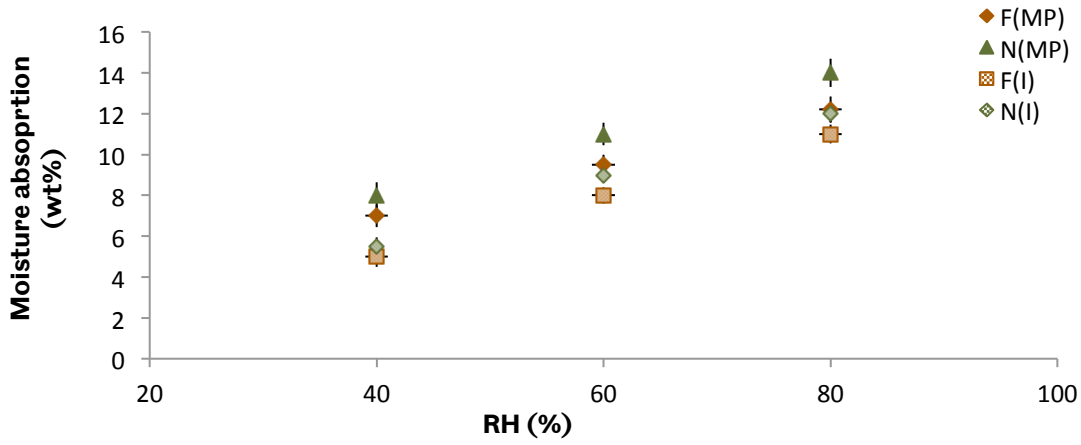

Figure 3.15 Moisture absorption of MPF, MPN, IF and IN fibres as a function of different humidity levels for 24 hours of exposure, for 5 fibres from each fibre type. The notation F(MP) is referred to the use of minimally processed flax fibres (brown rhombus) and N(MP) to the corresponding minimally processed nettle fibres (green triangles). The notation F(I) is referred to the use of industrial processed flax fibres (dashed brown squares) and N(I) to the corresponding industrial processed nettle fibres (dashed green rhombus) . The error bars represent ±1SD (samples tested for every set of error bars n=3).

It was observed that MP fibres had the highest levels of moisture absorption. MPN fibres absorbed 14 wt% of moisture, followed by MPF fibres at 12.2 wt% at 80% RH. Differences in the cellulose and hemicellulose content (Table 2.1) in nettle and flax fibres resulted in different moisture absorption rates [278]. From the aforementioned results, the industrially processed fibres had lower moisture absorption rates than the corresponding minimally processed fibres exposed to the same RH. Possible explanations may be the difference in the amount of physical voids included in the fibre structure, which can be either created by the different preparation processes or are included naturally in the structure of the plant. The

moisture absorption values reported in the literature for flax fibres vary from 7-8% and for ramie fibres between 12–17%, which are in agreement with the values calculated in the present project [148].

During the moisture absorption test, an increase in the fibre's weight was observed. Minimally processed and industrial flax and nettle fibres were weighted every 2 minutes until the end of the experiments. Fibre's weight was increased up to the first 40 minutes of the experiments. From that point onwards, the absorbed moisture remained sTable, as can be seen in Figure 3.16.

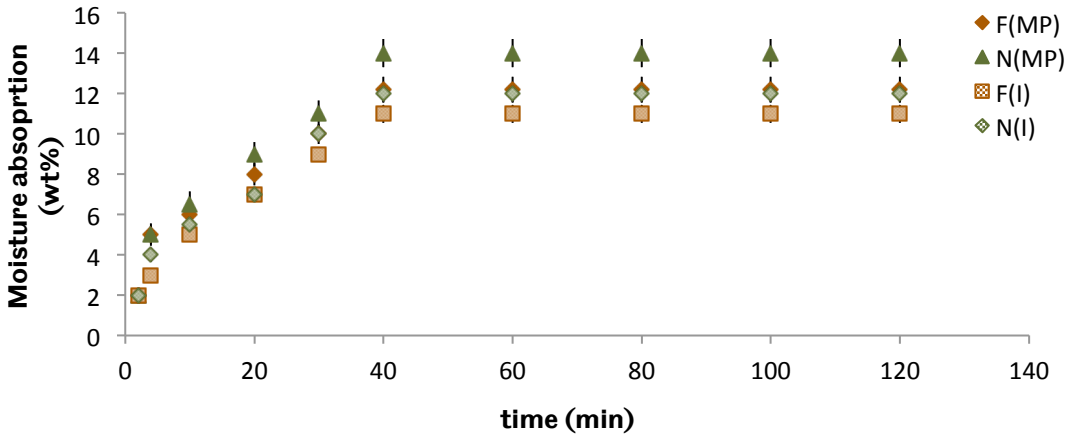

Figure 3.16 Moisture absorption as a function of exposure time of MPF, MPN, IF, and IN fibres at 80%RH, for 5 fibres from each fibre type. The notation F(MP) is referred to the use of minimally processed flax fibres (brown rhombus) and N(MP) to the corresponding minimally processed nettle fibres (green triangles). The notation F(I) is referred to the use of industrial processed flax fibres (dashed brown squares) and N(I) to the corresponding industrial processed nettle fibres (dashed green rhombus). The error bars represent ±1SD (samples tested for every set of error bars n=3).

Moisture absorption caused dimensional instability by increasing the fibre radius, as shown in Figure 3.17. MPN fibres had the larger increase in radius, by 92% at 80% RH, followed by MPF fibres at 77%. Similarly, with the lower moisture absorption rates, industrially processed fibres also had smaller increases in their radius, as can be seen in Figure 3.17.

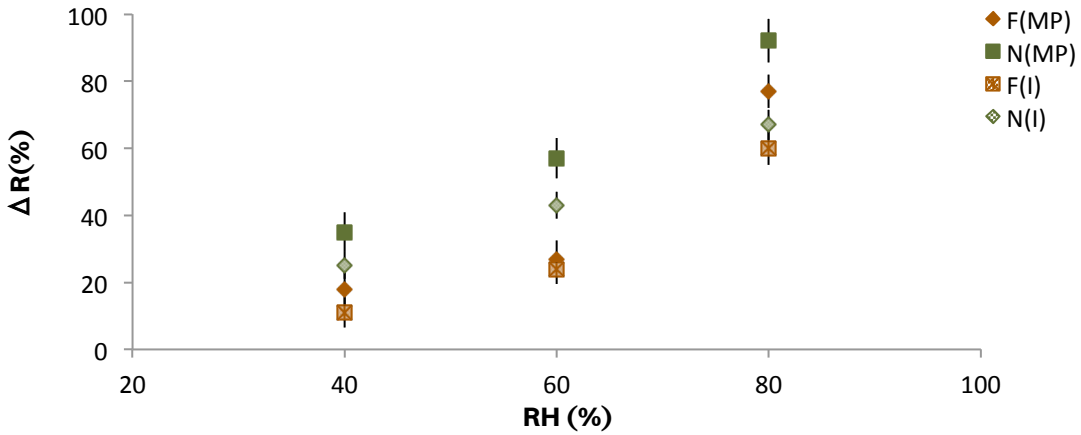

Figure 3.17 Increase in the radius of MPF, MPN, IF, and IN fibres as a function of different humidity levels for 24 hours of exposure, for 5 fibres from each fibre type. The notation F(MP) is referred to the use of minimally processed flax fibres (brown rhombus) and N(MP) to the corresponding minimally processed nettle fibres (green triangles). The notation F(I) is referred to the use of industrial processed flax fibres (dashed brown squares) and N(I) to the corresponding industrial processed nettle fibres (dashed green rhombus) .The error bars represent ±1SD (samples tested for every set of error bars n=3).

From the moisture absorption tests, differences in the physical properties of the fibres were observed. The question arises as to whether the mechanical properties of the fibres have been affected. The effect of moisture absorption on the tensile properties of fibres will be described in the following section. The water desorption tests followed in section 3.5.5.

3.5.4.1 Mechanical properties

The tensile strength results of fibres exposed to different humidity conditions illustrated a tensile strength reduction at higher RH. The reductions in the tensile strength results were affected by the humidity level and by the fibre type and preparation process. Figure 3.18 presents the average tensile strength of all tested fibres against different humidity levels. Figure 3.19 displays the percent reduction in the tensile strength.

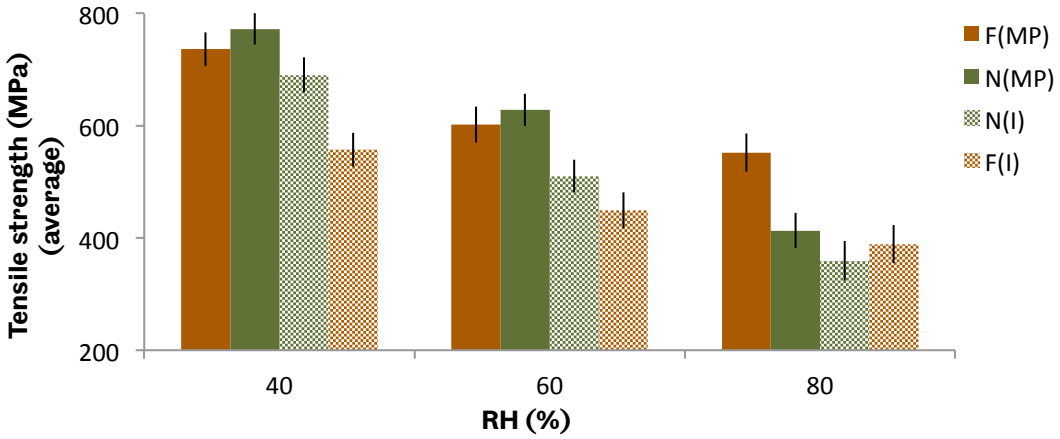

Figure 3.18 Tensile strength of MPF, MPN, IF, and IN as a function of different humidity levels for 24 hours of exposure, for 5 fibres from each fibre type. The notation F(MP) is referred to the use of minimally processed flax fibres (solid brown bars) and N(MP) to the corresponding minimally processed nettle fibres (solid green bars). The notation F(I) is referred to the use of industrial processed flax fibres (dashed brown bars) and N(I) to the corresponding industrial processed nettle fibres (dashed green bars). The error bars represent ±1SD (samples tested for every set of error bars n=3).

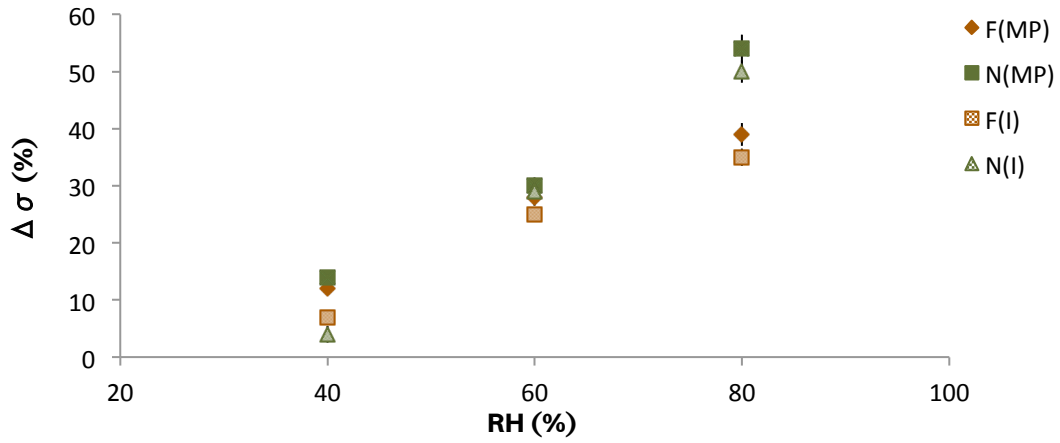

Figure 3.19 Reduction in the tensile strength of MPF, MPN, IF, and IN as a function of different humidity levels for 24 hours of exposure, for 5 fibres from each fibre type. The notation F(MP) is referred to the use of minimally processed flax fibres (brown rhombus) and N(MP) to the corresponding minimally processed nettle fibres (green triangles). The notation F(I) is referred to the use of industrial processed flax fibres (dashed brown squares) and N(I) to the corresponding industrial processed nettle fibres (dashed green rhombus). The error bars represent ±1SD (samples tested for every set of error bars n=3).

The decrease in tensile strength was related to the percentage of absorbed moisture. Fibres with the highest moisture absorption rates had the greatest

tensile strength reduction. Thus, MPN fibres had the highest tensile strength reduction, 54% at 80% RH. Table 3.7 summarises the amount of moisture absorption and the changes in fibre weight and radius for 40–80% RH.

Table 3.7 Influence of moisture absorption on fibres' physical and mechanical properties. The fibre's weight, radius and tensile strength were calculated as the arithmetic mean for 5 fibres from each fibre type, tested at each RH. The notation F(MP) is referred to the use of minimally processed flax fibres and N(MP) to the corresponding minimally processed nettle fibres. The notation F(I) is referred to the use of industrial processed flax fibres and N(I) to the corresponding industrial processed nettle fibres. The errors represent ±1SD (samples tested for every set of error bars n=3).

Single fibres n=5	**RH (%)**	**ΔW (%)**	**ΔR (%)**	**Δσ (%)**
Flax (I)	80	11±0.2	60±9	35±2
	60	8±0.1	24±8	25±2
	40	5±0.1	11±6	7±1
Nettle (I)	80	12±0.3	67±7	50±3
	60	9±0.2	43±6	29±2
	40	5.5±0.1	25±6	4±2
Flax (MP)	80	12.2±0.5	77±7	39±3
	60	9.5±0.5	27±7	28±2
	40	7±0.2	18±6	12±2
Nettle (MP)	80	14±0.6	92±9	54±3
	60	11±0.5	57±8	30±2
	40	8±0.3	35±8	14±2

Moisture affects the cellulosic fibres because of their chemical composition and structure [148]. Due to variations in cellulose, hemicellulose, and hydroxyl groups, the level of moisture absorption of plant fibres varies between 7–12 wt% for the most common bast fibres (i.e., flax, hemp, jute) and up to 25% for cotton fibres, according to the literature [279]. As it has been described in chapter 2 (section 2.2.7), each hydroxyl included in the molecular chain of the ligno-cellulosic fibres is joined with the molecules of water and in its attempted to carry more water molecules it expands and swelled [100]. According to the country of origin of the plant (such as climate, geographic location), which affects both the physical and mechanical properties of the fibres extracted, different amount of moisture absorption are reported. The moisture absorption of flax fibres was reported at 7% and for nettle fibres, between 12–17% [280]. The moisture absorption of the

nettle fibres was within the reference values from the literature, at 14%, as opposed to the moisture absorption of flax fibres, which were higher at 12% at 80% RH.

The reduction in the mechanical properties of the fibres was mainly due to the changes in the fibres' radius. A similar study from Davies and Bruce reported a reduction in the Young's modulus of flax and nettle fibres exposed to 30–70% RH [281].

3.5.5 Water desorption test

Industrial and minimally processed flax and nettle fibres were dried at 40, 60, 80 and 100 °C for 24 hours respectively. The fibres were previously placed in laboratory atmospheric conditions (T=23 ± 2 °C and 55 ± 5% RH). The amount of water lost was calculated based on the reduction in the fibre weight using Equation 3.5, presented in Figure 3.20. The fibres exposed to different drying temperatures were evaluated in terms of their physical properties for possible changes in the fibre radius. The difference in fibre radius was calculated using Equation 3.6.

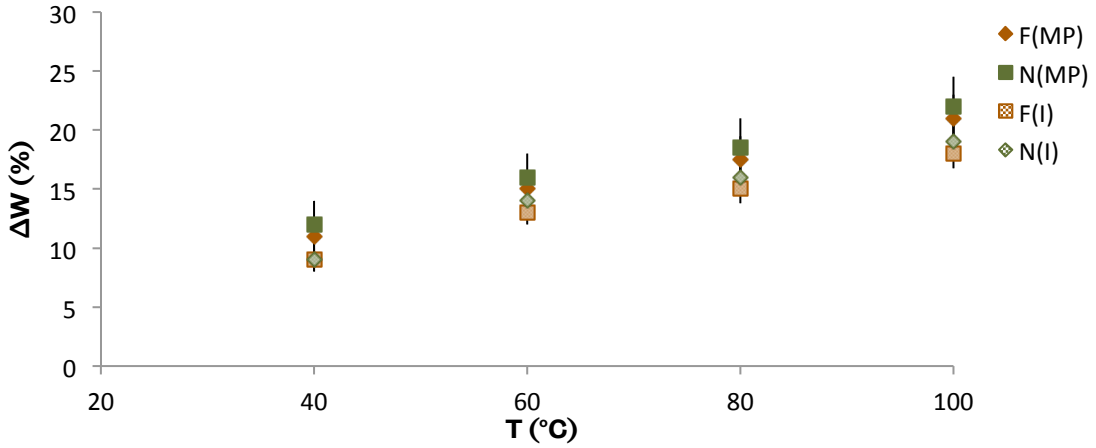

Figure 3.20 Weight loss of MPF, MPN, IF, and IN as a function of different drying temperatures for 24 hours of exposure, for 5 fibres from each fibre type. The notation F(MP) is referred to the use of minimally processed flax fibres (brown rhombus) and N(MP) to the corresponding minimally processed nettle fibres (green triangles). The notation F(I) is referred to the use of industrial processed flax fibres (dashed brown squares) and N(I) to the corresponding industrial processed nettle fibres (dashed green rhombus). The error bars represent ±1SD (samples tested for every set of error bars n=3).

Contrary to the results from moisture absorption tests (section 3.5.3), fibres exposed at different temperatures showed a decrease in their weight due to the desorption of water. The highest reduction of the fibre weight was observed at 100

°C for all types of fibres, with the highest reduction in the case of MP fibres. MPN and MPF fibres had a weight reduction of 22% and 21% at 100 °C, respectively.

The high temperatures caused changes not only in the fibre weight but also in the fibre radius. Using a Leica DM LM optical microscope, it was observed that the radius of fibres decreased as the drying temperature increased. Figure 3.21 shows the radius reduction of the different types of fibres according to the drying temperatures. The highest reduction was observed in the case of MPN and MPF fibres, by 35% and 34% at 100 °C respectively, as a consequence from the highest moisture absorption.

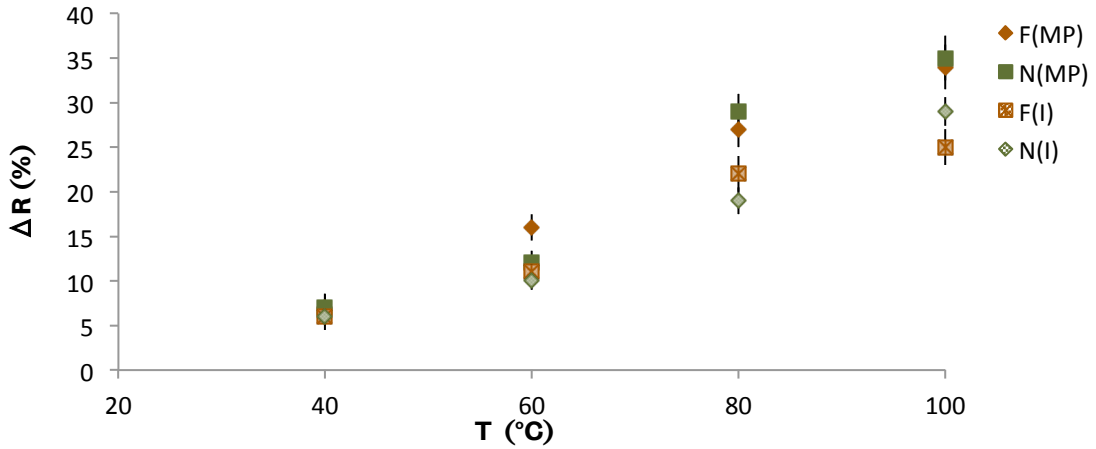

Figure 3.21 Decrease in the radius of MPF, MPN, IF and IN fibres as a function of different drying temperatures for 24 hours of exposure, for 5 fibres from each fibre type The notation F(MP) is referred to the use of minimally processed flax fibres (brown rhombus) and N(MP) to the corresponding minimally processed nettle fibres (green triangles). The notation F(I) is referred to the use of industrial processed flax fibres (dashed brown squares) and N(I) to the corresponding industrial processed nettle fibres (dashed green rhombus). The error bars represent ±1SD (samples tested for every set of error bars n=3).

The moisture content of fibres, below the fibre saturation point is a function of both relative humidity and temperature of surrounding air [104]. The equilibrium moisture content (EMC) of plant fibres was calculated at the point where the fibres were neither gaining nor losing moisture [282]. The EMC for minimally processed flax and nettle fibres, and for the industrially processed flax and nettle fibres was calculated at 40, 60 80 and 100°C as it can be seen in Figure 3.22.

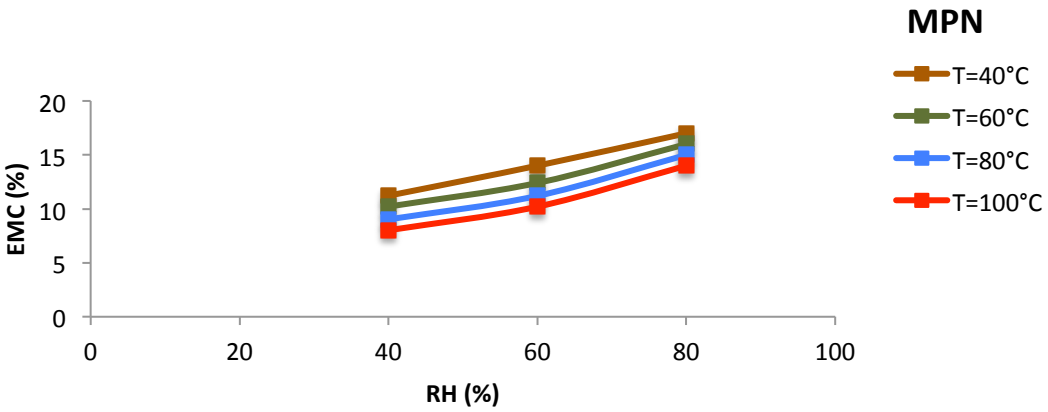
MPN
T=40°C
T=60°C
T=80°C
T=100°C
EMC (%)
RH (%)
0
5
10
15
20
0
20
40
60
80
100

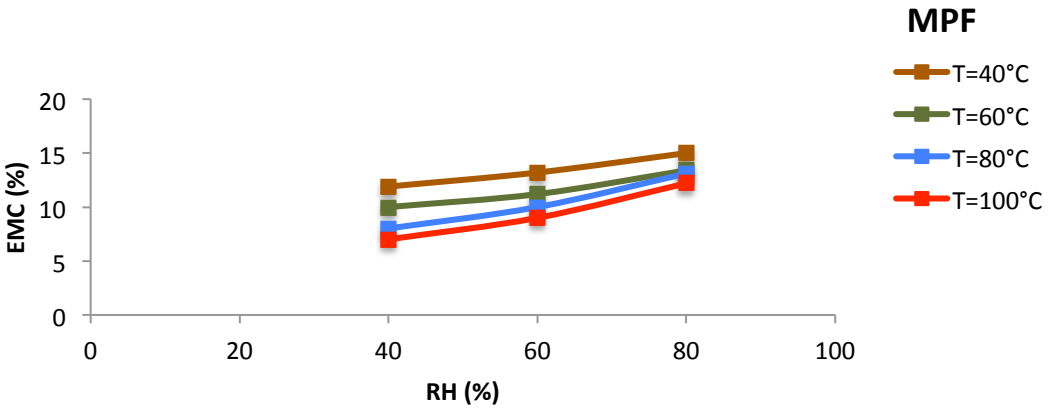
MPF
T=40°C
T=60°C
T=80°C
T=100°C
EMC (%)
RH (%)
0
5
10
15
20
0
20
40
60
80
100

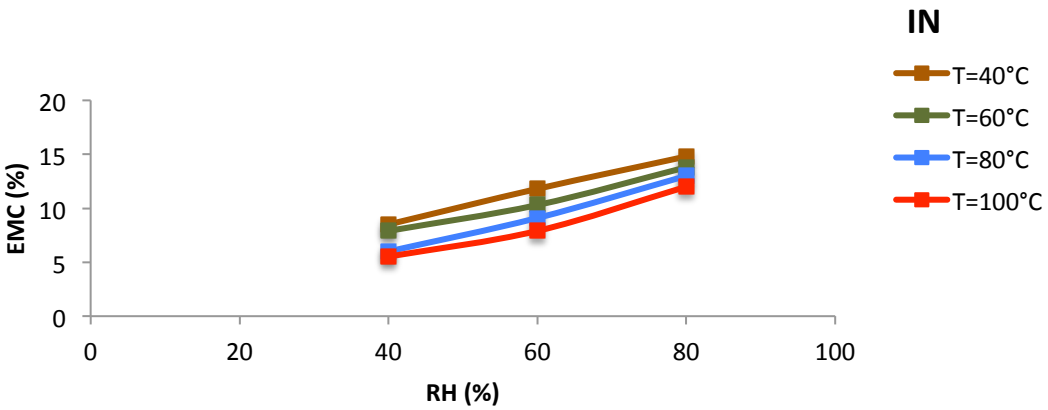
IN
T=40°C
T=60°C
T=80°C
T=100°C
EMC (%)
RH (%)
0
5
10
15
20
0
20
40
60
80
100

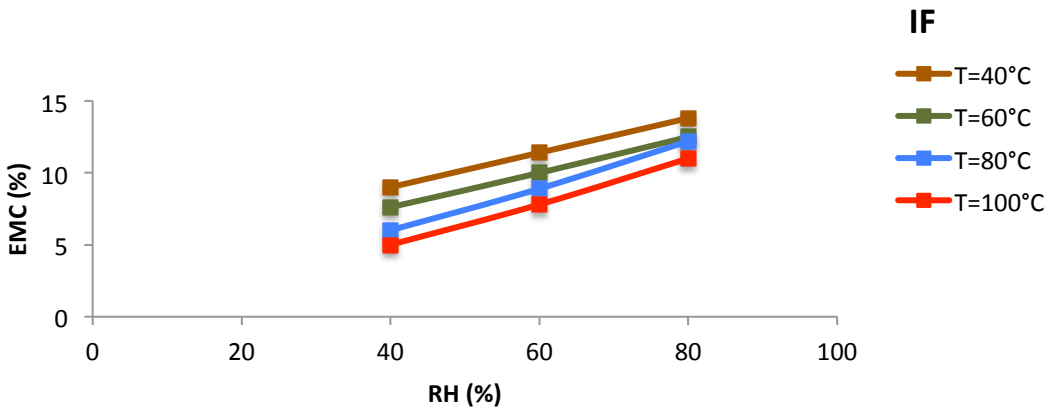

Figure 3.22 Moisture equilibrium content of MPN, MPF, IN and IF fibres at different relative humidity levels and temperatures.

In all fibre types, EMC was lower as the temperature increases. The lowest EMC was at 100°C and the highest at 40°C. The higher temperature and lower relative humidity level has as a results the lower EMC for fibres. The moisture contents increased from the lowest to the highest relative humidity. Minimally processed fibres had higher EMC levels compared to the respective industrial process fibres.

3.5.5.1 Mechanical properties

Due to changes observed in the physical properties of the fibres, the mechanical properties were examined for any changes after the water desorption tests. The tensile strength results increased as the drying temperature increased. The increase of the tensile strength was dependent on the drying temperature and the fibre type, as illustrated in Figure 3.23. Figure 3.24 shows the per cent increase in the tensile strength against the different drying temperatures. The highest increase in the tensile strength was observed in MPN fibres, at 33%, followed by MPF fibres at 26% at 100 °C. Table 3.8 summarises the changes in fibre weight, radius, and tensile strength results at drying temperatures between 40–100 °C.

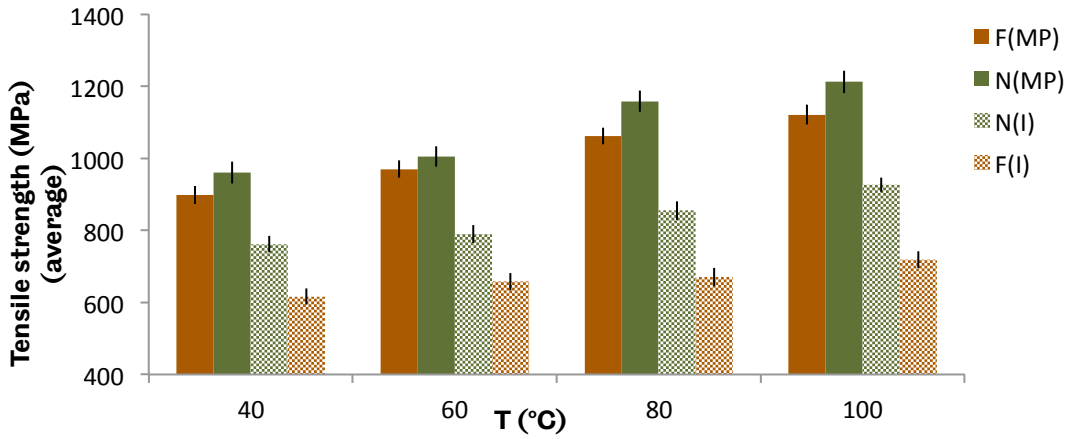

Figure 3.23 Tensile strength of MPF, MPN, IN and IF and fibres as a function of different drying temperatures, for 5 fibres from each fibre type. The notation F(MP) is referred to the use of minimally processed flax fibres (solid brown bars) and N(MP) to the corresponding minimally processed nettle fibres (solid green bars). The notation F(I) is referred to the use of industrial processed flax fibres (dashed brown bars) and N(I) to the corresponding industrial processed nettle fibres (dashed green bars). The error bars represent ±1SD (samples tested for every set of error bars n=3).

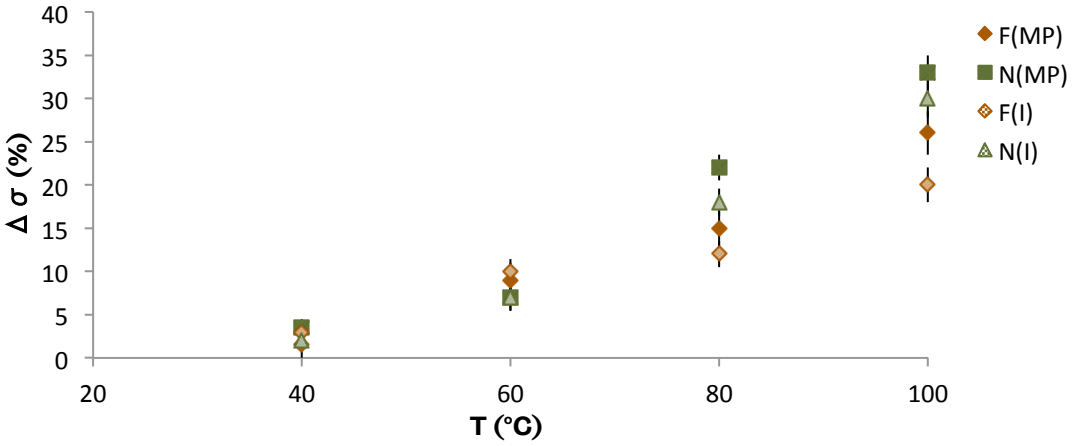

Figure 3.24 Tensile strength increase of MPF, MPN, IF and IN fibres as a function of different drying temperatures, for 5 fibres from each fibre type. The notation F(MP) is referred to the use of minimally processed flax fibres (brown rhombus) and N(MP) to the corresponding minimally processed nettle fibres (green triangles). The notation F(I) is referred to the use of industrial processed flax fibres (dashed brown squares) and N(I) to the corresponding industrial processed nettle fibres (dashed green rhombus). The error bars represent ±1SD (samples tested for every set of error bars n=3).

Table 3.8 Influence of drying temperatures on fibres' physical and mechanical properties. The fibre's weight, radius and tensile strength were calculated as the arithmetic mean, for 5 fibres from each fibre type, tested at each drying temperature. The notation F(MP) is referred to the use of minimally processed flax fibres and N(MP) to the corresponding minimally processed nettle fibres. The notation F(I) is referred to the use of industrial processed flax fibres and N(I) to the corresponding industrial processed nettle fibres. The error bars represent ±1SD (samples tested for every set of error bars n=3).

Single fibres n=5	**T (°C)**	**ΔW (%)**	**ΔR (%)**	**Δσ (%)**
Flax (I)	100	18±3	25±3	20±4
	80	15±2	22±2	12±3
	60	13±2	11±1	10±2
	40	9±2	6±1	3±1
Nettle (I)	100	19±3	29±2	30±3
	80	16±2	19±2	18±2
	60	14±2	10±1	7±1
	40	9±2	6±1	2±1
Flax (MP)	100	21±3	34±3	26±2
	80	17.5±3	27±2	15±2
	60	15±2	16±2	9±1
	40	11±2	7±1	1.5±0.6
Nettle (MP)	100	22±4	35±4	33±3
	80	18.5±4	29±3	22±2
	60	16±3	12±2	7±1
	40	12±3	7±1	3.5±1

In the moisture absorption tests, the weight and radius of fibres increased, causing a decrease in the fibres' mechanical properties (with the greatest decrease at 80% RH). Contrariwise, fibres exposed to different drying temperatures had improved mechanical properties as their weight and the radius decreased. The greatest increase in tensile strength was observed at 100 °C, where the water contained in the fibres was completely evaporated.

The moisture absorption and desorption experiments were conducted to determine the effect of humidity conditions on the physical and mechanical properties of the fibres. The ability of cellulose, hemicellulose, pectin and lignin to establish hydrogen bonds with the water molecules caused the dimension

instability (increase in weight and radius) of flax and nettle fibres. Additionally, plant fibres as porous materials can store water inside the free volume of their structure increasing rapidly their weight [148]. During the desorption tests, flax and nettle fibre's weight and radius were dramatically decreased due to water evaporation which led to shrinkage. Water desorption tests were also used as an indication of proper storage of fibres to prevent any alterations in the physical and mechanical properties of the fibres.

3.5.6 Surface morphology

The wider literature reported that the microstructure of fibre is highly connected to the mechanical properties of fibres [85], [144], [165]. The concentration of damage (voids) inside the fibre's structure is one of the main factors that reduce mechanical properties. For this reason, a Jeol JSM-6010la analytical SEM was used for a qualitative observation of the structure of industrial and minimally processed flax and nettle fibres. Figure 3.25 shows the appearance of voids inside flax and nettle fibres.

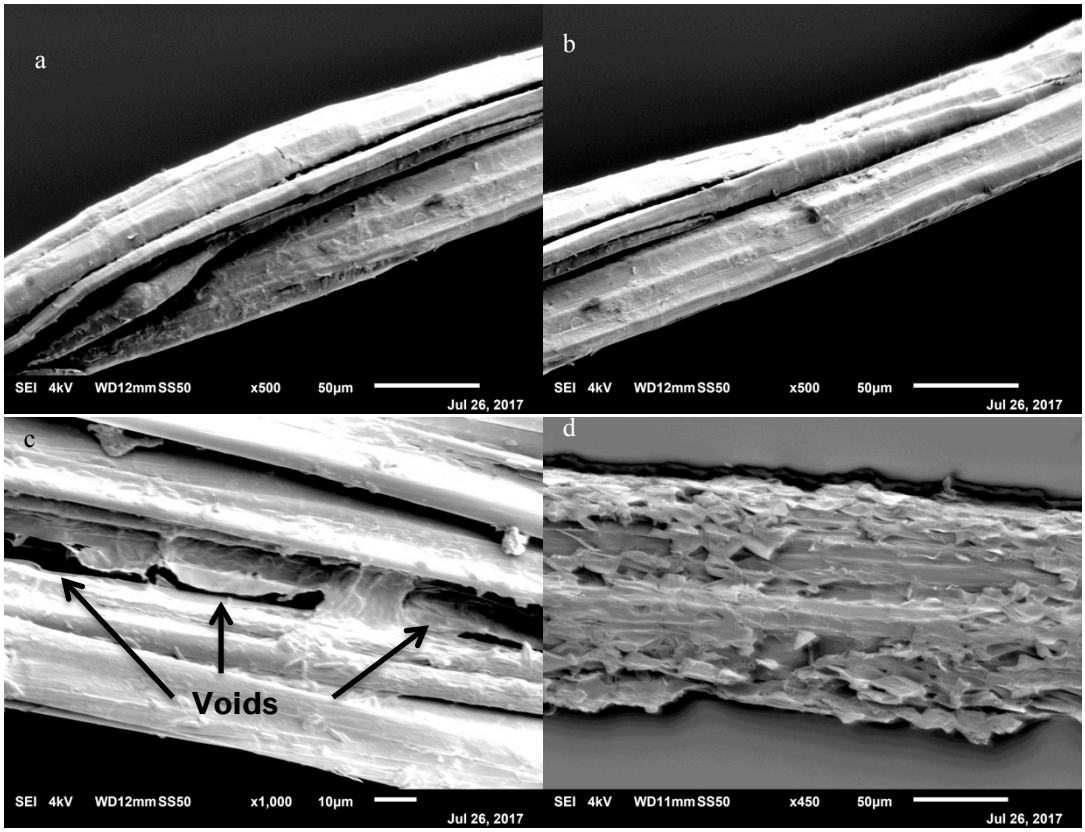

Figure 3.25 SEM micrographs of a) MPN b) MPF, c) IN and d) IF fibre. The magnification was changed to have better visibility on the voids.

It has been reported that the amount and size of voids in the fibre's structure affects the fibre tensile properties and the amount of absorbed moisture [77], [85]. According to the literature, there is a correlation between the amount of voids and the mechanical properties of fibres, with fibres with a lower number of voids presenting higher mechanical properties [77].

In this study, it is speculated that the formation of voids in the industrially processed flax and nettle fibres are increased, due to the fibre preparation method (i.e., retting) while the lower concentration of voids in the minimally processed fibres are only due to the natural structure of plant stems.

3.5.7 Chemical structure

The chemical structure of fibres was reported in the previous sections. To evaluate the difference in the chemical composition of the industrial and flax and nettle fibre, a Nicolet 380 spectrometer was used. From the spectra collected, a similar peak appearance was observed for the IN, IF, MPN, and MPF fibres. MPF fibres had peaks in different wavelengths, indicating a different chemical composition compared to MPN fibres, as seen in Figure 3.26. For the determination of the amount of cellulose, hemicellulose and lignin, wet chemistry analytical methods can be used. The Van Soest method, gravimetric (weighing) and volumetric analysis (measuring) are some quantitative wet chemistry techniques [283].

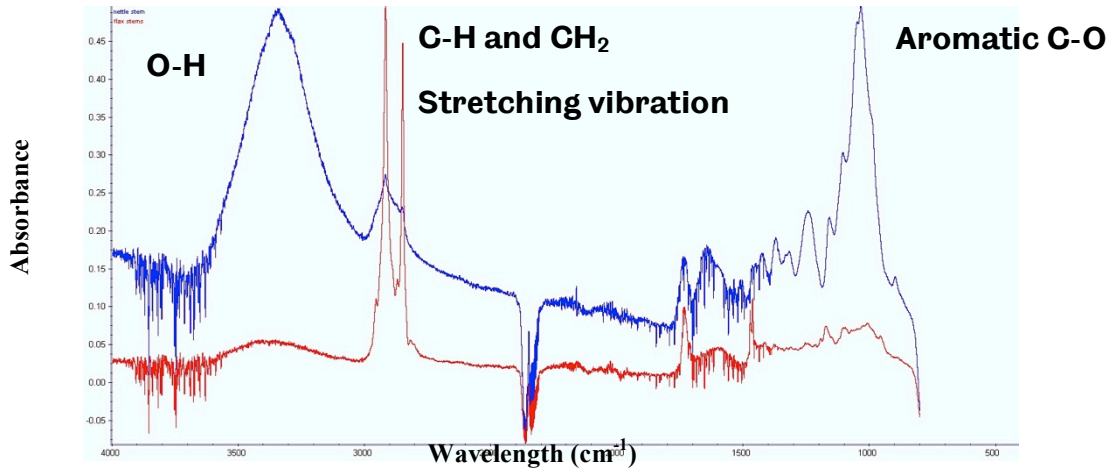

Figure 3.26 FTIR spectra of MPF and MPN fibres. The blue spectrum represents the minimally processed nettle fibres, and the red spectrum is for the minimally processed flax fibres.

The IF, IN, and MPN fibres had a major peak at 3400 cm^{-1} wavelength, showing the existence of O(3)H--O(5) bonds (intramolecular hydrogen bonging showing the bonding of a hydrogen with a atom with another atom within in the same

molecule) [39]. These bonds exists in the cellulose, hemicellulose, and lignin parts of the fibres [284]. A peak at 2400 cm^{-1} represents the C-H bonds due to symmetrical stretching of the chemical bonds of fibres, and the peak at 1000 cm^{-1} wavelength is due to the C-C, C-OH, and CH bonds [285].

According to Gardner-Blackwell, the hydrogen bonds include two intramolecular O(2)H---O(6) and O(3)H---O(5) bondings and one intermolecular bonding, O(6)H---O(3) [40]. Kataoka and Kondo showed by FTIR spectroscopy that the spectra deformations occurred only in the cellulose part of the plant. No molecular deformation has been observed in the lignin or hemicellulose parts [286], [287].

Table 3.9 summarises the peaks of IF, IN, and MPN fibres from the FTIR spectra. The MPF fibres had two peaks at wavelengths of 2900 and 2800 cm-^{1}, as seen in Figure 3.25, with a possible explanation the presence of linseed oil in the flax fibre structure [287]. Linseed oil (also known as flaxseed oil or flax oil) can be obtained in large quantities from flax plant seeds and, in some cases, from the dry flax stem. Flax oil has applications as a plasticiser and hardener [288].

Table 3.9 Corresponding wave numbers derived from the FTIR analysis associated with chemical bonds of IF, IN, and MPN fibres.

Fibres	Wavelength (cm^{-1})	Chemical bonds
F(I) N(I) N(MP)	3330-3400	OH
	2900	CH
	2830	CH_2
	1630	H_2O
	1450	C-OH
	1100	C-O-C
	1050	C-OH

3.6 Summary

Fibre properties were investigated to determine whether nettle fibres have sufficient mechanical properties to be used as reinforcing material in composite manufacturing and whether the fibre preparation process affects their properties.

From the analysis of their physical and mechanical properties, nettle fibres were found to have improved properties compared to flax fibres, making nettles a promising reinforcing material. MPN fibres had tensile strength of 898 ± 33 MPa, followed by MPF with tensile strength of 837 ± 31 MPa. Comparing the mechanical

properties between the industrial and minimally processed fibres, the industrially processed fibres had lower tensile strength and Young's modulus results, indicating possible modification of the fibres' strength and stiffness due to the preparation process. The IN and IF fibres produced tensile strength results of 719 ± 35 MPa and 599 ± 37 MPa, respectively.

The fibres' nature and preparation process affected the fibres when tested under different humidity conditions. Minimally processed fibres absorbed the highest amounts of moisture, leading to the highest reduction in mechanical properties (tensile strength reduction of 54% and 34% for MPN and MPF fibres respectively at 80% RH).

From the evaluation of the physical and mechanical properties of flax and nettle fibres, questions are raised about their performance as reinforcements to composite materials. In the follow chapters, a detailed analysis of the manufacture and characterisation of flax and nettle fibre-reinforced composites is presented.

4 COMPOSITE MANUFACTURE AND TESTING METHODOLOGIES

4.1 Introduction

This chapter outlines the approach used to create plant fibre reinforced composite materials and the physical, mechanical, and thermal tests performed on them before presenting the results in Chapter 5.

4.2 Materials

4.2.1 Material selection

Chapter 3 shows that both industrially and minimally processed flax and nettle fibres would be suitable for integration into a composite material as reinforcing materials.

As a binding matrix, thermoplastic polymers are widely used in the manufacture of composites [92], [113], [201], [289]. One example, described in chapter 2, is PLA, a biodegradable polymer which has received much interest due to its mechanical performance and bio credentials [195], [197], [204]. Recently, PLA has seen increased interest for combination with natural fibres for composite manufacture [5], [26], [63].

As previous discussed in section 2.4.1.2, Floreon is a new blend based on PLA [19]. Specifically, Floreon is a plant-based additive to PLA, which increases its mechanical properties (i.e., tensile strength and Young's modulus) while maintaining its biodegradability [19], [207], [290]. For the purposes of this work, samples of Floreon were obtained from the Floreon-Transforming Packaging Limited [19].

4.3 Fibre-reinforced composites

4.3.1 Composite manufacture process overview

To replicate an industrial approach towards processing, flax and nettle fibres were blended with Floreon in a twin-screw extruder to create 4 mm filament. This was further pelletised and used in an injection moulder to create samples for standardised testing.

4.3.2 Extruder setup

Extrusion is a useful technique to intensively mix materials of different physical and mechanical properties and produce a homogeneous material [125], [126]. A Rondol 21 mm laboratory scale twin-screw extruder was used to blend oven dry (section 3.3.6) industrially and minimally processed flax and nettle fibres with Floreon. The extruder configuration is illustrated in Figure 4.1. A hopper receives the unmixed samples and transports them via twin screws to the kneader, which consists of three heating zones and a final, heated 4 mm die through which the filament passes to a water bath and finally a Rondol pelletiser.

Figure 4.1 a) Rondol 21 mm scale twin-screw laboratory extruder and b) Rondol pelletiser used for the fibre/Floreon blending and pellet production.

4.3.3 Extrusion parameters

The melting temperature of Floreon varies between 170–190°C [19], [207]. Studies using flax fibre/PLA indicated a moulding temperature in the range of 180–200 °C, while temperatures higher than 200 °C may cause fibre degradation resulting in reduced tensile strength and strain properties [93], [115], [158], Therefore to evaluate the effects of extrusion temperature on the flax and nettle fibre-reinforced Floreon composites, extrusion temperatures in the range of 180–200 °C were tested.

Previous studies in this area indicated extrusion pressures of 10–100 bar can be used, depending on the material's viscosity, processing time, and temperature [19], [133], [139]. Therefore, to evaluate the effects of extrusion pressure in this study, extrusion pressures in the range of 10–40 bar were applied.

Thermoplastic polymers can withstand longer extrusion procedures (5–15 minutes) without undergoing thermal degradation [291]. However, studies on bio-composites have indicated that extrusion procedures, exceeding five minutes in combination with temperatures of 200 °C affect negatively the mechanical properties of cellulosic fibres [77], [133], [195].

4.3.4 Injection moulding setup

A Haake Minijet II micro-injection moulder with dog bone (75 x 10 x 4 mm) and rectangular shaped moulds (80 x 12 x 4 mm) available at the laboratory of the University of Manchester was used to create standardised composite samples for testing (Figure 4.2). A silicone release agent (Ambersil Formula 1 from Invotec Solutions) was used on the mould to facilitate sample demoulding

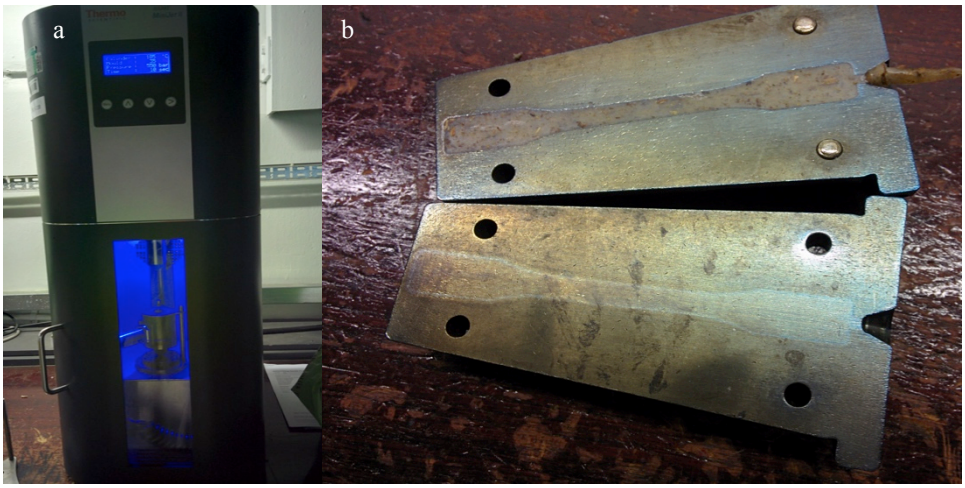

Figure 4.2 a) Haake Minijet II injection moulder and b) dog bone shaped mould.

4.3.5 Injection moulding parameters

Using the previous extrusion parameters and the wider literature as a guide, moulding pressures between 300–500 bar and temperatures between 180–200 °C were tested [58], [127], [130], [292].

4.4 Fibre-reinforced composite composition

Aside from the processing parameters, the fibre/matrix content ratio significantly affects the composite's mechanical properties [163], [165]. This ratio can be calculated by weight or by volume content. The matrix content should be sufficient to bond the fibres and create a strong fibre/matrix adhesion [165]. Typically, a satisfactory thermoplastic matrix content (e.g., PLA) in a composite structure varies between 40–70% for hand layup (open moulding method) and pre-preg

(reinforcing fabric which has been pre-impregnated with a resin system) uses and between 10–30% for injection moulding, depending on the ultimate application [92], [292].

Six compositions per fibre type were tested, split into three flax or nettle fibre/Floreon ratios and using either minimally processed (MP) or industrial (I) fibre sources for each. A summary of the compositions and the sample nomenclatures may be found in Table 4.1. The composition is determined by percent weight of the materials added to the hopper.

Table 4.1 Composites' composition and nomenclatures. Composites are consisting of MPF, MPN, IN and IF fibres of 20, 30, and 40 wt% fibre content. Each of the composite nomenclatures is as followings, fibre type and (fibre /matrix)% content.

	Industrial fibres (I)		**Minimally processed fibres (MP)**		
Name	**Nettle wt%**	**Flax wt%**	**Nettle wt%**	**Flax wt%**	**Floreon wt%**
IN (20/80)%	20				80
IN (30/70)%	30				70
IN (40/60)%	40				60
IF (20/80)%		20			80
IF (30/70)%		30			70
IF (40/60)%		40			60
MPN (20/80)%			20		80
MPN (30/70)%			30		70
MPN (40/60)%			40		60
MPF (20/80)%				20	80
MPF (30/70)%				30	70
MPF (40/60)%				40	60

*Note it was not possible to use higher fibre concentrations due to blockage of the extruder.

4.5 Experimental manufacture of flax and nettle fibre-reinforced Floreon composites

The complete preparation procedure for the flax fibre-reinforced Floreon composites and nettle fibre-reinforced Floreon composites were divided into three phases, described below. The composite-specific extrusion parameters, fibre type, and concentration may be seen in Table 4.2.

Phase A: Fibre preparation

Industrially processed flax and nettle fibres were separated by hand as single fibres and chopped manually into lengths of 2–5 mm, according to the critical fibre length (see chapter 5). Minimally processed flax and nettle fibres were extracted by hand from the dry stems and single fibres were chopped into 2–5 mm lengths. All fibres were oven dried at 100 ± 1 °C for 24 hours and weighed using a mass balance of 0.001 mg accuracy (Semi-Micro Analytical Balance GR-200, A&B company). The oven-dried fibres were then mixed in the appropriate ratio with Floreon.

Phase B: Fibres/matrix blend

Prior to blending, Floreon was oven dried at 50 ± 1 °C (to avoid moisture absorption) for 24 hours before weighing and mixing with the appropriate weight of fibres. After preheating the extruder (section 4.3.2), chopped fibres and Floreon pellets were placed in the feeding hopper and extruded under a range of temperatures, pressures, and times (Table 4.2) before being pelletised to 3–4 mm sections.

Phase C: Composites manufacturing

Prior to injection moulding, the Floreon/fibre pellets were oven dried at 65 °C for 24 hours to allow structural and stress relaxation before mechanical testing (Floreon's glass transition temperature is T_g = 65 ± 2 °C). After preheating the injection moulder (section 4.3.4), the blended pellets were placed in the feeding hopper (Figure 4.1 a) and injected into the moulds. A silicone release agent (Ambersil Formula 1) was used on the mould to facilitate demoulding. The extrusion parameters are presented in Table 4.2.

Table 4.2 Injection moulded MPN (20/80)% composite, manufactured with different processing parameters. Each of the composite's nomenclatures is as followings, fibre type and content; extrusion temperature and extrusion pressure.

Extrusion temperature (°C)	Extrusion pressure (bar)	Sample name
180	10	MPN20-180-10
	20	MPN20-180-20
	30	MPN20-180-30
	40	MPN20-180-40

An example of the separate components, pellets, and injection-moulded composites may be found in Figure 4.3.

Figure 4.3 a) MPN fibres and b) Floreon pellets used as raw material in the extrusion procedure, c) nettle/Floreon pellets, and d) injection-moulded MPN composites.

4.6 Characterisation equipment and procedures

The following section describes the characterisation and calculations used to derive the physical and thermal properties of Floreon and Floreon-based composites presented in later chapters.

4.6.1 Density

The density of Floreon was calculated by the immersion methods following the BS EN ISO 1183-1:2004 standard [293]. The weight of Floreon was measured in atmospheric conditions (m_1) and immersed in water (m_2) using a mass balance of 0.001 mg accuracy (Semi-Micro Analytical Balance GR-200, A&B company). The weight of the immersed Floreon specimen (m_2) was measured within a Glassware Duran volumetric tube and calculated by subtracting the weight of the tube from the final readings of the weight balance.

Water was used as an immersion liquid. Floreon was immersed in 100 ml of water and left for 10 minutes. The immersion time was short and therefore had no measurable influence on the weight of the immersed specimen. In total, five Floreon samples were tested to determine the average Floreon density.

The density of Floreon was calculated using Equation 4.1.

$$\rho = \frac{m_1 \times \rho_{liq}}{m_1 - m_2} \qquad \textbf{Equation 4.1}$$

where,

ρ is the density of Floreon (g/cm^3);

ρ_{liq} is the density of water (mg/ml);

m_1 is the mass of Floreon in atmospheric condition (g);

m_2 is the mass of Floreon immersed in water (g).

4.6.2 Mechanical properties

Tensile and three-point bending tests were used for the mechanical characterisation of Floreon.

4.6.2.1 Tensile testing

Tensile tests were performed on a Zwick Roell Z020TN testing machine with load cell of 25 kN and head speed of 0.125 mm/minute in accordance with the ISO 527-2-1BA standard [150], [151]. The tensile tests were performed in atmospheric conditions at T=23 $\pm$ 2 °C and 55 $\pm$ 5% RH. The gauge length of dog bone Floreon samples was measured at 50 mm between the testing grips. In total, 50 Floreon samples were tested to determine tensile properties.

The tensile stress at the breaking load was calculated using Equation 4.2.

$$\sigma = \frac{F}{A}$$ **Equation 4.2**

where,

σ is the tensile stress at break (MPa);

F is the force at break (N);

A is the cross-section area (mm^2).

The tensile strain at breaking load was calculated using the Equation 4.3

$$\varepsilon = \frac{\Delta L}{L} \cdot 100\%$$ **Equation 4.3**

where,

ε is the tensile strain expressed in percentage (%);

ΔF is the difference between the initial and final sample gauge length after the tensile test (mm);

L is the gauge length (mm).

The Young's modulus was calculated using Equation 4.4.

$$E = \frac{\sigma}{\varepsilon}$$ **Equation 4.4**

where,

E is the Young's modulus (MPa);

σ is the tensile stress (MPa);

ε is the tensile strain.

4.6.2.2 Flexural testing

Flexural properties of Floreon were assessed with a TA500 testing machine under three-point bending tests. The flexural testing was performed in accordance with BS EN ISO 14125: 1998 standards with a minimum span-to-thickness ratio of 16:1 [155], [294]. The three-point tests were performed in atmospheric conditions at

T=23 ± 2 °C and 55 ± 5% RH. The gauge length of rectangular Floreon samples was measured at 75 mm. Valid samples were those where the fracture occurred at the centre of the sample's gauge length (Figure 4.4). In total, 50 Floreon samples were tested to determine flexural properties.

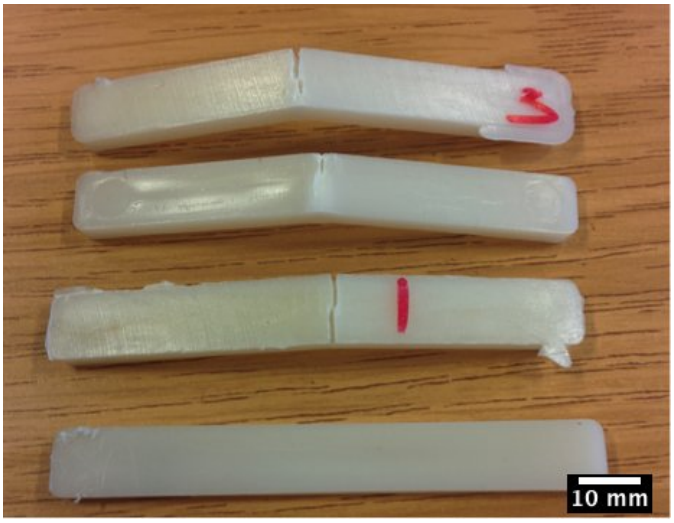

Figure 4.4 Valid Floreon samples after three point bending test.

The flexural stress was calculated using Equation 4.5.

$$\sigma = \frac{3FL}{2bd^2} \qquad \textbf{Equation 4.5}$$

where,

σ is the flexural stress at break (MPa);

F is the force at break (N);

L is the gauge length (mm);

b is the width (mm);

d is the depth (mm).

The flexural strain was calculated using Equation 4.6.

$$\varepsilon = \frac{6sd}{L^2} \qquad \textbf{Equation 4.6}$$

where,

ε is the flexural strain at break;

s is the deflection of the centre of the beam (mm);

d is the depth (mm);

L is the gauge length (mm).

The flexural modulus was calculated using Equation 4.7.

$$E_{flex} = \frac{L^3 m}{4bd^3}, \; m = \frac{\Delta F}{\Delta s} \qquad \textbf{Equation 4.7}$$

where,

E_{flex} is the flexural modulus (MPa);

L is the gauge length (mm);

m is the slope of the load displacement (Δs);

b is the width (mm);

d is the depth (mm).

4.6.3 Thermal properties

Techniques such as DSC and DMA were used to determine the thermal properties of Floreon.

4.6.3.1 DSC

The thermal behaviour of Floreon was studied using a TA Instrument DSC Q100 with a cooling attachment, purged under a nitrogen atmosphere. In total, five Floreon samples were cut into small pieces (5–6 mg) and hermetically sealed in pans.

Samples were subjected to two heating cycles, from 25 to 200 °C at 5 °C/min. The glass transition (T_g), melting temperature (T_m), and degree of crystallinity were determined from the first heating cycle. The melting temperature was determined from the maximum region of endothermic melting peak. Data was analysed using Pyris software.

The heat capacity of Floreon was calculated using Equation 4.8.

$$\Delta C_p = \frac{\Delta q}{m \cdot \Delta T} \qquad \textbf{Equation 4.8}$$

where,

ΔC_p is the change in heat capacity (J/mol °K);

q is the heat flow (Watts) from the DSC curve;

m is the mass (grams);

ΔT is the heating rate (°K).

The degree of crystallinity of Floreon was calculated using Equation 4.9 from the DSC curve of the first heating cycle:

$$X_c = \frac{\Delta H_f}{\Delta H_f^o} \times 100 \qquad \textbf{Equation 4.9}$$

where,

ΔH_f is the heat of fusion of the neat Floreon;

ΔH^0_f is the heat of fusion for 100% crystalline Floreon.

For 100% crystalline Floreon, the heat of fusion of 100% crystalline PLA, ΔH_{100}=93.7 J/g was used [207].

4.7 Flax and nettle fibre Floreon composites characterisation

Similar to the Floreon characterisation, the physical, mechanical, and thermal properties of the injection-moulded composites were determined.

4.7.1 Density

The density measurements of MPN, MPF, IN, and IF composites were calculated using Equation 4.1 and in accordance with the BS EN ISO 1183-1:2004 standard [293]. Composite weights were measured before and after immersion in 100 ml of water using a weighing balance with an accuracy of 0.001 mg (Semi-Micro Analytical Balance GR-200, A&B company). In total, five composites from each composite category were tested to determine the average composite density.

4.7.2 Composites composition

In order to calculate the constituents of the composites, the following Equations were used.

The fibre content by volume was calculated using Equation 4.10.

$$V_f = W_f \cdot \frac{\rho_c}{\rho_f} \qquad \textbf{Equation 4.10}$$

where ,

V_f is the fibre volume fraction as a percentage;

W_f is the fibre weight fraction as a percentage;

ρ_c is the density of the test sample (g/cm^3);

ρ_f is the density of the reinforcing fibres (g/cm^3).

The polymer content by volume was calculated using Equation 4.11.

$$V_m = (100 - W_f) \cdot \frac{\rho_c}{\rho_m} \qquad \textbf{Equation 4.11}$$

where,

V_m is the matrix volume fraction as a percentage ;

ρ_c is the density of the test sample (g/cm^3);

ρ_m is the density of the matrix (g/cm^3).

The void content by volume was calculated using Equation 4.12.

$$V_o = 100 - \left[W_f \cdot \frac{\rho_c}{\rho_f} + (100 - W_f) \cdot \frac{\rho_c}{\rho_m} \right] \qquad \textbf{Equation 4.12}$$

where,

V_o is the void content as a percentage of the initial volume.

4.7.3 Mechanical properties of minimally and industrial processed flax and nettle fibre Floreon composites

4.7.3.1 Tensile testing

Tensile tests were performed on a Zwick Roell Z020TN testing machine with a load cell of 25 kN and head speed of 0.125 mm/minute, in accordance with the ISO 527-2-1BA standard [150], [151]. The gauge length of composites was measured at 50 mm between the testing grips. Composites were attached on crocodile grips in a vertical direction, with end tabs on the edges of the composite to minimise the concentration of stress at these points. The tensile tests were performed in atmospheric conditions at T=23 $\pm$ 2 °C and 55 $\pm$ 5% RH. In total, 200 composites were tested (50 composites each of minimally processed nettle fibres, minimally processed flax fibres, industrially processed nettle fibres, and industrially processed flax fibres).

Samples that failed close to the grip were rejected. For the calculations of the tensile stress, strain, and Young's modulus, Equations 4.2–4.4 were used respectively.

4.7.3.2 Flexural test

The flexural testing was performed with a TA500 testing machine with a 500 N load cell at a constant speed of 2 mm/min. The gauge length of composites was measured at 75 mm. The flexural tests were performed in atmospheric conditions at T=23 $\pm$ 2 °C and 55 $\pm$ 5% RH. In total, 200 composites were tested (50 composites of each fibre type). For the calculations of flexural stress, strain, and flexural modulus, Equations 4.5–4.7 were used respectively.

As discussed in section 2.3.3.3, tested samples were the breaking point coincided with the loading point (in the middle of the sample) were taken into account as seen in Figure 4.5.

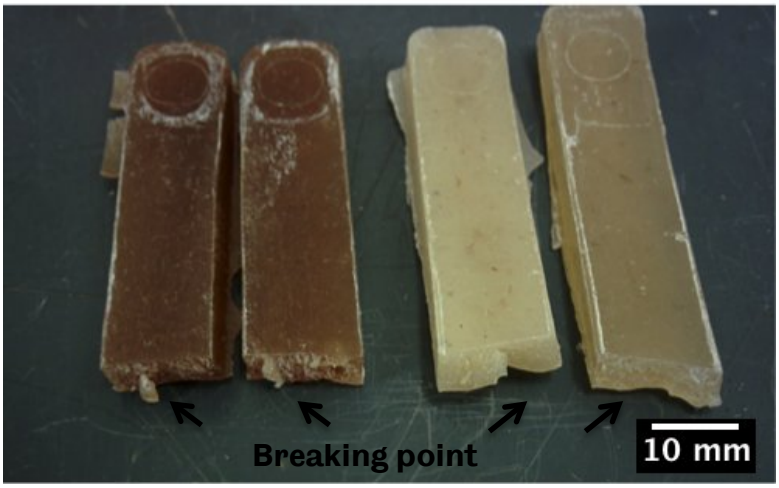

Figure 4.5 MPF, IN and MPN (40/60)% composites (left to right) after three-point bending test.

The rule of mixtures was used in a calculation of the weighted mean of composite properties, including the volume fraction and the individual volumes of fibres and polymer, respectively.

In the case of short fibre reinforced composites, were the fibres are shorter than the length of the composite the stress of fibre depends on it length, the elastic and plastic properties of the fibres and matrix and the fibre-matrix interfacial strength.

The Young's modulus based on the rule of mixtures was calculated using Equation 4.13, according to the Voigt model.

$$E_c = fE_f + (1-f)E_m,\ f = \frac{V_f}{V_f + V_m}$$ **Equation 4.13**

where,

E_c is the composite's Young's modulus (GPa);

E_f is the fibre's Young's modulus (GPa);

E_m is the polymer's Young's modulus (GPa);

f is the volume fraction of fibres.

4.7.4 Fibre/matrix adhesion investigation

The mechanical properties of composites are affected not only by the individual mechanical properties of the reinforcing fibres and matrix but also by their interfacial bonding [143], [162], [295]. The interfacial area of a composite is the area where debonding between fibres and matrix may occur when the applied forced is higher than the interface strength. There are a number of tests to determine the degree of fibre/matrix adhesion [143], [148]. For this work, a single fibre pull-out test was developed and explored to provide some initial insights into this phenomenon.

4.7.5 Single fibre pull-out test

Before the pull-out test, fibres were dried in the oven at 100 ± 1 °C for 24 hours (chapter 3, section 3.5.4) and Floreon pellets at 65 ± 1 °C for 24 hours to minimise the water content and moisture absorption. The diameter, length, and cross-section area of fibres were measured with an optical microscope (Leica DM LM) and calculated using ImageJ software (chapter 3, Table 3.5).

MPF and MPN fibres were partially embedded into a molten pellet of Floreon. The Floreon was softened by either placing the pellet on a hot plate at a temperature up to 120 °C (at that temperature the Floreon pellet became softer) or by using hot air. Tweezers were used to push the fibres into the softened polymer. The maximum length of the single fibres was 5 mm and the embedded fibre length was calculated using a Leica MZ6 optical microscope.

The pull-out tests were performed on a Zwick Reoll ZTN 0.5 tensile testing machine with load cell of 0.5 kN and head speed of 1 mm/minute. Samples that failed or broke during the pull-out test were not used in the analysis of results. For calculations, it was assumed that fibres had a cylindrical shape with uniform

diameter, homogeneous adhesion between the fibre and matrix, and a uniform distribution of stress during the pull-out test. In total, 15 samples from each fibre type were tested.

The interfacial shear strength was calculated using Equation 4.14 according to the Kelly and Tyson model [296].

$$\tau = \frac{F_{\max}}{d_f \cdot \pi \cdot l_{ef}} \qquad \textbf{Equation 4.14}$$

where,

τ is interfacial shear strength (N/mm^2);

F_{max} is the maximum applied force (N);

d_f is the fibre diameter (mm);

l_{ef} is the embedded length of fibres (mm).

The critical fibre length was calculated using Equation 4.15 according to the Kelly and Tyson model [296].

$$L_c = \frac{\sigma_f \cdot d_f}{2\tau} \qquad \textbf{Equation 4.15}$$

where,

L_c is the fibre critical length (mm);

σ_f is the tensile strength of a single fibre (MPa);

d_f is the fibre diameter (mm);

τ is the interfacial shear strength (N/mm^2).

Additionally, the critical fibre length can be used as an indication of the capability of adhesion between the fibre and the matrix in a composite. According to the literature, the majority of cellulosic fibres have typical fibre lengths of less than 30 mm and aspect ratios between 100–2000 [136]. Generally, the fibre length efficiency factor describes the ability and the effectiveness of fibres to transfer strength and stiffness to the composite. There are two types of fibre length efficiency factor, correlated with either stiffness or strength. The length efficiency factor has been determined by Bos *et al.* in the range of 0.17–0.20 for flax composites [58].

The fibre aspect ratio was calculated using Equation 4.16.

$$\text{Aspect ratio} = \frac{l_f}{d_f} \qquad \text{Equation 4.16}$$

where,

l_f is the fibre's length (mm);

d_f is the diameter of fibres (mm).

4.7.6 Thermal properties of minimally and industrially processed flax and nettle fibre Floreon composites -DMA

Composite samples of dimensions 10 x 9 x 4 mm were placed within a Perkin Elmer DMA 8000 in single cantilever mode with gauge length of 10 mm and tested in a heating cycle in a range of 25°C–100 °C at 3 °C min^{-1} and subjected to a single frequency of 1 Hz at a displacement of 0.05 mm. The glass transition temperature is defined as the tanδ peak of the dynamic modulus versus temperature curve. Dynamic modulus is the ratio of stress to strain under vibratory conditions and tanδ represents the ratio of the viscous to elastic response of a viscoelastic material [173]. In total, 20 composites (five composites from each composite category) were tested.

4.7.7 Moisture absorption test of flax and nettle fibre-reinforced Floreon composites

Due to the hydrophilic character of minimally and industrially processed flax and nettle fibres, the effect of moisture absorption was studied in the case of flax and nettle fibre-reinforced Floreon composites. The moisture absorption test was used to determine the amount of moisture absorbed along the thickness of composites. The moisture absorption tests were performed in accordance with ASTM D5229/D5229M-12 standards [282]. In total, 20 composites (five composites from each composite category) were exposed to 40,60% and 80% RH in a humidity chamber for 24 hours respectively. Before the measurements, the weight of fibres was measured with a weight balance of 0.001 mg accuracy (Semi-Micro Analytical Balance GR-200, A&B company).

The average moisture content in the composite was calculated using Equation 4.17.

$$M = \frac{W_f - W_i}{W_i} \cdot 100\% \qquad \textbf{Equation 4.17}$$

where,

M is the average moisture content of composites (%);

W_f is the final mass of composites after the exposure to RH (g);

W_i is initial mass of composites (g).

4.7.7.1 Moisture diffusivity

Moisture diffusivity is a parameter used for the optimisation of drying procedures in materials. Higher values describe a faster diffusion mechanism for the samples tested. To determine the moisture diffusivity parameter for flax and nettle fibre-reinforced Floreon composites, it was assumed they behaved as a single-phase Fickian specimen with constant moisture absorption properties through the thickness of the composite [213], [282].

The diffusivity was calculated using Equation 4.18.

$$D_z = \pi \left(\frac{h}{4M_m} \right)^2 \left(\frac{\Delta M}{\sqrt{t}} \right)^2 \qquad \textbf{Equation 4.18}$$

where,

D_z is the diffusivity of composite through its thickness (cm^2/s);

h is the thickness of the composite (mm);

M_m is the mass moisture equilibrium content (mg^2);

ΔM is the average moisture content (mg^2);

t is the exposure time $(\sqrt{\sec})^{-1}$.

4.7.8 Mechanical properties of flax and nettle fibre-reinforced Floreon composites after moisture absorption tests

The tensile and flexural properties of the composites after moisture absorption were calculated using Equations 4.2–4.4 and 4.5–47 respectively.

The residual mechanical properties were further calculated using Equation 4.19.

$$\text{Residual mechanical property (\%)} = \frac{P_f}{P_i} \cdot 100\% \qquad \text{Equation 4.19}$$

where,

P_f is the property of the composite after the moisture absorption tests;

P_i is the initial property of composite.

4.8 Summary

This chapter outlined the flax and nettle fibre-reinforced Floreon composites manufacture procedure and their subsequent physical, thermal, and mechanical characterisation and analysis. Chapter 5 presents the results of this comparison.

5 INJECTION MOULDED FIBRE-REINFORCED COMPOSITES

Physical, mechanical, and thermal properties of flax and nettle fibre-reinforced composites

5.1 Introduction

This chapter discusses the physical, mechanical, and thermal properties of minimally and industrially processed nettle and flax fibre-reinforced Floreon composites fabricated using injection moulding. The aim of this work is to provide insight into the effects of processing conditions on performance, defining a database of properties of composites and enabling researchers to make informed choices as to which fibre/matrix combination is suitable for their intended application.

5.2 Results and discussion

5.2.1 Density

The density of injection-moulded Floreon and the different types of composites were determined using the immersion method, as described in sections 4.6.2 and 4.7.1, and calculated using Equation4.1. For the injection moulded composites Floreon (FL 800), which is specifically made for injection moulding was used [19]. Table 5.1 presents the calculated density of Floreon and composites according to the different fibre/polymer contents.

Table 5.1 Density of Floreon, flax and nettle fibre-reinforced Floreon composites, for 5 Floreon samples and composites from each composite category.

Density (g/cm^3) Floreon 1.20-1.30 (g/cm^3) Flax 1.4-1.7 (g/cm^3), nettle 1.3-1.8 (g/cm^3)				
Composite concentration	**Flax/Floreon**		**Nettle/Floreon**	
Fibre/Floreon	**MP**	**I**	**MP**	**I**
(40/60)%	1.20-1.30	1.20-1.30	1.20-1.30	1.20-1.30
(30/70)%	1.30-1.35	1.20-1.30	1.30-1.35	1.20-1.30
(20/80)%	1.30-1.40	1.20-1.35	1.30-1.40	1.25-1.35

In composites with 20 wt% fibre content, those consisting of MP fibres had slightly higher density values. MPN (20/80)% had density of 1.40 g/cm^3 compared to IN (20/80)% with the density of 1.35 g/cm^3. Composites with 40 wt% fibre had the

same density values as the pure Floreon. However, from the calculated density values (Table 5.1) composites with lower fibre content such as MPF (20/80)% and MPN (20/80)% had higher densities. Given the higher densities of flax (1.4–1.7 g/cm^3) and nettle (1.3–1.8 g/cm^3) and lower density of Floreon (1.2-1.3 g/cm^3), the opposite trend would be expected. A possible explanation for the reduced density values in composites with higher fibre by weight content may be the creation of voids [140]. Voids can be formed during manufacturing when the air is trapped within compounded pelletised material and through moisture absorption by the reinforcing fibres [297]. The differences in density values between Floreon and the composites led to the void content calculations in the following section.

5.2.2 Void content

To help better understand the causes for the discrepancies in the predicted versus measured densities of the composites, the fibre and matrix content were calculated by weight. Table 5.2 presents the fibre, matrix, and void content by volume in the different types of composites. The difference between the sum of fibre (V_f) and matrix (V_m) versus the sample (100%) indicates the formation of voids during the manufacturing process. W_f was calculated as a percentage of the ratio of the oven-dried fibres to the fibres' initial mass.

Table 5.2 Composite composition and associated void content. For the calculation of the individual composite contents, Equations 4.10, 4.11 and 4.12 were used.

Composite type	Composite composition (Fibre/Matrix)	Fibre volume V_f (%)	Matrix volume V_m (%)	Void volume V_o (%)
MPF	(40/60)%	36	56	8
	(30/70)%	27	67	6
	(20/80)%	18	78	4
MPN	(40/60)%	33	55	12
	(30/70)%	25	66	9
	(20/80)%	17	77	6
IF	(40/60)%	36	58	6
	(30/70)%	28	68	4
	(20/80)%	19	79	2

IN	(40/60)%	36	57	7
	(30/70)%	27	68	5
	(20/80)%	19	78	3

In general, an increase in the void content was observed as the fibre content increased, confirming results from the density testing. The highest percentage of voids was calculated in the case of MPN (40/60)%, followed by MPF (40/60)%.

One possible explanation for void formation and especially in the case of composites consisting of minimally processed fibres is a nonhomogeneous mixture and poor adhesion between fibres and Floreon [144]. Minimally processed fibres, specifically MPN, have rougher surfaces than IN fibres, leading to weaker bond between the fibres and the matrix. Floreon is a thermoplastic polymer (similar to PLA) and has a high melting viscosity, meaning that it does not readily flow into small volumes [169]. During injection moulding, the surface of the sample loses heat rapidly as it hardens and the matrix (i.e., Floreon) shrinks, leaving holes within the composites [298].

Furthermore, the injection pressure, temperature, and the permeability of the flax and nettle fibres can all have significant effects on the formation of voids in a composite [135]. Generally, high injection pressures are preferred to avoid the formation of voids, which may cause deformation of the mould, fibre distortion, and uneven solidification of the moulded part [298].

The fracture surface of MPF composites via SEM (Jeol JSM-6010la, Jeol, Japan) can be seen in Figure 5.1 (a-b), showing the voids contained in the composites. On a microscale, flax and nettle fibres include natural voids along the fibre's length, resulting from the fibre morphology and structure and industrial preparation process (see chapter 2) [52], [59]. Also, the contrast between the hydrophobic behaviour of Floreon (small amount of water uptake) and hydrophilic flax and nettle fibres may cause problems with the wettability of the sample [290].

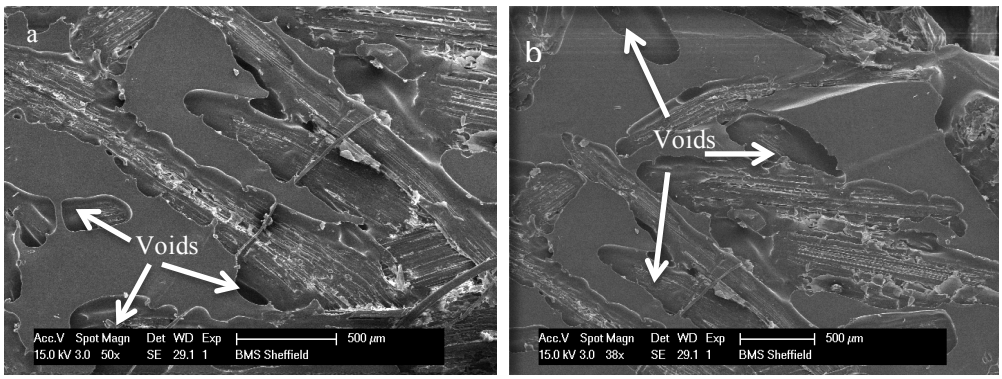

Figure 5.1 Fracture surface with Jeol JSM-6010la SEM of a) MPF (30/70)% and b) MPF (40/60)%.

From Figure 5.1, voids can be clearly seen inside the composites' structure. Air trapped during the moulding process remains the strongest hypothesis for void formation. Previous studies confirmed the influence of the composites' manufacturing, reporting that an insufficient selection of manufacturing and processing parameters can affect the composites' structure and therefore the composites' properties [77], [298].

5.2.3 Mechanical properties

A Rondol 21mm scale twin-screw laboratory extruder and Haake Minijet II micro-injection moulder were used to manufacture both dog bone and rectangular samples according to British standards for tensile and flexural testing [81], [294]. Compositions and nomenclatures based on the processing parameters were presented in chapter 4 (Tables 4.1 and 4.2). In the following section, the mechanical properties of Floreon, MPF, MPN, IF, and IN composites consisting of 20%, 30%, 40 wt% fibre content are presented. Composites with higher fibre contents could not be created due to clogging of the extruder nozzle.

5.2.3.1 Tensile properties

Samples for tensile testing were created using the following process parameters: extrusion pressure of 40 bar, moulding pressure of 500 bar, and cooling pressure of 300 bar (cooling and moulding time at 1 minute each). The extrusion and moulding temperature was 190 °C for MPF/MPN composites and 180 °C for IN/IF composites. Normally, the moulding temperatures are 10 °C to 20 °C higher than the melting temperature of the matrix. The 10 °C difference between the minimally and industrially processed fibres was found after a series of experiments [291], [292]. Previous studies do not refer to such differences. This temperature

difference may be due to the different fibre processes between the minimally and industrially processed fibres. MPN and MPF fibres had rougher and larger surfaces compared to the corresponding industrially processed fibres, and higher temperatures were needed for sufficient blending with Floreon.

The tensile properties of tensile stress, strain, and Young's modulus were calculated using Equations 4.2–4.4. Specifically for the strain measurements, the readings from the respective software were collected related with the initial and final length of the sample before and after the experiments. The strain measurements in this project were all done in the same way, in order to have consistency in the results. However, there may be improvements in the accuracy of strain measurement, such as using strain gauges. Strain gages are used as sensors that convert the applied force into a change in electrical resistance, which can then be measured. As a result of the applied external forces to the stationary sample, stress and strain are the result.

Figure 5.2 represents the stress–strain curves for Floreon, a) MPN, b) MPF, c) IF and d) IN fibre-reinforced Floreon composites consisting of 40%, 30% and 20% wt fibre content respectively (for nomenclature, please refer to Table 4.1).

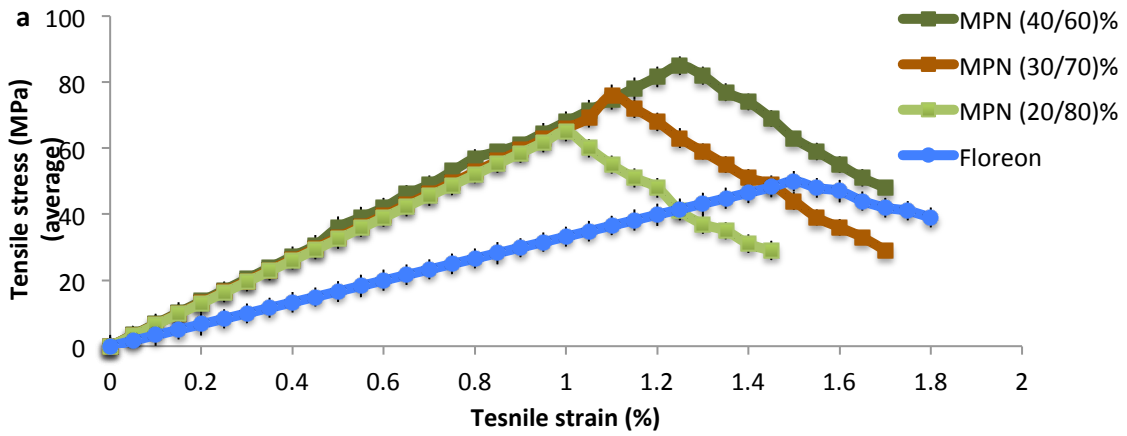

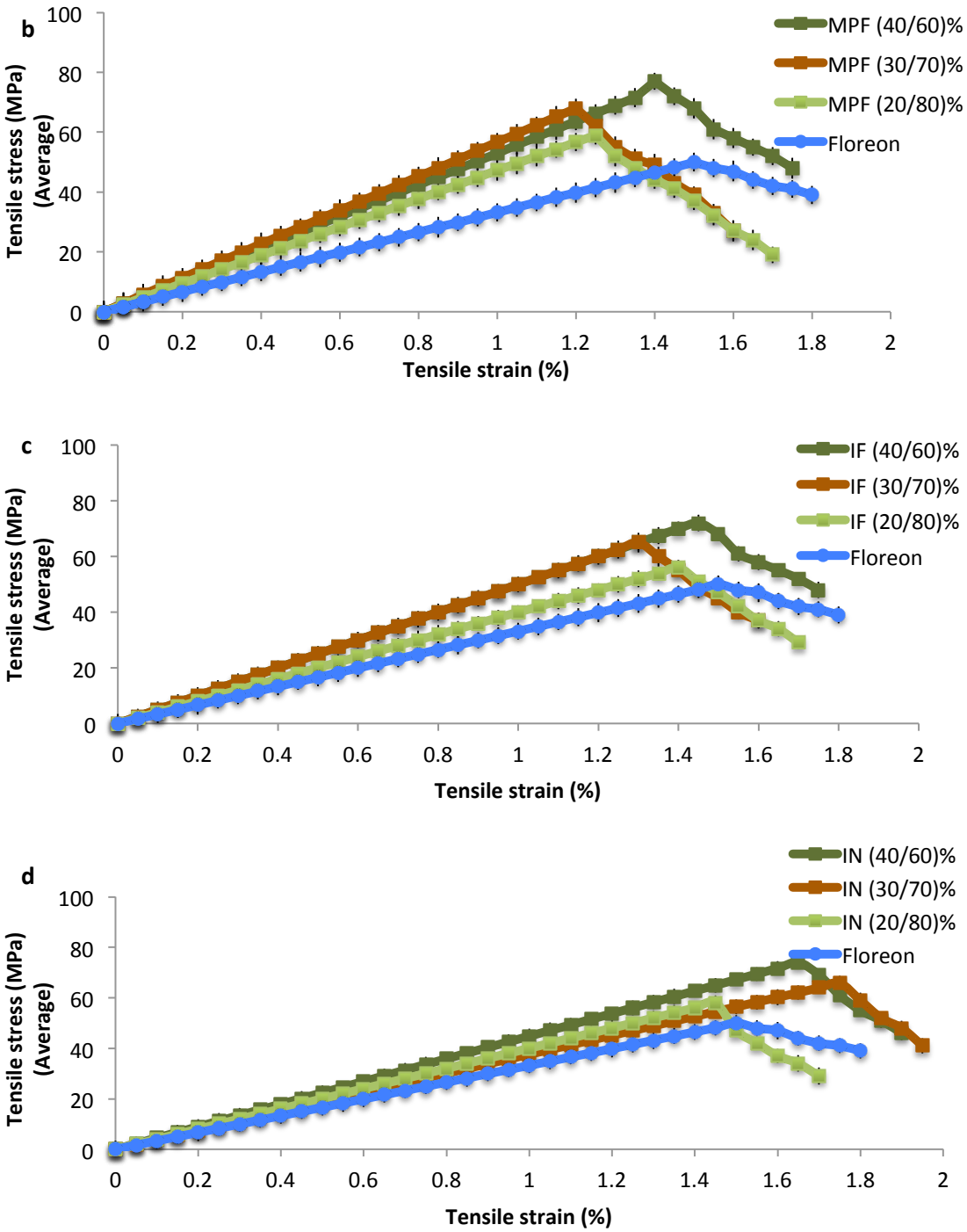

Figure 5.2 Tensile stress-strain curves of Floreon, a) MPN, b) MPF, c) IF and d) IN composites of 40%, 30%, 20 wt%, for 50 composites from each composite category. Floreon and composites were made using extrusion pressure of 40 bar, moulding pressure of 500 bar and moulding time at 1 minute moulding time. The moulding temperature for composites consisting of MP fibres was set up at 190 °C and at 180°C for the corresponding composites with I fibres. The error bars represent ±1SD (samples tested for every set of error bars n=10).

As illustrated in Figure 5.2, Floreon and composites exhibited a liner relationship between the tensile stress and strain, suggesting a linear deformation during

testing. Composites reached at a maximum tensile stress point before failure, which is higher than Florean's, known as tensile strength. The linear part of the tensile stress-strain curves was used for the calculation of Young's modulus. The failure of composites was caused by two main damage mechanisms that can occur during the tensile test. Firstly, micro-cracks form in the matrix when the polymer undergoes a plastic deformation [152], [162]. Secondly, fibre/matrix debonding can occur, leading to fibre failure [299]. Finally, fibres are pulled out from the surrounding polymer, resulting in matrix failure and composite failure.

Comparing the tensile stress and strength of Floreon with flax and nettle fibre-reinforced composites, both minimally and industrially processed flax and nettle fibres clearly increased the tensile strength (Figure 5.3). In general, the composites with the highest fibre contents, (40/60)%, had the highest tensile strength. The increased tensile strength is due to the fibres' ability to carry and transfer the applied load from the Floreon matrix and generate a uniform stress distribution during testing [152]. At lower fibre contents, composites have a lower tensile strength, causing local cracks and a weaker sample [162]. Upon increasing the fibre content, stress concentration is further avoided, increasing the strength of the whole composite [149], [276].

Comparing performance across the different types of composites, MPN and MPF composites have the highest tensile stress, strength and Young's modulus compared to the IN and IF composites. This is not surprising given that a composite's tensile properties are linked with the tensile properties of the constituent materials, and MPN and MPF fibres were stronger and stiffer than their industrial counterparts (chapter 3). MPN40-190-40-1 (see Table 4.2) composites had the highest tensile strength, at 85 ± 3 MPa, followed by MPF40-190-40-1 with a tensile strength of 77 ± 2 MPa (Figure 5.3).

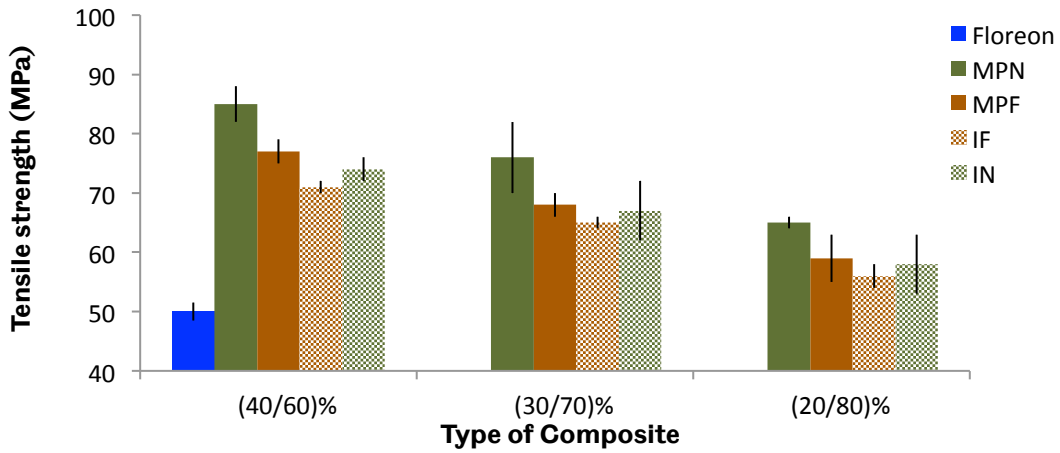

Figure 5.3 Tensile strength (average) of Floreon and Floreon based composites of 40%, 30%, 20 wt%, for 50 composites from each composite category. Floreon and composites were made using extrusion pressure of 40 bar, moulding pressure of 500 bar and moulding time of 1 minute. The moulding temperature for composites consisting of MP fibres was set up at 190 °C and at 180 °C for the corresponding composites with I fibres. The notation MPN is referred to composites consisting of minimally processed nettle fibres (solid green bars) and MPF to the corresponding composites with minimally processed flax fibres (solid brown bars). The notation IN is referred to composites consisting of industrial processed nettle fibres (dashed green bars) and IF to the corresponding composites with industrial processed flax fibres (dashed brown bars). Notice that the lower value of tensile strength axis are omitted in order to improve the readability of the plot. The error bars represent ±1SD (samples tested for every set of error bars n=10).

According to calculations using the rule of mixtures (Equation4.13), the Young's modulus for composites increased with the fibre volume content. The highest Young's modulus was again observed in the MPN40-190-40-1 and MPF40-190-40-1 composites, with values of 6.8 ± 1.2 GPa and 5.5 ± 1 GPa respectively, compared to 3.2 ± 0 .8 GPa for pure Floreon. Figure 5.4 summarises the calculated Young's modulus for MPN, MPF, IF and IN composites based on the different used fibre contents.

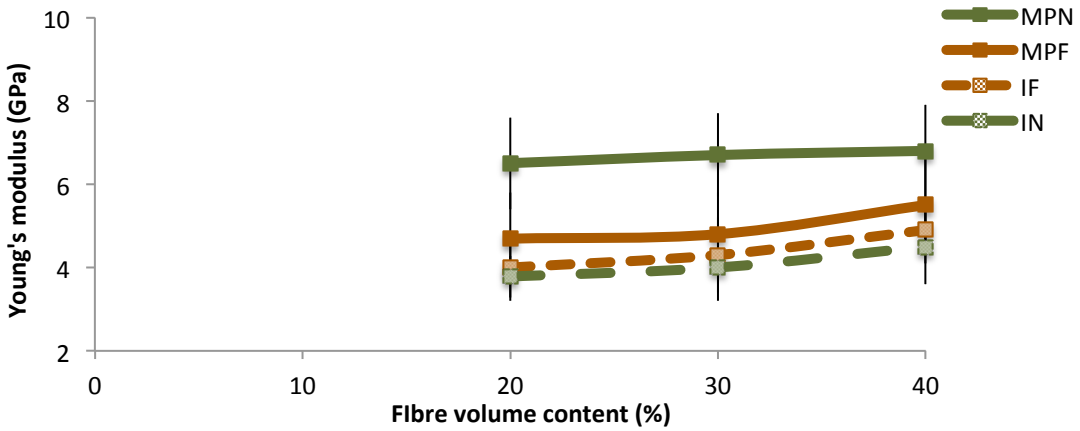

Figure 5.4 Young modulus as a function of fibre volume content of MPN, MPF, IF and IN composites of 40%, 30%, 20 wt% fibre content. The error bars represent ±1SD (samples tested for every set of error bars n=10).

The tensile properties of composites were characterised according to the different applied parameters (temperature and pressure). The results obtained show a correlation between the mechanical properties of the composites with the processing parameters, in agreement with the wider literature [133]. A range of different extrusion and moulding temperatures, extrusion and moulding pressures, and moulding times (the time needed to fill the mould) during the extrusion of fibres with Floreon were tested (Figures 5.4-5.5).

Figure 5.5 a–b shows the effects of moulding temperature and extrusion pressure on the tensile strength of MPF and MPN fibre-reinforced composites with different fibre content ratios. The highest tensile strength results were obtained at an extrusion pressure of 40 bar and extrusion temperature of 190 °C during the extrusion procedure. During the injection moulding the same temperature values as the extrusion temperatures were used and therefore the term moulding temperature is used. The moulding pressure was constant at 500 bar and cooling pressure set to 300 bar. After experiments with different moulding pressure values between 300–500 bar, the above values were chosen and remained consistent throughout all experiments, as they were sufficient to fill the mould without leaving (optical) gaps and without the overflow of Floreon. Lower moulding pressure values resulted in incomplete filling of the mould, where in most cases, the mould was filled up to 75% of the total mould area. At lower cooling pressure values, deformation was observed during the solidification stage of composites. Lesions were mainly present at the edges of composites. The maximum tested extrusion pressure was 40 bar, based on the capabilities of the extruder.

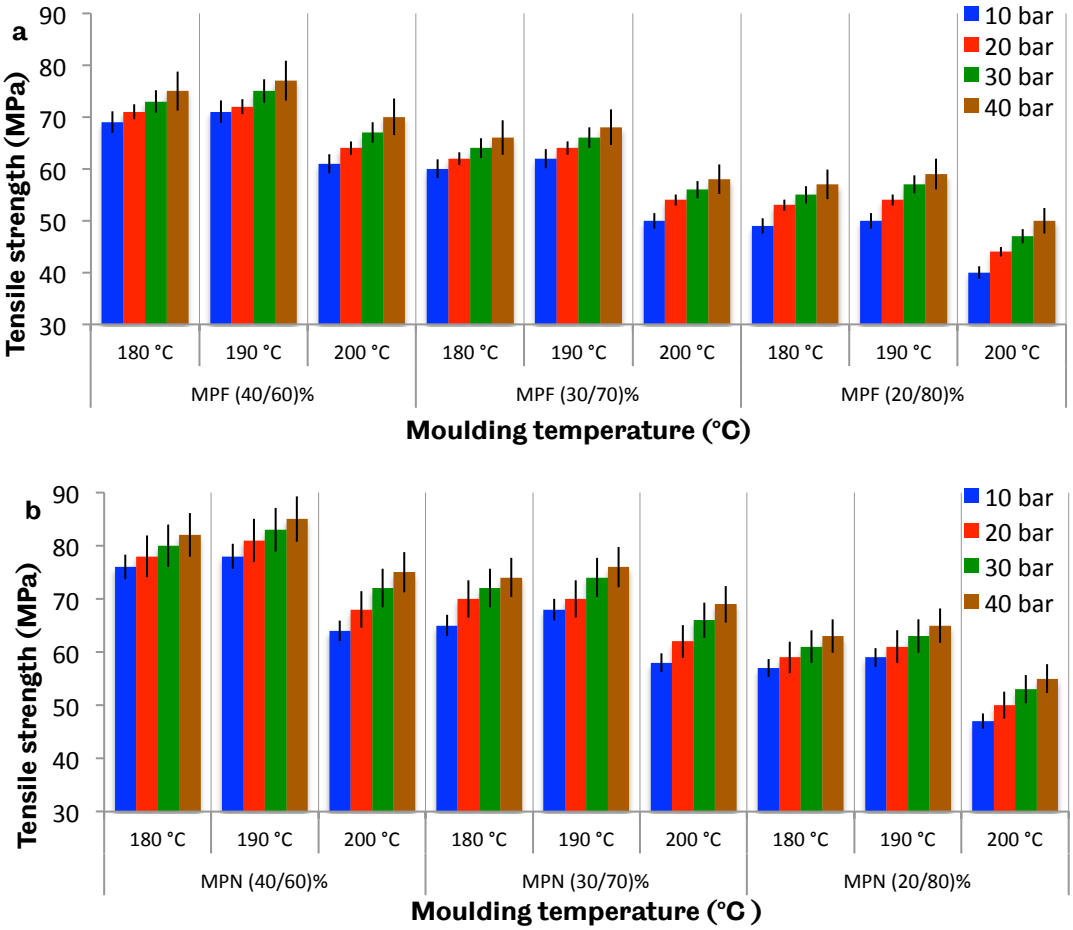

Figure 5.5 Effect of processing parameters on the tensile strength of a) MPF composites and b) MPN composites of 40%, 30%, 20 wt%, for 10 composites from each composite category, The x-axis presents the moulding temperatures tested from 180 °C to 200 °C. The blue, red, green and brown coloured bars represent the extrusion pressures tested at 10 bar, 20 bar, 30 bar and 40 bar, respectively. For each processing parameters tested, the composites were manufactured with constant values of moulding time of 1 min, moulding and cooling pressure at 500 bar and 300 bar respectively. Notice that the lower value of tensile strength axis are omitted in order to improve the readability of the plot. The error bars represent ±1SD (samples tested for every set of error bars n=5).

IF composites exhibited their highest tensile strength results at extrusion pressure of 40 bar and at moulding temperature of 180 °C. As the moulding temperature increased, the tensile properties decreased, with the greatest reduction observed at 200 °C in all fibre contents.

Figure 5.6 a presents the effect of moulding temperature and pressure on the tensile strength of IF composites. IN composites had the same outcome as the IF composites, with the highest results obtained at moulding pressure of 40 bar and moulding temperature of 180 °C, as seen in Figure 5.5 b. A moulding time between

1–10 minutes was also tested, but no significant changes were observed in the mechanical properties of any type of composite.

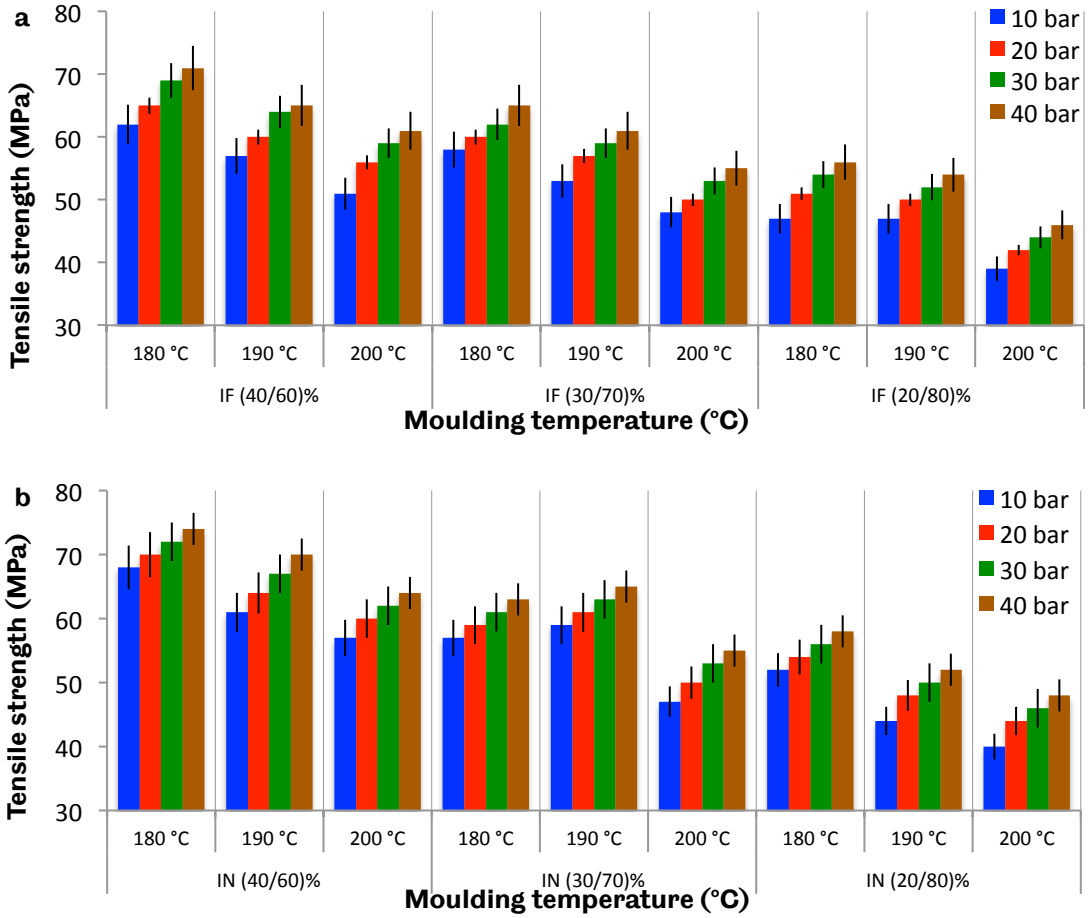

Figure 5.6 Effect of processing parameters on the tensile strength of a) IF composites and b) IN composites of 40%, 30%, 20 wt%, for 10 composites from each composite category, The x-axis presents the moulding temperatures tested from 180 °C to 200 °C. The blue, red, green and brown coloured bars represent the extrusion pressures tested at 10 bar, 20 bar, 30 bar and 40 bar, respectively. For each processing parameters tested, the composites were manufactured with constant values of moulding time of 1 min, moulding and cooling pressure at 500 bar and 300 bar respectively. Notice that the lower value of tensile strength axis are omitted in order to improve the readability of the plot. The error bars represent ±1SD (samples tested for every set of error bars n=5).

Composites manufactured with moulding temperature of 200 °C and above had decreased tensile strength and stiffness values due to the thermal degradation of the fibres. The variation in the Young's modulus values according to different values of moulding temperature and extrusion pressure can be seen in Table 5.3.

Table 5.3 Effect of processing parameters on the Young's modulus (GPa) of a) MPN and MPF and b) IN and IF composites of 40%, 30% and 20 wt%, The error bars represent ±1SD (samples tested for every set of error bars n=5).

a)	Extrusion pressure (Bar)/ Moulding temperature (°C)						
MPN (40/60)%	180	190	200		**MPF (40/60)%**	180	190	200
10	6.3±1.1	6.5±1.3	6.0±1.0		10	5.0±1.0	5.2±1.2	4.7±1.1
20	6.4±1.0	6.6±1.1	6.1±1.2		20	5.1±1.0	5.3±1.1	4.8±1.0
30	6.5±1.0	6.7±1.2	6.3±1.2		30	5.2±1.1	5.4±1.0	5.0±1.2
40	6.6±1.0	**6.8±1.2**	6.4±1.1		40	5.3±1.0	**5.5±1.1**	5.0±1.2
MPN (30/70)%	180	190	200		**MPF (30/70)%**	180	190	200
10	5.2±1.1	6.4±1.2	6.0±1.0		10	4.2±1.1	4.5±1.3	4.1±1.1
20	6.3±1.2	6.5±1.1	6.1±1.2		20	4.3±1.2	4.6±1.0	4.2±1.0
30	6.4±1.0	6.6±1.1	6.2±1.1		30	4.4±1.1	4.7±1.3	4.3±1.0
40	6.5±1.1	**6.7±1.1**	6.3±1.0		40	4.6±1.0	**4.8±1.2**	4.4±1.1
MPN(20/80)%	180	190	200		**MPF(20/80)%**	180	190	200
10	6.0±1.1	6.2±1.0	4.8±1.3		10	4.2±1.0	4.4±1.1	3.9±1.0
20	6.1±1.0	6.3±1.2	5.9±1.1		20	4.3±0.9	4.5±0.9	4.0±0.9
30	6.2±1.1	6.4±1.3	6.0±1.1		30	4.4±1.0	4.6±1.1	4.1±0.9
40	6.3±1.2	**6.5±1.2**	6.1±1.1		40	4.5±0.8	**4.7±0.9**	4.2±0.8

b)	Extrusion pressure (Bar)/ Moulding temperature (°C)						
IN (40/60)%	180	190	200		**IF(40/60)%**	180	190	200
10	4.2±1.1	4.1±1.3	3.8±1.2		10	4.6±1.1	4.5±1.1	4.3±1.0
20	4.3±0.9	4.2±1.0	3.9±1.1		20	4.7±1.2	4.6±1.2	4.4±0.9
30	4.4±1.1	4.3±1.1	4.0±1.0		30	4.8±1.1	4.7±1.0	4.5±1.0
40	**4.5±1.0**	4.4±1.2	4.1±0.9		40	**4.9±1.0**	4.8±1.1	4.6±1.2
IN (30/70)%	180	190	200		**IF(30/70)%**	180	190	200
10	3.7±1.1	3.6±1.0	3.3±1.0		10	3.7±1.0	3.6±1.0	3.3±1.1
20	3.8±0.9	3.7±1.2	3.4±1.0		20	3.8±1.0	3.7±1.2	3.4±0.9
30	3.9±1.1	3.8±1.2	3.5±1.2		30	3.9±1.1	3.8±1.1	3.5±1.3
40	**4.0±1.0**	3.9±1.1	3.6±1.1		40	**4.0±1.0**	3.9±1.1	3.6±1.1
IN (20/80)%	180	190	200		**IF(20/80)%**	180	190	200
10	3.5±1.0	3.4±0.8	3.1±1.0		10	3.7±1.0	3.6±1.0	3.3±1.1
20	3.6±0.8	3.5±1.0	3.2±1.0		20	3.8±1.0	3.7±1.2	3.4±0.9
30	3.7±1.0	3.6±1.0	3.3±0.9		30	3.9±1.1	3.8±1.1	3.5±1.3
40	**3.8±0.9**	3.7±0.8	3.4±0.8		40	**4.0±1.0**	3.9±1.1	3.6±1.1

Gassan and Bledzki studied the thermal degradation of flax fibres, testing the fibres between 170 °C and 210 °C, and reported reduction of the flax fibre properties as the temperature increased [93]. Shibata *et al.* also reported a reduction in the viscosity of PLA, which Floreon is based on, at temperatures close to 200 °C, which turned the composite into a more brittle material [300].

Summarising the tensile properties, a higher tensile strength and Young's modulus were obtained in the case of MPN (40/60)% and MPF (40/60)% composites. The optimised processing parameters were an extrusion pressure of 40 bar, and moulding and cooling pressure at 500 bar and 300 bar respectively. The moulding temperature was 190 °C for composites with MP fibres, and 180 °C for composites with I fibres.

The mechanical properties for flax/PLA composites reported in the literature vary. Nassiopoulos *et al.* reported a tensile strength and modulus of flax/PLA composites of 72 MPa and 13 GPa, respectively [301]. Different studies reported an average tensile strength of 54 MPA and 53 MPa for flax/PLA composites of 30 wt% fibre content [92], [302]. In the case of nettle/PLA composites, a tensile strength of 59 MPa (30 wt% fibre content) and 50.5. MPa was reported [192], [303].

Compared to the tensile properties of the injection-moulded composites obtained in previous studies, the composite's tensile strength results are higher in this study. These differences are due to the individual materials used, the fibre preparation processes, and selected processing parameters. This study used Floreon, rather than PLA, as in previous studies. Floreon has higher tensile strength than PLA. Additionally, flax and nettles fibres have significant variability in plant growth conditions (geographical origin, local climate), fibre extraction processes, and measurement conditions (tensile speed, initial gauge length, moisture, temperature, different cross section of fibres at different points), affecting both the fibre's mechanical properties and the final composite's properties [31], [63].

5.2.3.2 Flexural properties

The selected processing parameters were an extrusion pressure of 40 bar, moulding pressure of 500 bar, and cooling pressure of 300 bar (cooling and moulding time at 1 minute). The extrusion and moulding temperature for MPF and MPN composites was 190 °C, and 180 °C for the IF and IN composites. The flexural stress, strain, and flexural modulus were calculated using Equations 4.5–4.7. Composites showed a significant improvement on the flexural stress results compared to Floreon as it can be seen in Figure 5.7.

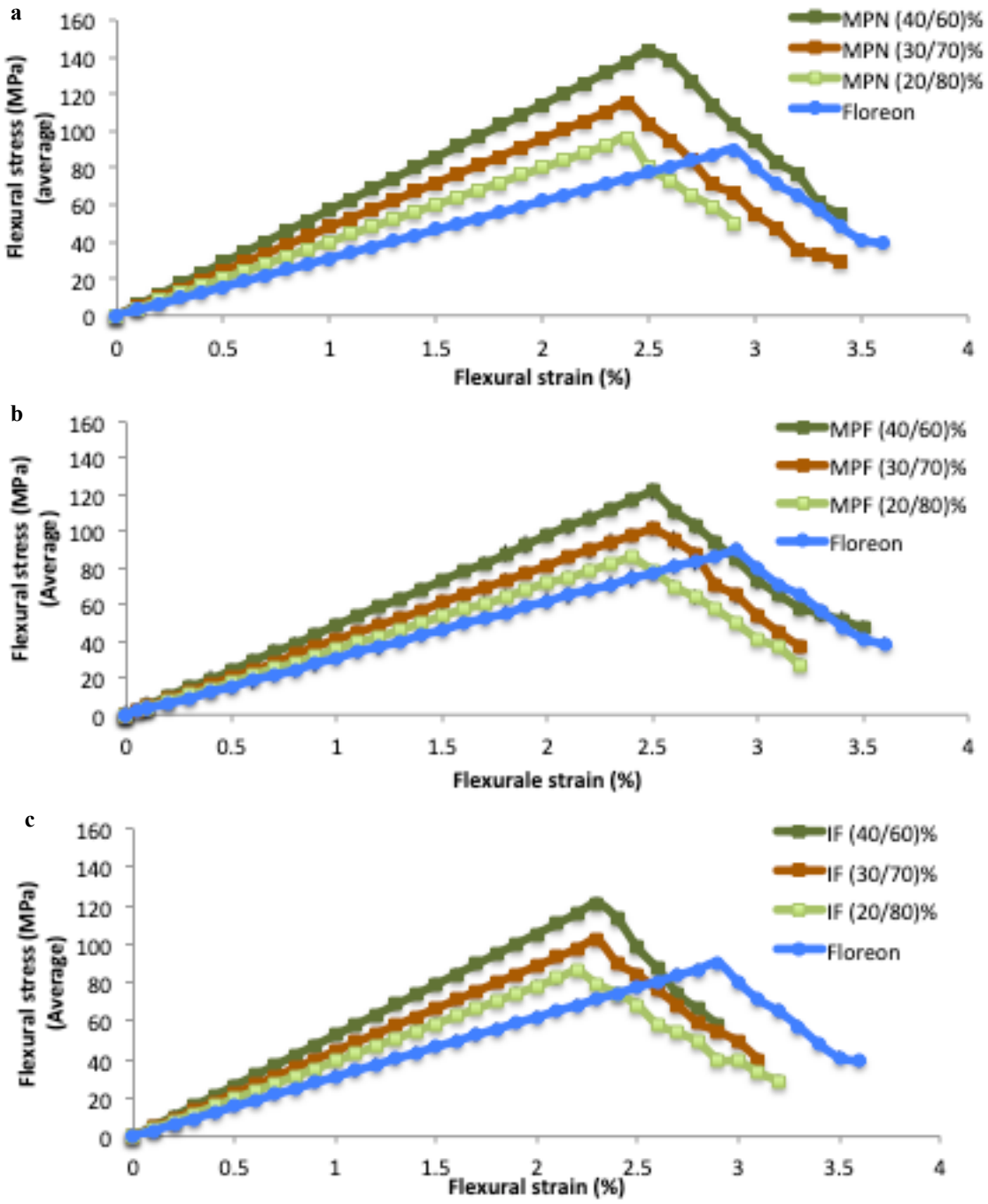
a
Flexural stress (MPa) (average)
Flexural strain (%)
MPN (40/60)%
MPN (30/70)%
MPN (20/80)%
Floreon
b
Flexural stress (MPa) (Average)
Flexurale strain (%)
MPF (40/60)%
MPF (30/70)%
MPF (20/80)%
Floreon
c
Flexural stress (MPa) (Average)
Flexural strain (%)
IF (40/60)%
IF (30/70)%
IF (20/80)%
Floreon

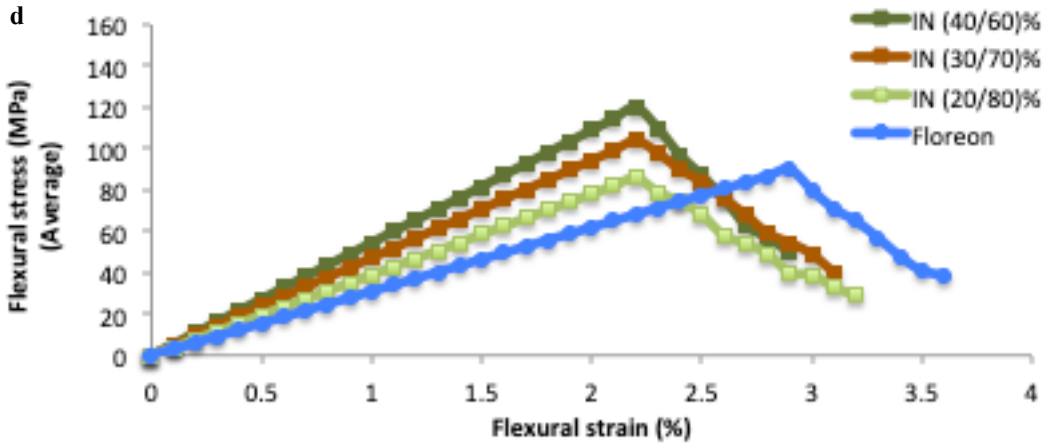

Figure 5.7 Flexural stress-strain curves of Floreon, a) MPN, b) MPF, c) IF and d) IN composites of 40%, 30%, 20 wt%, for 50 composites from each composite category. Floreon and composites were made using extrusion pressure of 40 bar, moulding pressure of 500 bar and moulding time at 1 minute moulding time. The moulding temperature for composites consisting of MP fibres was set up at 190 °C and at 180°C for the corresponding composites with I fibres. The error bars represent ±1SD (samples tested for every set of error bars n=10).

Figure 5.8 shows the flexural strength results (the maximum stress composites can withstand before failure) for Floreon and the different composite types.

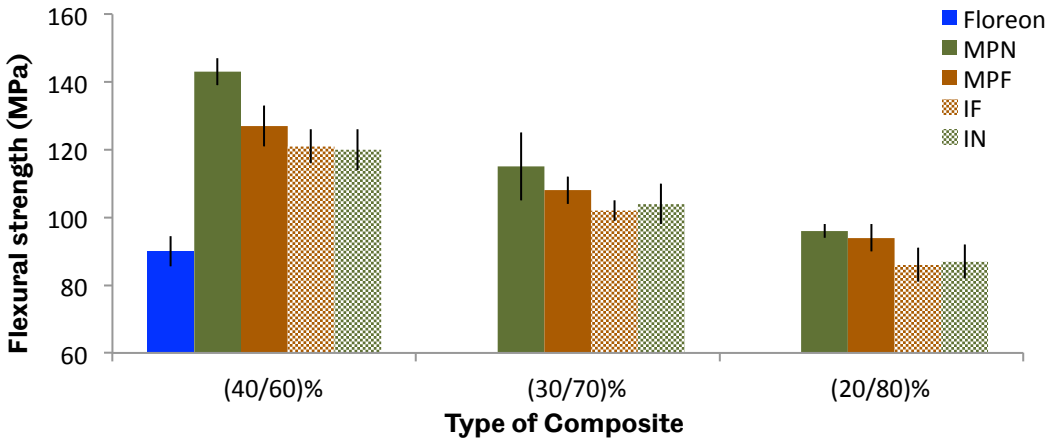

Figure 5.8 Flexural strength (average) of Floreon and Floreon based composites of 40%, 30%, 20 wt%, for 50 composites from each composite category. Floreon and composites were made using extrusion pressure of 40 bar, moulding pressure of 500 bar and moulding time of 1 minute. The moulding temperature for composites consisting of MP fibres was set up at 190 °C and at 180 °C for the corresponding composites with I fibres. The notation MPN and MPF referred to composites consisting of minimally processed nettle (solid green bars) and minimally processed flax fibres (solid brown bars) respectively. The notation IN and IF referred to composites consisting of industrial processed nettle (dashed green bars) and industrial processed flax fibres (dashed brown bars) respectively. Notice that the lower value of flexural strength axis are omitted in order to improve the readability of the plot. The error bars represent ±1SD (samples tested for every set of error bars n=10).

Flexural strength followed the same trend as the tensile strength results for composites, with the highest results obtained for composites with higher fibre content. Maximum flexural strength results were obtained for composites consisting of MPF and MPN of 40 wt% fibre content. MPN40-190-40-1 had the highest flexural strength at 143 ± 4 MPa, followed by MPF40-190-40-1 with a flexural strength of 127 ± 6 MPa.

The flexural strength results were much higher compared with the corresponding tensile strength results, as expected and reported in previous studies [157], [304]. The injection-moulded composites included small defects (voids), as presented in Table 5.2 that concentrate the applied force locally, making the composite weaker at these points. During three-point bending tests, the strongest fibres carry the applied force and contribute to the flexural strength results. In contrast, during the tensile tests, all reinforcing fibres carry the same applied force, and the tensile strength is based on the failure of the weaker materials [156], [305].

The highest flexural modulus was once again observed in the composites consisting of MP fibres. At higher fibre contents, flexural modulus reached higher values as it can be seen in Figure 5.9.

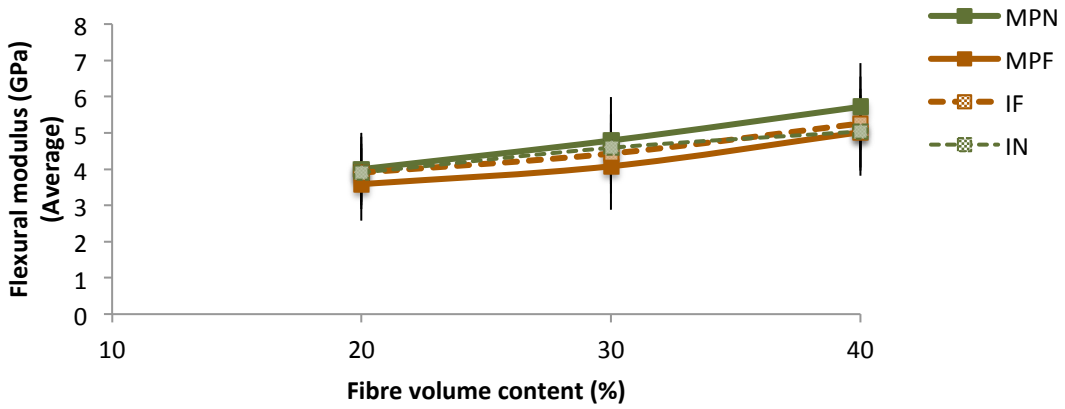

Figure 5.9 Flexural modulus as a function of fibre volume content of MPN, MPF, IF and IN composites of 40%, 30%, 20 wt% fibre content. The error bars represent ±1SD (samples tested for every set of error bars n=10).

The flexural properties of composites were studied according to the different applied processing parameters to identify potential effects of the moulding parameters on the composite's properties. Figure 5.10 a–b shows the flexural strength results obtained for MPF and MPN composites.

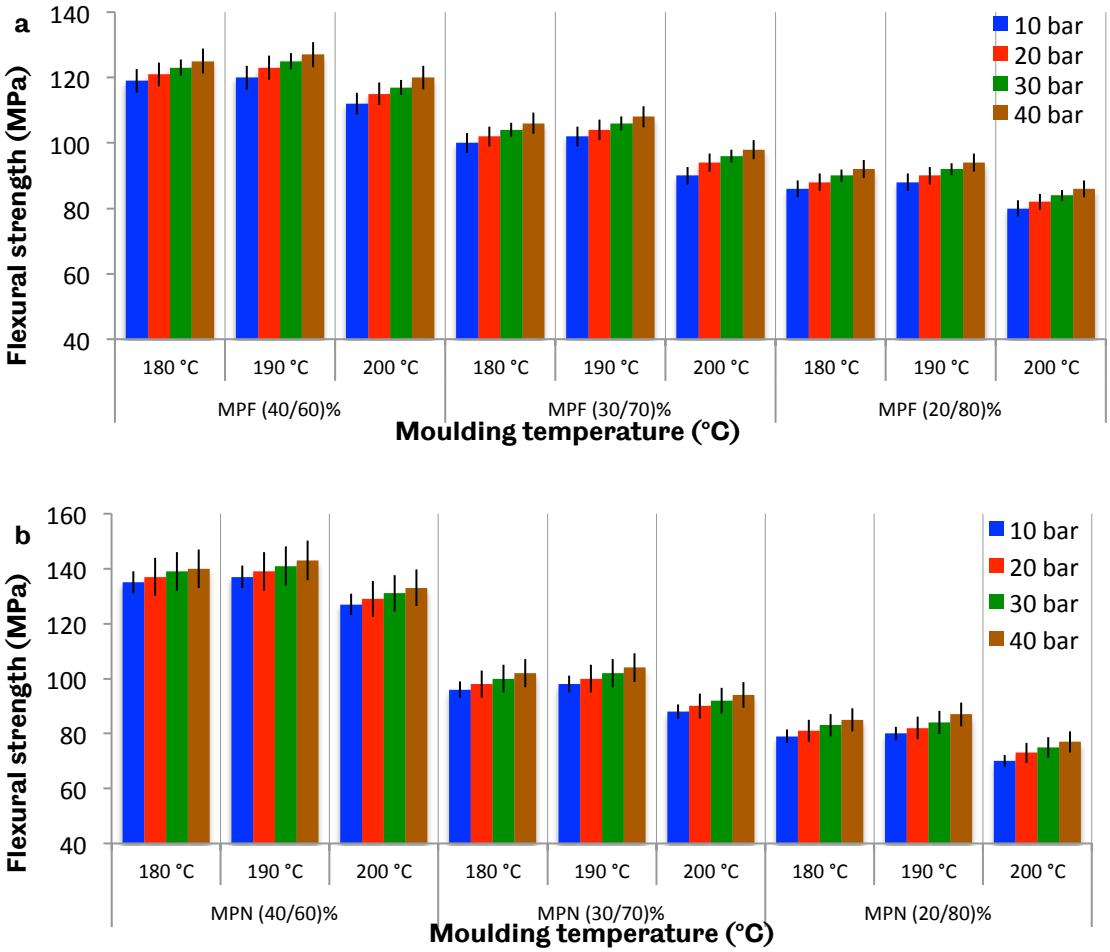

Figure 5.10 Effect of processing parameters on the flexural strength of a) MPF composites and b) MPN composites of 40%, 30%, 20 wt%, for 10 composites from each composite category, The x-axis presents the moulding temperatures tested from 180 °C to 200 °C. The blue, red, green and brown coloured bars represent the extrusion pressures tested at 10 bar, 20 bar, 30 bar and 40 bar, respectively. For each processing parameters tested, the composites were manufactured with constant values of moulding time of 1 min, moulding and cooling pressure at 500 bar and 300 bar respectively. Notice that the lower value of flexural strength axis are omitted in order to improve the readability of the plot. The error bars represent ±1SD (samples tested for every set of error bars n=5).

The highest flexural strength results were obtained at extrusion pressure of 40 bar and at moulding temperature of 190 °C during the extrusion procedure for MPF and MPN composites. The results are in agreement with previous studies, where Yuan *et al.* reported that the flexural strength of flax/PLA composites increased as the moulding temperature increased for fibre concentration between 30–50% [292]. No changes in the flexural strength results were observed with different moulding times, so a moulding time of one minute was applied for all composites during the extrusion procedure.

In the case of IF and IN composites, the highest flexural strength results were observed at a moulding temperature of 180 °C and at a moulding pressure of 40 bar, as can be seen in Figures 5.11 a–b. The IF40-180-40-1 composite had the highest flexural strength of 121 ± 5 MPa and IN40-180-40-1 had a flexural strength of 124 ± 6 MPa.

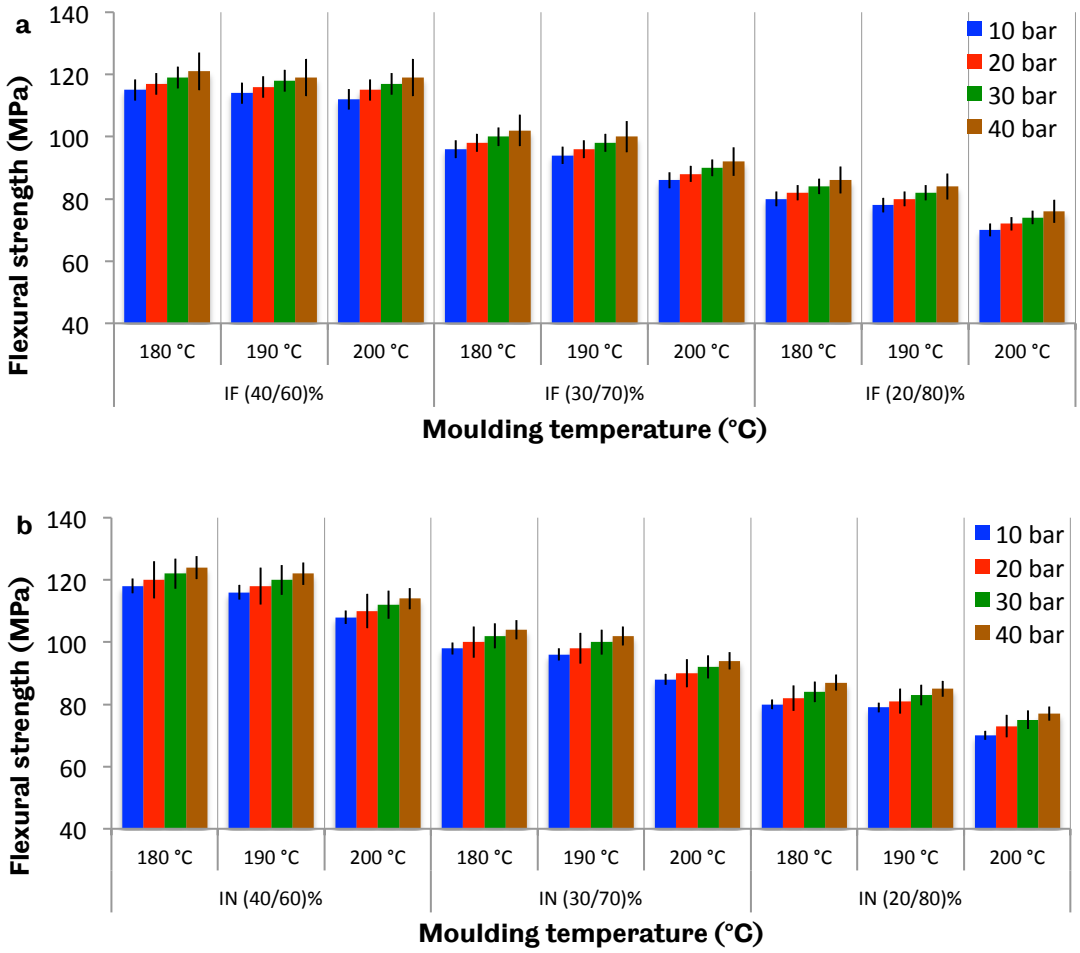

Figure 5.11 Effect of processing parameters on the flexural strength of a) IF composites and b) IN composites of 40%, 30%, 20 wt%, for 10 composites from each composite category. The x-axis presents the moulding temperatures tested from 180 °C to 200 °C. The blue, red, green and brown coloured bars represent the extrusion pressures tested at 10 bar, 20 bar, 30 bar and 40 bar, respectively. For each processing parameters tested, the composites were manufactured with constant values of moulding time of 1 min, moulding and cooling pressure at 500 bar and 300 bar respectively. Notice that the lower value of flexural strength axis are omitted in order to improve the readability of the plot. The error bars represent ±1SD (samples tested for every set of error bars n=5).

The maximum obtained flexural modulus were again observed in the case of MPF40-190-40-1 and MPN40-190-40-1, with 5.0 ± 2.2 GPa and 5.7 ± 1.9 GPa respectively, compared to the Floreon's flexural modulus of 3.1 ± 0.9 GPa. Table 5.4

summarises the flexural modulus according to the different applies processing parameters.

Table 5.4 Effect of processing parameters on the flexural modulus (GPa) of a) MPN and MPF and b) IN and IF composites of 40%, 30% and 20 wt%, The error bars represent ±1SD (samples tested for every set of error bars n=5).

a)	Extrusion pressure (Bar)/ Moulding temperature (°C)						
MPN (40/60)%	180	190	200		**MPF (40/60)%**	180	190	200
10	5.2±1.8	5.4±1.5	4.9±1.0		10	4.5±1.7	4.7±2.2	4.2±1.4
20	5.3±1.7	5.5±1.6	5.0±1.2		20	4.6±1.8	4.8±2.1	4.3±1.3
30	5.4±1.7	5.6±1.7	5.1±1.2		30	4.7±1.7	4.9±2.0	4.4±1.4
40	5.5±1.8	**5.7±1.9**	5.2±1.1		40	4.8±1.8	**5.0±2.2**	4.5±1.2
MPN (30/70)%	180	190	200		**MPF (30/70)%**	180	190	200
10	4.2±1.6	4.5±1.6	4.0±1.6		10	3.5±1.5	3.7±1.7	3.1±1.1
20	4.3±1.7	4.6±1.5	4.1±1.6		20	3.6±1.6	3.8±1.7	3.2±1.0
30	4.4±1.7	4.7±1.7	4.2±1.4		30	3.7±1.5	3.9±1.9	3.3±1.0
40	4.5±1.8	**4.8±1.7**	4.3±1.8		40	3.8±1.6	**4.0±2.0**	3.4±1.1
MPN(20/80)%	180	190	200		**MPF(20/80)%**	180	190	200
10	3.4±1.5	3.7±1.6	3.1±1.3		10	3.0±1.0	3.2±1.1	2.7±1.2
20	3.5±1.6	3.8±1.5	3.2±1.1		20	3.1±1.3	3.3±1.2	2.8±1.1
30	3.6±1.8	3.9±1.6	3.3±1.1		30	3.2±1.1	3.4±1.3	2.9±1.0
40	3.7±1.5	**4.0±1.7**	3.4±1.1		40	3.3±1.2	**3.5±1.2**	3.0±0.9

b)	Extrusion pressure (Bar)/ Moulding temperature (°C)						
IN (40/60)%	180	190	200		**IF(40/60)%**	180	190	200
10	4.7±1.7	4.5±1.7	4.2±1.2		10	4.9±1.0	4.5±1.5	4.3±1.5
20	4.8±1.8	4.6±1.8	4.3±1.4		20	5.0±1.2	4.6±1.4	4.4±1.4
30	4.9±1.6	4.7±1.7	4.4±1.4		30	5.1±1.2	4.7±1.5	4.5±1.3
40	**5.0±1.8**	4.8±1.8	4.5±1.5		40	**5.2±1.0**	4.8±1.4	4.6±1.5
IN (30/70)%	180	190	200		**IF(30/70)%**	180	190	200
10	4.3±1.3	4.1±1.0	3.8±1.2		10	4.1±1.0	3.9±1.2	3.8±1.1
20	4.4±1.4	4.2±1.2	3.9±1.3		20	4.2±1.2	4.0±1.2	3.9±1.2
30	4.5±1.2	4.3±1.4	4.0±1.3		30	4.3±1.4	4.1±1.1	4.0±1.3
40	**4.6±1.0**	4.4±1.0	4.1±1.4		40	**4.4±1.0**	4.2±1.2	4.1±1.5
IN (20/80)%	180	190	200		**IF(20/80)%**	180	190	200
10	3.6±1.2	3.4±0.9	3.1±1.0		10	3.2±1.1	3.0±1.0	2.7±1.0

20	3.8±1.1	3.5±1.0	3.2±1.1		20	3.3±1.2	3.1±1.0	2.8±1.0
30	3.8±1.0	3.6±0.9	3.3±1.0		30	3.4±1.2	3.2±1.0	2.9±0.9
40	**3.9±1.1**	3.7±0.8	3.4±0.8		40	**3.5±1.0**	3.3±0.9	3.0±0.9

Summarising the flexural properties, an increase in the composite's flexural properties was observed compared to pure Floreon samples, as seen in Figure 5.8. The fibres acted as reinforcing materials that strengthened both the flexural strength and flexural modulus of the composites. The flexural strength of all types of composites was higher at higher fibre contents (maximum fibre content used at 40 wt%); with the MPF and MPN fibres further enhancing the properties of the composites compared to industrially processed fibre composites.

A similar study reported a flexural strength of 138.5 MPa and maximum flexural modulus of 7.93 GPa (50% flax content at a moulding temperature of 180 °C and moulding time of 5 minutes) [147]. The reported flexural strength of nettle/PLA composites was 87 MPa (50% nettle content), which is much lower than the present results [192]. As observed in the tensile properties of the injection-moulded composites of the present study (section 5.2.3.1), the obtained flexural strength is much higher, highlighting the use of Floreon as the binding matrix and MP fibres (flax and nettles) as reinforcing materials to enhance the composite's properties.

The results of the investigation of composite tensile and flexural properties based on the fibre type, concentration, and processing parameters are presented in Table 5.3. Mechanical properties from the literature were compared with the values of industrial fibre composites, as the preparation processes for these fibres included additional steps compared to the minimally processed fibres.

The tensile and flexural properties of the injection-moulded composites are different than the corresponding values from the literature as it can be seen in Table 5.5. Specifically, the injection-moulded composites reinforced with MPF and MPN fibres have higher tensile and flexural properties compared with previous studies, proving that the fibre's preparation process has a significant influence on the fibre's (chapter 3) and composite's mechanical properties. The use of nettle fibres with minimal process as reinforcing materials has the greater improvement in the mechanical properties of Floreon compared to MPF, IN and IF fibres. In this study, the manufacture of a green-composite with the combination of nettle fibres and Floreon was achieved. Both individual raw materials extracted by renewable resources without the use of chemical treatment. The MPN composites produced had sufficient high tensile and flexural properties. Nevertheless, the limitations that have been occurred during manufacturing experiments such as the use of specific

fibre content and extrusion pressure values due to the limitations of the extruder should not be overlooked.

Table 5.5 Tensile and flexural strength (average), Young's and flexural modulus of MPN, MPF, IF and IN composites, for 50 tested composites from each composite category, compared to literature values.

Composite type	Tensile strength (MPa)	Young's modulus (GPa)	Flexural strength (MPa)	Flexural modulus (GPa)	Literature Tensile strength (MPa)/ Young's modulus (GPa) References	Literature Flexural strength (MPa)/ Flexural modulus (GPa) References
MPN (40/60)%	85	6.8	143	5.7		
(30/70)%	76	6.7	115	4.8		
(20/80)%	65	6.5	96	4		
MPF (40/60)%	77	5.5	127	5.0		
(30/70)%	68	4.8	108	4.0		
(20/80)%	59	4.7	94	3.5		
IF (40/60)%	71	4.9	121	5.4	100 MPa/ [2] 13 GPa / [306]	138 MPa/ [147] 7 GPa/ [292]
(30/70)%	65	4	102	4.4	54/ [23] 8 GPa/ [2]	
(20/80)%	56	4	86	4.0		
IN (40/60)%	74	4.5	120	5.0	(40-52) MPa/ [192]	87 MPa/ [192]
(30/70)%	67	4	104	4.6	59 MPa/ [25] 5 GPa/ [192]	
(20/80)%	58	3.8	87	3.9		

5.2.4 Statistical Analysis

For the evaluation of the statistical significant differences between composites consisting of different fibre contents and concentrations, ANOVA single factor test was performed. The p-value was calculated in order to identify the statistically significant differences between the produced composites.

Table 5.6 Statistical test for the identification of statistically significant difference. Anova-single factor test was applied for the calculation of p-value for tensile strength of MPN, MPF, IN and IF composites consisting of 20%, 30% and 40% fibre content. P- values smaller than 0.005 (yellow highlighted) present statistically significant difference between the tested composites, while P-values higher than 0.005 (red highlighted) represent not statistically significant differences between the tested composites. Table 5.6a) presented the p-values for the tensile strength, b) Young's modulus, c) flexural strength and d) flexural modulus of MPN, MPF, IN and IF composites.

a)		MPN	MPF	IN	IF	MPN	MPF	IN	IF	MPN	MPF	IN	IF
%		(20/80)%				(30/70)%				(40/60)%			
20/80	MPN	-	-	-	-	-	-	-	-	-	-	-	-
	MPF	3E-12	-	-	-	-	-	-	-	-	-	-	-
	IN	3E-12	2E-12	-		-	-	-	-	-	-	-	-
	IF	2E-12	2E-12	2E-3	-	-	-	-	-	-	-	-	-
30/70	MPN	5E-13	8E-13	7E-13	6E-13	-	-	-	-	-	-	-	-
	MPF	5E-13	5E-13	6E-13	6E-13	2E-13	-	-	-	-	-	-	-
	IN	7E-13	6E-13	1E-3	3E-3	3E-13	2E-12	-		-	-	-	-
	IF	9E-12	4E-13	3E-3	2E-3	3E-13	4E-12	5E-3	-	-	-	-	-
40/60	MPN	7E-15	3E-14	6E-14	4E-15	2E-17	5E-18	5E-19	2E-3	-	-	-	-
	MPF	6E-16	6E-15	3E-14	3E-14	4E-17	6E-18	7E-19	5E-3	5E-12	-	-	-
	IN	7E-15	4E-14	7E-3	7E-3	4E-17	7E-2	4E-2	4E-3	4E-12	2E-15	-	-
	IF	5E-15	4E-15	7E-3	7E-3	3E-17	7E-2	9E-2	2E-3	3E-11	3E-13	5E-3	-

b)		MPN	MPF	IN	IF	MPN	MPF	IN	IF	MPN	MPF	IN	IF
%		(20/80)%				(30/70)%				(40/60)%			
20/80	MPN	-	-	-	-	-	-	-	-	-	-	-	-
	MPF	4E-13	-	-	-	-	-	-	-	-	-	-	-
	IN	6E-13	2E-14	-		-	-	-	-	-	-	-	-
	IF	6E-13	4E-14	9E-2	-	-	-	-	-	-	-	-	-
30/70	MPN	8E-12	8E-13	5E-3	7E-2	-	-	-	-	-	-	-	-
	MPF	9E-12	5E-13	4E-3	7E-2	6E-12	-	-	-	-	-	-	-
	IN	3E-12	6E-13	5E-3	8E-2	4E-13	9E-12	-		-	-	-	-
	IF	6E-12	4E-13	4E-3	9E-2	5E-12	3E-13	5E-3	-	-	-	-	-
40/60	MPN	7E-16	4E-16	3E-3	2E-3	5E-11	9E-15	5E-13	2E-3	-	-	-	-
	MPF	8E-16	6E-16	3E-3	5E-3	6E-12	6E-15	6E-12	5E-3	4E-15	-	-	-
	IN	5E-16	7E-16	2E-3	5E-3	9E-12	8E-15	7E-2	4E-3	4E-15	2E-15	-	-
	IF	3E-16	8E-16	5E-3	2E-3	2E-12	2E-15	8E-2	2E-3	2E-15	8E-15	6E-3	-

c)		MPN	MPF	IN	IF	MPN	MPF	IN	IF	MPN	MPF	IN	IF
%		(20/80)%				(30/70)%				(40/60)%			
20/80	MPN	-	-	-	-	-	-	-	-	-	-	-	-
	MPF	7E-18	-	-	-	-	-	-	-		-	-	-
	IN	6E-18	5E-18	-		-	-	-	-		-	-	-
	IF	6E-18	2E-18	9E-3	-	-	-	-	-		-	-	-

30/70	**MPN**	5E-19	3E-19	5E-19	6E-19	-	-	-	-	-	-	-	-
	MPF	5E-19	2E-19	4E-19	4E-19	6E-18	-	-	-	-	-	-	-
	IN	5E-19	3E-19	5E-3	4E-3	3E-18	3E-18	-		-	-	-	-
	IF	7E-19	5E-19	6E-3	5E-3	4E-18	5E-18	4E-3	-	-	-	-	-
40/60	**MPN**	7E-18	7E-18	6E-18	-	2E-17	2E-17	5E-16	6E-14	-	-	-	-
	MPF	4E-18	4E-18	7E-18	-	5E-17	3E-17	5E-16	5E-14	7E-17	-	-	-
	IN	3E-18	6E-18	4E-3	2E-3	7E-17	7E-2	4E-2	8E-2	5E-17	2E-18	-	-
	IF	4E-18	7E-18	2E-3	4E-3	8E-17	7E-2	9E-2	2E-3	2E-17	7E-18	7E-3	-

d)		**MPN**	**MPF**	**IN**	**IF**	**MPN**	**MPF**	**IN**	**IF**	**MPN**	**MPF**	**IN**	**IF**
%		**(20/80)%**				**(30/70)%**				**(40/60)%**			
20/80	**MPN**	-	-	-	-	-	-	-	-	-	-	-	-
	MPF	4E-14	-	-	-	-	-	-	-	-	-	-	-
	IN	2E-14	6E-14	-	-	-	-	-	-	-	-	-	-
	IF	3E-14	7E-14	5E-3	-	-	-	-	-	-	-	-	-
30/70	**MPN**	7E-15	5E-14	5E-3	7E-3	-	-	-	-	-	-	-	-
	MPF	5E-15	5E-14	3E-3	3E-3	7E-15	-	-	-	-	-	-	-
	IN	3E-16	2E-14	4E-3	5E-3	4E-15	4E-16	-		-	-	-	-
	IF	2E-15	3E-14	7E-3	6E-3	2E-15	5E-16	7E-3	-	-	-	-	-
40/60	**MPN**	8E-15	4E-16	7E-2	8E-2	5E-17	6E-17	3E-2	6E-2	-	-	-	-
	MPF	2E-16	5E-16	4E-3	7E-2	4E-17	5E-17	4E-3	8E-2	3E-17	-	-	-
	IN	6E-15	4E-16	4E-3	3E-3	9E-17	3E-17	2E-2	4E-3	3E-17	3E-17	-	-
	IF	3E-15	8E-16	6E-2	2E-2	2E-17	2E-17	5E-3	8E-2	2E-17	2E-17	9E-3	-

Statistically significant differences were found between composites consisting of different fibre types and concentrations. Comparing the tensile strength, Young's modulus, flexural strength and flexural modulus of MPN and MPF composites of all fibre concentrations are statistically significant as the calculated p-values are smaller than 0.005 (Table 5.6). Statistical insignificant differences were found between the IN and IF composites.

5.2.5 Pull-out test

As the previous section has shown, increasing fibre content significantly improves the composite properties across all types of samples produced. However, in order to better understand how the fibre types and the preparation processes differ and interact with the matrix, single fibre pull-out tests were explored.

In order to identify the level of adhesion between the reinforcing fibres and matrix, MP and I, flax and nettle single fibres were embedded in Floreon and tested using a single fibre pull-out test. From the results of this pull-out test, the interfacial shear strength (IFSS) was calculated as an indication of the fibre/matrix adhesion. IFSS was measured by pulling a single fibre out of Floreon by using a Zwick Roell ZTN

0.5 tensile testing machine with load cell of 0.5 kN and head speed of 1 mm/minute. The IFSS was calculated using Equation4.14.

Figure 5.12 shows the calculated IFSS for different types of fibres. For the IFSS calculation, specimens that presented debonding between the fibre and matrix were taken into account, while specimens in which fibre failure was observed were dismissed. For the single fibre pull-out test, a uniform stress distribution, uniform fibre diameter, and homogenous adhesion between fibre and Floreon were assumed.

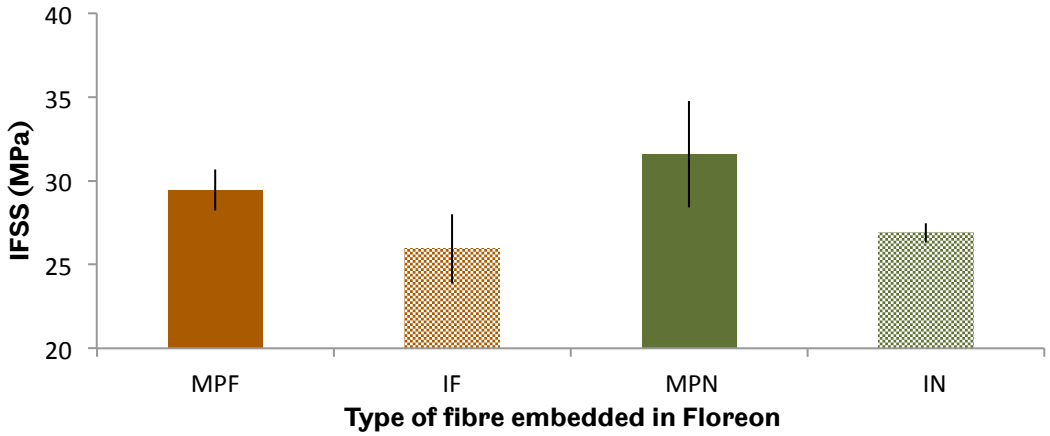

Figure 5.12 IFSS results of single fibres embedded in Floreon for 5 fibres from each fibre type. The notation MPF is referred to the use of minimally processed flax single fibre (solid brown bar) and MPN to the corresponding minimally processed flax single fibre (solid green bar). The notation IF is referred to the use of industrial processed flax single fibre (dashed brown bar) and IN to the corresponding industrial processed flax single fibre (dashed green bar). Notice that the lower value of IFSS axis are omitted in order to improve the readability of the plot. The error bars represent ±1SD (samples tested for every set of error bars n=3).

The highest IFSS results were obtained with MPF and MPN fibres at 29.5 ± 1.2 MPa and at 31.6 ± 3.1 MPa respectively, indicating better adhesion between MP fibres with Floreon. The IFSS results for IF and IN fibres were at, 25.9 ± 2.1 MPa and 26.9 ± 1.9 MPa respectively. After the pull-out tests, the fibres were examine under Leica DM LM optical microscope for the validity of the pull-out tests. The fibres were pulled cleanly out of the matrix, testifying that the tests were valid.

Values from the literature for flax fibres embedded in PLA was 28.3 MPa, indicating that the surface and chemical treatment of fibres increased the IFSS results and improved the adhesion between the fibres with the surrounding matrix [143]. Alkali treated flax fibres ended with a rougher fibre surface, while it formed more contacting points with PLA matrix leading to an enhanced adhesion between PLA

and flax fibres [307]. There are currently no references regarding pull-out tests for nettle/PLA samples.

The critical fibre length was calculated using Equation4.15, the fibre aspect ratio using Equation4.16, and the results presented in Table 5.7. The values of critical fibre length are presented as a range of results due to the non-uniform structure of fibres and the different diameters of each tested sample. The calculated critical fibre length was used as an indicator for the ideal chopped length of fibres used in composites. Reports indicate a critical fibre length of 1.95 mm for flax/PLA samples, highlighting the influence of cross-section area of the fibres [143].

The effect of the fibre aspect ratio on the mechanical properties of fibre-reinforced composites has been investigated. Higher tensile strength and Young's modulus at higher aspect ratios for flax fibre-reinforced composites have been reported [130], [143]. The tensile properties of composites increase as the fibre aspect ratio increases, reaching a plateau when the fibre aspect ratio overcome a specific value determined from the type and length of the reinforcing fibres [308].

Table 5.7 Critical fibre lengths and aspect ratio of MPF, MPN, IN and IF fibres.

Fibre	**L_c (mm)**	**Aspect ratio**	**Average Aspect ratio**
Flax (I)	2-3 ± 0.2	68.9-136	102.45 ± 34
Flax (MP)	2-5 ± 0.3	54.0-333	193 ± 139
Nettle (I)	2-3 ± 0.4	74.0-111	185 ± 74
Nettle (MP)	2-5 ± 0.4	44.4-333.3	188.7 ± 144.3

5.2.6 Thermal properties

Fibre-reinforced composites can be used in many applications as structural components including automotive and aerospace engine components. Therefore, in many cases the composites are exposed to high temperatures that might affect the composite's properties. The thermal properties of composites, especially the glass transition temperature (T_g) and melting temperature (T_m), can indicate if a material can be used in specific applications.

The thermal properties of Floreon and the different types of composites created were evaluated using DMA and DSC. The T_g of Floreon and different composites types was determined by DMA, testing three Floreon and composite samples from each composite category. Figure 5.10a shows the dynamic properties of the tested samples. The T_g of Floreon was 65 ± 0.2 °C and between 66–68 °C for composites. No significant difference in T_g was observed between the different types of composites. Additionally, the fibre content did not affect the T_g of composites, which is in agreement with the wider literature. Previous studies indicated that although the mechanical properties improved for higher fibre content, T_g did not change significantly [309], [310].

The introduction of reinforcing fibres affected the tanδ peak (Figure 5.13a). This may indicate a poor adhesion between the fibres and matrix, resulting in the dissipation of more energy and thus higher tanδ peaks compared to composites with stronger adhesion [311].

As seen in Figure 5.13b, enhancement of the storage modulus, a measurement of the elastic response of a material by calculating the stored energy, (E') of composites with 40 wt% fibre content compared to Floreon was observed over the entire temperature range. The increased E' of composites means that the reinforcing flax and nettle fibres increase Floreon's capacity to support the composite under mechanical pressures with recoverable viscoelastic deformation.

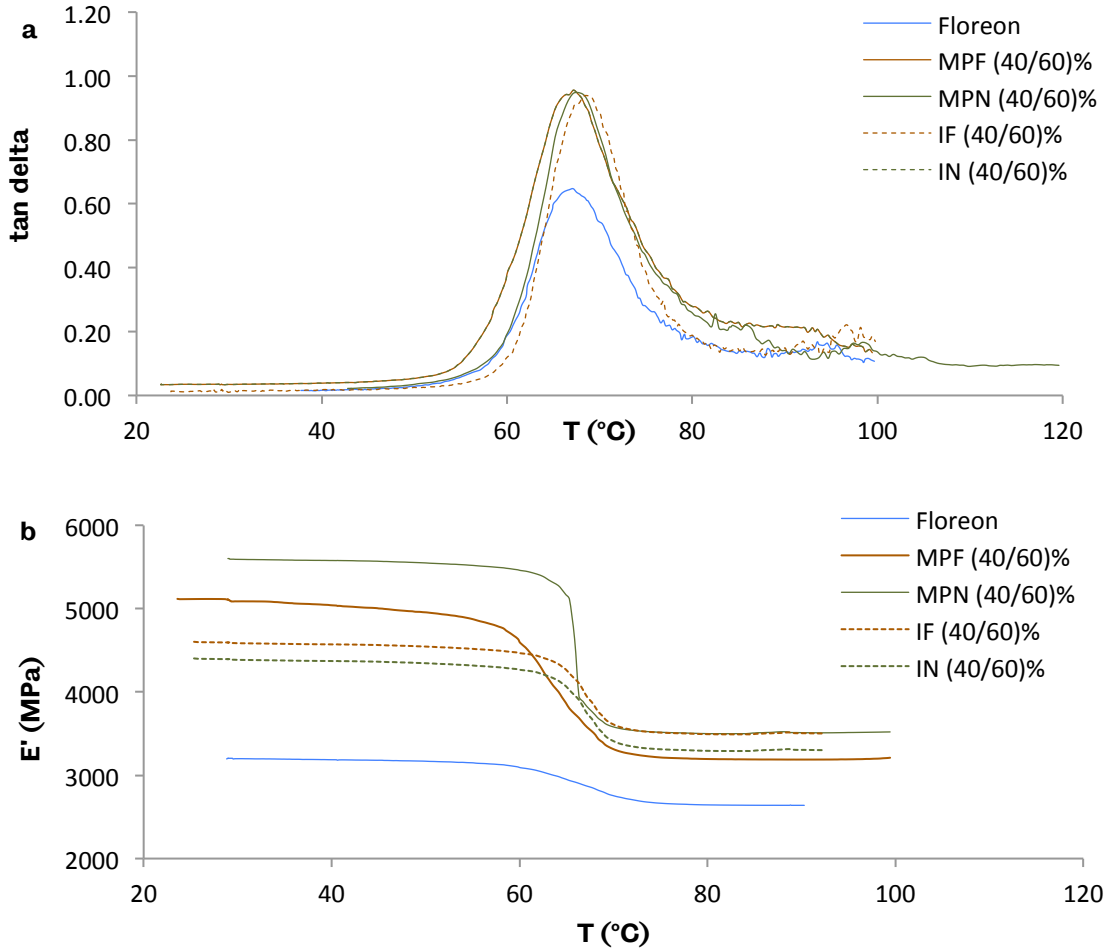

Figure 5.13 DMA curves a) tanδ and b) storage modulus (E') for Floreon and different composites types over temperature. The notation MPF (40/60)% is referred to composites consisting of minimally processed flax fibres of 40 wt% (brown line) and MPN (40/60)% to the corresponding composites with minimally processed nettle fibres of 40 wt% (green line). The notation IF (40/60)% is referred to composites consisting of industrial processed flax fibres of 40 wt% (dashed brown line) and IN (40/60)% to the corresponding composites with industrial processed nettle fibres of 40 wt% (dashed green line). Notice that the lower value of E' axis are omitted in order to improve the readability of the plot.

The melting temperature and melting enthalpy (ΔH_m) of Floreon and the different composite types were calculated by analysing the DSC curves of the first and second heating cycle, as shown in Figure 5.14a–b. The heat capacity and degree of crystallinity of Floreon was calculated using Equations 4.8 and 4.9. The thermal properties of Floreon and of the composites are presented in Table 5.8.

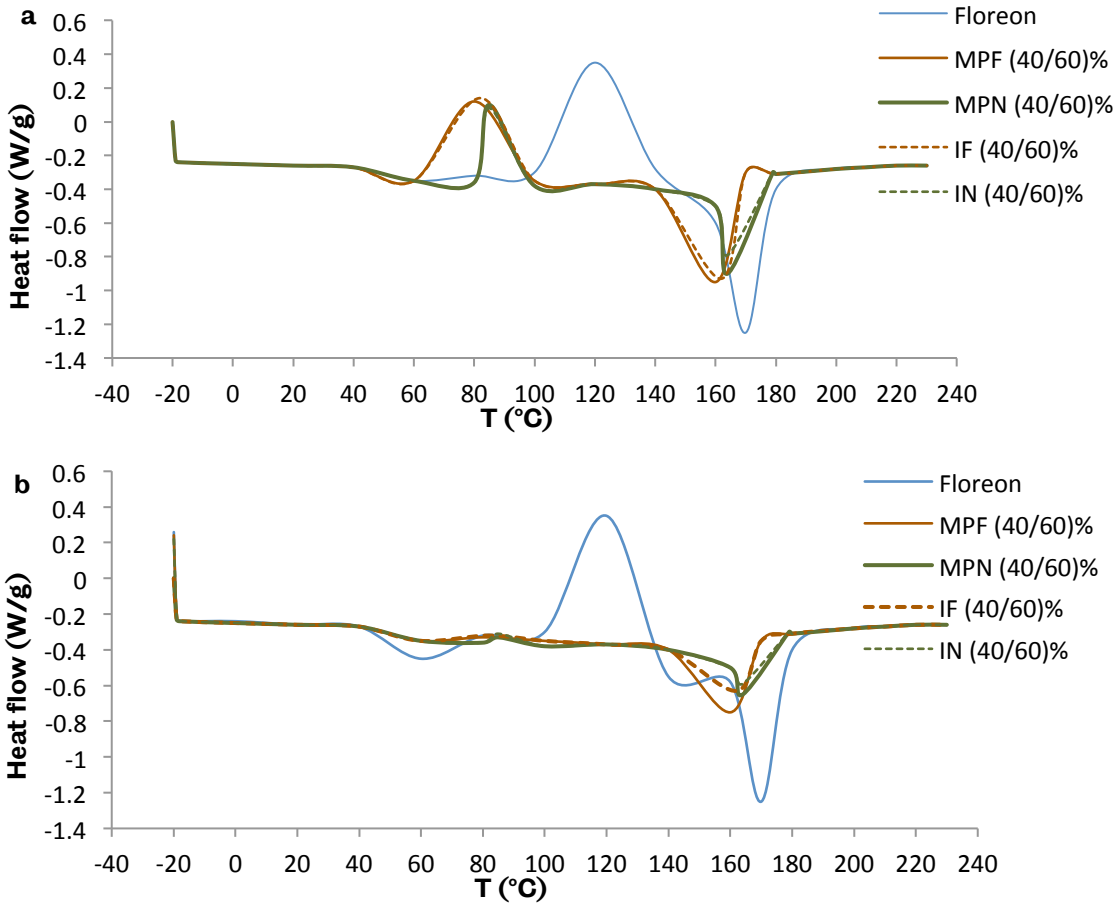

Figure 5.14 DSC curves of a) 1st heating cycle and b) 2nd heating cycle for Floreon and different composites types. The heating rate was 5 °C/min. The notation MPF (40/60)% is referred to composites consisting of minimally processed flax fibres of 40 wt% (brown line) and MPN (40/60)% to the corresponding composites with minimally processed nettle fibres of 40 wt% (green line). The notation IF (40/60)% is referred to composites consisting of industrial processed flax fibres of 40 wt% (dashed brown line) and IN (40/60)% to the corresponding composites with industrial processed nettle fibres of 40 wt% (dashed green line).

Table 5.8 Thermal properties of Floreon and different composites types.

Sample	T_g (°C) DMA	T_m (°C) DSC	ΔH_m(J/g) DSC	X_c (%)* DSC
Floreon	65	170	41	44
MPF (40/60)%	67	160	37	39
IF (40/60)%	67	162	31	33
MPN (40/60)%	68	164	29	30
IN (40/60)%	66	164	29	30

* For the calculations of X_c, the value of 100% crystalline PLA as the heat of fusion of 100% crystalline Floreon (ΔH_{100} = 93.7 J/g) was used, as Floreon and PLA share similar thermal properties, and the total mass of the samples was used [207]. The heat capacity change at T_g of Floreon was calculated at 43.1 $J.K^{-1} \cdot mol^{-1}$ at T_g = 338.2 K which is similar to PLA at 43.6 $J.K^{-1} \cdot mol^{-1}$ at T_g = 332.5 K [312].

The reported T_g of PLA from previous studies is 58–65 °C; Garlotta reported a T_g at 59–60 °C [22], while Martin and Averous determined 58 °C [313]. Floreon is expected to have thermal properties similar to PLA as PLA forms the base for Floreon. According to the literature, the use of flax fibres in PLA does not affect the T_g [314]. The calculated T_m of fibre-reinforced composites was slightly lower than Floreon, as was the melting enthalpy and degree of crystallinity.

Alimuzzaman observed a decrease in the T_g and T_m of flax/PLA composite compared to PLA and a reduction in the degree of crystallinity [147]. The decrease in the T_g and T_m of composites suggests that there are fewer molecular relaxations in the composite compared to Floreon [315]. The T_m of composites reduced as observed in similar studies using natural fibres. According to Choudhury, the reduced melting temperature of composites is due to strong nucleation on the reinforcing fibre surfaces, which shortens the time required for the polymer's crystallisation [316]. Xia *et al.* reported that the melting peak of flax/PLA composites shifted to lower temperatures, due to the cold crystallisation induced by flax fibres [163]. Li *et al.* agreed with the finding that the crystal structure of PLA changed in the presence of fillers in produced composites [317].

5.2.7 Moisture absorption test

Fibre-reinforced composites and especially cellulosic fibres behave differently according to the characteristics of the surrounding environment. As mentioned in chapters 2 and 3, cellulosic fibres are characterised as hydrophilic materials, meaning that they absorb moisture from the surrounding environment, causing problems in the fibre's and composite's mechanical and physical properties. As the content of fibres in the composites produced reached 40 wt%, moisture absorption in the manufactured MPF, MPN, IN and IF composites was studied to determine whether composite's properties were altered.

Composites were exposed under different moisture levels. The rate of moisture absorption over time of Floreon and the different composite types are shown in Figure 5.15 a–c. The amount of moisture absorption was calculated using Equation4.17.

Floreon and composites had the highest moisture absorption at 80% RH. Floreon absorbed 4 wt% of moisture at 80% RH, 3% at 60% and 1.5% at 40% RH. The level of moisture absorption was higher in composites, as expected; because both fibres and polymer absorb moisture form the surrounding environment and due to the void formation during the manufacturing. Moisture absorption was greater with higher fibre content, especially with MPN and MPF composites.

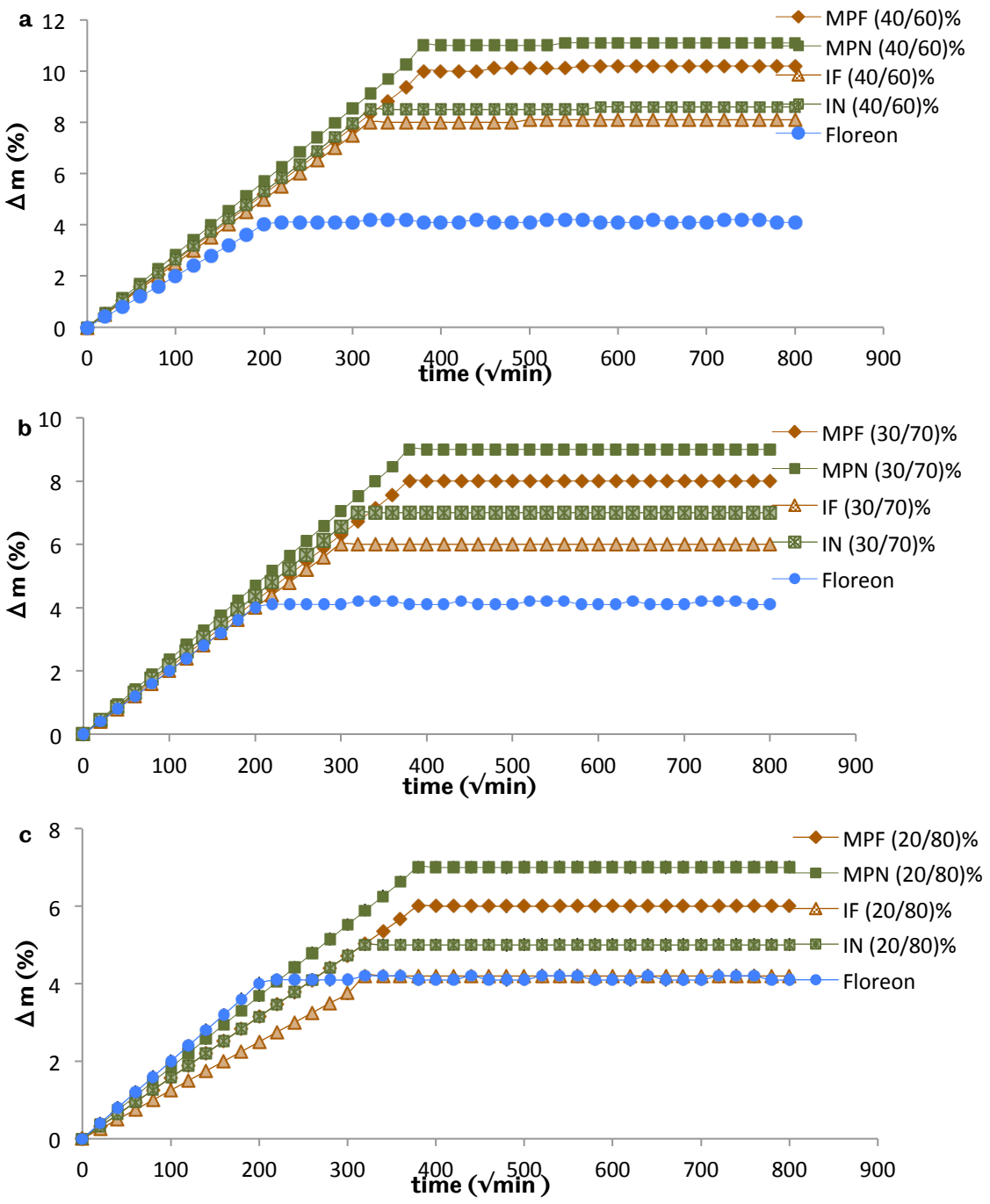

Figure 5.15 Moisture absorption (wt%) plots for Floreon and different composite types at 80% RH for 24 hours of exposure of a) 40wt%, b) 30wt% and c) 20wt% fibre, for 10 composites for each composite type. The notation MPF is referred to composites consisting of minimally processed flax fibres of 40,30,20 wt% (brown rhombus) and MPN to the corresponding composites with minimally processed nettle fibres of 40,30,20%wt (green squares). The notation IF is referred to composites consisting of industrial processed flax fibres of 40,30,20 wt% (dashed brown triangles) and IN to the corresponding composites with industrial processed nettle fibres of 40,30,20 wt% (dashed green squares). The error bars represent ±1SD (samples tested for every set of error bars n=5).

Figure 5.16 a–c illustrates the correlation between fibre content and maximum Δm (%) at 40, 60, and 80% RH levels respectively.

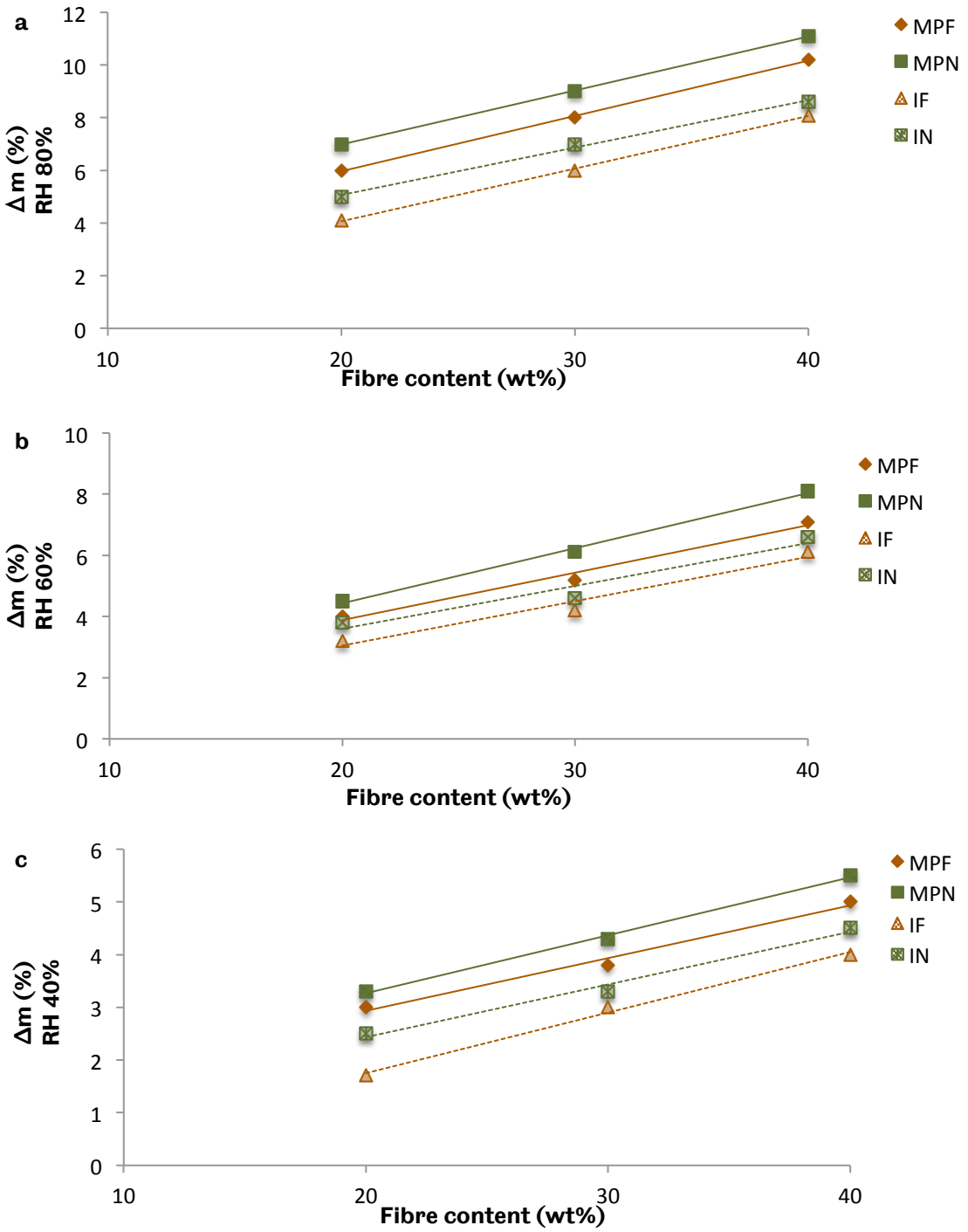

Figure 5.16 Maximum moisture absorption of different composite types at a) 80% RH b) 60% RH and c) 40% RH. The notation MPF is referred to composites consisting of minimally processed flax fibres (brown rhombus) and MPN to the corresponding composites with minimally processed nettle fibres (green squares). The notation IF is referred to composites consisting of industrial processed flax fibres (dashed brown triangles) and IN to the corresponding composites with industrial processed nettle fibres (dashed green squares).

Composites with 40 wt% fibre content from all fibre types had the highest moisture absorption at every tested RH. Due to the hydrophilic character of fibres (chapter 3) the composites were significantly affected. MPN and MPF composites absorbed the highest amounts of moisture. MPN (40/60%) absorbed 11.1 wt% of moisture at 80% RH, 8.1% at 60%, and 5.5% at 40% RH, followed by MPF (40/60%) with 10.2%, 7.1%, and 5% at the respective RHs. Moisture absorption values reported in the literature for flax/PLA composites were 11% and 12%, which is in the same range as the results calculated in this project [161]. Interestingly, composites with 40 wt% fibre content almost reached the moisture absorption rates of fibres (section 3.5.3), showing their effect on the entire composite.

In all samples tested, a linear behaviour between moisture absorption and the square root of time was observed, indicating Fickian behaviour [213]. The effect of moisture absorption was constant during the first hours of exposure, as water molecules penetrate more easily through the pores of the composite, and then flattened. Comparatively, Floreon's moisture absorption rate reached a plateau (the point at which the weight of sample reached a sTable maximum value) much earlier than the composites during the moisture absorption tests (Figure 5.12). All samples were removed after 24 hours of exposure.

The Fickian diffusion coefficient of Floreon and composites was calculated using Equation4.18 and the results are presented in Table 5.9 summarises at different humidity levels. Previous studies reported a diffusion coefficient for PLA at 6.7 x 10^{-9} (cm^2/sec) and diffusion coefficient of flax/PLA (40% fibre volume) at 4.8 x 10^{-6} (mm^2/sec) [306], [318]. Yew *et al.* immersed PLA samples in water at 30 °C for 30 days and reported a diffusion coefficient value of 5.6 x 10^9 cm^2/s [319].

Table 5.9 Diffusion coefficient of Floreon and composites of different fibre compositions.

D x10^{-9} (cm^2/sec)					
RH (%)	**Floreon**	**MPF**	**MPN**	**IF**	**IN**
		Composition: (40/60)%			
80	4.2	7.5	8.2	6.5	6.9
60	3.9	7.2	7.9	6.1	6.5
40	3.7	7.0	7.7	5.9	6.3
		(30/70)%			
80		6.6	8.0	6.1	6.4
60		6.3	7.6	5.8	6.0
40		5.9	7.2	5.4	5.6
		(20/80)%			
80		6.0	7.7	5.8	6.1
60		5.7	7.4	5.4	5.8
40		5.4	7.1	5.1	5.4

The diffusion coefficient increased linearly with the fibre content of composites, as shown in Figure 5.17 a–c. The hydrophilic character of natural fibres enhanced the absorption of water molecules, as indicated by the rate of the diffusion coefficient and reported in similar projects [320].

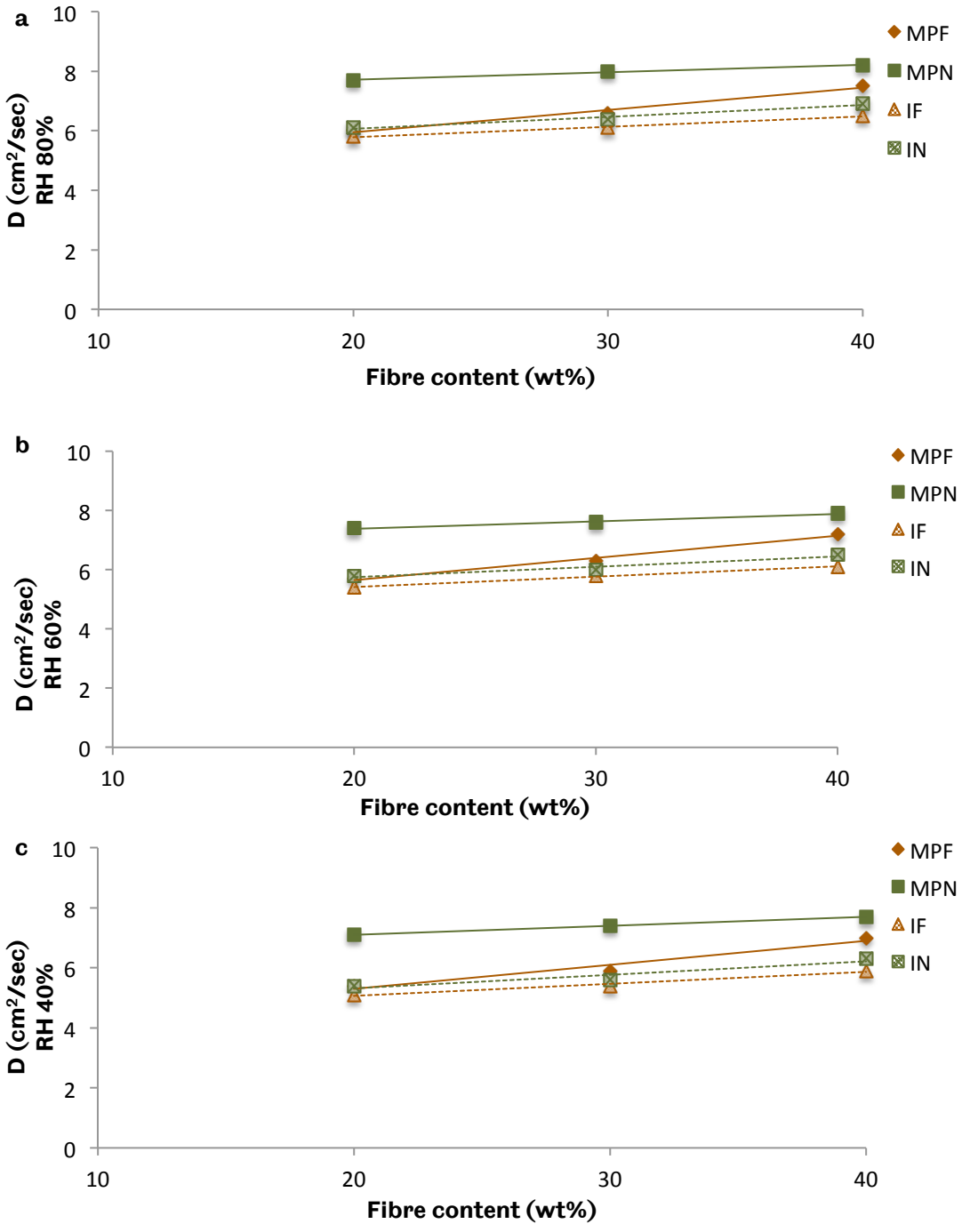

Figure 5.17 Diffusion coefficient of composite at a) 80% RH, b) 60% RH and c) 40% RH. The notation MPF and MPN referred to composites consisting of minimally processed flax fibres (brown rhombus) and to minimally processed nettle fibres (green squares). The notation IF and IN referred to composites consisting of industrial processed flax fibres (dashed brown triangles) and to industrial processed nettle fibres (dashed green squares).

The absorption of moisture is expected to affect the mechanical properties of composites, as it affected the fibres' mechanical and physical properties (chapter 3, section 3.5.3.1). Water molecules entering the composite structure change both the structure and properties of the fibres and matrix, as well as the interface between them. Moisture absorption in particular can cause incompatibility between fibres and matrix, as a result of shrinkage of the matrix and dimensional instability of fibres [106], [321].

5.2.7.1 Tensile test

Composites consisting of fibres of different types, preparation process, and contents had different diffusion coefficient values, as displayed in Table 5.8 and Figure 5.17 a–c. Higher values of diffusivity result in a faster diffusion of water molecules within the fibres and matrix. To investigate potential alternations on the composite properties, samples were exposed to different humidity conditions and mechanically tested.

Figure 5.18 a–c presents the tensile strength of Floreon and composites from each composite category at different humidity levels. Figure 5.16 a–c shows a decrease in the tensile strength of the tested samples according to the RH.

The main factors that contributed to the reduction of tensile strength in composites were the fibre content and humidity level. Composites consisting of 40 wt% fibre content exposed to 80% RH level had the largest decrease.

Specifically, MPN (40/60)% and MPF (40/60)% composites had the greatest tensile strength reduction, by 15% and 13% respectively at 80% RH. As illustrated in Figure 5.19 a–c, composites with 20 wt% fibre content (Figure 5.19c) of all fibre types have a smaller decrease in tensile strength. Because hydrophilic fibres absorb higher amounts of moisture than the surrounding matrix, Floreon had smaller decrease compared to the composites (Figure 5.19a).

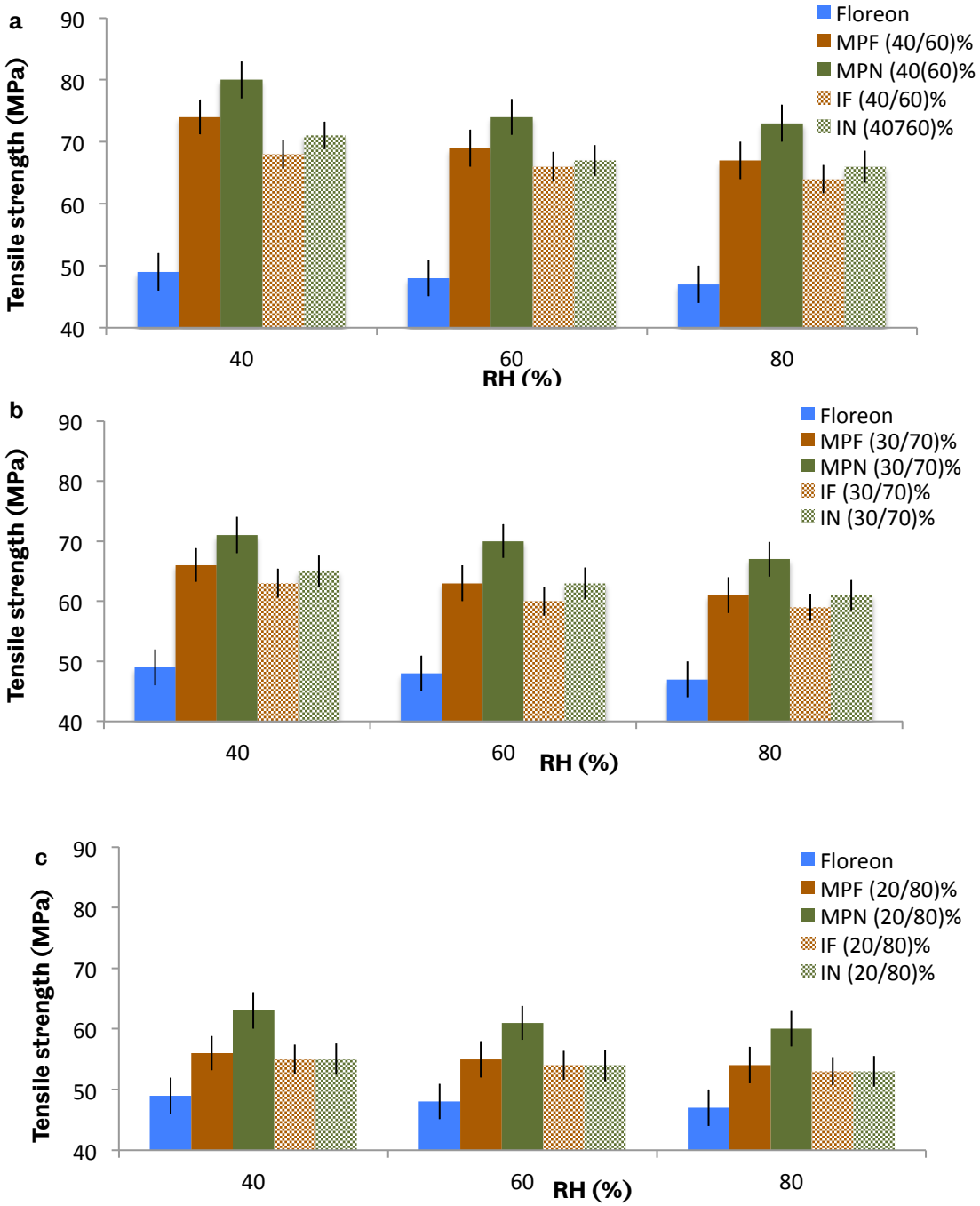

Figure 5.18 Tensile strength (average) of Floreon and Floreon based composites of 40%, 30%, 20 wt% as a function of different RH, for 5 composites from each composite category. Floreon and composites were made using extrusion pressure of 40 bar, moulding pressure of 500 bar and moulding time of 1 minute. The moulding temperature for composites consisting of MP fibres was set up at 190 °C and at 180 °C for the corresponding composites with I fibres. The notation MPN and MPF referred to composites consisting of minimally processed nettle fibres (solid green bars) and to minimally processed flax fibres (solid brown bars) respectively. The notation IN and IF referred to composites consisting of industrial processed nettle fibres (dashed green bars) and to industrial processed flax fibres (dashed brown bars) respectively. Notice that the lower value of tensile strength axis are omitted in order to improve the readability of the plot. The error bars represent ±1SD (samples tested for every set of error bars n=3).

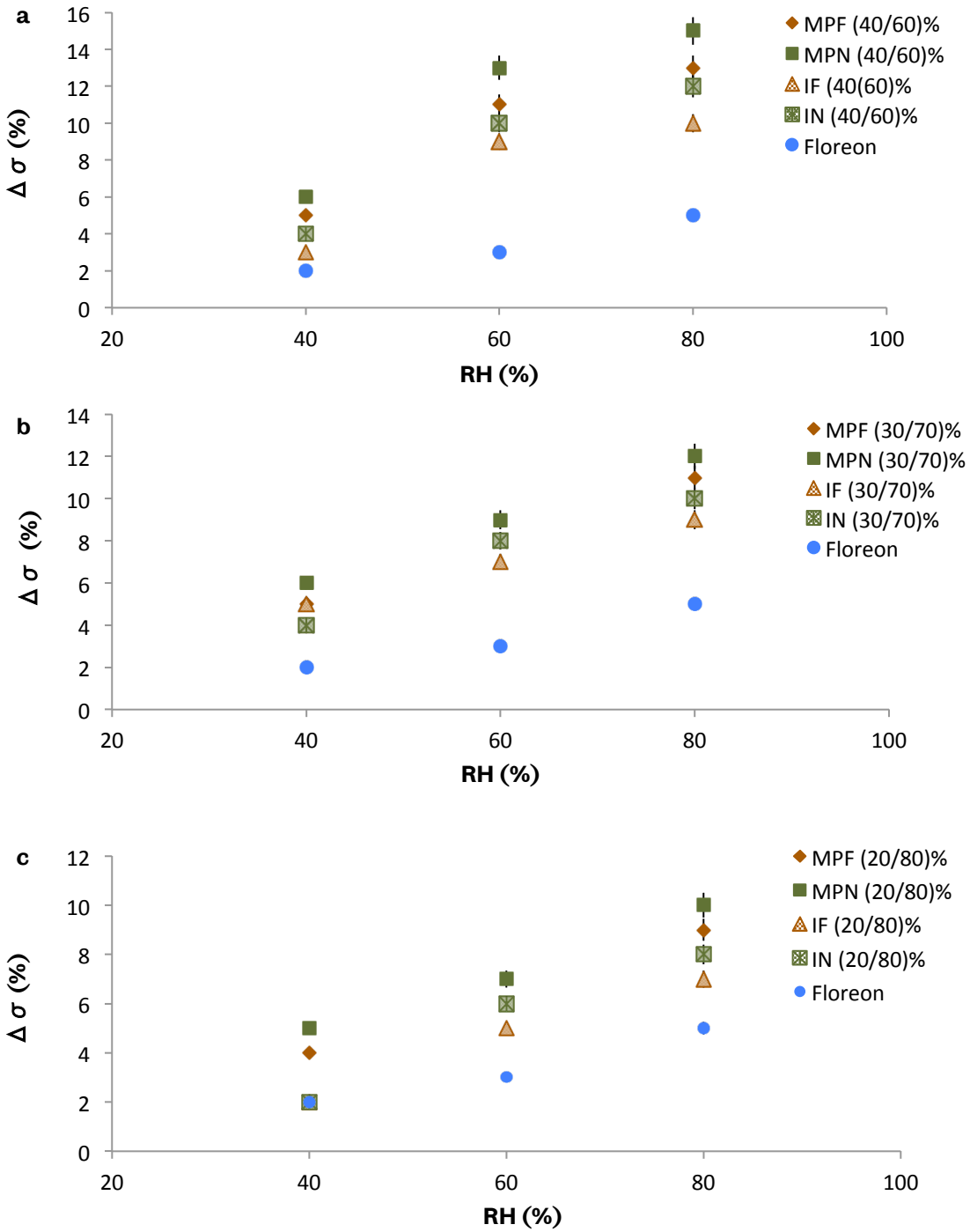

Figure 5.19 Reduction in the tensile strength of Floreon and Floreon based composites of a) 40wt%, b) 30wt% and c) 20wt% fibre as a function of different RH, for 5 composites from each composite category. The notation MPN is referred to composites consisting of minimally processed nettle fibres (green squares) and MPF to the corresponding composites with minimally processed flax fibres (brown rhombus). The notation IN is referred to composites consisting of industrial processed nettle fibres (dashed green triangle) and IF to the corresponding composites with industrial processed flax fibres (dashed brown triangle). The error bars represent ±1SD (samples tested for every set of error bars n=3).

Similarly with the tensile strength results, the Young's modulus of composites from all fibre categories had the highest reduction at 80% RH. At higher relative humidity levels, the tensile strength was reduce while the strain at failure remained at the same levels as a result the decrease of composites' Young's modulus. The different values of Young's modulus according the different relative humidity levels can be seen in Figure 5.20.

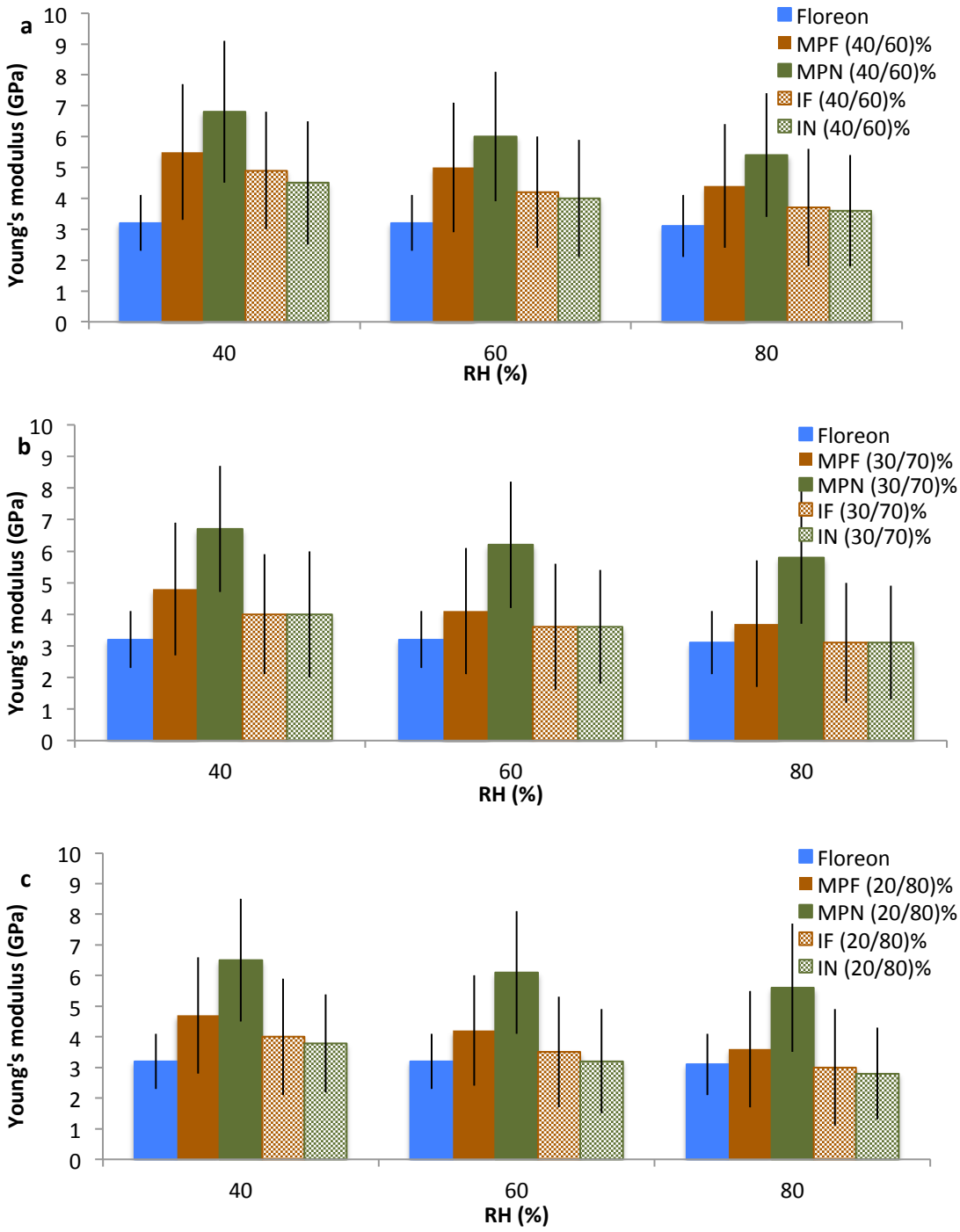

Figure 5.20 Young's modulus (average) of Floreon and Floreon based composites of a) 40wt%, b) 30wt% and c) 20wt% as a function of different RH, for 5 composites from each composite

category. Floreon and composites were made using extrusion pressure of 40 bar, moulding pressure of 500 bar and moulding time of 1 minute. The moulding temperature for composites consisting of MP fibres was set up at 190 °C and at 180 °C for the corresponding composites with I fibres. The notation MPN is referred to composites consisting of minimally processed nettle fibres (solid green bars) and MPF to the corresponding composites with minimally processed flax fibres (solid brown bars). The notation IN is referred to composites consisting of industrial processed nettle fibres (dashed green bars) and IF to the corresponding composites with industrial processed flax fibres (dashed brown bars). The error bars represent ±1SD (samples tested for every set of error bars n=3).

5.2.7.2 Flexural properties

Similar to the tensile strength (section 5.2.6.1), the flexural strength of Floreon and composites was affected when exposed to different humidity levels.

The reduction in the flexural strength of composites was affected by the humidity level and composite composition (fibre type and content). Figure 5.21 a–c presents the flexural strength and Figure 5.22 a–c shows the reduction of flexural strength in Floreon and composites over the different humidity levels.

As expected, the greatest reduction was observed at the highest tested RH of 80% and at composites with 40 wt% fibre content, showing poor adhesion between the reinforcing fibres and Floreon. MPF and MPN (40/60%) composites had a 13% and 12% reduction respectively in their flexural strength at 80% RH.

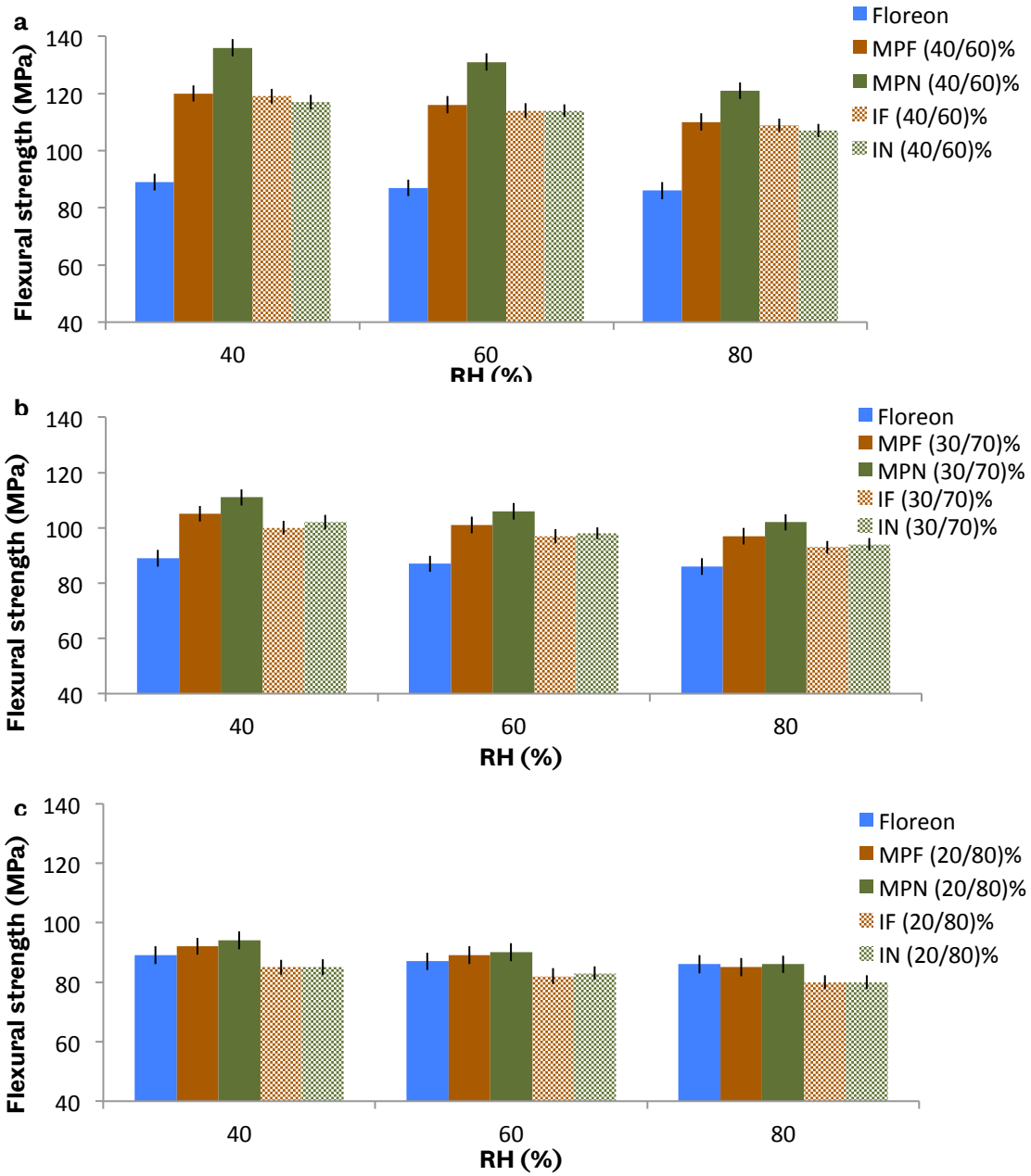

Figure 5.21 Flexural strength (average) of Floreon and Floreon based composites of 40%, 30%, 20 wt% as a function of different RH, for 5 composites from each composite category. Floreon and composites were made using extrusion pressure of 40 bar, moulding pressure of 500 bar and moulding time of 1 minute. The moulding temperature for composites consisting of MP fibres was set up at 190 °C and at 180 °C for the corresponding composites with I fibres. The notation MPN and MPF referred to minimally processed nettle fibres (solid green bars) and to the corresponding composites with minimally processed flax fibres (solid brown bars) respectively. The notation IN and IF referred to composites consisting of industrial processed nettle fibres (dashed green bars) and to the industrial processed flax fibres (dashed brown bars) respectively. Notice that the lower value of flexural strength axis are omitted in order to improve the readability of the plot. The error bars represent ±1SD (samples tested for every set of error bars n=3).

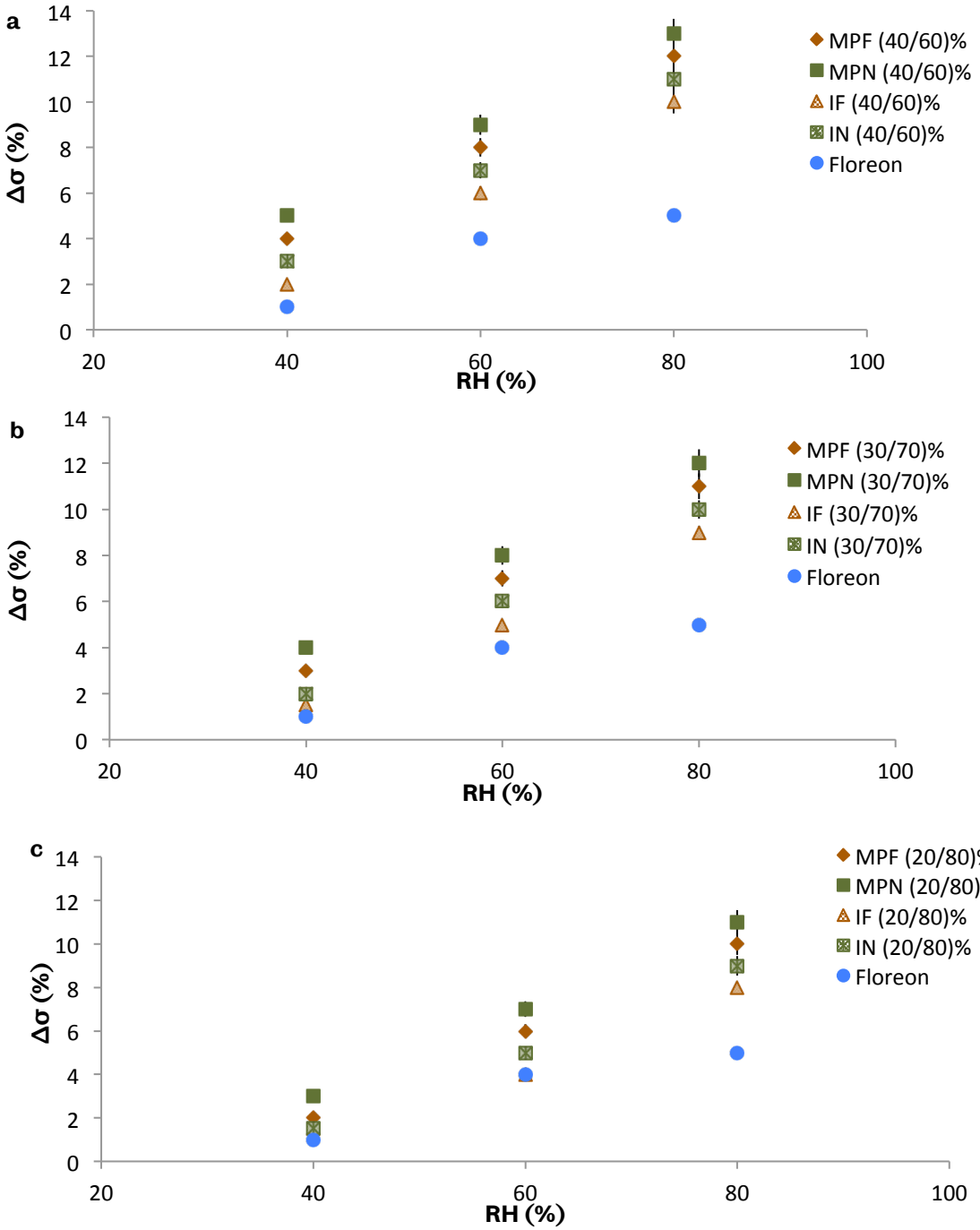

Figure 5.22 Reduction in the flexural strength of Floreon and Floreon based composites of a) 40wt%, b) 30wt% and c) 20wt% fibre as a function of different RH, for 5 composites from each composite category. The notation MPN is referred to composites consisting of minimally processed nettle fibres (solid green bars) and MPF to the corresponding composites with minimally processed flax fibres (solid brown bars). The notation IN is referred to composites consisting of industrial processed nettle fibres (dashed green bars) and IF to the corresponding composites with industrial processed flax fibres (dashed brown bars). The error bars represent ±1SD (samples tested for every set of error bars n=3).

Similarly with the flexural strength results and also following the same route as the Young's modulus values (Figure 5.20), flexural modulus had the highest reduction at 80% RH level. The reduction on the flexural modulus of composites form all categories are shown in Figure 5.23.

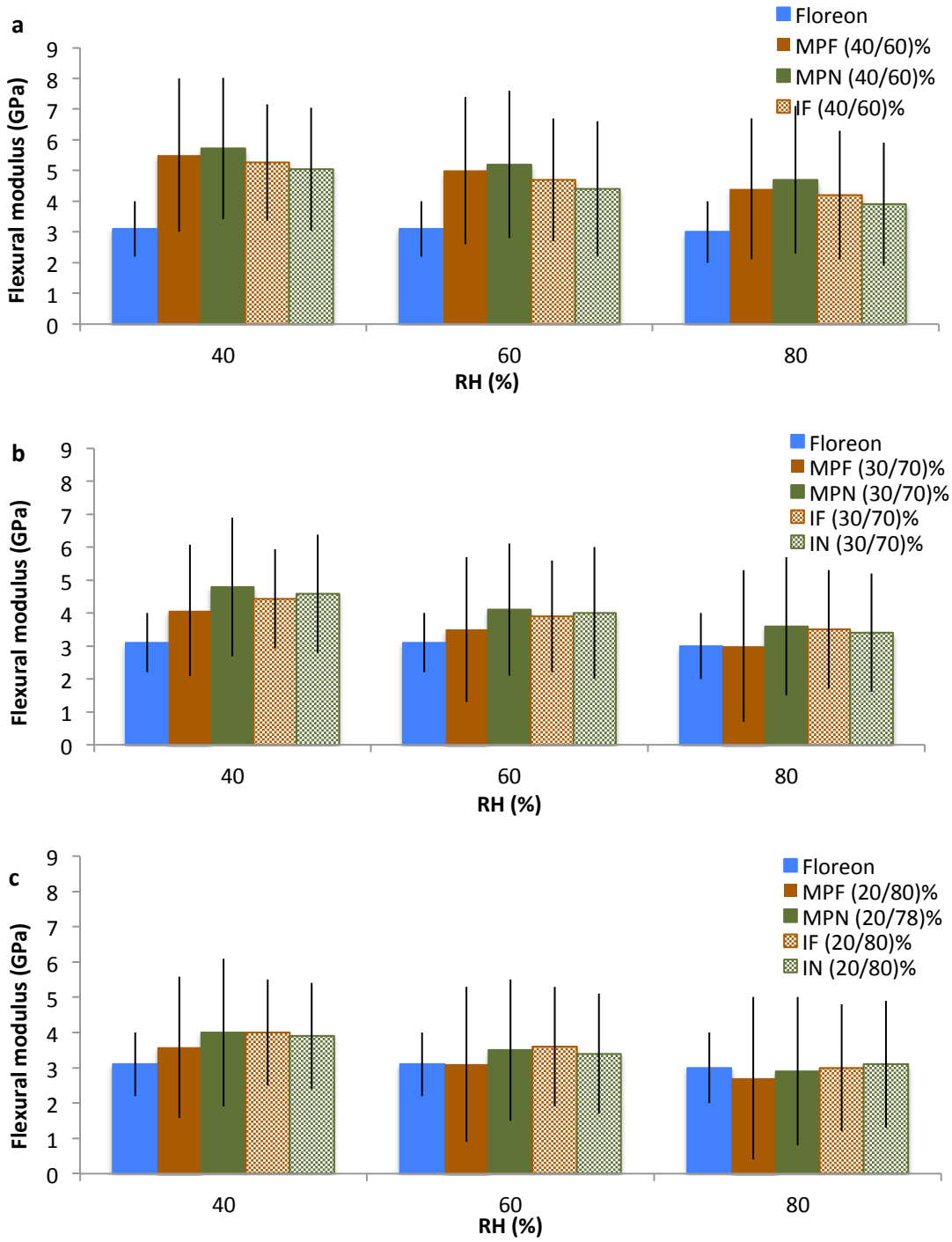

Figure 5.23Flexural modulus (average) of Floreon and Floreon based composites of a) 40%, b) 30%, c) 20 wt% as a function of different RH, for 5 composites from each composite category. Floreon and composites were made using extrusion pressure of 40 bar, moulding pressure of 500 bar and moulding time of 1 minute. The moulding temperature for composites consisting

of MP fibres was set up at 190 °C and at 180 °C for the corresponding composites with I fibres. The notation MPN is referred to composites consisting of minimally processed nettle fibres (solid green bars) and MPF to the corresponding composites with minimally processed flax fibres (solid brown bars). The notation IN is referred to composites consisting of industrial processed nettle fibres (dashed green bars) and IF to the corresponding composites with industrial processed flax fibres (dashed brown bars). Notice that the lower value of flexural strength axis are omitted in order to improve the readability of the plot. The error bars represent ±1SD (samples tested for every set of error bars n=3).

MPN composites had the largest decrease in both tensile and flexural strength results. Nettle fibre showed the highest moisture absorption and consequently the greatest reduction in MPN composites' tensile and flexural strength compared to the MPF, IN, and IF composites. This is consistent with the nettle fibre's behaviour under different humidity conditions as described in chapter 3.

Voids in the fibre structure occurring in the structure of the plant or created by the fibre and composite preparation processes probably intensify the moisture absorption. Moisture absorption is linked to the hydrophilic character of natural fibres as a result of the large concentration of hydroxyl groups (chapter 2 section 2.2.1) [40]. In the effort to minimise the effects of moisture absorption on the composite's physical and mechanical properties, chemical treatments are used to moderate the natural character of the fibres [25], [48].

5.3 Summary

The primary objective of this study was the manufacture of composites without chemical and/or surface treatment of the reinforcing nettle and flax fibres blended with Floreon. The injection-moulded flax and nettle fibre-reinforced composites were made and studied to verify that biodegrade and sustainable raw materials can be used to produce composites with sufficient mechanical properties while maintaining the physical nature of the flax and nettle fibres.

Analysing the mechanical properties of the injection-moulded composites, composites consisting of MPF and MPN fibres had much higher tensile and flexural strength results compared to composites with IF and IN fibres, which is consistent with chapter 3's observations of the individual fibre's mechanical properties. The highest mechanical properties were calculated at MPN (40/60%) and MPF (40/60%) composites, with a tensile strength of 85 ± 3 MPa and 77 ± 2 MPa and a flexural strength of 143 ± 4 MPa and 127 ± 6 MPa respectively.

It is worth stating that fibres with the minimal possible preparation process showed better performance as reinforcements, leading the material researchers

to examine alternative methods of preparing fibres for use as reinforcing materials. MPN fibres enhanced the composites' properties to a greater degree than flax fibres, making them a promising candidate as reinforcement materials.

Although the composite's mechanical properties were enhanced at higher fibre contents, the amount of moisture absorption was greater. MPN and MPF (40/60%) composites absorbed 11.1 wt% and 10.2 wt% of moisture at 80% RH level respectively, showing a significant reduction in their mechanical properties. Similarities were observed in the influence of moisture absorption on the physical and mechanical properties of fibres and fibre-reinforced composites. MPF and MPN fibres had the highest moisture absorption values, and their composites had the greatest reduction in mechanical properties.

The mechanical properties of the reinforcing fibres, Floreon, and injection-moulded composites were studied, compared, and presented in this chapter. In the following chapter, a different manufacturing approach was studied and the results obtained from the 3D printed composites are presented.

6 FUSED DEPOSITION MODELLING - 3D PRINTED COMPOSITES

Physical, mechanical, and thermal properties of flax and nettle fibre-reinforced composites

6.1 Introduction

The choice of 3D printing for composites for this project was based on the capabilities of 3D printers to control more parameters than other production processes, increasing the design flexibility and minimising the required quantity of material.

Composites consisting of minimally and industrially processed flax and nettle fibres and Floreon were 3D printed using FDM. The FDM technique allows changes in the orientation of the material being laid down relative to the sample and in the fill ratio (the amount of material printed inside the sample).

Both orientation and fill ratio can be combined, as a mesh-like structure is conventionally used to give design flexibility in the fill fraction. Furthermore, as the filament is extruded, the polymer and the fibres are oriented in the direction of movement of the printer head. Thus, FDM facilitates a more complete study of the effect of orientation on mechanical properties.

6.2 Research methodology

Of particular interest was the use of alternative manufacturing processes and the evaluation of the properties of the composite produced. Therefore, FDM as a technique, in which different processing parameters can be chosen, was used for the 3D printing of fibre-reinforced composites. The 3D printed composites were tested and characterised based on their physical, mechanical, and thermal properties. The properties of the 3D printed composites were compared with the injection-moulded composites (chapter 5).

6.2.1 Material selection

MPF and MPN fibres were used as reinforcing materials in the form of chopped short single fibres. Floreon 700 pellets obtained from Floreon-Transforming Packaging Limited were used as a matrix. The IF and IN fibres and were obtained from WildFibres Ltd., the MPF fibres were obtained as flax stems from a farm in Sussex and the MPN fibres were harvested from gardens and parks in Sheffield.

6.3 3D printed fibre-reinforced composites

The 3D printed flax and nettle fibre-reinforced Floreon composites were made using a LulzBot TAZ 3 3D printer, pictured in Figure 6.1. The classification of composites was based on the fibre/matrix ratio (determined by the percent weight of the materials added to the hopper) and the printing parameters used. The composition and nomenclatures used are presented in chapter 4, Table 4.1.

During the 3D printing of composites, fibre content greater than 40 wt% was not possible because the printer nozzle clogged with higher fibre content. The highest achieved fibre concentration was 30 wt%.

6.3.1 LulzBot TAZ 3.0 printer

The LulzBot TAZ 3.0 printer is a versatile and high performance desktop 3D printer designed for industrial use [322]. The material used in the 3D printing process was in the form of filament, which was fed into the extruder through a Polytetrafluoroethylene (PTFE) tube. Two idler screws were used to secure the filament in the extruder. The diameter of the nozzle end was fixed to 0.35 mm and determined by the extruder nozzle aperture. The diameter of the extruded filament was measured in the air (details to follow). The movement of the nozzle and print bed, the printing parameters, and the composites structure (i.e., shape and dimensions) are controlled by the Cura® host software [323].

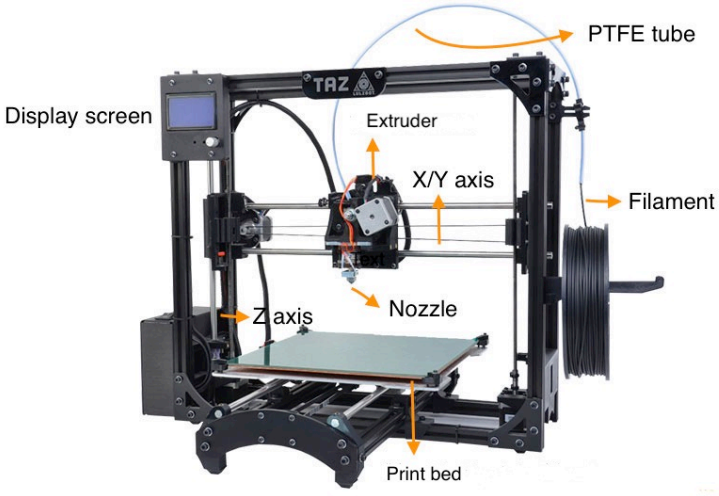

Figure 6.1 LulzBot TAZ 3 3D printer with its main components. The filament is wrap on a coil attached on the left side of the LulzBot TAZ 3 3D printer and is unwrapped during printing. The display screen is used to check the nozzle and bed temperature and the percentage of printed material. Reprinted from "LulzBot TAZ 3 Desktop 3D Printer by Aleph Objects, Inc. is licensed under CC BY-SA 4.0 International."

6.3.1.1 3D printing parameters

Processing parameters (e.g., moulding pressure and temperature) during manufacture affect the final properties of the composite produced [77], [139]. Similarly, the 3D printing parameters affect the physical and mechanical properties of the printed sample [324], [325], [326]. The printing parameters of the LulzBot TAZ 3 3D printer are characterised as primary and secondary parameters. Primary parameters depend on the printer model and the selected structure and composition of the printed part. Secondary parameters are mainly related to the appearance of the printed part [322].

The primary 3D print parameters that were intensively tested during this project are related to the nozzle temperature, values of fill density, and the thickness of the printed layers [224], [322], [223]. For this work, as Floreon is based on PLA, the nozzle extrusion temperature depended on the polymer's melting temperature and was usually set between 180–200 °C and the print bed heated to 50–60 °C [169], [322]. The applied heating parameters ensured the Floreon was molten and could flow smoothly during extrusion.

The extrusion speed (the speed of the nozzle travelling along the print bed) may also affect the filament temperature; generally faster extrusions require higher temperatures, as there is less time to transfer heat from the heated print head [326]. This extrusion speed controls the volume of the extruded filament and the cross-sectional geometry of the printed sample [322].

The fill density/ratio is a percentage between 0–100% and controls the amount of voids in the internal structure of the printed sample without affecting the perimeter [322]. Fill density defines the amount of plastic inside the print. Simply put, a completely solid part is printed with 100% fill density while a part printed with 0% fill density is completely hollow. Typically, filling density values vary between 20–60% according to the sample applications. Most plastic parts are printed with 100% fill density for extra stability [327]. The amount of filament used and the print time vary according to the selected fill density values [322].

The layer height thickness determines the number of printed layers. Layers printed with smaller height thickness produce a finer surface but require a longer print time [226]. Samples printed with greater height thickness reduce the print time but produce rougher surfaces [328].

The pattern structure and orientation determines the structure and orientation of the printed part [228]. There are two commonly available structure types: grid and line [322]. Grids are stiffer support structures and are printed as a continuous

piece. The line type consists of individual lines printed one at a time. The line type is much weaker compared to the grid pattern but is preferred for complex printed structures due to the independent movement of the nozzle [329]. The most advanced 3D printing software include patterns such as rectilinear and honeycomb structures [322]. The complex structure of the honeycomb pattern is preferred for applications requiring materials with high strength and stiffness [327].

The pattern orientation is highly connected to the applications of the printed sample. Different sets of pattern orientation such as -45°/45° and 0°/90° can be used. Samples with higher tensile strength are printed with the pattern orientation of 0°/90° because of the cohesion of the printing direction with the testing direction [324], [330].

For this work, pattern orientations of -45°/45° and 0°/90° were tested, as seen in Figure 6.2. Composites with the same fibre/matrix composition and different pattern orientations were evaluated to determine the effect of pattern orientation.

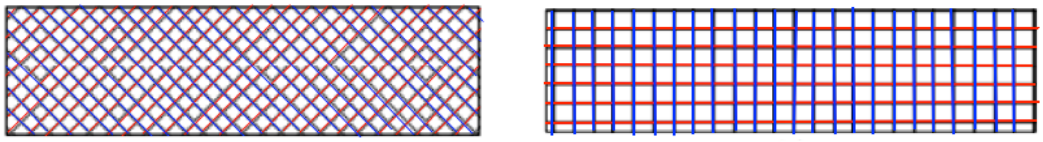

Figure 6.2 -45°/45° (diagonal) fill pattern, 0°/90° (linear) fill pattern orientations.

The nozzle temperature was tested at 180, 190, 200, and 210 °C. This temperature was limited by the melting temperature of Floreon, at 180 °C, and from the fibre degradation temperature at roughly 200 °C [93]. The print bed temperature was set at 60 ± 5 °C. Lower print bed temperatures caused problems with the stability of the first printed layers and led to problematic structures. Conversely, higher bed temperatures altered the thermal properties of the composite, mainly affecting the first printed layers. The ideal bed temperature is slightly below or in the range of the T_g of the polymer used [322].

Fill density was tested at 40, 60, 80, and 100%. According to the literature, 40% is the minimum suggested fill density for composites for applications required to withstand structural loading [327].

Layer height thickness was set to 0.2 mm, 0.3 mm, and 0.4 mm to investigate potential problems caused to the adhesion between the printed layers.

6.4 Experimental manufacture method of 3D printed flax and nettle fibre-reinforced Floreon composites

The manufacture process for 3D printed flax and nettle fibre-reinforced composites was performed in three phases.

Phase A: Fibre preparation

Phase A is identical to the preparation process of fibres described in chapter 4 (section 4.5).

Phase B: Filament manufacturing

A filament of chopped short flax or nettle fibres and Floreon was prepared by extrusion mixing. The fibres were blended with the polymer in a Rondol 21 mm scale twin-screw laboratory extruder and extruded as a continuous filament. The extrusion parameters used are described in chapter 4 (section 4.3.3). Phase B followed the same steps as described in section 4.5. Once cooled, the filament had a cylindrical shape with a diameter between 2.6 mm and 2.8 mm, as seen in Figure 6.3.

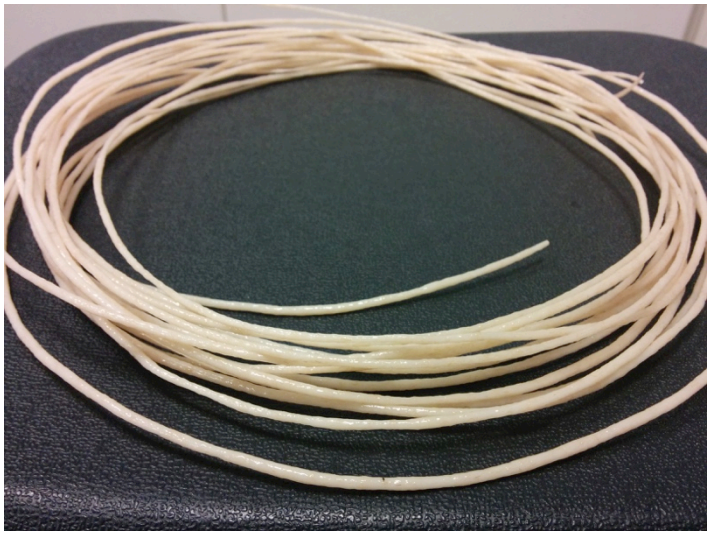

Figure 6.3 MPF/Floreon filament. The filaments were produced manually via extrusion and thus the diameter of the filaments along its length was unequal in some cases. The diameter of the filaments could not exceed the 3 mm due to the size limitation of the nozzle. Filaments with smaller diameter than 2.4 mm were too thin to be fed properly into the 3D printer's motor.

Phase C: 3D printing procedure

Before each printing operation, the PET printing bed (see Figure 6.1) was cleaned with acetone to prevent any contamination from previous materials and calibrated to maintain the ideal bed level for a successful adhesion of the first printed layer.

The print bed and nozzle were heated according to the selected bed and nozzle temperature. Low adhesion tape was applied to the print bed for easier detachment of the printed sample. The filament was loaded when the nozzle reached the desired temperature.

The printing parameters were applied as discussed in section 6.3.1.1. Prior to printing, the extrusion was tested to verify that the material was able to flow by moving the nozzle to the Z axis above the print bed and extruding approximately 40–60 mm of filament.

Cura®[**] software was used to design the sample [323]. The final form, shape, and dimensions of the desired 3D printed sample were illustrated as a 3D model on Cura® software and saved as an .stl file, as seen in Figure 6.4. Once ready to print, the .stl file was uploaded and printing begun. At the end of the 3D printing, the nozzle and print bed were left to cool down to room temperature (T = 25°C) before removing the printed composite. A clam knife blade was used to pry the sample off the low adhesion tape. This procedure was repeated for the manufacture of all composites with the different combinations of fibre/matrix concentrations and printing parameters.

The 3D printed samples were placed in an oven set to Floreon's glass transition temperature (T_g= 65 ± 2 °C) for 24 hours to allow for structural relaxation of Floreon before the mechanical testing.

[**] Cura® is a tradename of Ultimaker B.V developed by David Braam

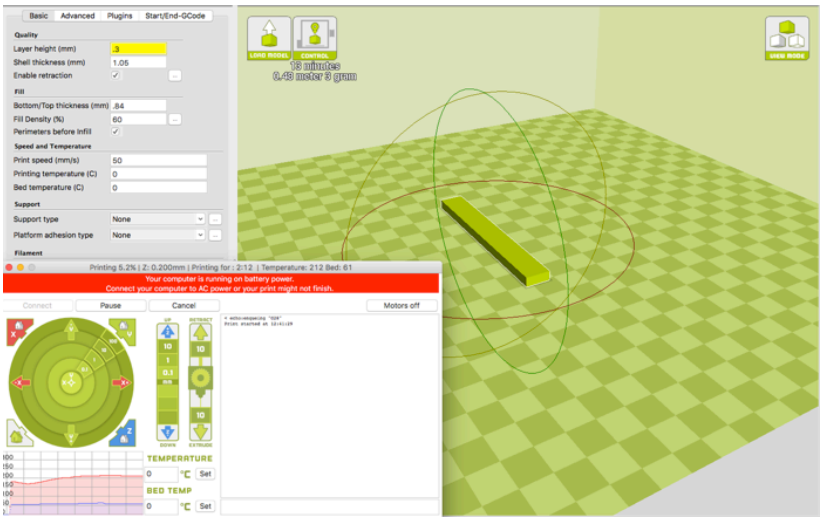

Figure 6.4 Rectangular sample designed on Cura® software. The structure, shape and dimensions of composite and the position on the print bed are controlled and set up from Cura® software before the 3D printing procedure. Reprinted from Ultimaker Cura, © 2018 Ultimaker B.V., https://ultimaker.com/

The 3D printing parameters tested and the composite nomenclatures resulting from these combinations are presented in Table 6.1. Each of the composite nomenclatures is as follows: fibre type and content; pattern orientation; fill density; layer height thickness; and nozzle temperature. For example, a composite consisting of minimally processed nettle fibres of 20 wt%, with pattern orientation of -45°/45°, fill density of 40%, layer height thickness of 0.2 mm, and nozzle temperature of 180 °C is named as MPN20-45-40-2-180.

Table 6.1 Composite nomenclatures of MPN (20/80)% based on the 3D printing parameters.

Pattern orientation (%)	Fill density (%)	Layer height thickness (mm)	Nozzle temperature (°C)	Sample name
-45°/45°	40	0.2	180	MPN20-45-40-2-180
			190	MPN20-45-40-2-190
			200	MPN20-45-40-2-200
			210	MPN20-45-40-2-210
		0.3	180	MPN20-45-40-3-180
			190	MPN20-45-40-3-190
			200	MPN20-45-40-3-200
			210	MPN20-45-40-3-210
		0.4	180	MPN20-45-40-4-180
			190	MPN20-45-40-4-190
			200	MPN20-45-40-4-200
			210	MPN20-45-40-4-210
	60	0.2	180	MPN20-45-60-2-180
			190	MPN20-45-60-2-190
			200	MPN20-45-60-2-200
			210	MPN20-45-60-2-210
		0.3	180	MPN20-45-60-3-180
			190	MPN20-45-60-3-190
			200	MPN20-45-60-3-200
			210	MPN20-45-60-3-210
		0.4	180	MPN20-45-60-4-180
			190	MPN20-45-60-4-190
			200	MPN20-45-60-4-200
			210	MPN20-45-60-4-210
	80	0.2	180	MPN20-45-80-2-180
			190	MPN20-45-80-2-190
			200	MPN20-45-80-2-200
			210	MPN20-45-80-2-210
		0.3	180	MPN20-45-80-3-180
			190	MPN20-45-80-3-190
			200	MPN20-45-80-3-200
			210	MPN20-45-80-3-210
		0.4	180	MPN20-45-80-4-180
			190	MPN20-45-80-4-190
			200	MPN20-45-80-4-200
			210	MPN20-45-80-4-210
	100	0.2	180	MPN20-45-100-2-180
			190	MPN20-45-100-2-190
			200	MPN20-45-100-2-200
			210	MPN20-45-100-2-210
		0.3	180	MPN20-45-100-3-180
			190	MPN20-45-100-3-190
			200	MPN20-45-100-3-200
			210	MPN20-45-100-3-210

		0.4	180 190 200 210	MPN20-45-100-4-180 MPN20-45-100-4-190 MPN20-45-100-4-200 MPN20-45-100-4-210

6.5 3D printed composites evaluation tests

The tensile tests of dog bone (75 x 10 x 4 mm) samples, pictured in Figure 6.5, were performed with a Zwick Roell Z020TN machine with load cell of 25 kN and head speed of 0.125 mm/minute and gauge length of 50 mm in accordance with the ISO 527-2-1BA standard [150], [151]. The tensile properties of the 3D printed Floreon and composites—tensile strength, strain, and Young's modulus—were calculated using Equations 4.2–4.4.

The flexural properties of rectangular (80 x 12 x 4 mm) samples of Floreon and composites, pictured in Figure 6.5, were determined by a three-point bending test using a TA500 testing machine in accordance with the British standards [294]. The flexural properties of Floreon and composites as the flexural strength, strain, and flexural modulus were calculated using Equations 4.5–4.7.

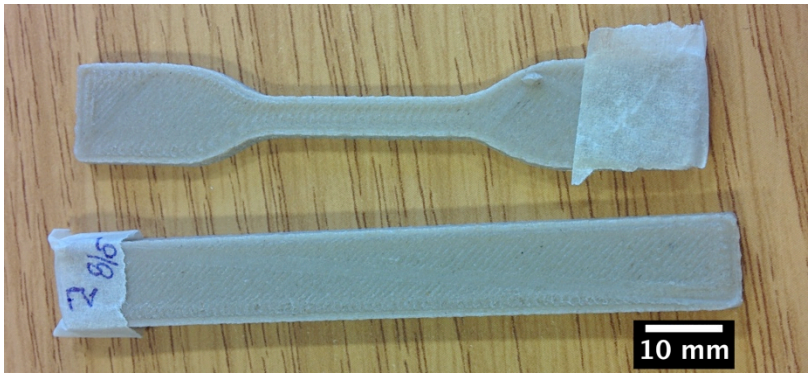

Figure 6.5 Dog done and rectangular IF20-45-100-2-190 samples 3D printed with constant secondary parameters. Dog bone specimen is refereed to a sample with two wider areas at each end and a gauge length between them. The wider areas are used to concentrate the stress in the middle when the sample is loaded with a tensile force.

The fibre/Floreon filament was made via a Rondol 21 mm scale twin-screw laboratory extruder with the extrusion pressure at 40 bar and a temperature of 180 °C. The printing parameters for tensile and bending tests were set to a layer height thickness of 0.2 mm, fill density of 100%, and a nozzle temperature of 200 °C for composites consisting of MPF and MPN fibres and at 190 °C for composites with the IF and IN fibres. The pattern orientation for the tensile tests was 0°/90°, and -45°/45 for the bending tests. The main printing parameters (section 6.3.1.1) were determined after analysing the results obtained from the tensile and bending

tests. A detailed description of the printing parameters follows in the next sections. The dog bone and rectangular samples were 3D printed with constant secondary printing parameters, as presented in Table 6.2.

Table 6.2 Secondary printing parameters. The nozzle's diameter is set up from the manufacturer while the remaining three parameters were set up after multiple tests based on the ideal adhesion between the printing layers and print bed, on the continuous flow and uniform distribution of the filament.

Secondary parameters	
Nozzle diameter	0.35 mm
Bed temperature	60-65 °C
Printing speed	50 mm/s
Shell thickness	1.05 mm

6.6 Results and discussion

6.6.1 Tensile properties

Figure 6.6 presents the tensile stress versus strain curves of Floreon, MPN, MPF, IF and IN composites consisting of different fibre contents. The 3D printed Floreon and composites had a linear stress–strain relationship until the point of fracture, as it was observed on the injection moulded composites (Figures 5.2).

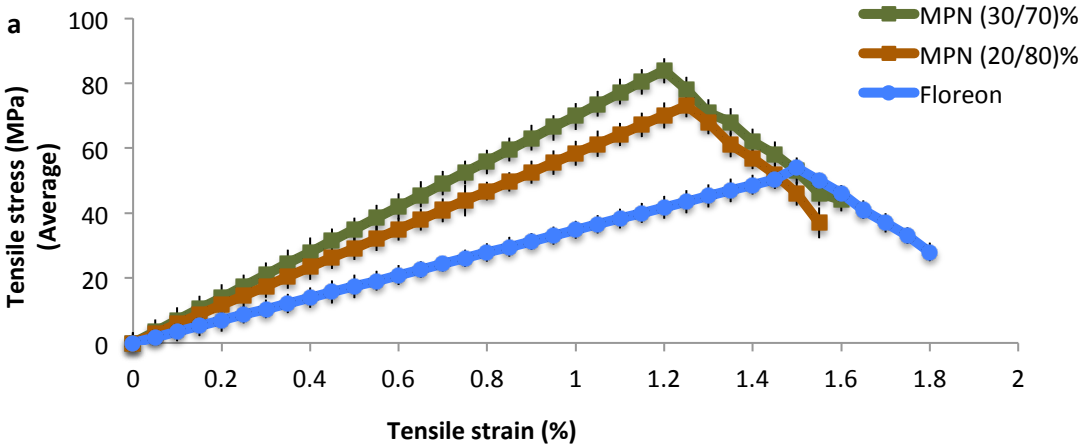

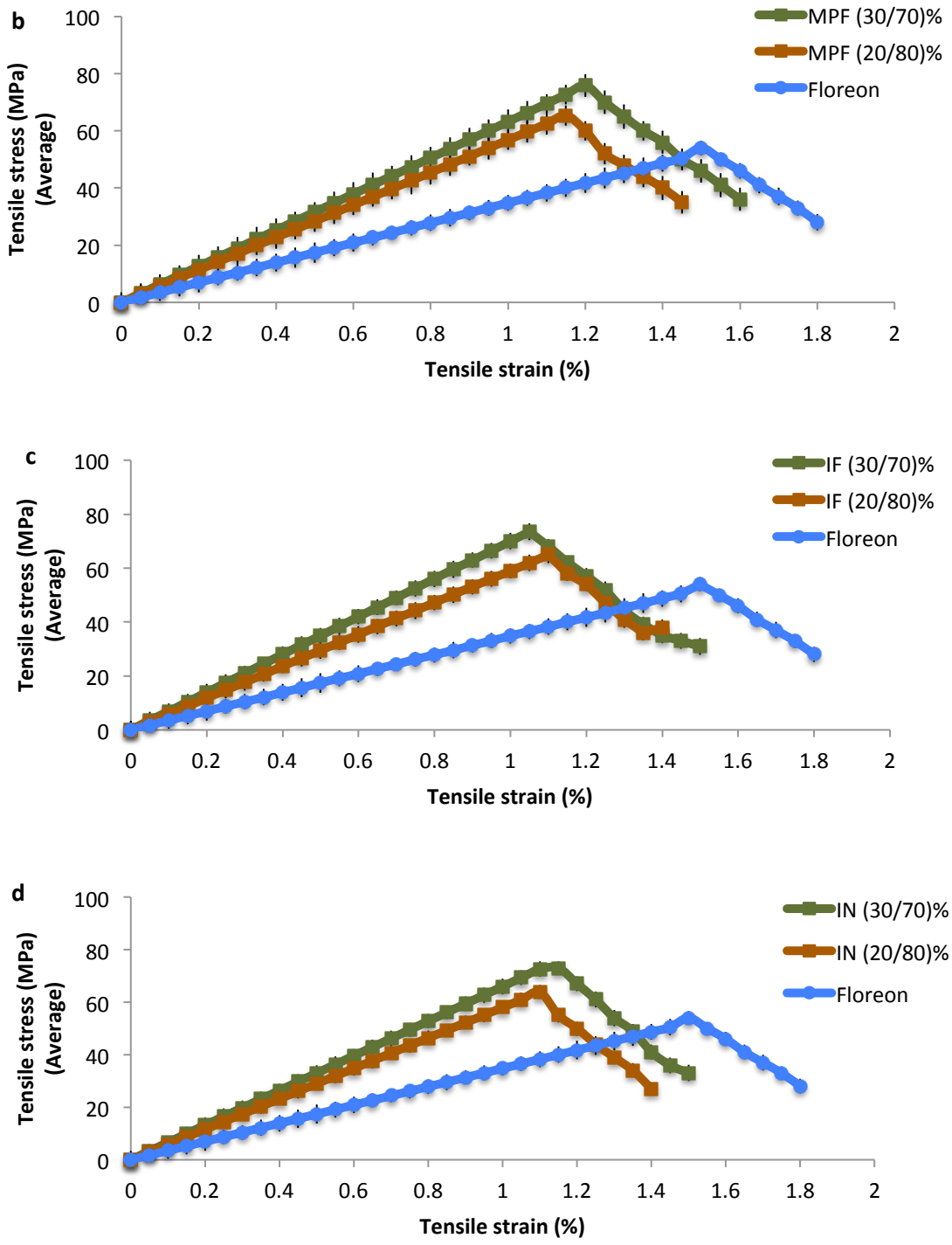

Figure 6.6 Tensile stress-strain curves of Floreon, a) MPN, b) MPF, c) IF and d) IN composites of 30%, 20 wt%, for in total 25 samples of each composite category. Floreon and composites were 3D printed with layer height thickness of 0.2 mm, pattern orientation of 0°/90° and fill density of 100%. The nozzle temperature composites consisting of MPN fibres was set up at 200 °C and at 190 °C for the corresponding composites with I fibres. The error bars represent ±1SD (samples tested for every set of error bars n=15).

Composites with higher fibre content had higher tensile strength results (the point with the maximum tensile stress before the failure occurs), as would be expected by the rule of mixtures. The combination of flax and nettle fibres with Floreon increased significantly the tensile strength of composites, compared to Floreon's tensile strength of 54 ± 3 MPa. The MPN30-90-100-2-200 composites had a tensile strength of 84 ± 4 MPa, followed by MPF30-90-100-2-200 with a tensile strength of 76 ± 4 MPa as seen in Figure 6.7. The IN composites had slightly higher tensile strength results than the IF composite (Figure).

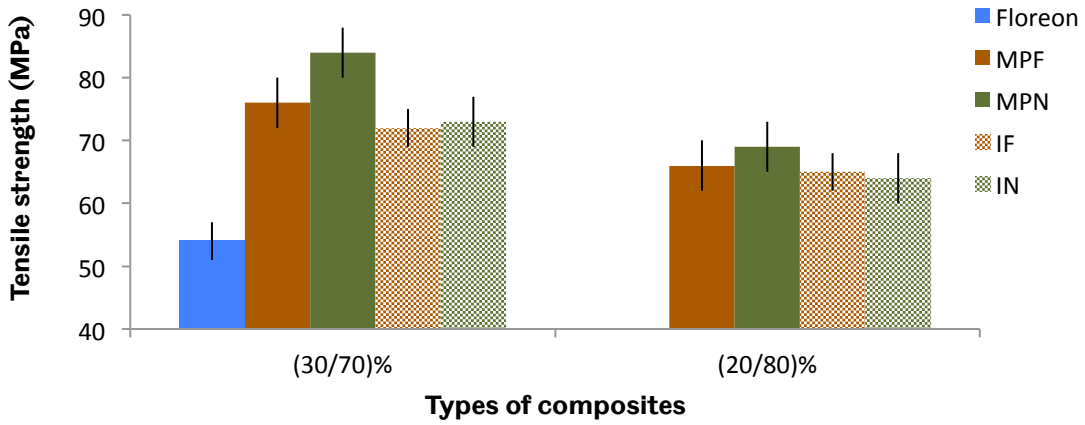

Figure 6.7 Tensile strength (average) of Floreon and Floreon based composites of 30%, 20 wt%, for 25 samples of each composite category. Floreon and composites were 3D printed with layer height thickness of 0.2 mm, pattern orientation of 0°/90° and fill density of 100%. The nozzle temperature for composites concisting of MPN fibres was set up at 200 °C and at 190 °C for the corresponding composites with I fibres. The notation MPN is referred to composites consisting of minimally processed nettle fibres (solid green bars) and MPF to the corresponding composites with minimally processed flax fibres (solid brown bars). The notation IN is referred to composites consisting of industrial processed nettle fibres (dashed green bars) and IF to the corresponding composites with industrial processed flax fibres (dashed brown bars). Notice that the lower value of tensile strength axis are omitted in order to improve the readability of the plot. The error bars represent ±1SD (samples tested for every set of error bars n=15).

The Young's modulus results were also higher in the case of the composites compared to Floreon. The Young's modulus results are presented in Table 6.3.

Table 6.3 Young's modulus of Floreon and Floreon based composites. Composites concisted of MP fibres had higher Young's modulus compared to composites consisting of I fibres. The nomenclatures of composites are according to Table 6.1. The error bars represent ±1SD (samples tested for every set of error bars n=15).

Sample	Young's modulus (GPa)
Floreon	3.6±0.8
MPN30-90-100-2-200	7.0±1.4
MPF30-90-100-2-200	6.8±1.1
IN30-90-100-2-190	6.3±1.0
IF30-90-100-2-190	5.9±0.9
MPN20-90-100-2-200	5.8±0.8
MPF20-90-100-2-200	5.6±0.7
IN20-90-100-2-190	5.8±1.0
IF20-90-100-2-190	5.7±1.1

Based on the calculations using the rule of mixtures (Equation4.13), the Young's modulus for composites increased according to the fibre volume fraction (20% and 30 wt%). As can be seen in Figure 6.8, composites consisting of MP fibres have higher Young's modulus results.

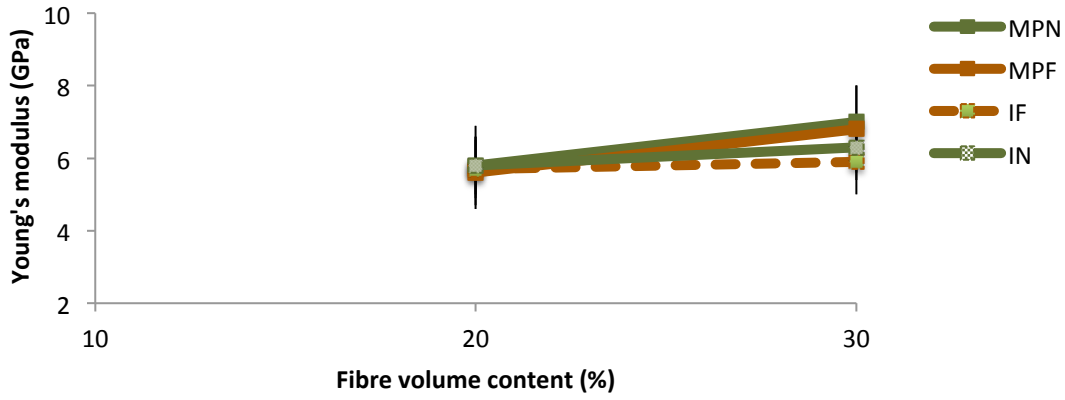

Figure 6.8 Young modulus as a function of volume fraction of MPN, MPF, IF Aand IN nettle composites of 30%, 20 wt%. The notation MPN is refered to compoites concisting of minimally processed fibres. The upper bound (blue line) corresponds to loading parallel to the fibres and the lower bounds (dashed red line) to the transverse loading according to the rule of mixtures . The error bars represent ±1SD (samples tested for every set of error bars n=15).

6.6.2 Tensile properties according to the printing parameters

After repeated tests, it was observed that the tensile properties of the 3D printed samples were affected by the selected printing parameters. A variety of

combinations between the fill density, layer height thickness, nozzle temperature, and pattern orientation were evaluated in terms of the tensile properties of the 3D printed composites.

6.6.2.1 Nozzle temperature and layer height thickness

Figures 6.9 a–b and 6.10 a–b show the effect of nozzle temperature and layer height thickness on the tensile strength results of MPF, MPN, IN and IF composites respectively.

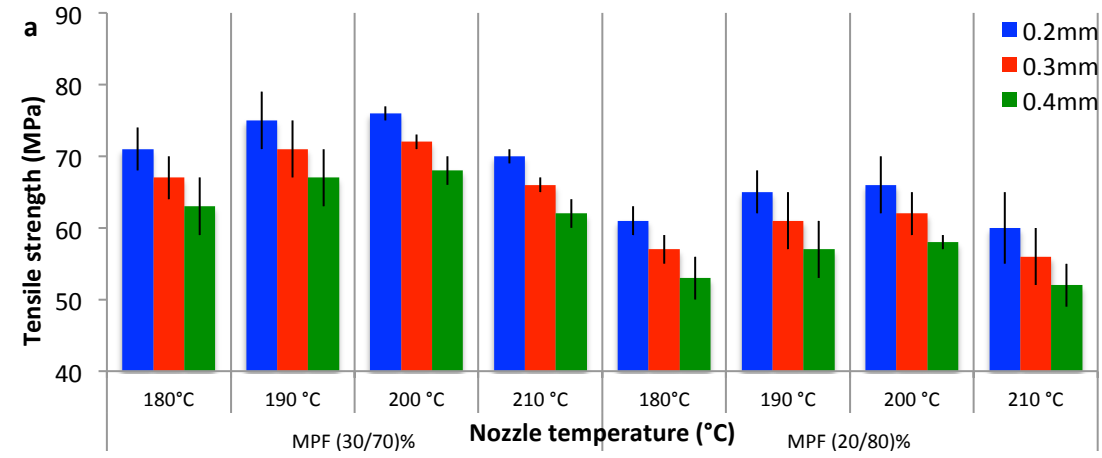

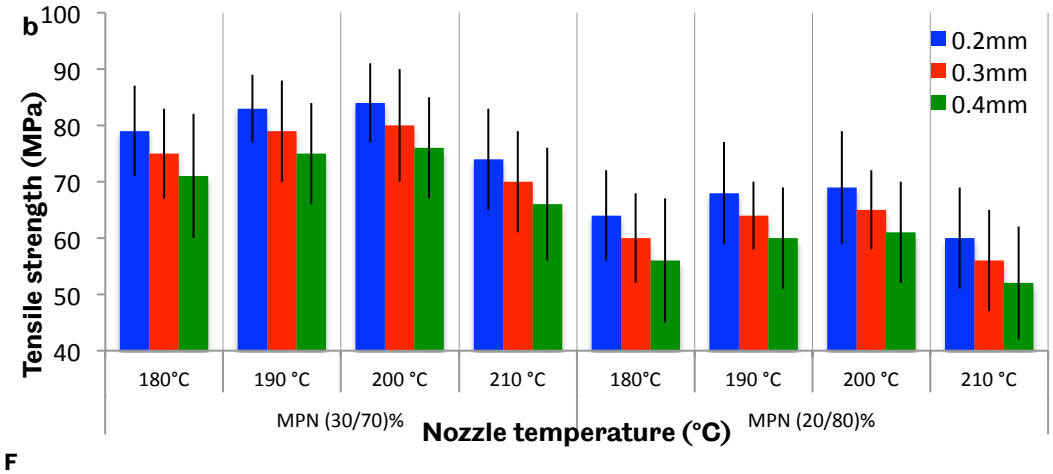

F

Figure 6.9 Effect of printing parameters on the tensile strength of a) MPF composites and b)MPN composites of 30%,20 wt%, for 10 composites from each composite category. The x-axis presents the applied nozzle temperatures from 180 °C to 210 °C. The blue, red, green coloured bars represent the layer height thickness tested at 0.2 mm, 0.3 mm and 0.4 mm respectively. For each printing parameters tested, the composites were 3D printed and tested with constant values of fill density of 100% and printing pattern orientation of 0°/90°. Notice that the lower value of tensile strength axis are omitted in order to improve the readability of the plot. The error bars represent ±1SD (samples tested for every set of error bars n=5).

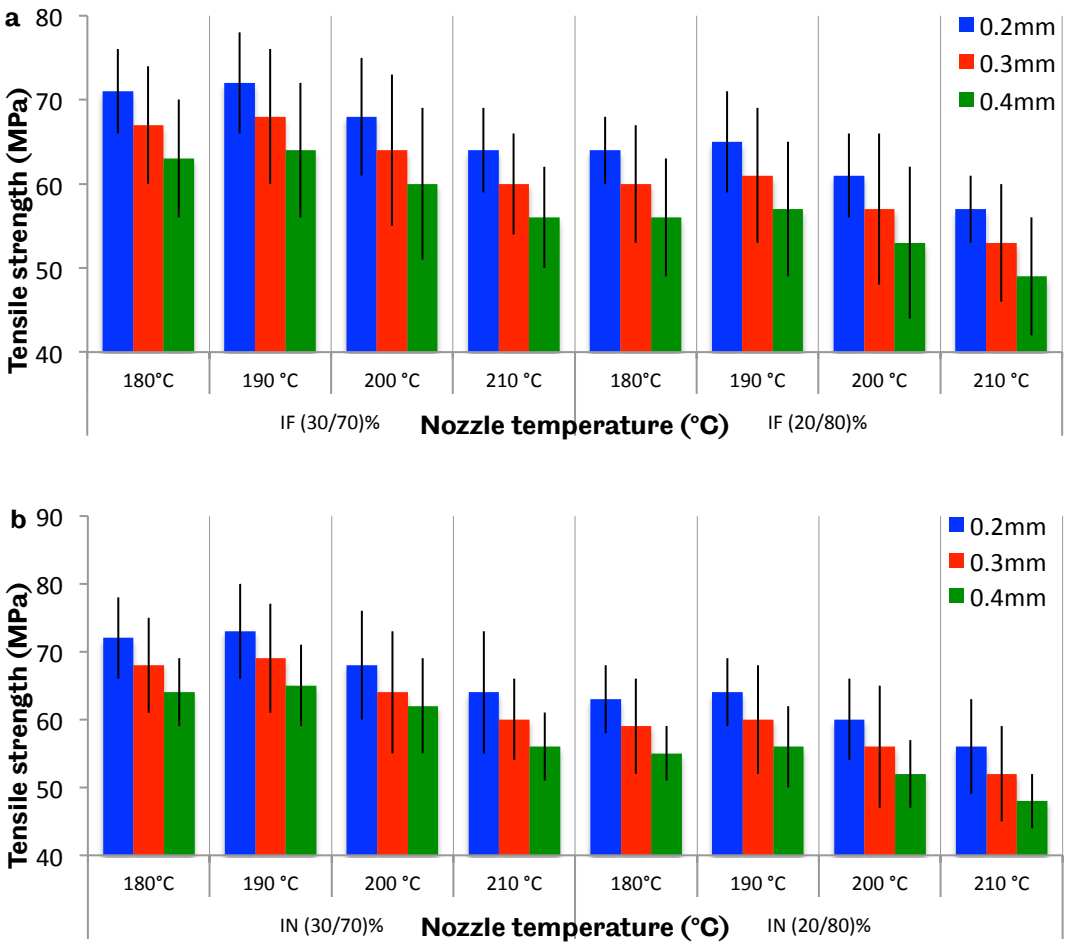

Figure 6.10 Effect of printing parameters on the tensile strength of a) IF composites and b) IN composites of 30%,20 wt%, for 10 composites from each compostie category. The x-axis presents the applied nozzle temperatures from 180 °C to 210 °C. The blue, red, green coloured bars represent the layer height thickness tested at at 0.2 mm, 0.3 mm and 0.4 mm respectively. For each printing parameters tested, the composites were 3D printed and tested with constant values of fill density of 100% and printing pattern orientation of 0°/90°. Notice that the lower value of tensile strength axis are omitted in order to improve the readability of the plot. The error bars represent ±1SD (samples tested for every set of error bars n=5).

The 3D printed dog bone composites had total height of 4 mm. In total, 20 layers were printed at 0.2 mm layer height thickness, 13 layers at 0.3 mm layer height thickness, and 10 layers at 0.4 mm layer height thickness. Comparing the tensile strength (Figures 6.9 and 6.10), of composites consisting of MP and I fibres, the highest results were obtained at a layer height thickness of 0.2 mm.

Reduced tensile strength results were observed at values higher than 0.2 mm layer height thickness (Figures 6.9 and 6.10), which is consistent with the wider literature [222]. Ning *et al.* reported a reduction in tensile strength and Young's modulus results for carbon fibre-reinforced plastic composites at layer height

thicknesses higher than 0.35 mm [328]. Tymrak *et al.* investigated the tensile properties of PLA and ABS polymers printed with different values of layer height thickness. The highest tensile strength was reported for both polymers with 0.2 mm layer height thickness, compared to results obtained from samples printed with 0.3 mm and 0.4 mm layer height thicknesses [227]. Independent from the material, lower values of layer height thickness produced samples with tighter interlayer bonding, with the nozzle acting as a pressure lever between the 3D printed layers, resulting in increased adhesion between the printed parts and reduced concentration of voids [328], [331] As the newly printed layer overlays the previous one, there is a degree of shrinkage during the solidification stage that traps air between the printed layers, resulting in weak adhesion between layers and lower mechanical properties [226], [331].

The tensile strength of the 3D printed composites is also affected by the nozzle temperature (Figures 6.9 and 6.10). Composites consisting of MPF and MPN fibres had a higher tensile strength at 200 °C nozzle temperature. This is contrary to composites made from IF and IN fibres that had the highest tensile strength at 190 °C (Figures 6.9&6.10).

The temperature of the nozzle was determined based on the melting temperature of Floreon (T_m = 180 °C) and the degradation temperature of the fibres (about 200 °C) [19], [93], [207]. Temperatures below 180 °C caused problems in the continuous flow of Floreon and generated weak bonding between the printed layers [328]. Due to flax and nettle degradation at 200 °C and above, the mechanical properties of the 3D printed samples decreased at 210 °C, as seen in Figures 6.9 and 6.10 [332]. The same 10 °C difference between the MP and I fibres in the 3D printed composites was also observed in the injection-moulded composites (chapter 5, section 5.2.3.1). The MP fibres require higher temperatures than the corresponding I fibres, probably because of their rougher untreated surface.

Comparing the Young's modulus results (Table 6.4) of composites consisting of MP and I fibres, the highest results were obtained at a layer height thickness of 0.2 mm. Composites 3D printed with MP fibres had higher Young's modulus compared to the corresponding composites with I fibres. The nozzle temperature and layer height thickness had the same impacts on the composites Young's modulus as on the tensile strength results.

Table 6.4 Effect of printing parameters on the Young's modulus (GPa) of a) MPN and MPF and b) IN and IF composites of 30%,20 wt%, The error bars represent ±1SD (samples tested for every set of error bars n=5).

Young's modulus (GPa) Nozzle temperature (°C) / Layer height thickness (mm)							
a)	**MPN (30/70)%**				**MPN (20/80)%**		
	0.2	0.3	0.4		0.2	0.3	0.4
180	6.8±1.4	6.7±1.3	6.6±1.4		5.6±1.0	5.5±0.9	5.4±0.8
190	6.9±1.3	6.8±1.4	6.7±1.2		5.7±0.9	5.6±0.8	5.5±0.9
200	**7.0±1.4**	6.9±1.3	6.8±1.4		**5.8±0.8**	5.7±0.9	5.6±0.8
210	6.6±1.2	6.4±1.4	6.1±1.5		5.3±0.9	5.1±0.8	4.9±0.8
	MPF (30/70)%				**MPF (20/80)%**		
	0.2	0.3	0.4		0.2	0.3	0.4
180	6.6±1.1	6.5±1.2	6.4±1.0		5.4±1.1	5.3±1.2	5.2±1.1
190	6.7±1.2	6.6±1.3	6.5±1.1		5.5±0.9	5.4±0.8	5.4±0.8
200	**6.8±1.1**	6.7±1.0	6.6±1.1		**5.6±0.7**	5.5±0.9	5.4±0.9
210	6.4±0.8	6.1±0.9	5.7±0.8		5.2±1.1	4.9±1.2	4.6±1.1
Nozzle temperature (°C) / Layer height thickness (mm)							
b)	**IN (30/70)%**				**IN (20/80)%**		
	0.2	0.3	0.4		0.2	0.3	0.4
180	6.1±0.8	6.0±0.9	5.9±0.8		5.6±0.9	5.4±0.8	5.3±0.8
190	**6.3±1.0**	6.2±0.8	6.1±0.9		**5.8±0.8**	5.7±0.9	5.6±0.8
200	6.2±0.8	6.1±1,0	6.0±0.8		5.7±0.9	5.6±0.8	5.5±1.0
210	6.0±0.8	5.8±0.9	5.7±0.8		5.5±0.8	5.2±0.7	4.9±0.8
	IF (30/70)%				**IF (20/80)%**		
	0.2	0.3	0.4		0.2	0.3	0.4
180	5.7±0.8	5,6±1.0	5.5±0.9		5.4±1.1	5.3±1.2	5.2±1.1
190	**5.9±0.9**	5.8±0.8	5.7±0.7		**5.7±1.1**	5.6±0.8	5.5±0.8
200	5.8±0.9	5.7±1.0	5.6±0.8		5.6±0.7	5.5±0.9	5.4±0.9
210	5.6±0.9	5.3±1.0	5.1±0.8		5.2±1.1	4.9±1.2	4.6±1.1

6.6.2.2 Fill density and pattern orientation

The parameters of fill density and pattern orientation affect the mechanical properties of composites consisting of both MP and I fibres. The highest tensile strength and Young's modulus of all 3D printed composites were observed at 100% fill density. The tensile properties of composites were reduced as the fill density decreased. Composites with fill density of 40% had a tensile strength reduction of 10 MPa compared to composites printed with fill density of 100% (Figure 6.11).

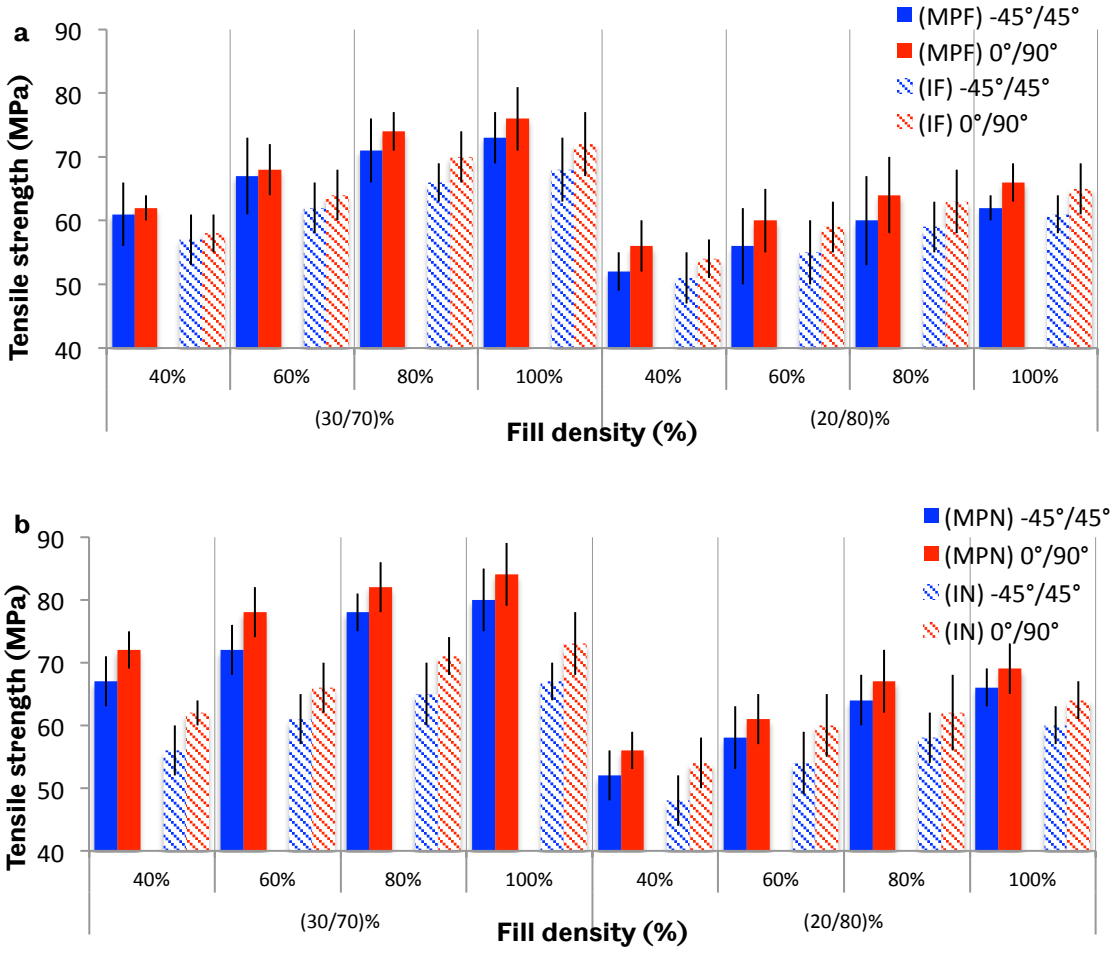

Figure 6.11 Effect of printing parameters on the tensile strength of a) MPF (solid coloured bars) and IF (dashed coloured bars) composites and b) MPN (solid coloured bars) and IN (dashed coloured bars) composites of 30%,20 wt%, for 10 composites from each composite category. The x-axis presents the applied fill density values from 40-100%. The blue and red colours represent the printing pattern orientation tested at -45°/45° and 0°/90 respectively. For each printing parameters tested, the composites were 3D printed and tested with constant values of layer height thickness of 0.2 mm, nozzle temperature of 200 °C for composites consisting of MP fibres and of 190°C for the corresponding composites with I fibres. Notice that the lower value of tensile strength axis are omitted in order to improve the readability of the plot. The error bars represent ±1SD (samples tested for every set of error bars n=5).

The higher Young's modulus was observed at fill density of 100% and pattern orientation of 0°/90° for composites of all categories. Specifically MPN30-90-100-2-200 (pattern orientation of 0°/90°) had Young's modulus at 7.0±1.4 GPa compared to MPN30-45-100-2-200 (pattern orientation of 45°/-45°) at 5.8 ±0.9 GPa. MPF30-90-100-2-200 had Young's modulus at 6.8 ±1.1 GPa while MPF30-45-100-2-200 had Young's modulus at 5.9 ±1.3 GPa.

Higher densities increased the amount of material used and the printing time, as seen in Table 6.5.

Table 6.5 Required printing time and composites' weight due to different fill density values, for MPN30-90-100-2-200 and MPF30-90-100-2-200.

Fill density (%)	Printing time (min)	Composites weight (gr)
100	15	3.2
80	13	3.0
60	11	2.7
40	7	2.4

The literature reports that composites printed with a fill density lower than 80% include voids (air trapped during printing), thereby reducing the mechanical properties [225]. Kim *et al.* reported a reduction in the mechanical properties of ABS and PLA samples 3D printed with a fill density of 50% compared to samples printed with a fill density of 100% [333].

The pattern orientations significantly affect the tensile properties of 3D printed composites. Regardless of the type and concentration of fibre, composites printed at a pattern orientation of 0°/90° had higher tensile strength results than composites printed with -45°/45° orientation. The different tensile strength results based on the pattern orientation and fill density values can be seen in Figure 6.11 a–b.

At a 0°/90° printing pattern orientation, the fibres have the same orientation as the applied force during the tensile tests and therefore, as expected, the tensile properties of these composites are higher than composites 3D printed at -45°/45°. The tensile strength of 3D printed PLA and ABS samples observed by Tymak *et al.* were also greater using the 0°/90° orientation [227]. PLA samples 3D printed with -45°/45° pattern orientation had a 20% reduction in tensile strength and a 14.5% reduction in Young's modulus [216].

6.6.3 Flexural properties

Figure 6.12 presents the flexural stress versus strain curves for 3D printed Floreon, MPN, MPF, IF and IN composites of different fibre concentrations. Floreon and composites had had a linear stress–strain deformation during the bending tests before failure occurs, The linear stress–strain relationship of composites represents the elastic deformation of the polymer up to the maximum reached point of flexural stress; the flexural strength. After that point the first crack occurs in the matrix, and the reinforcing fibres withstand the applied force until the final failure of the composite [305].

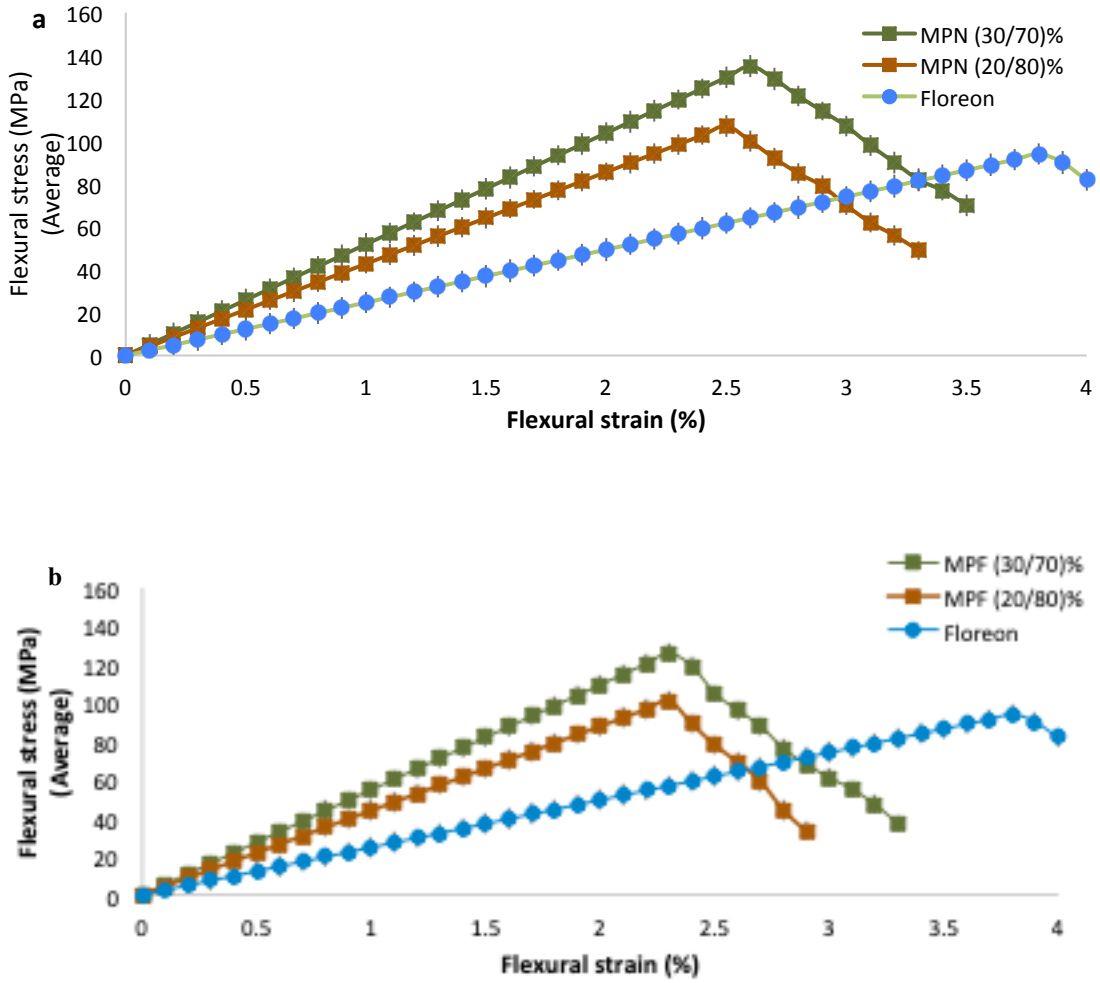

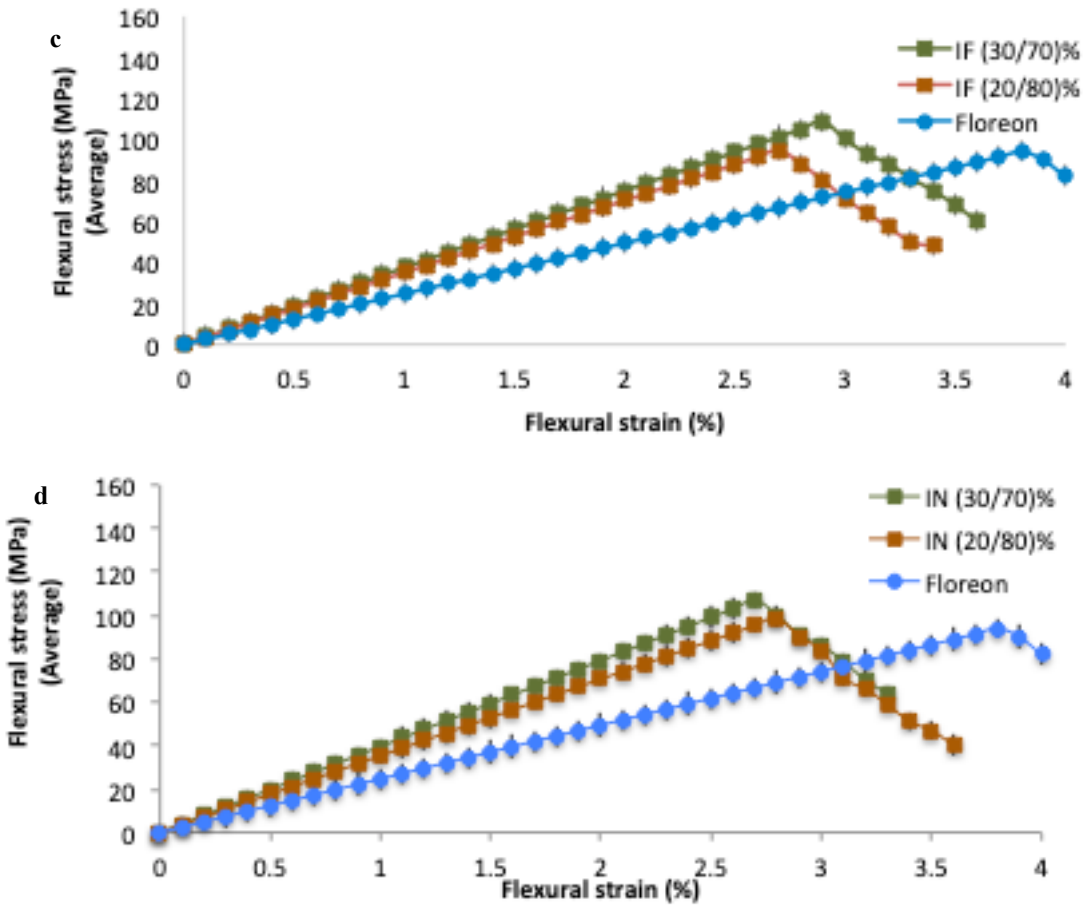

Figure 6.12 Flexural stress-strain curves of Floreon, a) MPN, b) MPF, c) IF and d) IN composites of 30%, 20 wt%, for in total 25 samples of each composite category. Floreon and composites were 3D printed at layer height thickness of 0.2 mm, pattern orientation of -45°/45°, and fill density of 100%. The nozzle temperature composites consisting of MPN fibres was set up at 200 °C and at 190 °C for the corresponding composites with I fibres. The error bars represent ±1SD (samples tested for every set of error bars n=15).

The flexural strength (the maximum stress at the time of failure) of 3D printed Floreon is clearly lower than Floreon-based composites, as seen in Figure 6.13. MPN and MPF (30/70)% composites had the highest flexural strength of all composites produced and had a significant differences compared to the IN and IF (30/70%) composites. MPN30-45-100-2-200 had a flexural strength of 139 ± 7 MPa, compared to IN30-45-100-2-200 with 107 ± 4 MPa. The enhanced flexural properties of composites consisting of MP fibres, especially MPN, are the result of the higher mechanical properties of the fibres derived from the fibre type and preparation process (chapter 3, section 3.5.2.2).

The bending properties of the composites increased at higher fibre concentrations. MPF30-45-100-2-200 had flexural strength of 126 ± 5 MPa,

compared to MPF20-45-100-2-200 with 101 ± 5 MPa. Floreon's flexural strength was 94 ± 5 MPa.

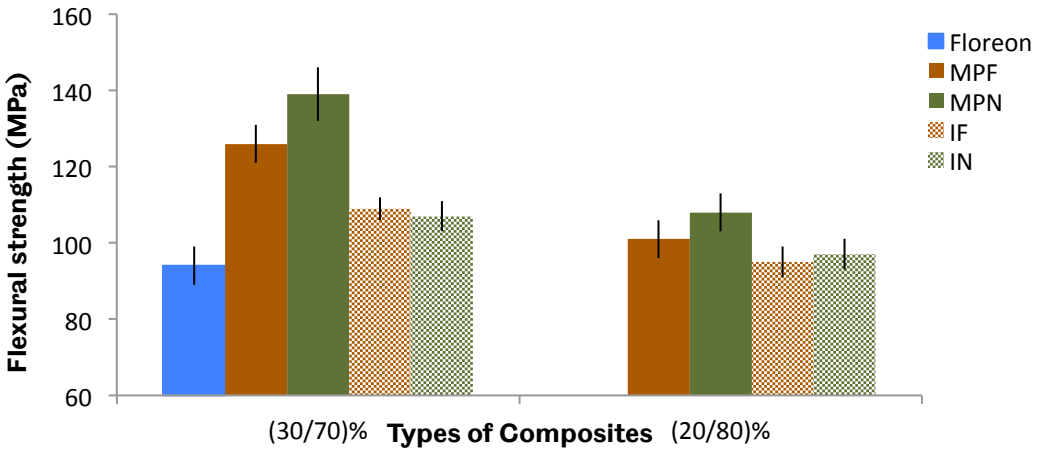

Figure 6.13 Flexural strength (average) of Floreon and Floreon based composites of 30%, 20 wt%, for 25 samples of each composite category. Floreon and composites were 3D printed using a layer height thickness of 0.2 mm, pattern orientation of -45°/45° and fill density of 100%. The nozzle temperature for composites consisting of MP fibres was set up at 200 °C and at 190 °C for the corresponding composites with I fibres. The notation MPN is referred to composites consisting of minimally processed nettle fibres (solid green bars) and MPF to the corresponding composites with minimally processed flax fibres (solid brown bars). The notation IN is referred to composites consisting of industrial processed nettle fibres (dashed green bars) and IF to the corresponding composites with industrial processed flax fibres (dashed brown bars). Notice that the lower value of flexural strength axis are omitted in order to improve the readability of the plot. The error bars represent ±1SD (samples tested for every set of error bars n=15).

The calculated flexural modulus of composites was also higher compared to Floreon. MPN30-45-100-2-200 composites had a flexural modulus of 5.19 ± 1.7 GPa, and MPF30-45-100-2-200 had 5.9 ± 2.5 GPa. The Floreon flexural modulus was 4.9 ± 0.8 GPa. Figure 6.14 shows the increase in flexural modulus in composites as the fibre content increases.

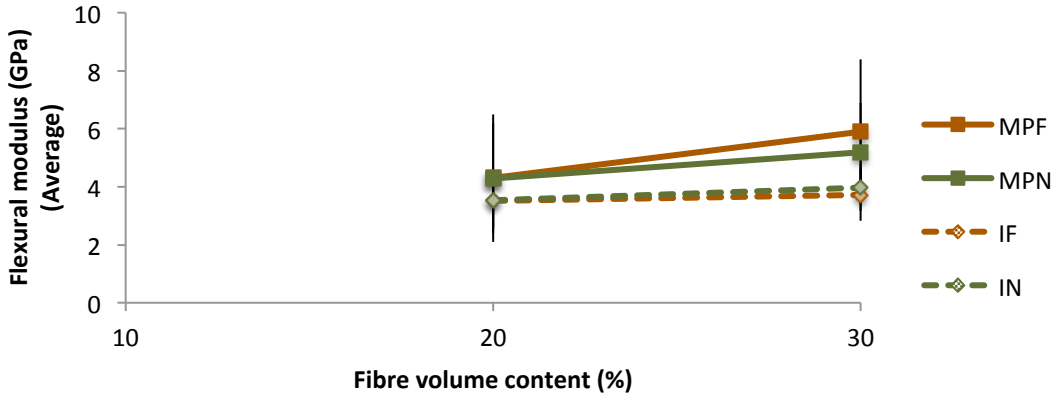

Figure 6.14 Flexural modulus as a function of fibre volume content of MPN, MPF, IF and IN composites of 30% and 20 wt% fibre content. The error bars represent ±1SD (samples tested for every set of error bars n=10).

The results obtained from the bending tests cannot be compared to the wider literature because of the different combination of materials used in this study.

6.6.4 Flexural properties according to the printing parameters

The results of the tensile tests (section 6.6.1.1) indicated that the print parameters affected the tensile properties of composites. Therefore, the composites were tested with different sets of printing parameters (section 6.3.1.1) to evaluate their flexural properties.

6.6.4.1 Nozzle temperature and layer height thickness

Figures 6.15 a–b and 6.16 a–b show the effect of nozzle temperature and layer height thickness on the flexural strength of MPF and MPN composites.

In all composite categories, the highest flexural strength was observed at a layer height thickness of 0.2 mm. Similar to the tensile strength calculations (section 6.6.1.1), increasing the layer height thickness decreases the flexural strength.

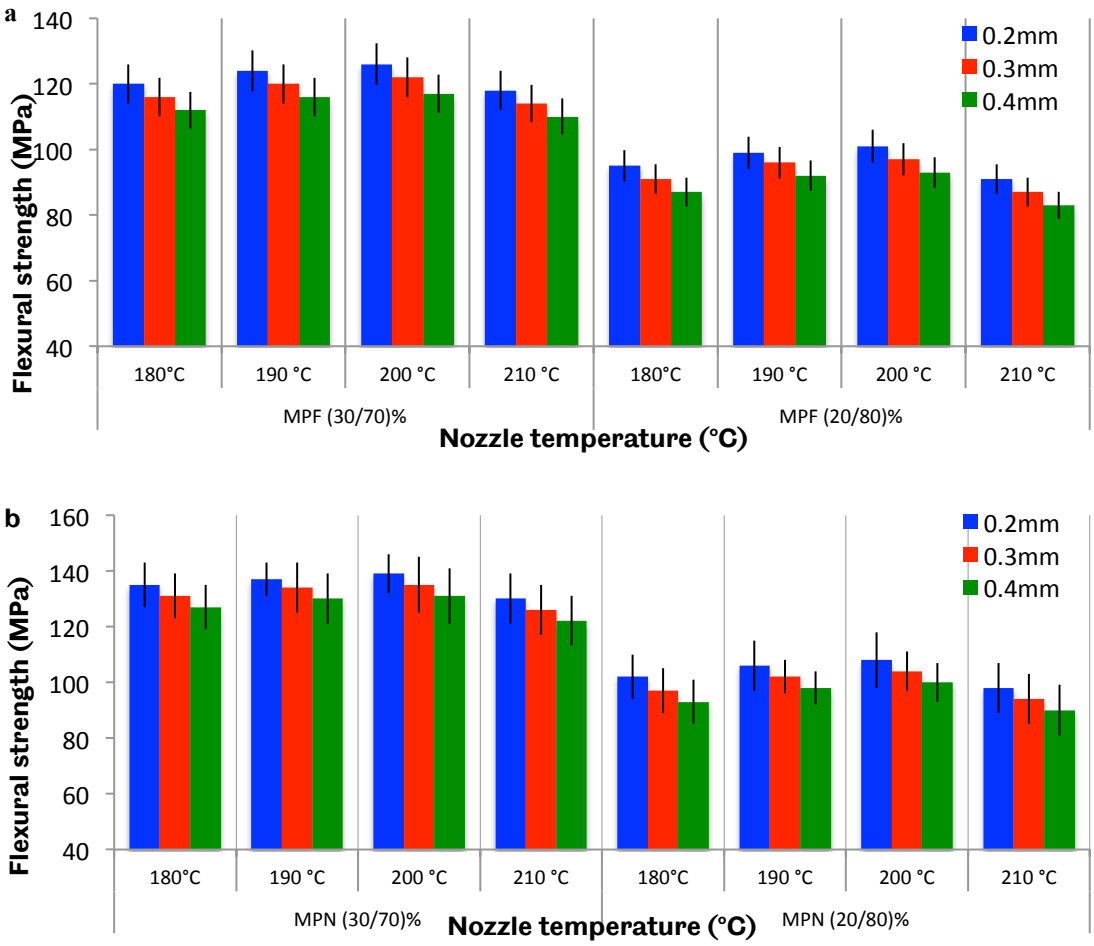

Figure 6.15 Effect of printing parameters on the flexural strength of a) MPF composites and b) MPN composites of 30%,20 wt%, for 10 composites from each composite category. The x-axis presents the applied nozzle temperatures from 180 °C to 210 °C. The blue, red, green coloured bars represent the layer height thickness tested at 0.2 mm, 0.3 mm and 0.4 mm respectively. For each printing parameters tested, the composites were 3D printed and tested with constant values of fill density of 100% and printing pattern orientation of -45°/45°. Notice that the lower value of flexural strength axis are omitted in order to improve the readability of the plot. The error bars represent ±1SD (samples tested for every set of error bars n=5).

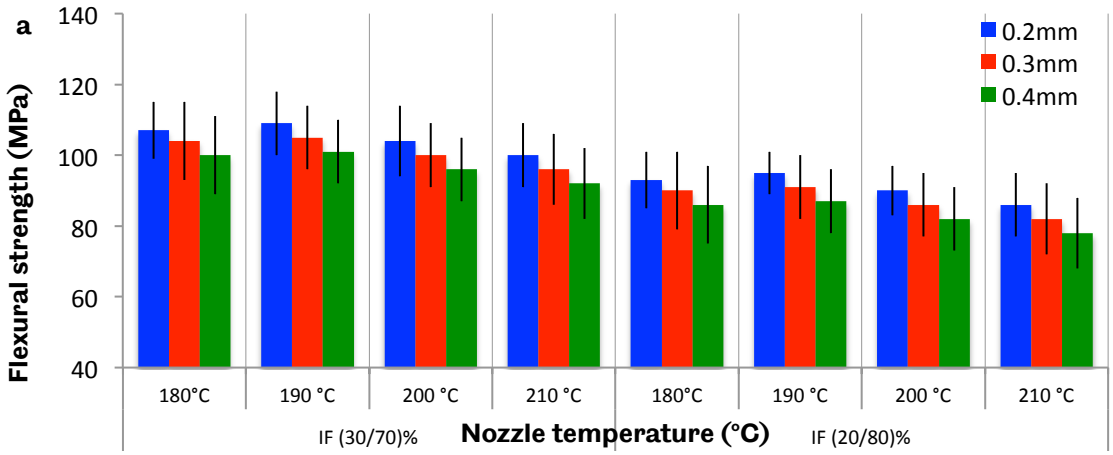

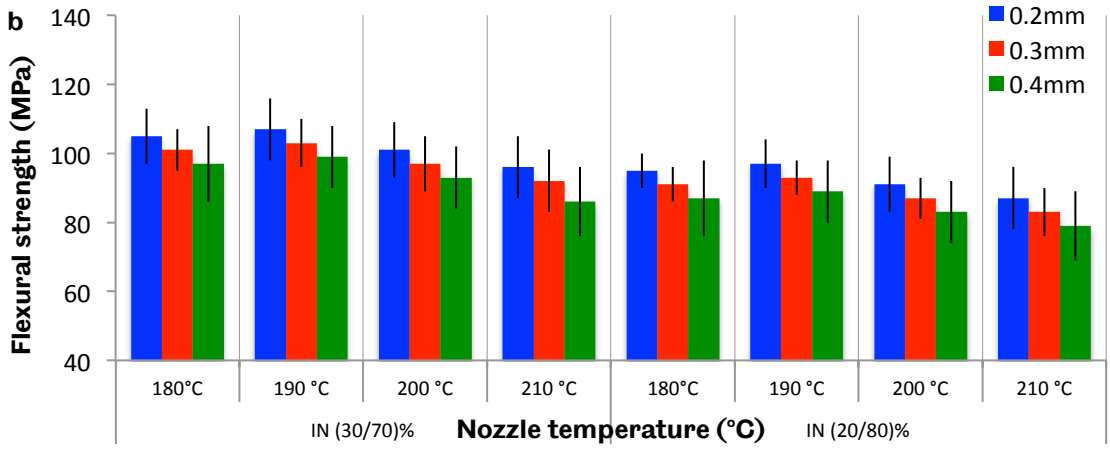

Figure 6.16 Effect of printing parameters on the flexural strength of a) IF composites and b) IN composites of 30%,20 wt%, for 10 composites from each composite category. The x-axis presents the applied nozzle temperatures from 180 °C to 210 °C. The blue, red, green coloured bars represent the layer height thickness tested at 0.2 mm, 0.3 mm and 0.4 mm respectively. For each printing parameters tested, the composites were 3D printed and tested with constant values of fill density of 100% and printing pattern orientation of -45°/45°. Notice that the lower value of flexural strength axis are omitted in order to improve the readability of the plot. The error bars represent ±1SD (samples tested for every set of error bars n=5).

The layer height thickness significantly affects the interlayer adhesion within the composite structure [226]. Reducing the value of layer height thickness to 0.2 mm, the printed structure was tighter, more compact and with reduced probability of trapping quantities of air due to the fact that more layers were 3D printed in one composite, as illustrated in Table 6.6. Comparing the results from the different layer height thickness values, both the tensile (Figures 6.9 and 6.10) and the flexural strength results decreased as the layer height thickness values increased. Kuznetsov *et al.* studied the cross-section area of PLA samples printed with different layer height thickness values, reporting that the voids were significantly decreased at lower layer thicknesses values, resulting in an increase in the mechanical properties of the material [334]. However, it should not be overlooked that the current results are obtained in combination with the secondary print parameters (Table 6.2). Different combinations of secondary print parameters with layer height thickness values can have the opposite results, as reported by Chacón *et al* [335].

Table 6.6 Correlation between the numbers of the printed layers with the different layer height thickness values in a rectangular shaped composite. Each composite had the exact same dimensions with height of 4 mm. Composites with fewer printed layers were lighter compared to composites with higher values of layer height thickness.

Layer height thickness (mm)	Number of printed layers
0.2	20
0.3	13
0.4	10

The flexural properties of the composites were also affected by the nozzle temperature (Figures 6.14 and 6.15). As in the tensile strength calculations, MPN and MPF composites had the highest flexural strength results at a nozzle temperature of 200 °C, while IN and IF composites had the highest flexural strength results at 190 °C. The lowest flexural properties were calculated at 180 °C for composites consisting of MP fibres. Composites consisting of I fibres had the lowest flexural strength at a nozzle temperature of 210 °C. Above 210 °C, the flexural strength of composites of all composite categories was dramatically decreased due to the fibre's thermal degradation [93]. Composites consisting of MP and I fibres behave differently at different nozzle temperatures based on the different degradation temperatures of IN, IF, MPN, and MPF fibres that were mainly affected by the fibres preparation process [336]. Torres *et al.* reported higher strength values at higher nozzle temperatures due to the increase in cohesiveness between the printed layers [337]. However, comparison of the current results with the wider literature was not possible due to the use of Floreon and especially the use of MPN fibres, which have not been used in previous studies.

Comparing the flexural modulus results (Table 6.7) of composites consisting of MP and I fibres, the highest results were obtained at a layer height thickness of 0.2 mm. Composites 3D printed with MP fibres had higher flexural modulus compared to the corresponding composites with I fibres. The nozzle temperature and layer height thickness had the same impacts on the composites flexural modulus as on the flexural strength results. Composites consisting of MP fibres had the highest flexural modulus at nozzle temperature of 200°C, while composites with I fibres at 190°C as it can be seen in Table 6.6.

Table 6.7 Effect of printing parameters on the flexural modulus (GPa) of a) MPN and MPF and b) IN and IF composites of 30%,20 wt%, The error bars represent ±1SD (samples tested for every set of error bars n=5).

Flexural modulus (GPa) Nozzle temperature (°C) / Layer height thickness (mm)							
a)	**MPN (30/70)%**				**MPN (20/80)%**		
	0.2	0.3	0.4		0.2	0.3	0.4
180	5.0±1.2	4.9±1.1	4.8±1.2		4.1±1.2	4.0±1.2	3.9±1.3
190	5.1±1.3	5.0±1.2	4.9±1.0		4.2±1.2	4.1±1.3	4.0±1.3
200	**5.2±1.7**	5.1±1.7	5.0±1.6		**4.3±1.9**	4.2±1.8	4.1±1.8
210	4.9±1.1	4.5±1.0	4.1±1.1		4.0±1.1	3.5±1.0	3.1±1.1
	MPF (30/70)%				**MPF (20/80)%**		
	0.2	0.3	0.4		0.2	0.3	0.4
180	5.7±2.3	5.6±2.1	5.5±2.2		3.9±2.2	3.8±2.1	3.7±2.3
190	5.8±2.4	5.7±2.3	5.6±2.3		4.1±2.1	4.0±2.2	3.9±2.2
200	**5.9±2.5**	5.8±2.3	5.7±2.3		**4.2±2.2**	4.1±2.1	4.0±2.1
210	5.4±2.0	5.0±2.0	3.6±2.1		3.9±2.1	3.4±2.2	3.0±2.1
Nozzle temperature (°C) / Layer height thickness (mm)							
b)	**IN (30/70)%**				**IN (20/80)%**		
	0.2	0.3	0.4		0.2	0.3	0.4
180	3.7±0.8	3.6±0.9	3.5±0.8		3.3±0.9	3.2±0.8	3.1±1.0
190	**3.9±0.8**	3.8±0.8	3.7±0.9		**3.5±0.9**	3.4±0.9	3.3±0.8
200	3.8±0.8	3.7±1,0	3.6±0.9		3.4±0.9	3.3±1.0	3.2±1.1
210	3.5±0.9	3.2±0.9	3.9±0.8		3.1±0.8	2.9±0.7	2.4±0.8
	IF (30/70)%				**IF (20/80)%**		
	0.2	0.3	0.4		0.2	0.3	0.4
180	3.5±0.8	3.4±0.9	3.3±0.8		3.3±1.1	3.2±1.0	3.1±1.0
190	**3.7±1.0**	3.6±0.9	3.5±0.9		**3.5±1.0**	3.4±0.8	3.3±0.9
200	3.6±0.9	3.5±1.0	3.4±0.9		3.4±0.9	3.3±0.9	3.2±0.8
210	3.3±0.9	3.0±1.0	2.7±0.9		3.0±1.1	2.7±1.0	2.4±0.9

6.6.4.2 Fill density and pattern orientation

Fill density and pattern orientation greatly affected the tensile properties of the composites (Figure 6.11). Similarly, these two parameters were tested for the flexural properties of composites, as shown in Figure 6.17 a–b.

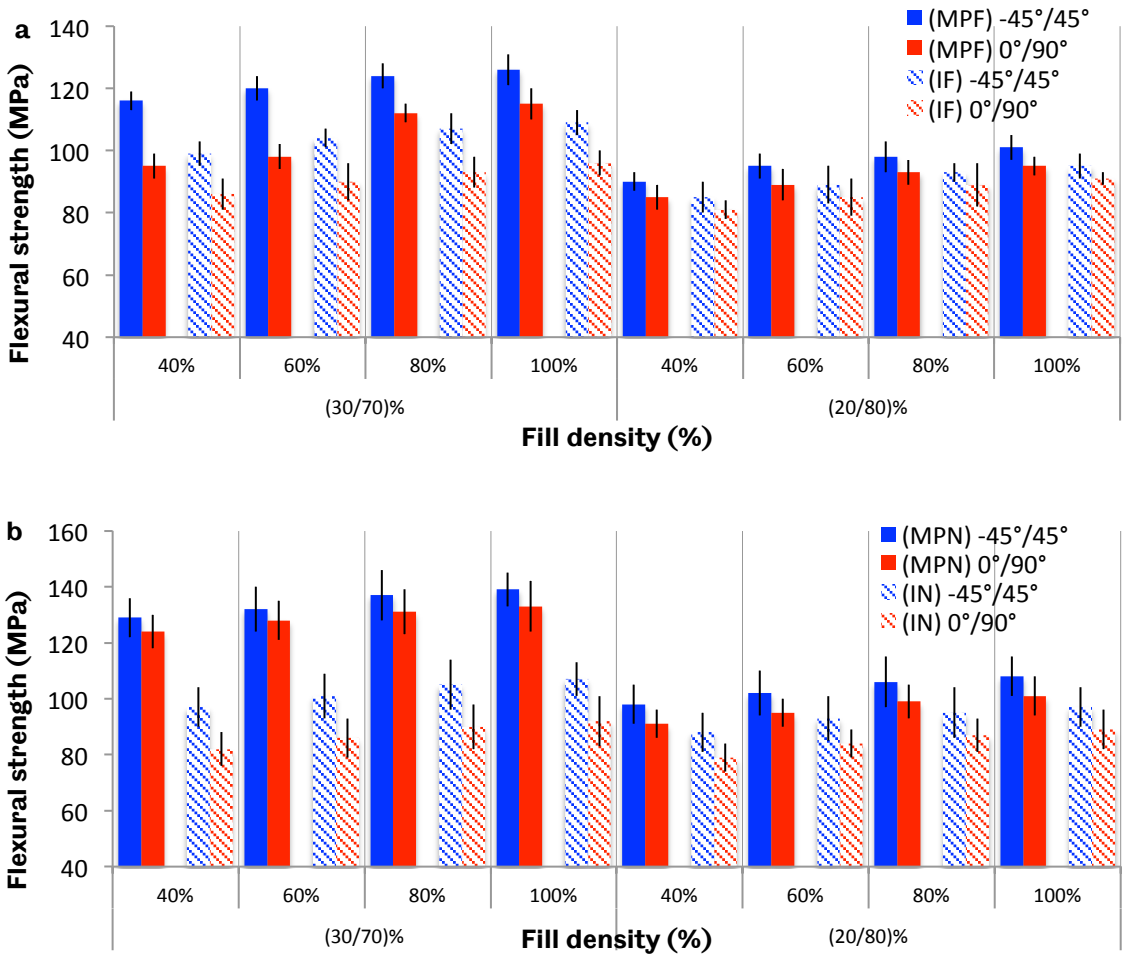

Figure 6.17 Effect of printing parameters on the flexural strength of a) MPF (solid coloured bars) and IF (dashed coloured bars) composites and b) MPN (solid coloured bars) and IN (dashed coloured bars) composites of 30%,20 wt%, for 10 composites from each composite category. The x-axis presents the applied fill density values from 40-100%. The blue and red colours represent the printing pattern orientation tested at -45°/45° and 0°/90 respectively. For each printing parameters tested, the composites were 3D printed and tested with constant values of layer height thickness of 0.2 mm, nozzle temperature of 200 °C for composites consisting of MP fibres and of 190°C for the corresponding composites with I fibres. Notice that the lower value of flexural strength axis are omitted in order to improve the readability of the plot. The error bars represent ±1SD (samples tested for every set of error bars n=5).

The lowest flexural strength results of all composites categories were obtained at a 40% fill density (Figure 6.17). At this value, the 3D printed composites were lighter compared to more densely printed composites. The specific strength (the force per unit area at failure over density) of composites at 40% fill density was higher compared to composites printed at a fill density of 100%, due to the lower mass of the composites. Although composites printed with lower fill densities had higher specific strength values, the final flexural strength results were higher for composites with 100% fill density. The flexural strength of composites printed at 40% fill density was reduced by 7% compared to composites printed at 100%.

Contradictory to the tensile strength, the maximum flexural strengths were obtained using a -45°/45° pattern orientation for all composite categories. The diagonal pattern orientation offered flexibility to the composites. The flexural strength and strain of composites were improved due to the printing direction and fibre orientation being in a plane with the applied bending force [230], [333]. Composites printed at pattern orientation of 0°/90° were oriented parallel (at 0°) and perpendicular (at 90°) to the load direction during the three-point bending tests, resulting in a reduction of flexural strength.

Flexural modulus of 3D printed composites was also affected by the fill density and pattern orientation. Lower amounts of fill density as 40% and 60% reduced significantly the flexural modulus of Floreon and composites as it can be seen in Table 6.8.

Table 6.8 Flexural modulus at different fill density values. The error bars represent ±1SD (samples tested for every set of error bars n=5).

Flexural modulus (GPa)/Fill Density (%)				
	40	**60**	**80**	**100**
Floreon	3.6 ± 0.7	3.9 ± 0.8	4.6 ± 0.9	4.9 ± 0.8
MPN30-45-100-2-200	4.1± 2.0	4.4 ± 1.9	4.9 ± 1.8	5.2 ± 1.9
MPN20-45-100-2-200	3.1 ± 1.8	3.6 ± 1.7	4.0 ± 1.8	4.3 ± 1.7
MPF30-45-100-2-200	4.5 ± 1.8	4.9 ± 2.0	5.3 ± 2.3	5.9 ± 2.5
MPF20-45-100-2-200	3.6 ± 2.3	3.9 ± 2.1	4.1 ± 2.3	4.3 ± 2.2
IF30-45-100-2-190	2.7± 0.9	3.0 ±0.8	3.4 ±0.9	3.7 ± 1.0
IF20-45-100-2-190	2.3 ± 1.0	2.6 ±0.9	3.1 ±0.8	3.5 ± 0.9
IN30-45-100-2-190	2.9±0.9	3.2 ±0.6	3.6 ± 0.7	3.9 ± 0.9
IN20-45-100-2-190	2.6 ±0.9	2.9 ±0.9	3.2 ±0.9	3.5 ± 0.8

The highest recorded flexural modulus was at composites 3D printed at -45°/45° pattern orientation compared to composites 3D printed at 0°/90°. At -45°/45° the flexural modulus of MPN30-45-100-2-200 was at 5.2 ± 1.9 GPa compared to 4.8 ± 0.9 GPa at 0°/90°. Similarly, MPF30-45-100-2-200 had a flexural modulus of 5.9 ± 2.5 GPa at -45°/45° compared to 5.0 ± 1.6 GPa at 0°/90° pattern orientation.

Fatimatuzahraa *et al.* determined improved flexural strength results for ABS 3D printed at a pattern orientation of -45°/45° [228]. Additional studies investigated the flexural properties of thermoplastic polymers according to different pattern orientations such as 0°, 90°, 45°/0°, and -45°/45°, and reported that the highest flexural modulus was observed at pattern orientations of 0° and -45°/45,° which are equivalent [220], [338]. Ang *et al.* correlated the porosity levels of ABS scaffold structures with the samples' flexural properties. Samples with lower porosity levels had the highest compressive modulus and strength. The level of porosity was connected to the applied layer height thickness, fill density, and pattern orientation values [338]. Pollard *et al.* investigated the relation between the specific strength and compressive forces in honeycomb PLA samples, concluding that parts with lower specific strength (because of lower mass) had lower compressive forces during bending tests [339].

To summarise the mechanical properties of the 3D printed composites, the tensile and flexural properties of all composites were much higher than the respective properties of Floreon. MPN (30/70%) composites had the highest tensile strength, Young's modulus, flexural strength, and flexural modulus compared to composites consisting of MPF, IN, and IF fibres indicating that MP fibres are suitable for use as reinforcements. As expected from the rule of mixtures, the mechanical properties of the 3D printed composites were higher at 30 wt% fibre concentration compared to composites with 20 wt%.

The mechanical properties of the 3D printed composites were evaluated based on different sets of printing parameters. The highest tensile and flexural properties were obtained for all composite categories at a fill density of 100% and a layer height thickness of 0.2 mm. During the tensile test, higher results were obtained in the pattern orientation of 0°/90°. Higher results were obtained for the -45°/45° orientation in the three-point bending test. The nozzle temperature affected the mechanical properties of composites differently based on the type and preparation process of the fibres used. Composites consisting of MP fibres had the highest mechanical properties at nozzle temperature of 200 °C, but composites consisting of IN and IF fibres had the highest mechanical properties at 190 °C.

6.6.5 Statistical Analysis

In order to identify if there are any statistically significant differences between the 3D printed composites of different fibre content and type, ANOVA single factor test was applied. By calculating the p-values as it can be seen in Table 6.9, the differences between the mechanical properties of 3D printed composites can be categorised as statistically significant or not.

Table 6.9 Statistical test for the identification of statistically significant difference. Anova-single factor test was applied for the calculation of p-value for tensile strength of MPN, MPF, IN and IF composites consisting of 20% and 30% fibre content. P- values smaller than 0.005 (yellow highlighted) presenti statistically significant difference between the tested composites, while P-values higher than 0.005 (red highlighted) represent not statistically significant differences between the tested composites. Table 6.9a) presented the p-values for the tensile strength, b) Young's modulus, c) flexural strength and d) flexural modulus of MPN, MPF, IN and IF composites.

a)		MPN	MPF	IN	IF	MPN	MPF	IN	IF
%		(20/80)%				(30/70)%			
20/80	MPN	-	-	-	-	-	-	-	-
	MPF	3E-13	-	-	-	-	-	-	-
	IN	4E-13	8E-14	-		-	-	-	-
	IF	6E-13	8E-14	8E-2	-	-	-	-	-
30/70	MPN	6E-14	2E-13	3E-13	4E-13	-	-	-	-
	MPF	3E-14	4E-13	5E-13	4E-13	6E-14	-	-	-
	IN	5E-14	4E-13	9E-2	6E-2	5E-14	3E-14	-	
	IF	2E-14	4E-13	9E-2	4E-2	5E-14	5E-14	7E-2	-

b)		MPN	MPF	IN	IF	MPN	MPF	IN	IF
%		(20/80)%				(30/70)%			
20/80	MPN	-	-	-	-	-	-	-	-
	MPF	2E-17	-	-	-	-	-	-	-
	IN	8E-17	7E-17	-		-	-	-	-
	IF	2E-17	3E-17	2E-3	-	-	-	-	-
30/70	MPN	5E-16	2E-16	4E-3	5E-3	-	-	-	-
	MPF	3E-16	3E-16	2E-3	2E-3	2E-16	-	-	-
	IN	3E-16	6E-16	3E-3	3E-3	3E-16	5E-16	-	
	IF	2E-16	2E-16	4E-3	3E-3	4E-16	4E-16	3E-3	-

c)		MPN	MPF	IN	IF	MPN	MPF	IN	IF
%		(20/80)%				(30/70)%			
20/80	MPN	-	-	-	-	-	-	-	-
	MPF	2E-15	-	-	-	-	-	-	-
	IN	6E-15	6E-15	-		-	-	-	-
	IF	4E-15	2E-15	4E-3	-	-	-	-	-

30/70	**MPN**	6E-15	8E-15	8E-15	9E-15	-	-	-	-
	MPF	5E-15	5E-15	8E-15	1E-15	6E-14	-	-	-
	IN	6E-15	2E-15	4E-3	2E-3	5E-14	3E-14	-	
	IF	4E-15	6E-15	5E-3	2E-3	5E-14	5E-14	4E-3	-

d)		**MPN**	**MPF**	**IN**	**IF**	**MPN**	**MPF**	**IN**	**IF**
%		**(20/80)%**				**(30/70)%**			
20/80	**MPN**	-	-	-	-	-	-	-	-
	MPF	6E-18	-	-	-	-	-	-	-
	IN	4E-18	9E-17	-		-	-	-	-
	IF	6E-17	9E-17	10E-2	-	-	-	-	-
30/70	**MPN**	6E-17	2E-16	5E-2	7E-4	-	-	-	-
	MPF	5E-17	3E-16	6E-2	10E-2	2E-17	-	-	-
	IN	7E-17	6E-16	2E-2	6E-2	5E-17	5E-17	-	
	IF	8E-17	2E-16	7E-2	6E-2	6E-17	8E-17	4E-2	-

As it can be seen from Table 6.9, the calculated tensile strength, Young's modulus, flexural strength and flexural modulus are statistically significant different between the MPN and MPF composites consisting of 20% and 30% fibre content.

6.6.5.1 Limitations during 3D printing

Using fibre-reinforced filaments for 3D printing with the FDM technique faces some limitations. During this project, problems arose due to the fibre concentration and length in combination with the applied printing parameters.

There is a clear operational window where these fibres can be used for FDM [322]. The current maximum fibre concentration in the 3D printed composites was up to 30 wt%, as higher fibre concentrations blocked the printer nozzle. A proposed solution for the blocked nozzle is to increase the nozzle temperature. However, higher nozzle temperatures (above 210 °C, see Figures 6.15 and 6.16), caused a reduction in the mechanical properties due to fibre thermal degradation

In addition, the fibres' length (chapter 5, Table 5.6) in the filament caused problems for the smooth and continuous flow of the filament during the extrusion. Fibres with lengths longer than the allowable limit for the LulzBot TAZ 3 3D printer model blocked the printer nozzle [322].

6.6.6 Comparison between 3D printed and injection-moulded composites

In order to compare injection moulding and 3D printing for the production of fibre-reinforced composites, samples with the same fibre content of MPF and MPN fibres and Floreon as a binding matrix were tested.

Before the evaluation of the mechanical properties obtained from the different techniques, the material required for dog bone and rectangular samples was compared. Less filament was required for 3D printing of composites, because of the ability to adjust different printing parameters. For example, materials 3D printed with fill density less than 80%, were much lighter due to the smaller amount of material used. During the injection moulding, mould overfilling occurred frequently and led to a significant amount of wasted material.

The 3D printed composites had also higher tensile and flexural properties compared to the respective injection-moulded composites, as presented in Figure 6.18.

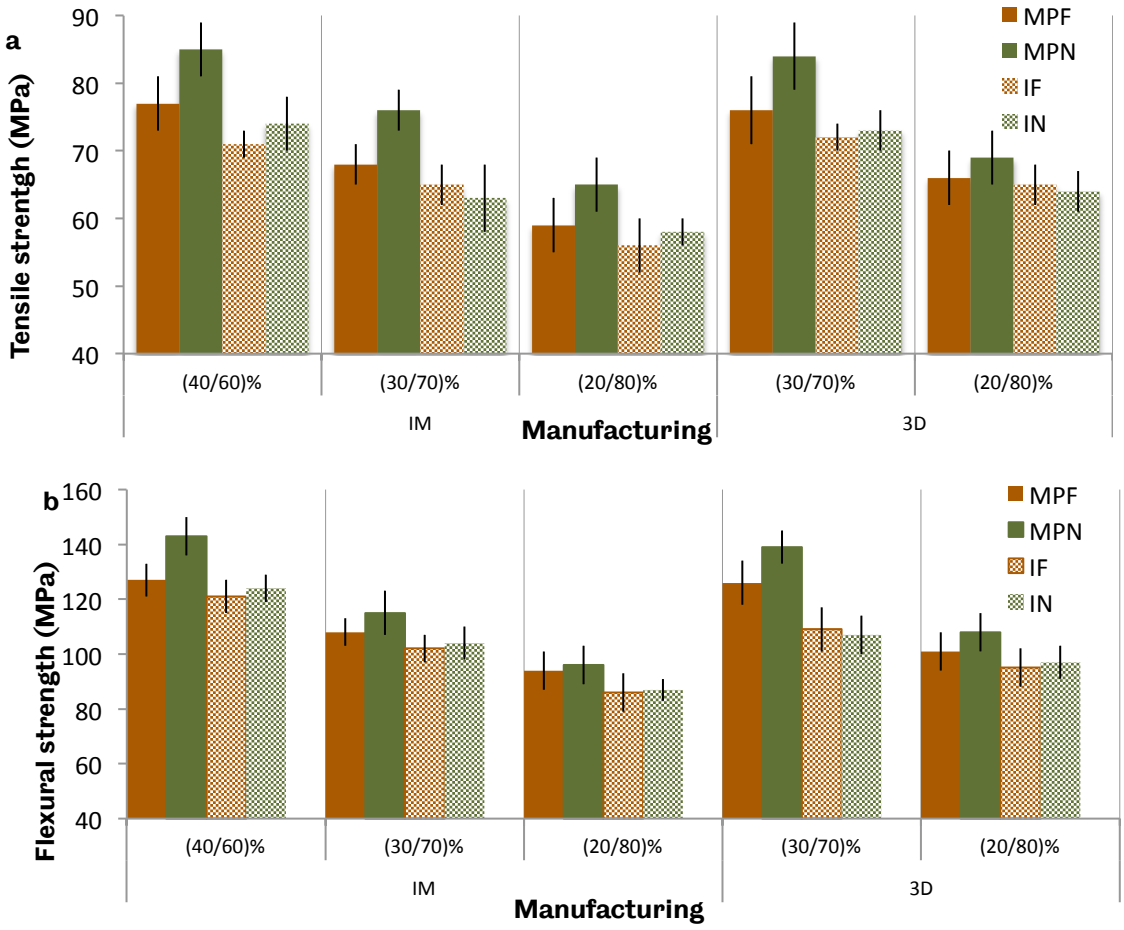

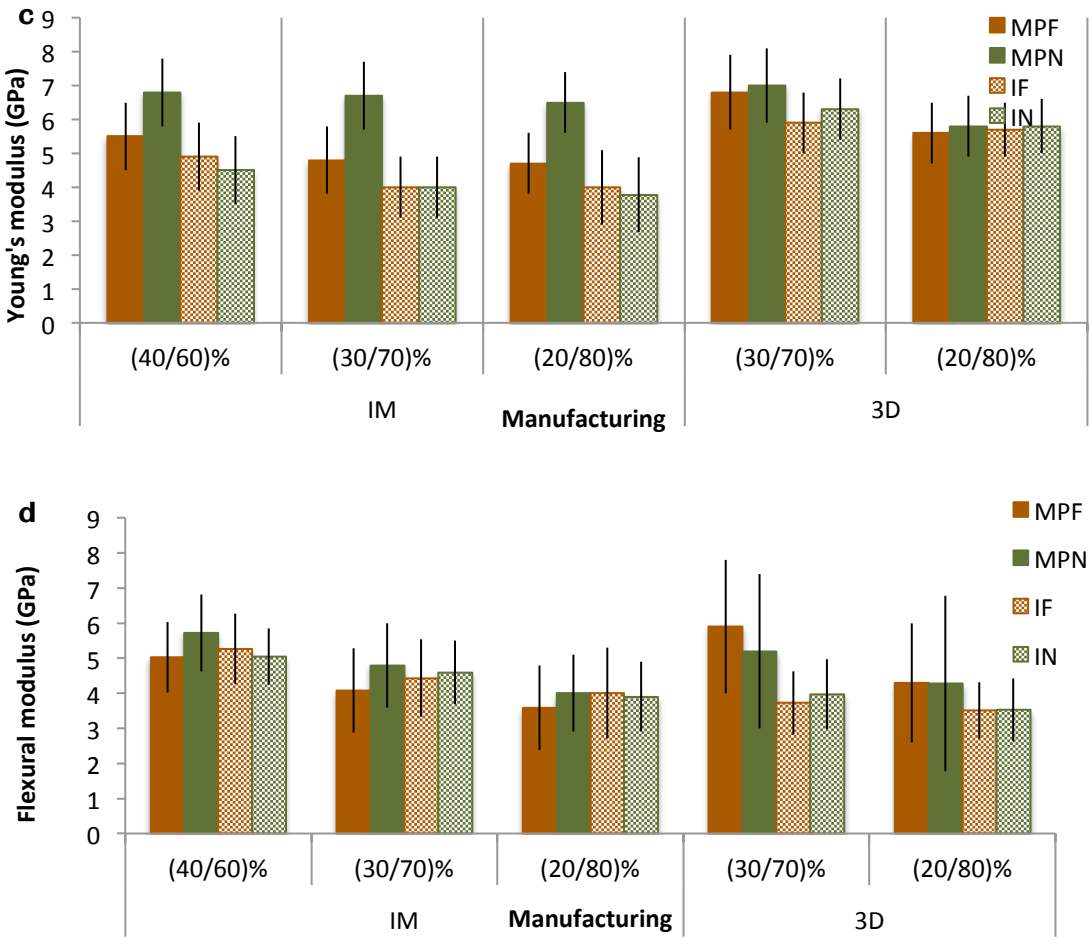

Figure 6.18 Injection moulding Vs. 3D printing, a) tensile strength and b) flexural strength, c) Young's modulus and d) flexural modulus of injection moulded (IM) and 3D printed composites (3D) of 40%, 30%, 20 wt%. The notation MPN is referred to composites consisting of minimally processed nettle fibres (solid green bars) and MPF to the corresponding composites with minimally processed flax fibres (solid brown bars). The notation IN is referred to composites consisting of industrial processed nettle fibres (dashed green bars) and IF to the corresponding composites with industrial processed flax fibres (dashed brown bars). The IM composites were made using extrusion pressure of 40 bar, moulding pressure of 500 bar and moulding time of 1 minute. The moulding temperature for composites consisted of MP fibres was set up at 190 °C and at 180°C for the corresponding composites with I fibres. The 3D printed composites were made using layer height thickness of 0.2 mm, pattern orientation of 0°/90° for tensile testing and at -45°/45° for bending testing, fill density of 100%. The nozzle temperature for composites consisted of MP fibres was set up at 200°C and at 190 °C for the corresponding composites with I fibres. Notice that the lower value of tensile and flexural strength axis are omitted in order to improve the readability of the plot. The error bars represent ±1SD (samples tested for every set of error bars n=15).

6.6.7 Statistical Analysis

An ANOVA single factor statistical test was performed on the 3D printed and injection moulded composites. ANOVA test was perform to evaluate the p-value and identify statistically significant differences between composites of the same fibre type and content manufacture with the two different techniques. The calculated p-values for the injection moulded (IM) and 3D printed (3D) composites are presented in Table 6.10.

Table 6.10 Statistical test for the identification of statistically significant difference between the 3D printed and injection moulded composites. Anova-single factor test was applied for the calculation of p-value for mechanical properties of 3D and injection moulded MPN, MPF, IN and IF composites consisting of 20% and 30% fibre content. P- values smaller than 0.005 (yellow highlighted) present statistically significant difference between the tested composites, while P-values higher than 0.005 (red highlighted) represent not statistically significant differences between the tested composites. Table 6.9a) presented the p-values for the tensile strength, b) Young's modulus, c) flexural strength and d) flexural modulus of 3D and injection moulded MPN, MPF, IN and IF composites.

a) Tensile strength		MPN	MPF	IN	IF		MPN	MPF	IN	IF
%		IM (20/80)%					IM (30/70)%			
3D (20/80)	MPN	3E-16	2E-16	5E-16	5E-16		6E-17	7E-17	7E-16	6E-17
	MPF	7E-16	4E-16	2E-16	7E-16		3E-17	8E-17	2E-17	4E-17
	IN	6E-16	8E-16	9E-16	7E-16		5E-17	5E-17	2E-17	6E-17
	IF	7E-16	8E-16	8E-16	2E-16		2E-17	6E-17	3E-17	5E-17
3D (30/70)	MPN	5E-16	7E-15	8E-15	2E-15		4E-15	1E-15	9E-15	5E-15
	MPF	7E-16	6E-15	4E-15	7E-15		7E-15	7E-15	2E-15	6E-15
	IN	2E-15	7E-15	3E-15	6E-15		7E-15	7E-15	3E-15	9E-15
	IF	4E-16	2E-15	3E-15	6E-15		3E-15	8E-15	5E-15	3E-15

b) Young's modulus		MPN	MPF	IN	IF		MPN	MPF	IN	IF
%		IM (20/80)%					IM (30/70)%			
3D (20/80)	MPN	2E-13	2E-16	5E-16	5E-16		5E-19	8E-19	7E-19	6E-19
	MPF	5E-13	4E-16	2E-16	7E-16		8E-19	3E-19	8E-19	4E-19
	IN	2E-13	8E-16	6E-16	7E-16		6E-19	5E-19	8E-19	6E-19
	IF	4E-13	8E-16	6E-16	2E-16		4E-19	7E-19	9E-19	5E-19
3D (30/70)	MPN	4E-13	6E-13	5E-13	2E-13		8E-19	9E-19	8E-19	5E-19
	MPF	4E-13	4E-13	6E-13	7E-13		2E-19	2E-19	3E-19	3E-19
	IN	2E-13	8E-13	8E-13	6E-13		8E-19	3E-19	4E-19	6E-19
	IF	4E-13	4E-13	4E-13	6E-13		9E-19	4E-19	7E-19	4E-19

c) Flexural strength		MPN	MPF	IN	IF		MPN	MPF	IN	IF
%		IM (20/80)%					IM (30/70)%			
3D (20/80)	MPN	1E-15	2E-15	5E-15	7E-15		8E-19	6E-19	8E-19	9E-19
	MPF	8E-15	8E-15	8E-15	5E-15		4E-19	4E-19	7E-19	8E-19

	IN	5E-15	3E-15	4E-15	8E-15		6E-19	7E-19	6E-19	7E-19
	IF	4E-15	7E-15	3E-15	6E-15		7E-19	1E-19	4E-19	3E-19
3D (30/70)	**MPN**	5E-14	7E-14	6E-14	4E-14		4E-18	6E-18	6E-18	6E-18
	MPF	3E-14	8E-14	3E-14	8E-14		6E-18	4E-18	4E-18	7E-18
	IN	8E-14	4E-14	7E-14	8E-14		9E-18	6E-18	7E-18	3E-18
	IF	7E-14	9E-14	8E-14	5E-14		3E-18	2E-18	7E-18	5E-18

d) Flexural modulus		**MPN**	**MPF**	**IN**	**IF**		**MPN**	**MPF**	**IN**	**IF**
%		**IM (20/80)%**					**IM (30/70)%**			
3D (20/80)	**MPN**	7E-12	2E-12	7E-12	4E-12		2E-15	6E-15	4E-15	3E-15
	MPF	5E-12	6E-12	5E-12	4E-12		3E-15	7E-15	4E-15	4E-15
	IN	3E-12	7E-12	3E-12	3E-12		7E-15	2E-15	6E-15	5E-15
	IF	7E-12	4E-12	3E-12	2E-12		8E-15	6E-15	2E-15	6E-15
3D (30/70)	**MPN**	5E-11	7E-11	5E-11	4E-11		4E-14	6E-14	6E-14	2E-14
	MPF	4E-11	3E-11	5E-11	5E-11		3E-14	8E-14	6E-14	3E-14
	IN	4E-11	2E-11	3E-11	5E-11		3E-14	8E-14	8E-14	3E-14
	IF	3E-11	4E-11	2E-11	7E-11		6E-14	9E-14	9E-14	3E-14

The statistical analysis and the calculated p-values between the 3D printed and injection moulded composites (Table 6.10) have shown that the obtained tensile and flexural results (tensile strength, Young's modulus, flexural strength and flexural modulus) have statistically significant differences.

It is remarkable that the 3D printed composites with6 a fibre content of 30 wt% and 100% infill approached, and in some cases exceed, the tensile strength values obtained from the injection-moulded composites of 40 wt% fibre content. Specifically, the tensile strength of the 3D printed IN30-90-100-2-190 was 15% greater than the injection-moulded IN30-180-40-1. Furthermore, the tensile strength of the MPN30-90-100-2-200 and MPF30-90-100-2-200 was 12% and 11% greater, respectively, compared to the injection-moulded counterparts.

A possible explanation for the improvement of the tensile strength is that the layer-by-layer 3D printing enhanced the fibre/polymer adhesion. The pattern orientation helped align the fibres, resulting in increased tensile and flexural properties in the direction of applied force during mechanical tests [340]. The ability to control the fill density at every printed layer reduced the void content, creating a homogeneous structure over the sample's length [325], [333].

In order to identify the significance between the tensile and flexural strength results of the injection-moulded and 3D printed composites, ANOVA single factor statistical tests were performed. The obtained p-values were always lower than the significance level α, indicating that the properties of the 3D printed composites

are indeed higher compared to the injection-moulded composites (results of ANOVA tests are presented in Appendix A and B).

6.6.8 Moisture absorption

Part of the evaluation of the mechanical properties of the 3D printed composites was to examine the behaviour of the samples in different humidity conditions. The 3D printed composites were exposed to 40, 60, and 80% RH for 24 hours respectively. Table 6.11 presents the moisture absorption (wt %) of 3D printed composites calculated using Equation4.17.

Table 6.11 Average moisture absorption (wt%) of Floreon and composite of different fibre compositions, for 10 composites from each composite category. The notation MPN is referred to composites consisting of minimally processed nettle fibres and MPF to the corresponding composites with minimally processed flax fibres. The notation IN is referred to composites consisting of industrial processed nettle fibres and IF to the corresponding composites with industrial processed flax fibres. The composites were exposed from 40-80% RH for 24 hours.

		Composites			
RH (%)	**Floreon**	**MPF**	**MPN**	**IF**	**IN**
		Composition: (30/70)%			
80	3.5	7	8	5	6
60	2.5	4	5	3	3.5
40	1.5	3	3.5	2	2.5
		(20/80)%			
80		5	6	3.6	4
60		3	4	3	3
40		2.5	2.7	1.8	2

From the aforementioned results, composites with 30 wt% fibre concentration absorbed the most moisture in all RH levels tested. Moisture absorption was more prevalent at 80% RH and was reduced at lower RHs. Composites consisting of MP fibres absorbed the highest percentage of moisture, which is in agreement with the results obtained from the injection-moulded composites (chapter 5, section 5.2.6).

MPN (30/70)% and MPF (30/70)% composites had average Δm absorption of 8 wt% and 7 wt% respectively, compared to 3.5 wt% for Floreon (the values referred to 80% RH). Even though the manufacturing of composites was different, the 3D printed composites from all composite categories absorbed higher amounts of

moisture due to the hydrophilic character of fibres compared to Floreon (chapter 3), affecting both the physical and mechanical properties of the composites.

Floreon reached a moisture equilibrium stage earlier than the fibre-reinforced composites, similar to the results for injection-moulded Floreon (chapter 5, Figure 5.15c), presented in Figure 6.19 a–b. As displayed in Figure 6.19 a–b, composites with I fibres reached an equilibrium stage faster than composites with MP fibres. The moisture equilibrium stage is related to the rate of moisture absorption of the hydrophilic fibres, which bond water molecules to the hydroxyl groups (chapter 2, section 2.2.2). Moisture absorption results in the appearance of micro-cracks in the fibre structure, which increase moisture absorption and cause dimensional instability in the fibres and ultimately in the whole composite. [320], [341].

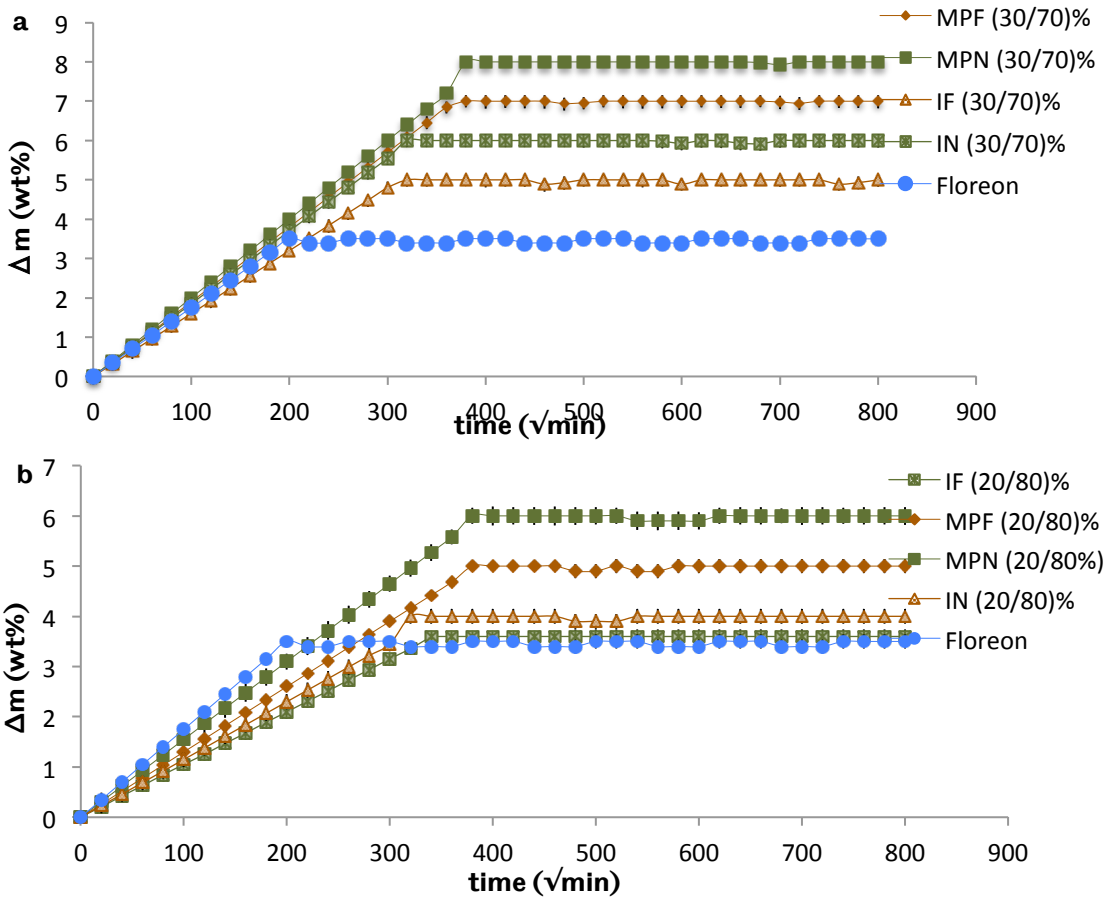

Figure 6.19 Moisture absorption (wt%) plots for Floreon and composite exposed at 80% RH for 24 hours of exposure of a) 30 wt% and b) 20 wt% fibre, for 10 composites for each composite type. The notation MPF is referred to composites consisting of minimally processed flax fibres of 30,20 wt% (brown rhombus) and MPN to the corresponding composites with minimally processed nettle fibres of 30,20 wt% (green squares). The notation IF is referred to composites consisting of industrial processed flax fibres of 30,20 wt% (dashed brown triangles) and IN to the corresponding composites with industrial processed nettle fibres of 30,20 wt% (dashed green squares). The error bars represent ±1SD (samples tested for every set of error bars n=5).

6.6.8.1 Tensile test

The appearance of micro-cracks in the fibre structure due to moisture absorption affected the physical properties of the fibres (swelling). To investigate whether the change in fibre dimensions (chapter 3, Table 3.6) causes problems to the composites, they were tested by tensile and bending tests.

The tensile strength of the 3D printed composites, calculated after moisture absorption tests, was affected by the fibre concentration and by the RH, as shown in Figure 6.20 a-b.

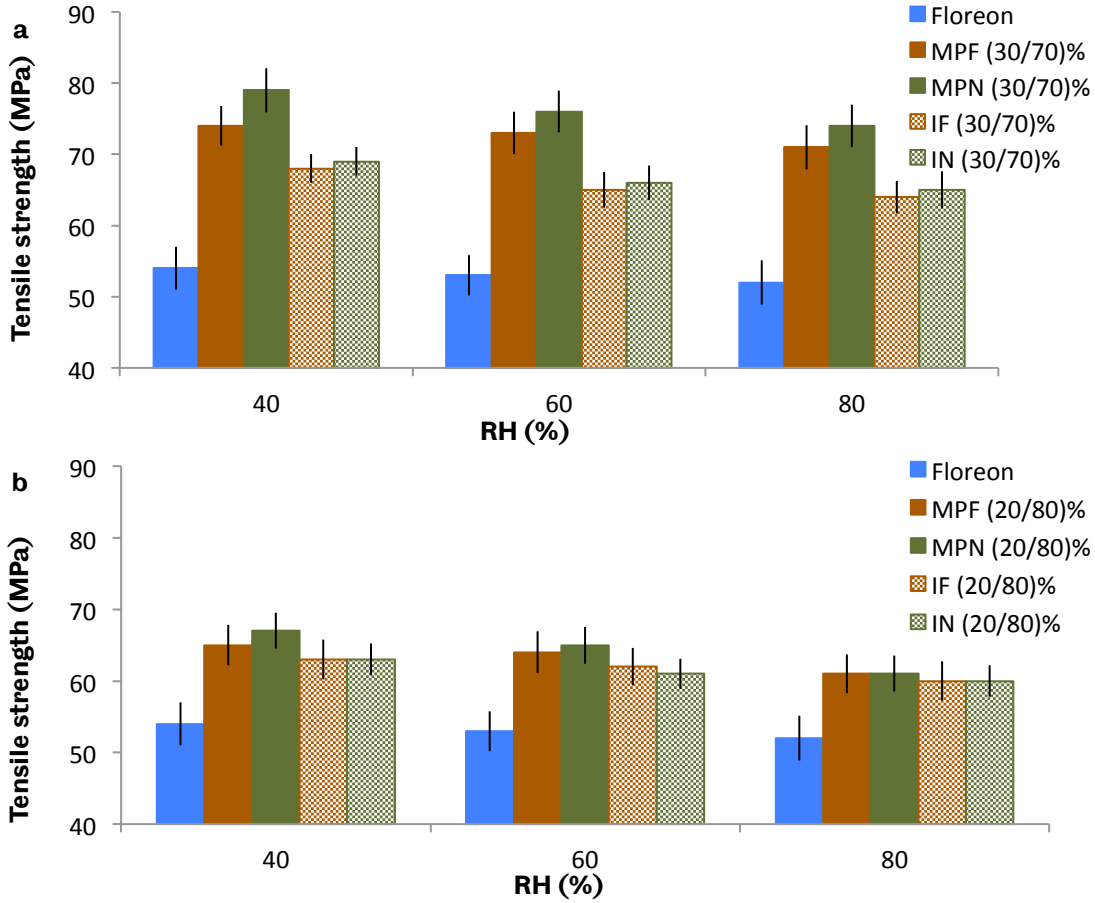

Figure 6.20 Tensile strength (average) of Floreon and Floreon based composites 30%, 20 wt% as a function of different RH, for 5 composites from each composite category. The composites were made using layer height thickness of 0.2 mm, pattern orientation of 0°/90°, fill density of 100%. The nozzle temperature for composites consisted of MP fibres was set up at 200 °C and at 190 °C for the corresponding composites with I fibres. The notation MPN and MPF referred to composites consisting of minimally processed nettle fibres (solid green bars) and to minimally processed flax fibres (solid brown bars) respectively. The notation IN and IF referred to composites consisting of industrial processed nettle fibres (dashed green bars) and to industrial processed flax fibres (dashed brown bars) respectively. Notice that the lower value of tensile strength axis are omitted in order to improve the readability of the plot. The error bars represent ±1SD (samples tested for every set of error bars n=3).

MPN (30/70%) and MPF (30/70%) composites had the largest decrease in tensile strength at all RH levels. MP nettle and flax fibres had the highest moisture absorption and largest decrease in their mechanical properties (chapter 3, section 3.5.3.1) and were similarly affected when included in composites. The decrease in the tensile strength of the 3D printed composites over different RHs is presented in Figure 6.21 a–b.

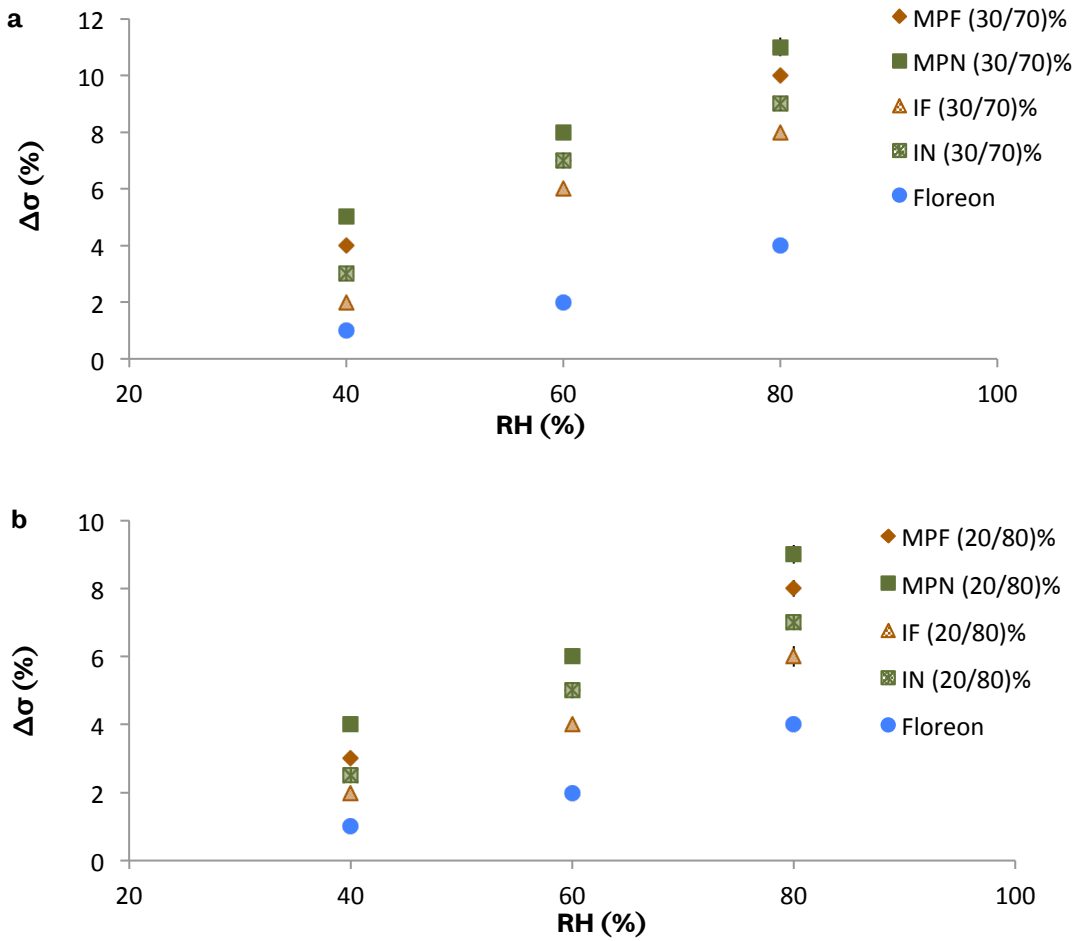

Figure 6.21 Reduction in the tensile strength of Floreon and Floreon based composites of a) 30 wt% and b) 20 wt% fibre as a function of different RH, for 5 composites from each composite category. The notation MPN is referred to composites consisting of minimally processed nettle fibres (green squares) and MPF to the corresponding composites with minimally processed flax fibres (brown rohmbus). The notation IN is referred to composites consisting of industrial processed nettle fibres (dashed green squares) and IF to the corresponding composites with industrial processed flax fibres (dashed brown triangles). The error bars represent ±1SD (samples tested for every set of error bars n=3).

The fibre-reinforced composites had a greater reduction in tensile strength and Young's modulus results compared to pure Floreon. The highest reduction of the Young's modulus results of the 3D printed composites was observed at 80% RH as

it can be seen in Figure 6.22. According to the literature, this is the result of the fibre/matrix debonding due to moisture absorption [106], [161]. At 80% RH, the tensile strength of Floreon decreased by 4%, compared to MPN (30/70%) with an 11% reduction.

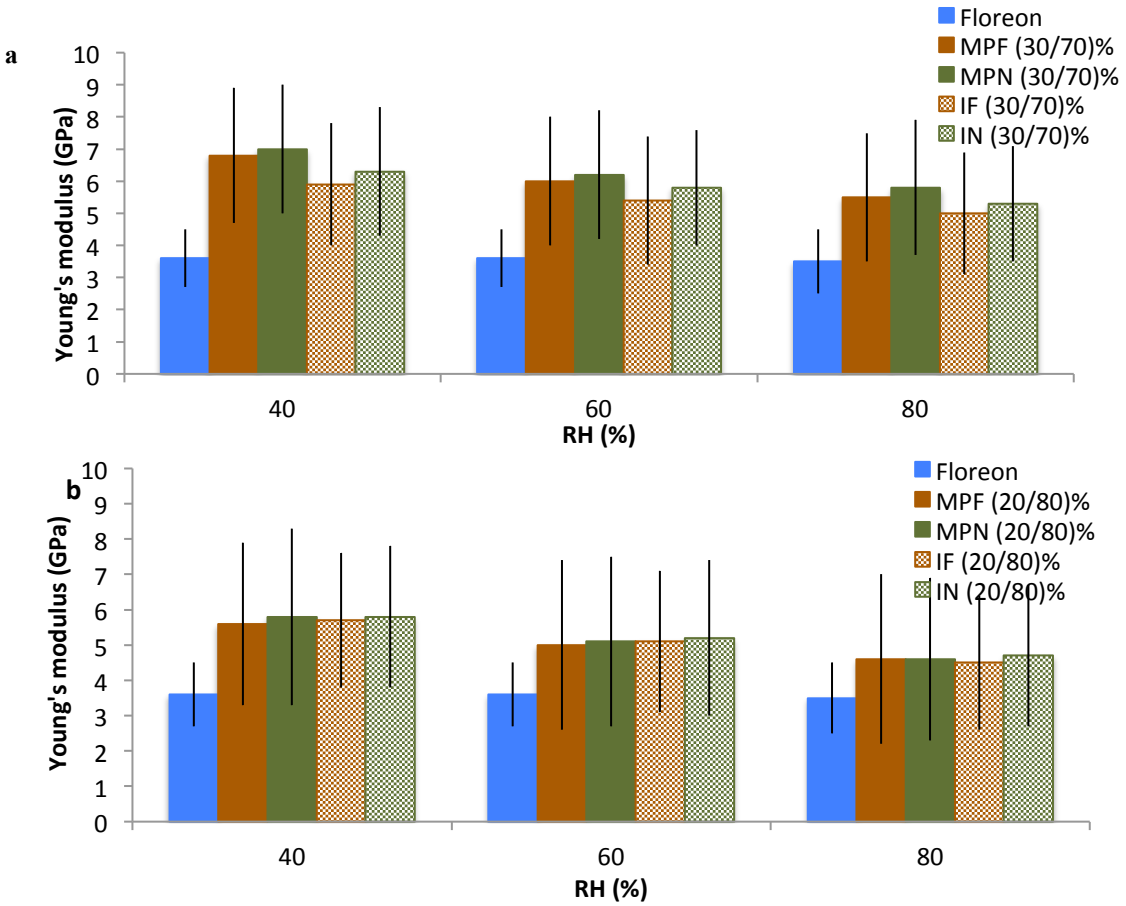

Figure 6.22 Young's (average) of Floreon and Floreon based composites a) 30%, b) 20 wt% as a function of different RH, for 5 composites from each composite category. The composites were made using layer height thickness of 0.2 mm, pattern orientation of 0°/90°, fill density of 100%. The nozzle temperature for composites consisted of MP fibres was set up at 200 °C and at 190 °C for the corresponding composites with I fibres. The notation MPN is referred to composites consisting of minimally processed nettle fibres (solid green bars) and MPF to the corresponding composites with minimally processed flax fibres (solid brown bars). The notation IN is referred to composites consisting of industrial processed nettle fibres (dashed green bars) and IF to the corresponding composites with industrial processed flax fibres (dashed brown bars). The error bars represent ±1SD (samples tested for every set of error bars n=3).

6.6.8.2 Flexural properties

As presented in Figure 6.23 a–b, composites consisting of 30 wt% fibre content had a greater reduction in flexural properties compared to composites consisting of 20 wt% fibre content.

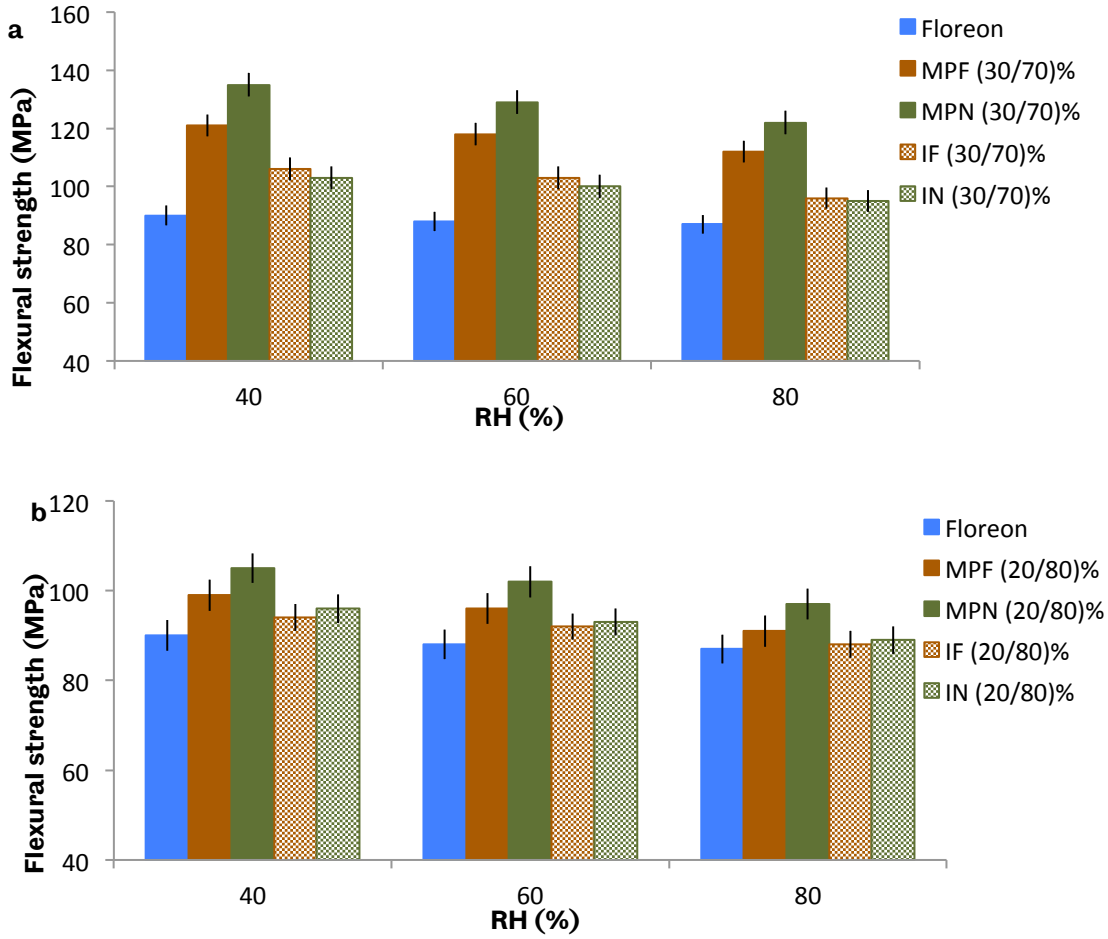

Figure 6.23 Flexural strength (average) of Floreon and Floreon based composites 30%, 20 wt% as a function of different RH, for 5 composites from each composite category. The composites were made using layer height thickness of 0.2 mm, pattern orientation of -45°/45°, fill density of 100%. The nozzle temperature for composites consisted of MP fibres was set up at 200 °C and at 190 °C for the corresponding composites with I fibres. The notation MPN is referred to composites consisting of minimally processed nettle fibres (solid green bars) and MPF to the corresponding composites with minimally processed flax fibres (solid brown bars). The notation IN is referred to composites consisting of industrial processed nettle fibres (dashed green bars) and IF to the corresponding composites with industrial processed flax fibres (dashed brown bars). Notice that the lower value of flexural strength axis are omitted in order to improve the readability of the plot. The error bars represent ±1SD (samples tested for every set of error bars n=3).

Similar to the tensile tests, the composites had largest reduction in flexural strength compared to pure Floreon. Composites from all composite categories exposed to 80% RH had a larger reduction in flexural strength compared to Floreon, as shown in Figure 6.24 a–b.

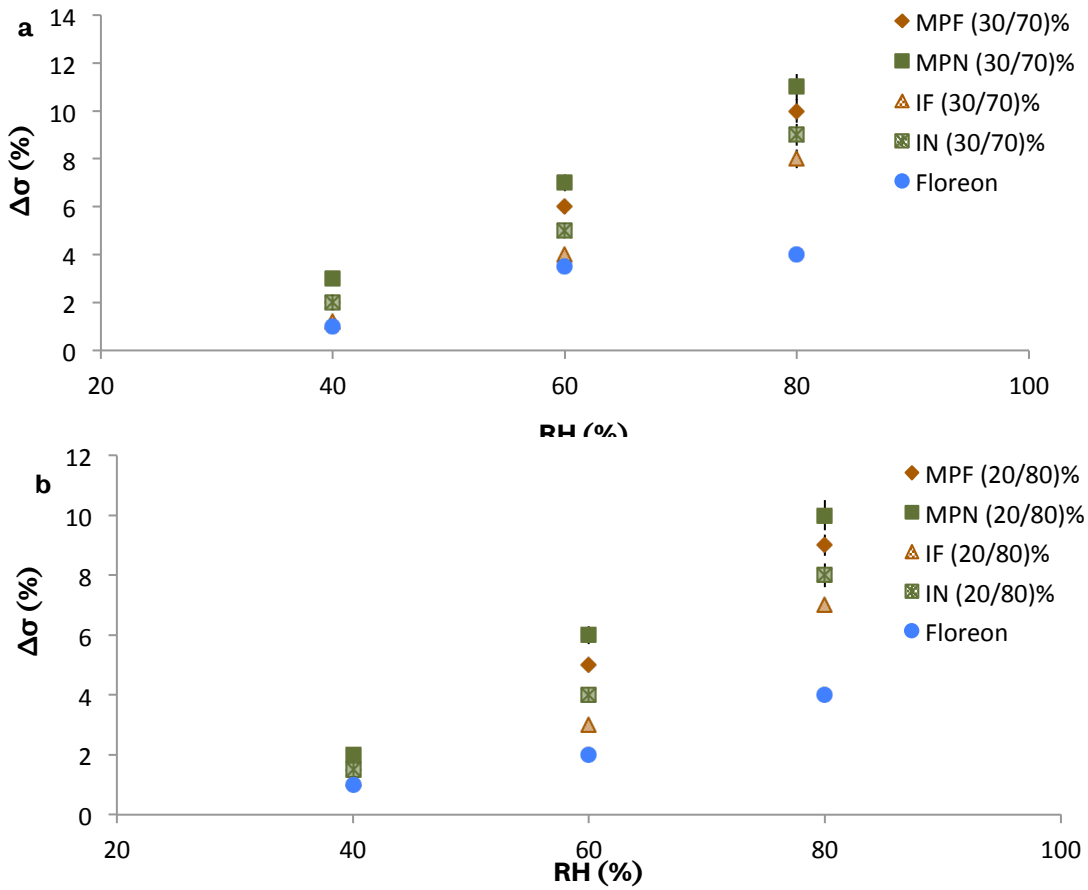

Figure 6.24 Reduction in the flexural strength of Floreon and Floreon based composites of a) 30wt% and b) 20 wt% fibre as a function of different RH, for 5 composites from each composite category. The notation MPN is referred to composites consisting of minimally processed nettle fibres (green squares) and MPF to the corresponding composites with minimally processed flax fibres (brown rhombus). The notation IN is referred to composites consisting of industrial processed nettle fibres (dashed green squares) and IF to the corresponding composites with industrial processed flax fibres (dashed brown triangles). The error bars represent ±1SD (samples tested for every set of error bars n=3).

The flexural strength of Floreon was reduced by 4% (80% RH), which was the smallest observed decrease. The flexural strength of MPN (30/70)% composites decreased by 11%, compared to 9% for IN (30/70)% at 80% RH.

Composites consisting of MP fibres, especially nettles had the largest reduction in the flexural modulus, which is most likely the result of the response of the constituent fibres under different humidity conditions (chapter 3). The influence of moisture absorption on the flexural modulus of 3D printed composites can be seen in Figure 6.25.

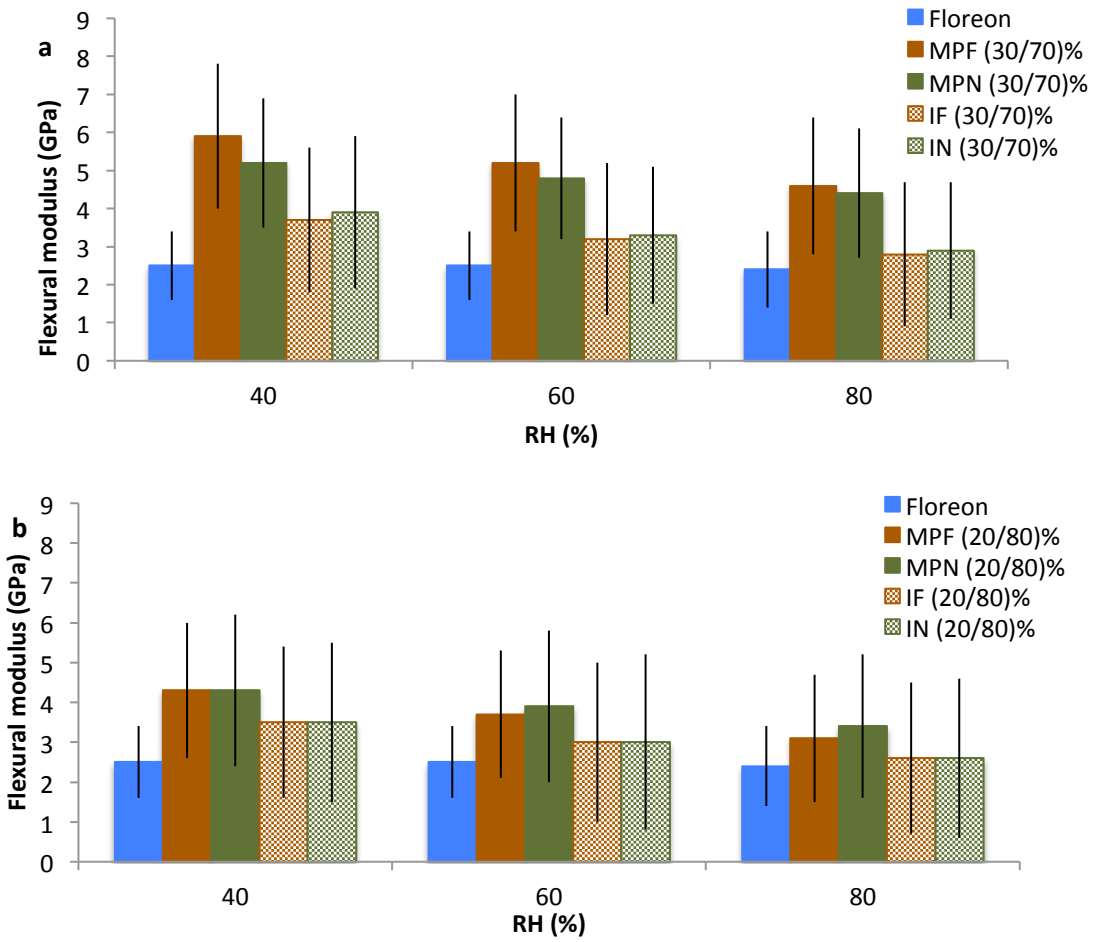

Figure 6.25 Flexural modulus (average) of Floreon and Floreon based composites a) 30%, b) 20 wt% as a function of different RH, for 5 composites from each composite category. The composites were made using layer height thickness of 0.2 mm, pattern orientation of -45°/45°, fill density of 100%. The nozzle temperature for composites consisted of MP fibres was set up at 200 °C and at 190 °C for the corresponding composites with I fibres. The notation MPN is referred to composites consisting of minimally processed nettle fibres (solid green bars) and MPF to the corresponding composites with minimally processed flax fibres (solid brown bars). The notation IN is referred to composites consisting of industrial processed nettle fibres (dashed green bars) and IF to the corresponding composites with industrial processed flax fibres (dashed brown bars). The error bars represent ±1SD (samples tested for every set of error bars n=3).

6.6.8.3 Comparison between 3D printed and injection moulded composites

Comparing the effects of moisture absorption on composites made by injection moulding and 3D printing revealed that all samples absorbed the highest amount of moisture at 80% RH and thus displayed the highest reduction in their tensile and flexural properties at this RH.

A possible explanation for the lower amounts of moisture absorption is better fibre/matrix adhesion of the 3D printed composites compared to the injection-moulded composites. Additionally, composites with higher fibre content (40 wt% for the injection-moulded composites and 30 wt% for the 3D printed) had the highest alterations in their tensile and flexural strength results. Figure 6.26 compares the reduction in tensile and flexural strength of the injection-moulded and 3D printed composites at 80% RH.

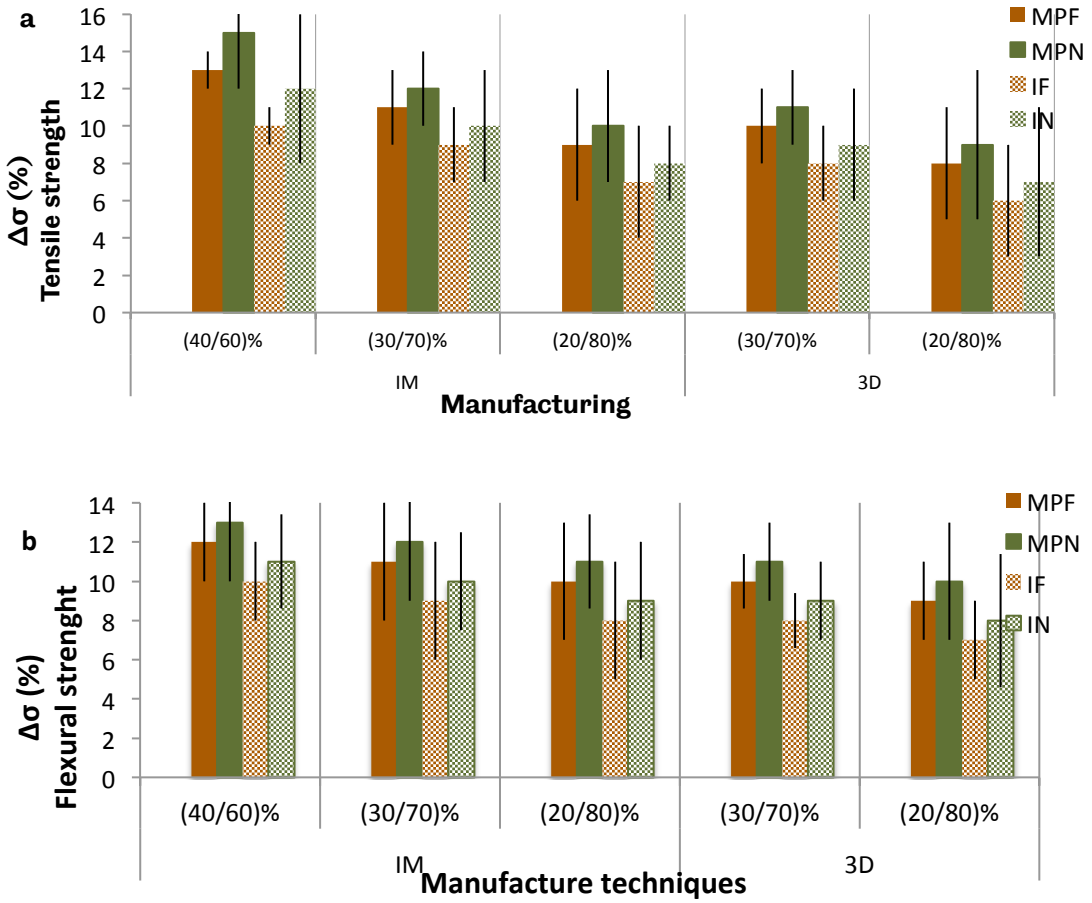

Figure 6.26 Reduction in the a) tensile strength and b) flexural strength of the injection moulded (IM) and 3D printed composites (3D) of 40%, 30%, 20 wt%. The notation MPN and MPF referred to composites consisting of minimally processed nettle fibres (solid green bars) and to minimally processed flax fibres (solid brown bars) respectively. The notation IN and IF referred to composites consisting of industrial processed nettle fibres (dashed green bars) and to industrial processed flax fibres (dashed brown bars) respectively. The IM composites were made using extrusion pressure of 40 bar, moulding pressure of 500 bar and moulding time of 1 minute. The moulding temperature for composites consisted of MP fibres was set up at 190 °C and at 180 °C for the corresponding composites with I fibres. The 3D printed composites were made using layer height thickness of 0.2 mm, pattern orientation of -0°/90°, fill density of 100%. The nozzle temperature for composites consisted of MP fibres was set up at 200 °C and at 190 °C for the corresponding composites with I fibres. The error bars represent ±1SD (samples tested for every set of error bars n=3).

The 3D printed composites had a slightly smaller decrease in tensile and flexural strength compared to injection-moulded composites. The tensile strength for 3D printed MPN (30/70)% and MPF (30/70)% decreased by 11% and 10% respectively, compared to 12% and 11% reductions for the corresponding injection-moulded composites at 80% RH.

The benefits of 3D printing are highlighted in terms of flexibility, capability, and application [217], [221]. It has been reported using 3D printing in aerospace projects reduced manufacturing costs and minimised production time [342]. Manufacturing costs are reduced due to the ability of one 3D printer to print samples made of different materials, shapes, and dimensions [343], [344].

In the current project, FDM provides advantages in material consumption and time, as well as in improved tensile and flexural properties of composites.

6.7 Summary

FDM was used for the 3D printing of MPF, MPN, IN, and IF composites. The 3D printed composites were mechanically tested and the results analysed based on the type and concentration of fibres and the selected printing parameters and were compared to results for the injection-moulded composites.

The 3D printed MPN and MPF composites had higher tensile (tensile strength and Young's modulus) and flexural (flexural strength and flexural modulus) properties compared to composites consisting of industrial fibres. The highest mechanical properties were obtained for MPN (30/70)% 3D printed composites, with an 84 ± 4 MPa average tensile and 139 ± 7 MPa average flexural strength. Next was MPF (30/70)%, with a 76 ± 4 MPa tensile and 126 ± 5 MPa flexural strength.

The properties of the 3D printed composites were affected significantly by the printing parameters. After a series of tests, the highest tensile and flexural strengths, Young's and flexural modulus for composites from all categories were obtained at a layer height thickness of 0.2 mm and fill density of 100%, agreeing with previous studies. The pattern orientation was selected based on the mechanical test results, with the highest tensile properties obtained at a pattern orientation of 0°/90° and -45°/45° for bending tests. The nozzle temperature was controlled by Floreon's melting temperature and by the fibre degradation temperature, with composites consisting of MP fibres set at 200 °C and composites with I fibres at 190 °C. The 3D printed composites had increased mechanical properties and decreased material consumption and time requirements compared to the injection-moulded composites (chapter 5).

Given the advantages of 3D printing on the mechanical properties of composites produced, 3D printing was next evaluated based on environmental emissions. The environmental analysis of 3D printing is presented in the next chapter.

7 LIFE CYCLE ASSESSMENT

ENVIRONMENTAL ANALYSIS OF FLAX AND NETTLE FIBRE-REINFORCED FLOREON COMPOSITES

7.1 Introduction

This chapter includes an LCA of fibre-reinforced composites and their individual constituents. The raw materials were evaluated in terms of environmental emissions, biodegradability and their potential for recycling using the Supply Chain Environmental Analysis Tool (SCEnAT). Specifically, this chapter describes the LCA procedure, total environmental emissions, and related environmental categories as a result of the analysis of minimally and industrially processed flax and nettle fibres, Floreon, and flax and nettle fibre-reinforced Floreon composites.

7.2 Research methodology

Government regulations now require manufacturing companies to report the environmental impacts of materials. This regulatory assessment emphasizes the recycling potential and end-of-life treatment [12], [13], [345]. LCA is an environmental analysis tool used for the evaluation of biodegradability and sustainability for different types of materials, applied manufacture processes, recycling, and reusability [265]. For composite manufacturing industries, LCA is often used as a qualitative analytical tool to assess the environmental emissions of composites [235].

The present LCA study analysed the environmental impacts and CO_2 emissions of MPF and MPN fibres according to their cultivation, fibre extraction, and sample preparation methods. The LCA was performed to highlight the differences in CO_2 emissions between the industrially and minimally processed fibres. The matrix component, Floreon, was assessed according to its biodegradability and sustainability potential and then compared to other types of polymers used in the manufacture of composite materials. Following this, flax and nettle fibre-reinforced Floreon composites were evaluated based on the recycling and reuse potential and final CO_2 emissions. The impact of the selected manufacturing methods (injection moulding and 3D printing) on the total composite emissions was also analysed.

7.2.1 Characterisation procedures

LCA is separated into five main phases (chapter 2, section 2.6). The output data and emissions from the LCA are then linked to their respective environmental

categories to help with an overall assessment. According to ISO/TR 14047:2003, there are eight important environmental impact classification factors (EICF), which were correlated in this LCA [236]:

1. Acidification potential (AP)
2. Aquatic toxicity potential (ATP)
3. Human toxicity potential (HTP)
4. Eutrophication potential (EP)
5. Global warming potential (GWP)
6. Non-renewable/abiotic resource depletion potential
7. Ozone depletion potential (ODP)
8. Photochemical oxidants creation potential (POCP)

For the LCA data analysis, a supply chain tool called SCEnAT was used. It was developed by the Management School of the University of Sheffield in partnership with the University of Hull and the Stockholm Environment Institute at the University of York and funded by the Centre for Low Carbon Futures [346]. To ensure rigour, SCEnAT operates according to the international standards and policy requirements ISO14040 and ISO14044 [232], [235], [346].

The SCEnAT software translates input data from a supply chain into a map and correlates the consumption sources of the raw material related to different preparation procedures. It then calculates direct and indirect CO_2 emissions with respect to the corresponding environmental impacts [346].

For CO_2 emission calculations, SCEnAT uses a hybrid LCA model. The hybrid LCA model combines two LCA methodologies, Process LCA and Environmental Input-Output LCA. This hybrid LCA enables the use of an extended system boundary of input-output analysis to estimate indirect emissions [347]. From the resulting supply chain map, CO_2 emissions hotspots can be identified and alternative solutions for the reduction of CO_2 emissions suggested based on a range of categories such as economic, environmental, and social factors.

It is important to note that LCA is still a model and therefore only as good as its design and input data. There is the possibility that the LCA (section 7.2.1) is compromised by these factors. For this reason, the definition of the functional unit and the boundary selection in the goal and scope phases varies according to the type and origin of the material and the input data source. Furthermore, during the LCI and LCIA phases, the impact category selection and the applied criteria may

vary according to the environmental regulations of each country. Finally, in the interpretation phase, the results may be affected by the availability and quality of data and the quality of other comparison studies. Therefore, until more progress is made in standardising this field, conclusions from LCA should be considered qualitatively.

7.3 LCA investigation phases for flax and nettle fibres

Goal: The environmental analysis of flax and nettle fibres focused on three main parts: agricultural operations (from plant cultivation to harvesting), fibre extraction, and the fibre preparation process. The aim of this LCA was to determine the sustainability of flax and nettle fibres used as reinforcement materials in composites compared to other cellulosic and synthetic fibres (e. g., carbon and E-glass fibres). In addition, a comparison between IF, IN, MPF, and MPN fibres was also highly relevant given the differences in fibre properties as a result of preparation processes (chapter 3).

Input data was collected from farmers in UK and European databases, (chapter 2, section 2.5) [238]. The National Farmers' Union provided information on the geographic locations, climate, and land use for the fibre production across the UK [348].

Scope: A specific product system was defined for the investigation of the environmental impacts.

The product system for flax and nettle fibres included the growth period (from seed to harvesting), fibre extraction (including specific extraction steps and procedures such as retting and decortication), and the fibre and yarn preparation process (including preparation steps such as hackling, scutching, and spinning).

Functional unit: The functional unit for both flax and nettle fibres was set to the same level for a more accurate correlation. All the collected data in the following sections refers to the fibre functional unit of '1 kg of flax/nettle fibres ready to be used as a reinforcement in a polymer matrix composite'.

System boundary: The system boundary defines the starting and endpoints of a LCA. Two different system boundaries were set due to the interest to investigate firstly the environmental impacts of the extraction process of fibres and secondly the fibre preparation process. The starting point was the flax and nettle seed and the endpoint was the final processing stages of fibres. For the IF and IN fibres, the endpoint was the spinning processes in which the fibres became yarn. For the MPF

and MPN fibres, the endpoint was at the end of cultivation, where flax and nettle plants were ready to be harvested.

LCI analysis: During the inventory step, the collected input data were combined with the corresponding output data. Input data considered were the amount of seed, fertiliser, and pesticides applied during the agricultural operations and water, diesel fuel, and electricity requirements during the flax and nettle fibre extraction and preparation processes. The outputs were a consequence of material waste and consequential emissions to water, air, and soil. The majority of emissions were due to fuel combustion, electricity generation, and the use of chemicals as fertiliser and pesticides.

LCIA: During LCIA, the data collected were analysed and correlated according to their environmental impacts in the aforementioned environmental categories (section 7.2.1).

Life Cycle Interpretation: During the final step, the carbon footprint was calculated using the SCEnAT software and a comparison made between flax and nettle fibres in terms of environmental and specifically CO_2 emissions.

7.4 LCA investigation phases for Floreon

The LCA of Floreon followed the same investigation phases as flax and nettle fibres (section 7.3).

Goal and scope: The goal of the LCA was the evaluation of the environmental impacts of Floreon, based on its biodegradable character, energy consumption during manufacturing and recycle/reuse applications, potential for recycling, and overall CO_2 emissions. Of great interest and importance was the comparison of Floreon's emissions with other biodegradable and thermoplastic polymers.

The production system of Floreon was related to the blend's manufacturing and included data from raw material (sugarcane and corn starch) extraction and acquisition through the energy consumption for the final formation of Floreon. For the recycling phase of Floreon, the potential energy consumption and use of any types of chemicals for the decomposition of the material were calculated.

Input data for Floreon was collected from the official Floreon website and from the ECO calculator and SimaPro databases [19], [238], [240]. These include data related to the environmental emissions and the corresponding affected environmental categories. The data collected were analysed by using SCEnAT, highlighting hotspots of CO_2 emissions.

Functional unit: The functional unit of Floreon is referred to as 'one kg of Floreon as a polymer matrix for composites'.

System boundary: The system boundary for Floreon was related to the blend's manufacturing. The starting point was the cultivation of corn seeds and the ending point the formation of Floreon through the fermentation process.

The remaining phases for the investigation of the environmental behaviour of Floreon in LCI, LCIA, and interpretation were the same as the aforementioned steps for flax and nettle fibres (section 7.3).

7.5 LCA investigation phases for flax and nettle fibre-reinforced Floreon composites

Goal and scope: The environmental behaviour and characterisation of the fibre-reinforced composites is directly connected to the environmental characteristics of the individual raw materials used (flax and nettle fibres as reinforcing materials and Floreon as the binding matrix). The goal of the LCA was the evaluation of the environmental impacts and calculation of the total CO_2 emissions of the composites produced. This evaluation was based on the degradability and biodegradability of the composite and the biodegradability of the reinforcing fibres and polymer. The sustainability of the composites produced was based on an environmentally friendly material, from extraction of raw materials to disposal of the final product, taking into consideration recycling options (including energy and chemical requirements) and CO_2 emissions. An example of an environmentally friendly material is household items (e.g., plates and bowls) made of biodegradable coconut fibres that can be recycled without using chemicals.

Special emphasis during the environmental analysis was paid to the evaluation of the composites' manufacturing (extrusion, injection moulding, or 3D printing). These techniques were evaluated and the sustainability of injection moulding and 3D printing were compared.

The product system of the composites included the composite manufacturing. The input data included the required amount of material, time and energy consumption for the production of dog bone and rectangular shaped composites, and consumptions during recycling.

Functional unit: The functional unit of flax and nettle fibre-reinforced Floreon composites was referred as 'one kg of composites produced'.

System boundary: The system boundary for the injection moulded and 3D printed composites was related to the composites' manufacturing. The starting

point was related with the individual material and energy requirements for the production of the composites using the two different techniques and the ending point was the calculation of the CO_2 emissions.

The LCI, LCIA, and interpretation of the LCA phases were compared to the corresponding procedures for composites (section 7.3).

7.6 Limitations in applying LCA

Variations in LCA analysis are expected due to the diversity of the input data. Different estimation factors may be used that influence the calculations of environmental emissions [238], [240], [346]. Different conclusions can be reached depending on the country, government laws, and selected method of carbon footprint calculation for LCA analysis [244], [265].

In the case of the fibres, the input data may vary according to the plant species, agricultural practices, and amount of water, energy, fertilisers, and pesticides used during the growing period and preparation processes [10]. For example, nettle fibres are often confused with ramie fibres because nettle and ramie (also known as Asian nettle), belong to the same plant family, the Urticaceae. However, differences in their stem morphology require different processing methods [265].

Significant differences in the energy and water consumption are observed between the different retting procedures during the fibre extraction process. In the UK, there are three frequently used procedures for fibre production [59]. One procedure uses a warm water retting process, which requires minimal energy consumption but higher water consumption. A second procedure uses a stand/dew retting process, with an intermediate level of energy and water consumption. The third procedure uses a bio-retting process, which requires the most energy but has the lowest water consumption [59], [242].

7.7 Results and discussion

7.7.1 LCA for IF and IN fibres

Data for the IF and IN fibres were obtained from various sources. Data related to the agricultural operations were collected from farmers in the UK and from agricultural reports [348]. For the fibre extraction and preparation process, the input and output data were collected from the DEFRA and ECO calculator databases [191], [240], [244]. The LCA preparation steps for the production of one tonne of flax or nettle fibres are summarised and presented in Figure 7.1.

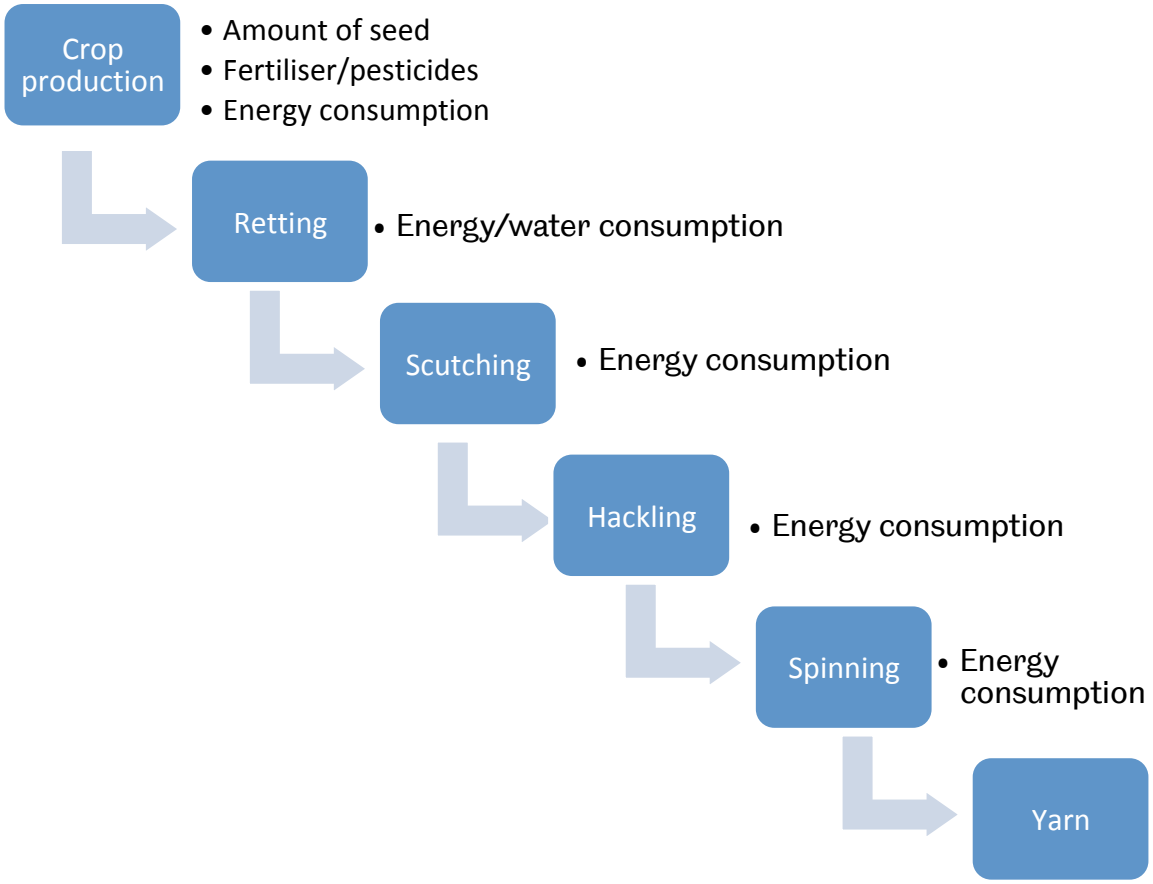

Figure 7.1 Flax and nettle fibre's processing starting from the crop production up to the final processing step, in which fibres end up as yarns. The input data collected mainly concerned the consumption of energy and water during the main preparation processes.

LCI for IF fibres

Part of the agricultural operation is soil preparation before cultivation. The average energy consumption for agricultural actions (e.g., tillage) was considered as the energy requirement to operate agricultural tractors [349]. The amount of seeds in Table 7.1 refers to the amount of dry seeds needed for the production of one tonne of flax yarn [242], [271]. The applied chemicals refer to N-, K-, and P-fertilisers and insecticides, herbicides, and fungicides (which are collectively referred as pesticides). The quantities of fertilisers and pesticides listed in Table 7.1 were based on a soil with pH6. Higher or lower pH levels would require different amounts of chemicals [256]. The energy consumption for the flax fibre preparation procedures was calculated based on the machine's energy consumption [242]. The output data are in the form of direct emissions, mainly due to diesel consumption and applications of fertilisers and pesticides [240], [241]. Table 7.1 presents the collected input and output data for the production of one tonne of flax yarn.

Table 7.1 Input and output data for the production of one kg of flax yarn [240]–[242], [269], [349].

Procedure	Input data	Output data
Crop production	Seeds: 0.423 kg Fertilisers: 2.445 kg lime 0.444 kg ammonium nitrate 0.400 kg triple superphosphate 0.305 kg potassium chloride Pesticides: 0.009 kg Energy consumption: 0.35 MJ/l diesel	Direct emissions: 9.334 kg CO_2 0.06 kg NH_3 0.014 kg N_2O 0.06 kg NO_X 0.03 kg SO_2 2.824 kg Dust
Retting and Scutching A) Warm water retting B) Stand/dew retting C) Bio-retting	Energy consumption: A) 15-16 MJ/tonne of yarn B) 24-25 MJ/tonne of yarn C) 80 MJ/tonne of yarn Water consumption: A) Warm water required for the immersion of fibre stems B) Stems left in the field and exposed to rain, sun and fungi C) Water enhanced with bacteria required for the immersion of fibre stems	
Hackling and Spinning	Energy consumption: ~60 GJ/tonne of yarn	

LCI for IN fibres

The input data and environmental emissions for the production of one tonne of nettle yarn are presented in Table 7.2. The energy consumption for nettle fibres was based on the diesel requirements of agricultural tractors (hours of tractor use per tonne). As nettle has a greater resistance to insect pests and diseases, lower amounts of fertilisers and no pesticides are applied. In the case of ramie (Asian nettle) fibres, the additional process of degumming is necessary to remove the gum from the fibre structure [191]. Degumming is energy intensive and harmful to the environment process as chemical solutions are used. The amount of energy required during the degumming and spinning processes varies by application. Softer ramie fibres require lower energy than stiffer ramie fibres. The input data

collected from ramie fibres were used as an identification of the energy requirements during the fibres preparation processes.

The output data collected are in the form of direct emissions, mainly due to the diesel consumed during the agricultural and extractions procedures and from the fibre preparation process. The exact calculation of the emissions was not possible so the LCA studies for nettle fibres are qualitative.

Table 7.2 Input and output data for the production of one kg nettle yarn [247], [350]–[352]**.**

Procedure	**Input data**	**Output data**
Crop production	Seeds: 0.250-0.275 kg Fertilisers: 0.214 kg N 0.06 kg P_2O 0.130 kg K_2O 0.383 kg CaO 0.093 kg MgO 0. 363-0.387 kg N Pesticides: no requirement Energy consumption: 30-40 KJ/l diesel Water consumption: 30 KT/ha	Direct emissions: Emissions associated with diesel consumption: CO, CO_2, NO_x, SO_2 Emissions associated with fertilisers consumption: CO_2, N_2O, NO_3, NH_3, SO_2
Retting and Degumming A) Microbial degumming B) Chemical degumming	Energy consumption: A+B) ~30-40 MJ/tonne of yarn Water consumption: A) Water enhanced with bacteria required for the immersion of fibre stems B) Aqueous alkaline solution required (i.e. caustic soda, sodium phosphate, sodium sulphate), followed by water bath	~ 6.500-7.350 kg CO_2 0.015-0.020 kg Ash 0.280 kg Gum
Spinning	Energy consumption: ~20-35 MJ/tonne of yarn	

Environmental impacts (LCIA)

The input data collected for the production of one tonne of IF and IN fibres were analysed and evaluated according to EICFs, as described in section 7.2.1. The analysis was conducted using SCEnAT and the ECO calculator in accordance with

ISO/TR 14047:2003 standards [266]. Eight environmental categories, as mentioned in section 7.2.1, were considered and their results are shown in Figure 7.2.

Global warming potential (GWP) (emissions of CO_2 and carbon monoxide (CO)) is affected primarily by diesel consumption, followed by chemicals applied during agricultural operations, and the fibre extraction process [7]. Evaluating the three retting procedures for lF fibres (section 7.6), the highest emissions were observed in the bio-retting process due to its large energy consumption. Dissanayake reported that the GWP can be reduced by approximately 25% in procedure 1, 18% in procedure 2, and 15% in procedure 3 by eliminating the spinning operation [241]. The spinning process (chapter 2, section 2.2.3) can be omitted for fibres in composite applications because the fibres do not need to be in form of a yarn.

Acidification (AP) and eutrophication potential (EP) are primarily caused by SO_2, NO_x and NH_3 emissions from the use of nitrogen, phosphate, fertilisers and pesticides [247], [254]. Generally, AP values are lower in the case of nettle yarn due to the lack of pesticides compared to flax yarn. The highest AP value was reported in the stand/dew retting process of flax fibres because of increased use of agro-chemicals. The use of nitrogen fertilisers increased the emissions in the EP category, recording emissions of 0.24 kg nitrogen equivalent (NEq) in the chemical degumming process of ramie yarn followed by 0.203 kg (NEq) in the stand/dew retting process of flax yarn.

Human toxicity potential (HTP) is defined as a calculated index reflecting the potential harm of the chemicals released into the environment. The calculations are based on the inherent toxicity and used/released amount of gases [353]. Released gases during the agricultural and preparation process, such as CO, NO_x, and SO_2, are the main contributors. From this analysis it was found that the HTP values for flax and nettle yarn are in the same range.

Aquatic toxicity potential (ATP) is caused by the use of pesticides. Between flax and nettle yarn production there is a significant difference, primarily due to the large amount of pesticide used during the flax growing period (up to 0.009 kg per kg of flax seeds). The ATP values of flax fibres reached at 200 m^3 compared to 8 m^3 of nettle yarn. The highest ATP is reported once again in the stand/dew retting process, due to high amount of pesticides applied.

Ozone depletion potential (ODP) is affected by the diesel consumption during the agricultural and extraction preparation processes. Due to the high energy consumption during the stand/dew retting process of flax yarn, the highest ODP

recorded value was 0.240 kg, compared to 0.131 kg in the case of the chemical degumming process of ramie yarns.

Photochemical oxidants creation potential (POCP) is a result of the diesel combustion and is calculated based on released ethylene. Nettle and flax yarn have POCP emissions at the same level up to 0.03 kg of ethylene with a significant reduction during the warm water and bio-retting process of flax yarn.

To summarise these findings, Figure 7.2 presents the environmental impacts for each category affected for flax and nettle yarns. In the case of flax, three scenarios were analysed based on the different retting procedures (warm water retting, stand/dew retting, and bio-retting). The eight environment impact classification factors for nettle yarn were calculated based on the two different degumming scenarios (microbial degumming and chemical degumming).

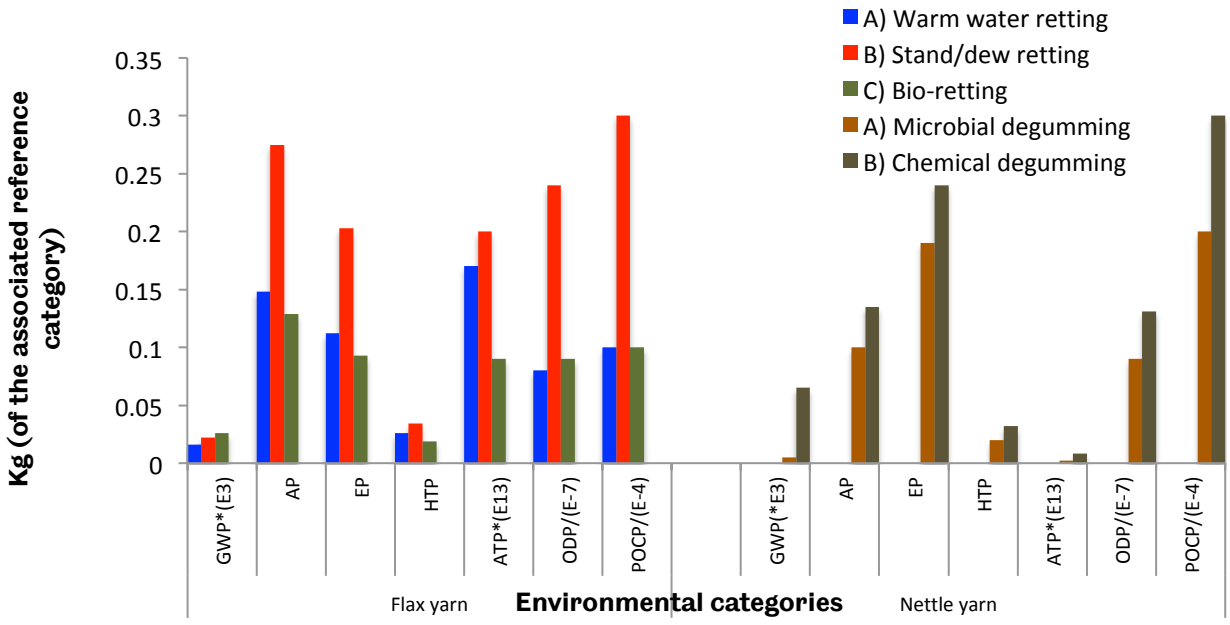

Figure 7.2 Environmental impacts (EICF) of flax and nettle yarn. Flax yarn was analysed according to three different retting scenarios (warm water retting, blue, stand/dew retting, red and bio-retting, green) and nettle yarn based on two different degumming scenarios (microbial degumming, brown and chemical degumming, dark green). Each preparation scenario requires different amounts of energy, water and chemicals and thus the final total emissions varied. Each of the acronyms for the eight categories are as followings, GWP*(E3) = Global warming potential (by 3 orders of magnitude, AP = Acidification Potential, EP = Eutrophication Potential, HTP = Human Toxicity Potential, ATP = Aquatic Toxicity Potential (by 13 orders of magnitude), ODP= Ozone Depletion Potential (divided by 7 orders of magnitude), POCP= Photochemical Oxidants Creation Potential (divided by 4 orders of magnitude *ATP has units of m^3, all others kg.

7.7.1.1 LCA for MPF and MPN fibres

MPF and MPN fibres have been carefully and manually extracted from the flax and nettle stems by the researcher (chapter 3, sections 3.3.2-3.3.4), avoiding any industrial preparation processes (such as hackling, degumming, spinning, and use of chemicals). The LCA analysis for MPF and MPN fibres followed the same procedure as shown in Figure 7.1.

The LCA investigation of MPF and MPN fibres is more qualitative than quantitative due to lack of input data. In addition, input data provided by farmers were estimations rather than accurate values. The analysis was based on estimation of the amount of fertilisers and pesticides used, and of the water and energy consumption for the cultivation of flax fibres (based on the data collected from farmers in Sussex). Additionally, nettle plants can be characterised as weeds in this research due to the fact that nettle plants are often found in home gardens and parks in Sheffield (i.e., no specific cultivating procedure was followed). The water consumption was estimated from rainwater and the researcher conducted the harvesting process manually (no diesel consumption was recorded). However, cultivation on an industrial scale would require equivalent fuel inputs and as such the harvesting impacts would be similar to flax. The European nettle thrives best in phosphate- and nitrogen-rich soils [354]. As such, the environmental impact of a large-scale cultivation could be as high as that of flax, considering different scenarios related to the processing methods (section 7.6). Therefore in the future, optimising the amount of chemicals required and evaluating the processing steps is crucial to produce an accurate LCA for MPN fibres.

CO_2 emissions of MPF and MPN fibres

The total CO_2 emissions were calculated using SCEnAT by uploading all the input data. A supply chain was created to evaluate the total CO_2 emissions of MPF and MPN fibres. SCEnAT serves as a carbon calculator engine and through the supply chain, the total CO_2 emissions were calculated for the production of 1 kg of fibres. The input data for flax and the estimated values for nettle for production of 1 kg of flax and nettle fibres are summarised in Table 7.3.

Table 7.3 Input data for the production of 1kg flax and nettle fibres. There are no references to fertilizers, pesticides and energy requirements for nettle fibres as they were harvested from gardens and parks and characterized as weeds.

Procedure	**Input data**
Flax fibres: Crop production	Seeds: ~0.6-0.9 kg Fertilisers: ~2.5-3. 6kg Pesticides: ~0.2 kg Energy consumption: ~0.03-0.06 MJ/l diesel Water consumption: 0.02 MT/ha
Nettle fibres: Crop production	Seeds: ~0.2-0.4 kg Fertilisers: - Pesticides: - Energy consumption: - Water consumption: ~0.02-0.4 MT/ha

The supply chain for flax fibres translated the amount of fertiliser and pesticide, the water and energy consumption and the related environmental emissions into CO_2 equivalent emissions, as seen in Figure 7.3. Based on the degree of influence of the input data on the total CO_2 emissions, the input data were automatically coloured (red, yellow, and green coloured boxes pictured in Figure 7.3).

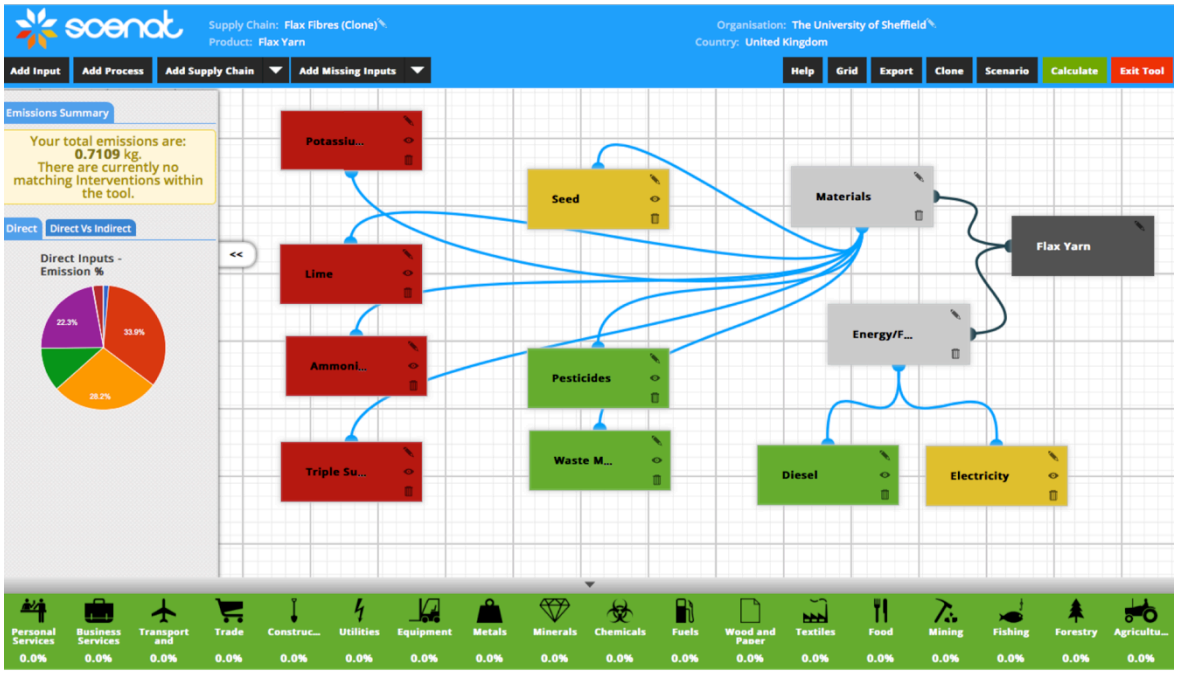

Figure 7.3 CO_2 emissions for the production of 1 kg of MPF fibres. The red sections are carbon hotspot emissions. These sections are related to the applied fertilisers, indicating input data with the highest CO_2 emissions. The yellow sections are mainly related to the electricity consumption, indicating lower CO_2 emissions than the red sections. Green coloured sections are based on the amount of waste material (i.e. seeds), pesticides and diesel consumption presenting the lowest carbon emissions.

Summarising the results from the LCA analysis, the estimated total CO_2 emissions for MPF fibres (production of 1 kg of fibres) were up to 0.711 kg and the emissions of MPN fibres were 0.436 kg. MPN fibres had lower CO_2 emissions due to the absence of any chemical additives such as fertilisers or pesticides. The estimated CO_2 emissions of the IF and IN fibres (9.3 kg and 6.5 kg CO_2 eq/kg of fibres respectively) are significantly higher than those of MP fibres, indicating clear preparation processes-based differences.

Previous LCA studies evaluated the greenhouse gas emissions based on the CO_2 emissions of different types of plant fibres [241]. Taken from the literature, Figure 7.4 presents a comparison of the greenhouse gas emissions per tonne of plant fibres (hemp, flax, jute, and kenaf). The GHG emissions presented no significant differences between the different types of fibres, with fertilisers having the greatest impact on the CO_2 emissions. Increased use of fertilisers (independent from the plant type) intensify the greenhouse gas problem [8], [247].

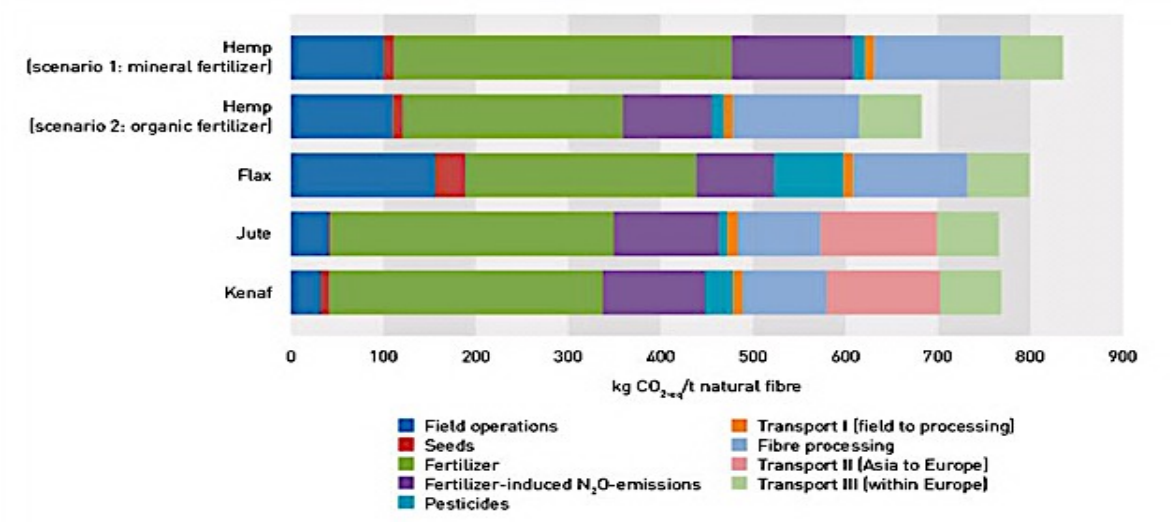

Figure 7.4 Comparison of the greenhouse gas emissions per tonne of plant fibres [268]. **Reprinted from Carbon footprint and sustainability of different natural fibres for biocomposites and insulation material (p.28), by Martha Barth (nova-Institute), Michael Carus (nova-Institute),2015-04, © 2015 nova-Institut GmbH, http://bio-based.eu/ecology/.**

The results obtained from the LCA analysis for the industrial and minimally processed fibres raise a question concerning the sustainability of the fibre preparation processes. The field/crop procedures, the extraction and preparation processes, from the cellulosic fibres to the production of fibre yarns, can be described as harmful environmental procedures. Qualitative comparison between the MPF and MPN fibres compared to the IF and IN fibres led to lower environmental emissions due to the absence of a series of preparation procedures. Certainly it should not be overlooked that the production and processes of fibres on an industrial scale will change significantly the final emissions.

Fibres intended for use as reinforcing materials in composite materials do not need to follow the same preparation steps as fibres used for other applications (e.g., cloth). Processing procedures such as hackling and spinning are used to increase the flexibility of the fibres that are necessary to fabricate cloths. However, for composite applications, these steps can be avoided, thus reducing energy consumption with consequent reductions in environmental emissions.

7.7.2 LCA for Floreon

The LCA for Floreon focused on the evaluation of the polymer's manufacturing. The input and output data were collected from Floreon and NatureWorks websites and ECO calculator [19], [355]. Figure 7.5 presents the system boundary for Floreon production, with the corresponding input and output emissions during the LCI analysis.

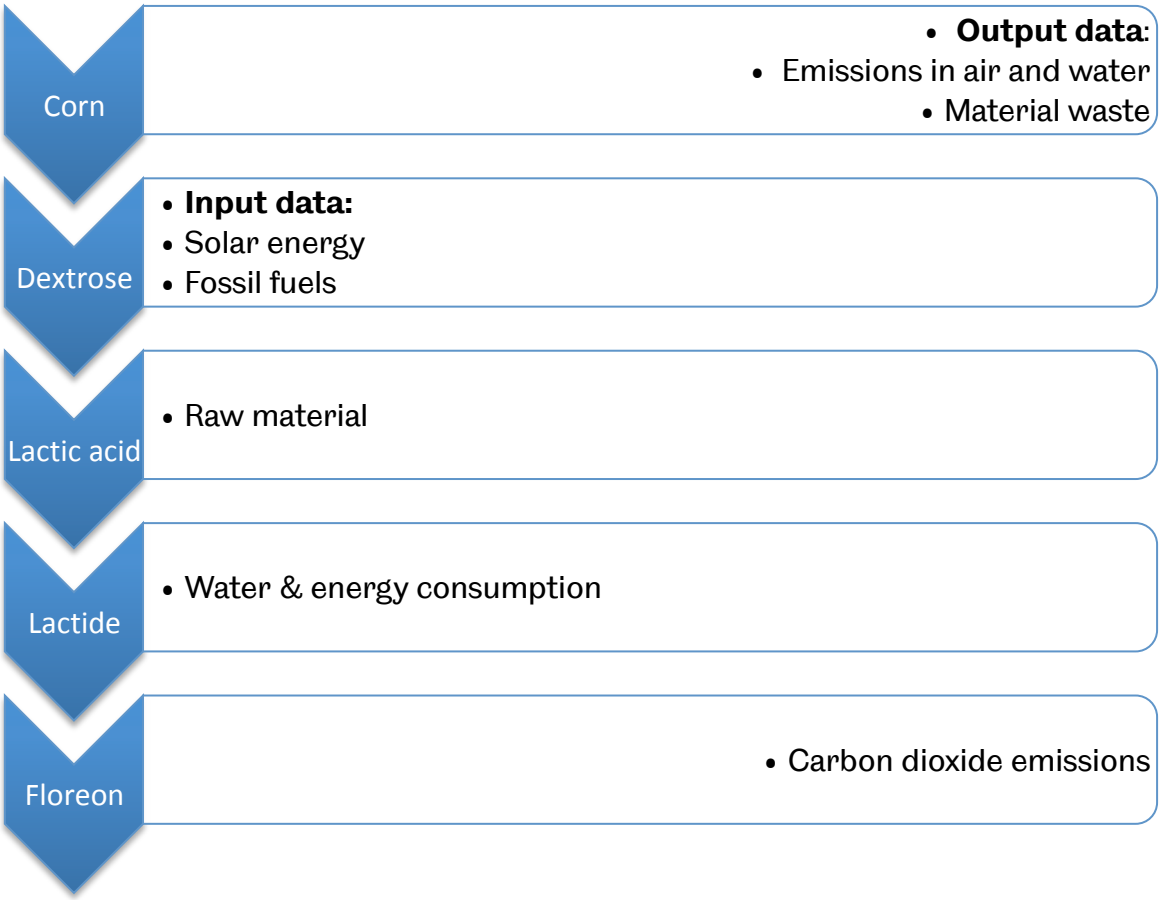

Figure 7.5 System boundaries for the production of Floreon. Floreon is characterised as a renewable polymer and natural origin material made by corn through a fermentation process. Input data include values of the amount of seeds, water and energy consumption while the output data were related with emissions into air.

Floreon (LCI)

Table 7.4 summarises the input and output data collected for the production of 1 kg of Floreon. A detailed description of Floreon production is provided in chapter 2 (section 2.4.1.2). The values of the energy and water consumption referred to the energy and water requirements during the crop production, such as planting the corn seeds, operating agricultural tractors, and applying fertilisers and pesticides. Energy consumption during the dextrose fermentation process for the production

of 1 kg of Floreon was calculated based on the energy requirements of the machine [193]. The output data referred to emissions in water and air, caused by diesel consumption and from the chemicals used (fertilisers and pesticides) [355].

Table 7.4 Input/ output data for the production of 1 kg of Floreon [21], [348], [355]**.**

Procedure	**Input data**	**Output data**
Corn Crop production	Fertilisers: ~2-3 kg (nitrogen and phosphorus) Pesticides: ~0.4 kg Energy consumption: 28.4.3 MJ/1kg (renewable energy) for corn feedstock 3.8 MJ/1kg diesel Water consumption: 2.7 kl/1kg	Direct emissions Emissions to air: CO_2 SO_4 NO_3 CH_4 NH_3 HCL CO Emissions to water: COD NH_4 CO_2
Dextrose	Energy consumption: 9.4 MJ/1kg	
Lactic acid	Energy consumption: 26.3 MJ/1kg	
Lactide	Energy consumption: 13.2 MJ/1kg	

Environmental impacts (LCIA)

The collected input data for the production of 1 kg of Floreon were analysed and evaluated according to the impacts on specific environmental categories (EICF) as described in section 7.2.1 The analysis was undertaken using ECO calculator in accordance with ISO/TR 14047:2003 standards [266]. The environmental impacts for each environmental category are presented in Figure 7.6.

GWP refers mainly to emissions into air as a CO_2 equivalent measurement. During Floreon production, emissions of CO_2, N_2O, and CH_4 were the main contributors.

AP and EP primarily indicate emissions into air, soil, and water. Emissions of NO_x, NH_3, and SO_4 had the highest impacts on the AP and EP categories,

POCP is a result of the diesel combustion during Floreon's production. Emissions of NO_x and CH_4 gases intensify the POCP.

HTP and **ATP** are calculated based on the NO_x, SO_x, and NH_3 emissions into the air. The increased amount of fertilisers and pesticides led to high HTP and ATP impacts.

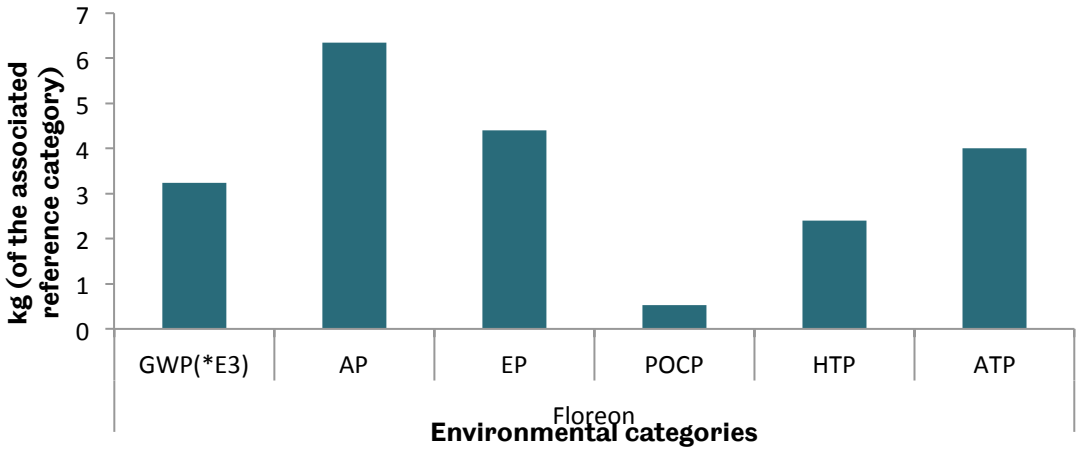

Figure 7.6 Environmental impacts (EICF) of Floreon [9], [355]**. Each of the acronyms for the eight categories are as followings, GWP*(E3) = Global warming potential (by 3 orders of magnitude, AP = Acidification Potential, EP = Eutrophication Potential, POCP= Photochemical Oxidants Creation Potential, HTP = Human Toxicity Potential, ATP = Aquatic Toxicity Potential, The calculations are measured in kg of the associated reference materials except ATP values are measured in m^3.**

7.7.2.1 Recycling of Floreon (LCI)

The LCA methodology was used to evaluate possible mechanisms for Floreon recycling. The environmental emissions during the recycling phases of Floreon were analysed. Floreon, a thermoplastic polymer, can be mechanically or chemically recycled or composted [19], [356].

For mechanical recycling, Floreon undergoes procedures such as separation, grinding, washing, drying, extrusion, cooling, and granulation [356]. During these different recycling steps, the energy and water required were considered as input data. During chemical recycling of Floreon, additional processing steps are required, such as decantation. In order to perform chemical recycling, precipitation agents are used, such as lime, aluminium sulphate, and inorganic chemicals [356]. Composting is the simplest type of recycling for thermoplastic polymers, consisting of separation of the polymer, grinding, and degradation [263], [264], [356]. Table 7.5 summarises the energy and water consumption with the related output data for the different recycling types for 1 kg of Floreon.

Table 7.5 Input and output data based on the different recycling mechanism for 1 kg of Floreon [19], [355].

Input data	Output data
Mechanical recycling:	
Energy consumption: 2649kJ /1kg	Material waste: 0.04.0.05 kg/1kg
Water consumption: 0.5L /1kg	Released heat: 286kJ/1kg
Chemical recycling:	
Energy consumption: 11211kJ /1kg	Material waste: 0.01 kg/1kg
Water consumption: 0.6-0.8L /1kg	Released heat: 7638kJ/1kg
Composting:	
Energy consumption: 39.7kJ /1kg	Material waste: 0.33 kg/1kg
	CO_2 emissions: 1.2kg/1kg

Environmental impacts (LCIA)

The collected input data (i.e., energy and water consumption) were analysed using SCEnAT software according the impacts on the different environmental categories. Figure 7.7 presents the environmental impacts on climate change, human toxicity, and fossil depletion for the three different mechanisms when recycling 1 kg of Floreon.

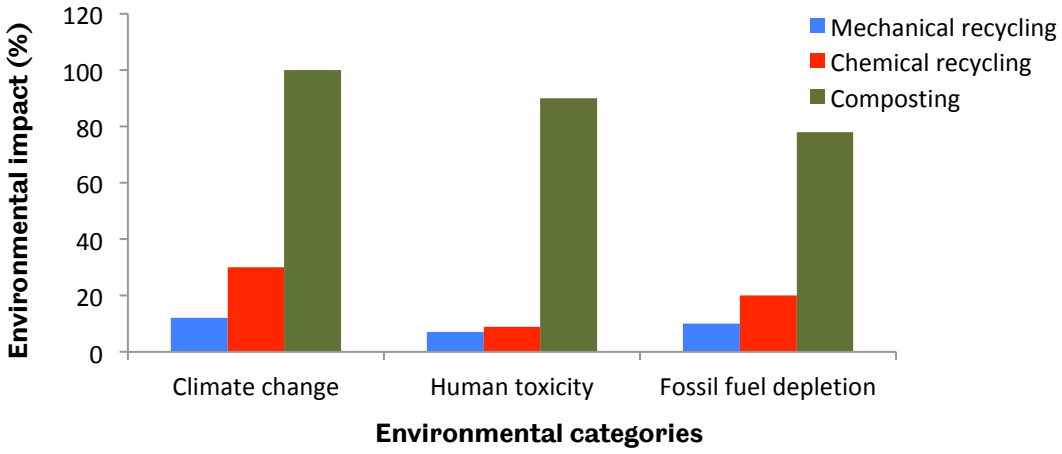

Figure 7.7 Environmental impacts according to the different recycling types.

Based on the input data collected, composting has the highest environmental cost, due to the high levels of energy consumption and released CO_2. Mechanical recycling has the lowest impacts in climate change, human toxicity, and fossil depletion categories. Thus, mechanical recycling is the best option for recycling Floreon. This supports a previous study by Piemonte *et al.*, which indicated that

mechanical recycling is the most energy efficient and environmentally friendly process for PLA [357]. However, this conclusion does not take into account the effect of recycling on polymer degradation (i.e., reduction in the polymer's molecular weight) and thus the recycled material may have a limited number of applications [139], [169].

To better interpret the results of Floreon, results from this work were compared to previous studies, in which CO_2 emissions for different types of polymers were calculated [23], [193], [356], [358]. Thermoplastic and thermosetting polymers were evaluated according to ISO 14040 and 14044 standards for energy consumption and impact on different environmental categories and compared to the polymers used in this study [232], [235]. Special emphasis was paid to the total CO_2 emissions, which are the main contributor to global warming. Figure 7.8a shows the greenhouse gases and Figure 7.8b presents the energy consumption for the production of 1 kg of different types of polymers.

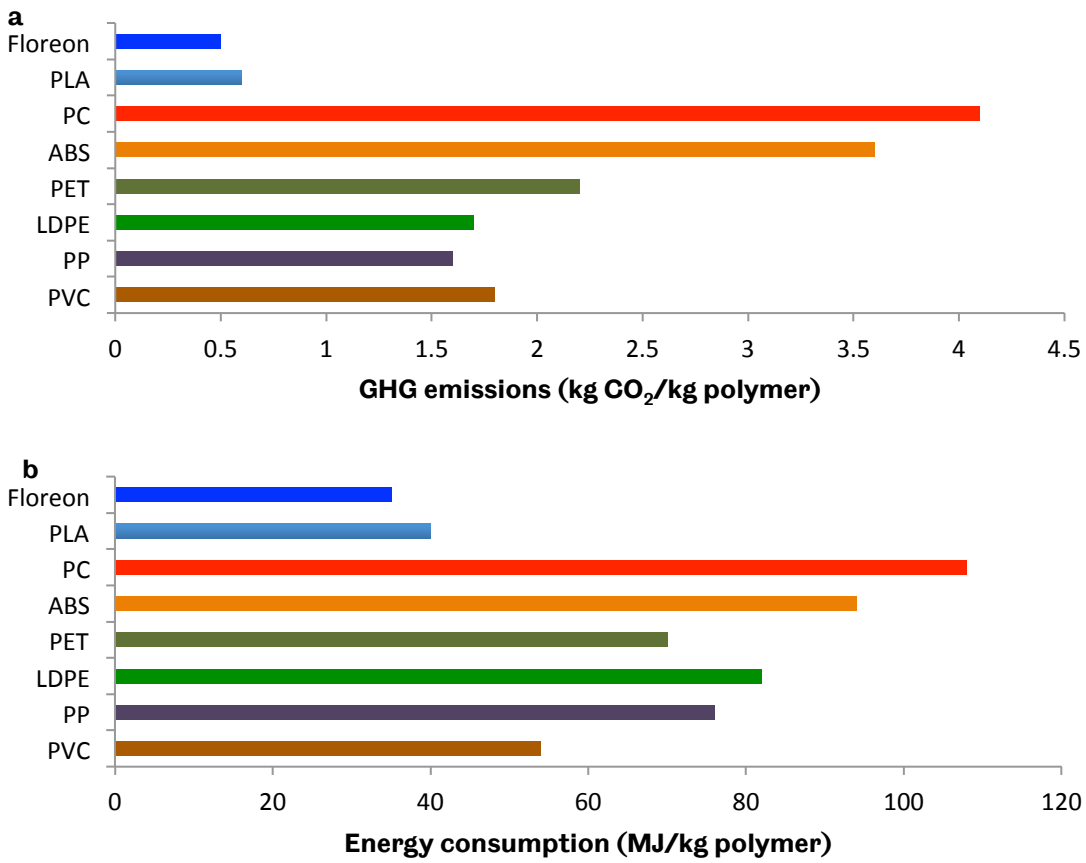

Figure 7.8 a) Greenhouse gas emissions and b) energy consumption [355]**. The GHG emissions and energy consumption of Floreon were added to the adapted GHG results from NatureWorks** [355]**. Each of the acronyms of polymers are as followings, PLA= Polylactic acid, PC= Polycarbonates, ABS= Acrylonitrile butadiene styrene, PET= Polyethylene terephthalate, LDPE= Low-density polyethylene, PP= Polypropylene, PVC= Polyvinyl chloride.**

The increased CO_2 emission of thermoplastic polymers such as PC, ABS, and PET, seen in Figure 7.8a is a result of the high energy consumption (Figure 7.8b). Use of non-renewable energy resources enhance the production of greenhouse gas emissions, contributing to global warming.

From Figure 7.8a–b, Floreon and PLA have much lower CO_2 emissions than other fossil-based polymers. Furthermore, both Floreon and PLA, being biodegradable and requiring fewer processing steps, consume less energy during manufacture and recycling [356]. This is due to the fact that the fossil-based polymers (e.g., LDPE) are subjected to specific processing steps, such as the formation of small carbon-based molecules that are combined using chemical polymerisation mechanisms. The use of chemicals such as benzene and xylenes (isolated from petroleum) require more energy during manufacturing and by extension the energy requirements for recycling is even greater [89], [259].

In order to reduce energy consumption and therefore CO_2 emissions, renewable sources of energy such as wind and solar power can be used. LCAs show that polymers from renewable resources have great potential to reduce environmental emissions and have lower impacts on environmental categories such as global warning, human toxicity, and acidification [20], [345].

Floreon has the potential among other biodegradable and bioplastic polymers to become the most environmentally friendly and green polymer for composite manufacturing. The combination of low CO_2 emissions during manufacturing with renewable energy resources and recycling can be the solution to decrease the use of non-recyclable plastic materials.

7.7.3 LCA for flax and nettle fibre-reinforced Floreon composites

The LCA of flax and nettle fibre-reinforced Floreon composites focused on the evaluation of different manufacturing processes (injection moulding and 3D printing) and on the impacts of the individual raw materials used (flax and nettle fibres and Floreon) on the total emissions created from the production of these composites.

The input data corresponded to the manufacture of 1 kg of composites. Energy consumption was based reported power supply values from the respective machine suppliers [322], [359]. The input data for the amount of materials (fibres and polymer) and time requirements were recorded during the composite manufacturing experiments. For the calculation of the composites emissions using

SCEnAT software, the impacts of the individual materials (sections 7.7.1 and 7.7.2) were used.

Flax and nettle fibre-reinforced Floreon composites manufacturing (LCI)

Table 7.6 summarises the input data collected for the production of 1 kg of flax and nettle fibre-reinforced Floreon composite. Detailed descriptions of the manufacturing process for injection-moulded and 3D printed composites are described in chapters 4 and 6.

Table 7.6 Input data according to the different manufacturing for the production of 1 kg of composites [322], [359]**. The energy consumption during manufacturing was based on the electricity consumption of the machines used (extruder, pelletiser, injection moulder and 3D printer).**

Procedure	Input data
Injection moulded composites: 1. Extrusion 2. Pelletiser 3. Injection moulder	**Energy consumption:** 1. 2.5 kWh 2. 1.5 kWh 3. 11.4 kWh **Material consumption:** 1. 3.2 kg 2. 2.9kg **Time consumption:** 1. 12 Hours 2. 6 Hours 3. 70 Hours
3D printed composites: 1. Extrusion 2. 3D printer	**Energy consumption:** 1. 2.5 kWh 2. 7.62 kWh **Material consumption:** 1. 3.2 kg 2. 1.5 kg **Time consumption:** 1. 12 Hours 2. 62.5 Hours

Environmental impacts (LCIA)

The input data collected (i.e., energy and material consumption) were analysed using SCEnAT software for calculations of total CO_2 emissions. The injection-moulded composites had a total energy consumption of 15.4 kWh and CO_2 emissions of up to 5 kg. The 3D printed composites had a total energy consumption of 10.12 kWh and CO_2 emissions of 4 kg (CO_2 eq. emissions).

From the aforementioned data, the injection moulding technique had higher energy consumption requirements and CO_2 emissions. The energy requirements are higher due to the required use of a pelletiser prior to the use of the injection moulder for the composite production. Therefore, 3D printing is a technique that saves time, material, and energy due to its adjustability in printing parameters and simultaneous multi-print capability (chapter 6), resulting in a reduction in CO_2 emissions.

Impacts of the individual materials used

The CO_2 emissions of composites were analysed according to the individual materials used. The fibre's nature (flax or nettle fibres), preparation processes (MP and I fibres), and the fibre's concentration in the composites structure were analysed. The functional unit was referred as '1 kg of composites produces'. The system boundary started at the fibres cultivation and ended up until the composite manufacturing. The aforementioned input data (Tables 7.1–7.4 and 7.6) were uploaded to SCEnAT software and are presented as CO_2 emissions in Figure 7.9.

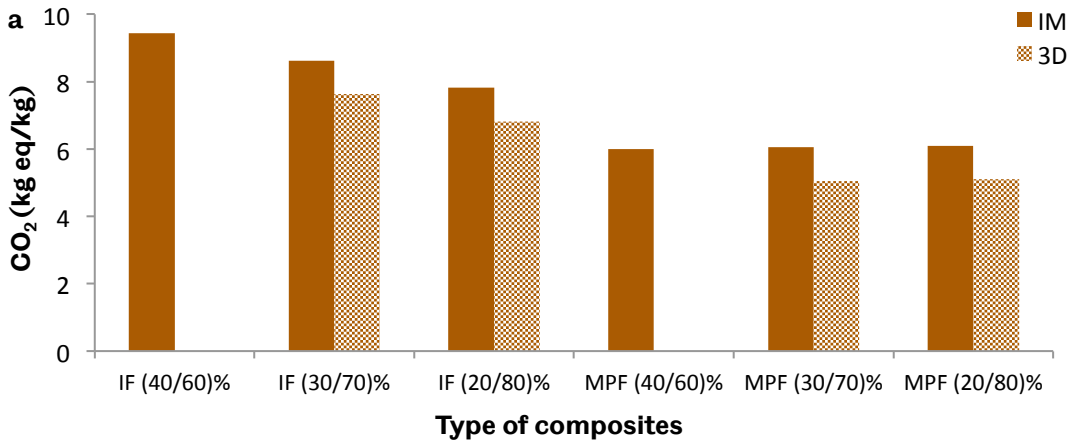

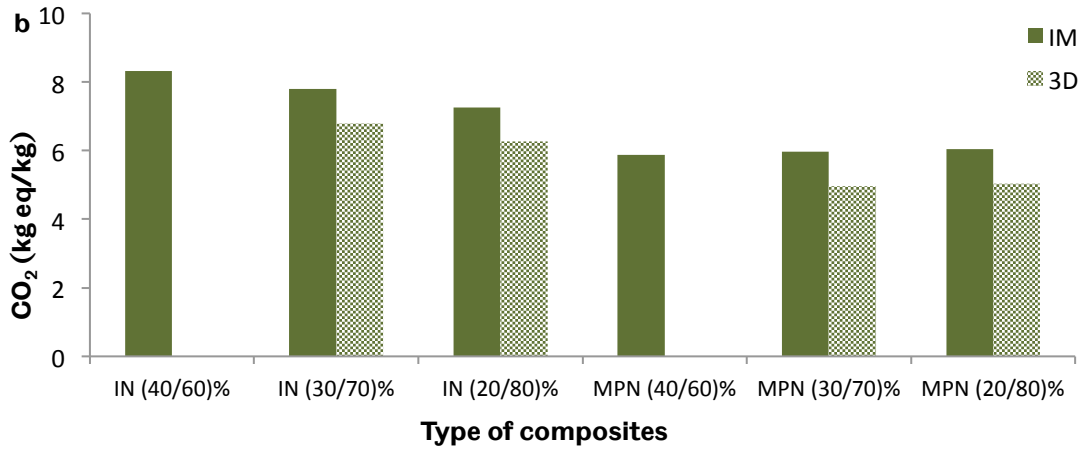

Figure 7.9 CO_2 emissions for the production of 1 kg of a) MPF and IF (brown bars) and b) MPN and IN (green bars) composites. The solid brown and green bars represent the injection moulded composites and the dashed brown and green the 3D printed composites. The notation (IF and IN) is referred to the use of industrially processed flax and nettle fibres and (MPF and MPN) to the corresponding minimally processed fibres.

The CO_2 emissions of the composites were affected by the CO_2 emissions in the preparation of the components and the manufacturing of the composites.

As illustrated in Figure 7.9, injection-moulded composites (independent of the fibre nature, preparation process, and concentration) had higher CO_2 emissions compared to 3D printed composites due to higher electricity consumption. The CO_2 emissions of the injection-moulded composites based on the manufacturing and individual materials used can be seen in Figure 7.10. Approximately 50% of the total CO_2 emissions of the injection-moulded composites are due to the manufacturing process, while the reinforcing fibres account for 40% of the final emissions.

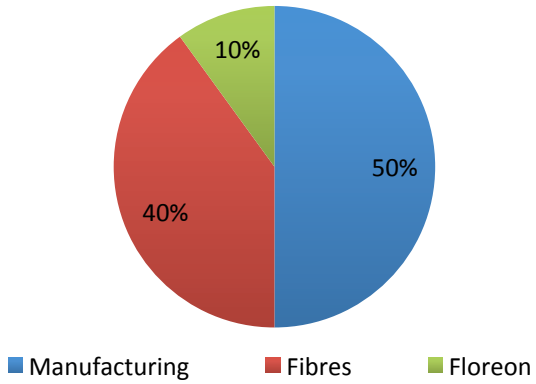

Figure 7.10 Percent representation of the total composite's CO_2 emissions of the injection moulded composites. The calculations of CO_2 emissions are based on the collected data for the production of 1kg injection moulded IF (40/60)% composites.

Composites made with nettle fibres had slightly lower emissions (Figure 7.9b). This is in agreement with the lower CO_2 emissions of nettle fibres (section 7.7.1.1), mainly due to the lower amounts of chemicals used during agricultural operations (section 7.7.1). Evaluating the results based on the type of fibres used, composites consisting of IF and IN fibres had higher overall emissions. The agricultural procedures, the use of fertilisers and pesticides, and the fibre preparation processes for IF and IN composites resulted in higher CO_2 emissions compared to composites of MPF and MPN fibres.

IN (40/60)% composites had 8.32 kg CO_2 eq. emissions compared to 5.88 kg CO_2 eq. emissions in the case of MPN (40/60)% composites consisting (Figure 7.9). The increased CO_2 emissions of composites using industrially processed fibres indicate the need for different fibre preparation procedures. The fibre preparation processes increase the emissions of the fibres themselves (section 7.7.1), resulting in even higher emissions compared to composites composed of them.

The fibre content had the least effect on the overall emissions, although more pronounced results were found in composites composed of industrially processed fibres. The CO_2 emissions for the use of Floreon in composites were in the range of 10%, highlighting the importance and the advantages of using a biodegradable polymer.

Therefore, future research should focus on developing ways to reduce emissions from the fibre preparation processes. In addition, researchers should work with farmers to develop more environmentally friendly and sustainable fertilisers and pesticides to reduce overall emissions.

It should not be overlooked that the results presented are based on the assumptions that MPF and MPN fibres require minimal amounts of fertilisers and fewer preparation processes compared to IF and IN fibres.

7.7.3.1 Recycling mechanisms of fibre-reinforced composites (LCI)

According to environmental regulations on waste management, the composite industries have to consider end-of-life treatment of the materials produced, alongside with the environmental emissions, material, and water usage [13]. Figure 7.11 shows the suggested EU waste framework, including potential options for end-of-life treatments. The different options are presented hierarchically from the most environmentally friendly to less desirable solutions [11]. The ‘prevention stage’ is one of the most desirable options for composite manufacturing, since it considers the use of the smallest possible amount of material and processes that extend the life of the product [11].

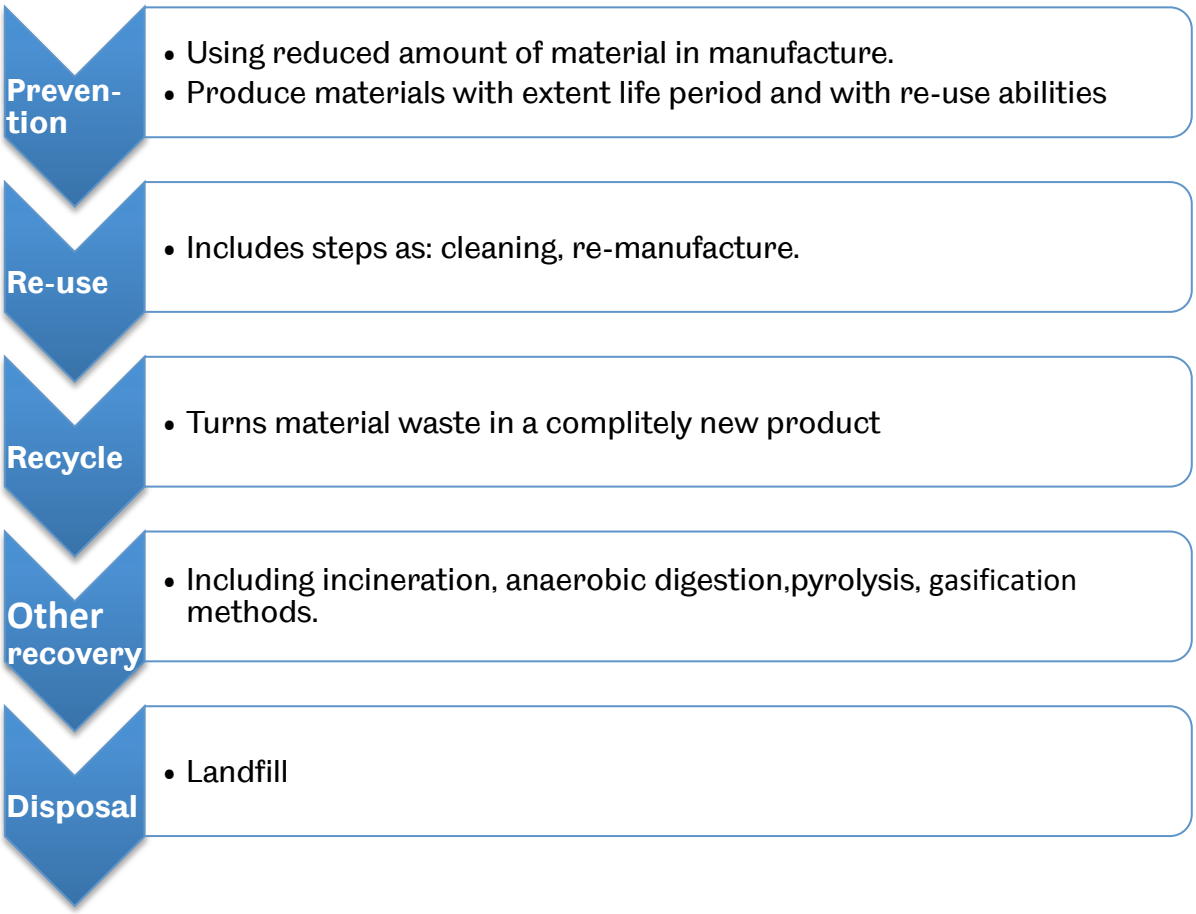

Figure 7.11 EU waste framework (adapted from [244]). The different end-of-life options are presented hierarchically from the most environmentally friendly to the least desirable options.

Composites made with thermoplastic polymers and MP fibres can be recycled into a completely new material and/or have reuse potentials [11], [208], [345]. Reusable fibre-reinforced composites are first cleaned, crushed, and mixed with other materials before being used in further applications (e.g., reused as fillers in thermoplastics) [263], [345]. Other recovery or recycling potentials for composite and plastics included anaerobic digestions, pyrolysis, and gasification methods [263], [264]. These methods use external heat, bacteria, and/or chemicals to break down composites into their initial components, fuel oils, or fuel gases [360]. Note that pyrolysis produces fuel oils and may not be considered a recycling method [6], [13]. Landfill, while the cheapest disposal method, is the least preferable option. Composite materials in landfill may undergo a time-consuming microbiological degradation [360].

According to the UK government policy, only waste that cannot be recycled may be incinerated [6], [244]. Incineration of plastics used to be common until high levels of dioxins and heavy metals released into atmosphere led the government to adopt

more strenuous restrictions [13]. Despite the fact that biodegradable polymers such as Floreon and PLA are made from renewable resources and do not produce dioxins during incineration, incineration is still avoided as a disposal method [193].

The energy requirements of the machines used for the different recycling processes are again based on estimations [13], [244]. Qualitative LCAs indicate that recycling through pyrolysis and gasification has the highest energy requirements [10], [201]. Use of a landfill may save energy because no machine is used for the decomposition of materials [345]. The sustainability of each recycling process is also determined by the amount of product recycled and by the amount of unused raw materials [201]. Fully recycled materials have the second highest levels of energy consumption, followed by materials that are reused [201].

7.8 Summary

EU legislation requires environmental studies to justify the use of the term 'green' material. In this chapter, the environmental analysis was conducted via LCA. The LCA methodology can be used as a qualitative tool for the environmental analysis and evaluation of the fibre's, polymer's, and composite's emissions. MPF and MPN fibres were analysed. The MP fibres presented lower CO_2 emissions due to the lower amounts of applied chemicals and fewer preparation processes. Floreon exhibits lower CO_2 emissions compared to other polymers because of its origin, manufacturing, and biodegradable character. Composites consisting of MPF and MPN fibres had lower emissions and environmental impacts compared to those created using IF and IN fibres, as a result of the lower CO_2 emissions of the MP fibres. In terms of manufacturing processes, injection-moulded composites produced higher emissions due to increased energy demand compared to the 3D printed composites.

These environmental research results were combined with results for the physical, mechanical, and thermal properties of flax and nettle fibre-reinforced composites, presented in the previous chapters, to conclude this research on the manufacturing and characterisation of natural fibre-reinforced composites.

8 THESIS SUMMARY

This thesis addressed the development and LCA of a series of bio-composites incorporating nettle and flax fibres as reinforcing materials and Floreon as the continuous matrix. Specifically, this work was conducted in three investigative stages, starting with the properties of the natural fibres, then the manufacture of fibre-reinforced composites, and culminating in an environmental analysis. A summary of the key findings in this thesis is presented in Table 8.1.

8.1 Technical achievements

The results presented in this work clearly indicate that the use of MP fibres for reinforcing materials can improve the strength of fibre-reinforced composites. Chapter 3 demonstrated that MPN fibres had the highest tensile properties, with a maximum reached tensile strength of 1.4 GPa and Young's modulus of 47 GPa. MPF fibres had a maximum tensile strength of 1.2 GPa and Young's modulus of 36 GPa, indicating clear species-based differences. Furthermore, it is clear that current industrial preparation and processing methods for these fibres reduce their mechanical properties, with IN fibres having a maximum tensile strength of 1.1 GPa and Young's modulus of 37 GPa. The IF fibres had a maximum tensile strength of 0.8 GPa and Young's modulus of 22 GPa.

These results raise a few questions on the feasibility of nettle use for composite reinforcing and on changes to fibre preparation processes in order to minimise the impact on a fibre's mechanical properties.

Given the results from the fibre testing experiments (chapter 3), I personally believe that nettle fibres have a future in the composite manufacturing industry. Nettle fibres have shown tensile properties comparable to, and even higher than, other established reinforcing fibres as flax and hemp (chapters 2 and 3). Additionally, as a plant that can be grown in the UK without special care, nettles have the potential to be a local alternative for reinforcing materials. Considering the fibre's preparation processes, one approach to be examined in the future is to specialise the preparation processes according to the intended application of the composite. The extraction methods used in this project were time consuming but they retained more of the fibre's natural properties. Mechanisation of the extraction technique (as described in chapter 3, section 3.3.4) will lead to a faster and larger preparation of fibres without destroying the fibre's structure.

To broaden the understanding of their potential use in and response to different environments, nettle and flax fibres were tested under a range of different

humidity levels (chapter 3 section 3.5.3). MP fibres had higher levels of moisture absorption compared to industrially processed fibres, resulting in a reduction of mechanical properties. The processing and humidity conditions are linked to the mechanical properties of nettle and flax reinforcing fibres. However, altering a fibre's preparation process can have a great impact on the associated environmental emissions, according to the environmental research and analysis described in chapter 7. The environmental impacts of fibres studied using LCA methodology highlight that specific agricultural operations, such as the use of fertilisers, significantly increase the CO_2 emissions (chapter 7, section 7.7.1). Based on the environmental analysis, the CO_2 emissions of IF and IN fibres were much higher compared to MPF and MPN fibres due to agricultural operations (e.g., retting and degumming). Nevertheless, LCA methodology is a qualitative tool and results should be used for guidance rather than as strict indications (chapter 7, section 7.6).

For the manufacture of biocomposites, a biodegradable blend called Floreon was used (chapter 2, section 2.4.1.2). Processing parameters during the extrusion and injection moulding process of flax and nettle fibre reinforced Floreon composites affected the final properties of the composites. Therefore, the processing parameters have to be carefully studied. Investigations of injection-moulded biocomposites (chapter 4) determined moulding parameters suitable for the individual materials used (chapter 5). It was observed that the moulding time had no significant effect on the composite manufacturing and on the tensile and flexural properties. However, it was found that moulding pressures lower than 40 bar were insufficient for the injection-moulded composites, forming voids and creating a nonhomogeneous composition (chapter 5). The moulding temperature was required to be above Floreon's melting temperature (~ 180°C) and the upper limit was dictated by the fibre degradation temperature.

In order to determine the influence of the fibre type and preparation process on a composite's mechanical properties, composites consisting of MPF, MPN, IN and IF fibres with Floreon were tested under tensile and three-point bending tests (chapter 5). Echoing results from chapter 3, the composites produced with MP fibres had the highest tensile and flexural strength. Injection-moulded MPN and MPF (40/60)% composites had tensile strengths of 85 ± 3 MPa and 77 ± 2 MPa respectively, compared to Floreon's tensile strength of 50 ± 5 MPa (chapter 5, section 5.2.3.1). The obtained Young's modulus for MPN (40/60)% and MPF (40/60)% were at 6.8 ± 1.2 GPa and 5.5 ± 1 GPa respectively. The flexural strength (chapter 5, section 5.2.3.2) of MPN and MPF (40/60)% were 143 ± 4 MPa and 127 ±

6 MPa respectively, compared to Floreon's flexural strength of 90 ± 5 MPa). MPN (40/60)% composites had flexural modulus at 5.7 ± 1.9 GPa , the MPF (40/60)% at 5 ± 2 GPa which are much higher than Floreon's flexural modulus at 3.1 ± 0.9 GPa. MPN composites exhibited the highest tensile and flexural strength and Young's and flexural modulus results compared to the MPF, IN, and IF composites (chapter 5), indicating a clear advantage based on the fibre type.

As minimally processed fibres enhanced the composites' tensile and flexural properties, fibre concentration also affected the composites' properties. Composites with higher fibre concentrations (by weight) had enhanced mechanical properties. The highest fibre concentration achieved in this project was up to 40 wt%, with the remaining 60 wt% Floreon (chapter 5). Higher percentages of fibres were not used because the extruder nozzle and die of the injection moulder continually clogged during the filament extrusion at higher fibre ratio contents. The use of a modified extruder nozzle specifically designed for the use of natural fibres would be of particular interest to investigate all possible composite manufacturing potentials. For example, a larger nozzle diameter as well as extruders with higher processing pressure potentials would be beneficial for the composite's manufacturing.

Investigating the different fibre types, preparation processes, and fibre concentration regarding to the composites' final mechanical properties, the question arises whether a composites' moisture absorption is associated with the fibres involved. Composites consisting of 40 wt% fibres absorbed the highest amount of moisture (chapter 5 section 5.2.6).

Summarising the results obtained from the composite research (chapter 4 and chapter 5), the composites' properties were affected by the properties of the individual raw materials as well by the parameters applied during manufacturing.

Noteworthy was the investigation of 3D printing as an alternative composite manufacturing process by using FDM AM (chapter 6). Once again, as in the case of injection-moulded composites (chapter 5), the 3D printing parameters such as the nozzle temperature, layer height thickness, fill density, and pattern orientation significantly affected the composites' mechanical properties (chapter 6, sections 6.3.1.1 and 6.3.4). The advantage of using 3D printing lies in the fact that the printing parameters can be adjusted according to the applications of the materials. Investigating the printing parameters, the highest tensile and flexural properties of the 3D printed composites were obtained at a fill density of 100% and at a 0.2 mm minimum layer height thickness (sections 6.7.1.1 and 6.7.1.2), as this created sample with a minimum amount of voids. For pattern orientation, the highest tensile

strength was obtained with composites printed at 0°/90° orientation, while the highest flexural strength was at -45°/45° pattern orientation (sections 6.7.1.1 and 6.7.1.2). The nozzle temperature was determined by the fibre type. Composites consisting of MPN and MPF fibres were printed at 200 °C, while composites consisting of IN and IF fibres were printed at 190 °C. The 10 °C increase in the processed temperature for MPN and MPF fibres was also found in the injection-moulded composites.

The mechanical properties of 3D printed composites were affected by the composite composition (fibre type and concentration), similar to the injection-moulded composites. Composites consisting of MPN and MPF fibres had higher tensile and flexural properties than composites with industrially processed fibres. The 3D printed MPN (30/70)% composite had the highest tensile strength at 84 ± 4 MPa, followed by MPF (30/70)% at 76 ± 4 MPa. The tensile strength of the IN (30/70)% and IF (30/70)% were 73 ± 4 MPa and 72 ± 3 MPa respectively (chapter 6, section 6.7.1.1). The Young's modulus of MPN (30/70)% and MPF (30/70)% reached at 7 ± 1.4 GPa and 6.8 ± 1,1 GPa, compared to Floreon's at 3.6 ± 0.8 GPa.

The 3D printed composites consisting of 30 wt% fibre approached the tensile and flexural strength of injection-moulded composites of 40 wt% fibre content (section 6.7.2). Higher fibre contents were not possible with the 3D printed composites because the increasing fibre content blocked the 3D printer nozzle. The problem was even more intense in the case of MPN and MPF fibres because of the fibres' stiffer surface, making it impossible to increase the fibre content.

Another interesting fact about the 3D printed composites was that the levels of moisture absorption were lower compared to the injection-moulded composites, resulting in a smaller reduction in the composites' mechanical properties (chapter 6, section 6.6.3). Overall, the 3D printed composites had improved tensile and flexural properties, were less affected by the humidity conditions, and had lower material waste and faster production time compared to the injection-moulded composites.

Using 3D printing for the manufacture of composites (chapter 6) provides many advantages, but requires adaptations depending on the type of materials and applications. Using 3D printers for composite manufacturing would require larger nozzle diameter, higher extrusion pressures, and lower nozzle temperatures to prevent fibre thermal degradation and allow the use of higher fibre contents. Future research could also explore more complex printing pattern orientations in relation to the mechanical properties of the composites.

In order to determine whether 3D printing is the most appropriate method, the environmental analysis has also been considered (chapter 7). Regarding energy and material consumption, 3D printing is more environmentally efficient, with reduced CO_2 emissions compared to injection moulding (chapter 7, section 7.7.3). However, it should not be forgotten that the CO_2 emissions of flax and nettle fibre-reinforced composites were mainly based on the emissions of the individual materials used (chapter 7, section 7.7.3).

8.2 Future work and suggestions

At the end of this project and based on the results observed, some improvements can be made in the future. Starting from the fibre preparation process, automation is required for the fibres collected from plants, especially during the extraction process from the stems. The fibres should be exported so that they remain intact and causing as little damage as possible. During the composite manufacturing, the selected extruders should have the capability of high pressures in a short period of time in order to protect the fibres from thermal degradation and also manufacture composites with the least possible void content.

The 3D printing technology has improved the time requirements of simultaneous manufacture of composite materials (more than 12 samples, based on the selected composites dimensions during this project). Although, it is necessary to identify the proper 3D printer with the ability to increase the pressure during the extrusion process in order to avoid the nozzle blockage.

LCA as an environmental analysis tool requires the detailed and continuous collection of input data. Input data related to the fibres cultivation need to be collected and recorded during the whole cultivation process. A close collaboration with farmers is required for the continuous monitor of the required amount of seed, chemical and energy requirements.

Natural fibre-reinforced composites have plenty of applications. It's suggested the composites to be manufactured and analysed according to the intent application, specifically for application requiring high temperatures.

8.3 Concluding remarks

The numerous reports on the use of natural fibres prove that they can be used in many different applications, even to construct a completely natural composite. From the outcomes of this project, nettle fibres have great potential as reinforcing materials. Special emphasis in the future should be paid to the fibre preparation

process to maintain the natural character and the mechanical properties of the fibres.

The manufacture of a completely ‘green’ bio-composite was achieved by incorporating a biodegradable PLA blend, Floreon, with MPF and MPN fibres. The possible combinations of natural fibres with biodegradable polymers are numerous. Advanced manufacturing processes allow the production of more complex materials with improved mechanical and physical properties. However, the need to use and manufacture materials with full recycling and reuse capabilities is more vital than ever because of the growing amount of plastic ending up in landfills. Therefore, the need for continuous research on bio-composites is necessary to open new horizons in the field of materials.

Table 8.1 Key findings.

Chapter	Materials	Key Findings
3: Fibre bundle-single fibres	MPN, MPF, IN, and IF fibres	**Tensile properties:** nettle fibres were stronger and stiffener than flax fibres. MPN and MPF single fibres showed greater tensile strength and Young's modulus results compared to IN and IF single fibres. **Moisture absorption:** Nettle and flax fibres absorbed higher rates of moisture at higher RH. Fibres with the highest moisture absorption rates had the greatest tensile strength reduction. MPN and MPF fibres had the larger tensile strength reduction compared to IN and IF fibres. **Water desorption:** the tensile properties of oven dried nettle and flax fibres improved at higher drying temperatures.
4: Experimental process		Description of the experimental manufacture of injection-moulded flax and nettle fibre-reinforced composites.
5: Injection moulded composites	Floreon MPN, MPF, IN, and IF composites	**Mechanical properties:** MPN, MPF, IN, and IF composites presented greater mechanical properties compared to Floreon. The mechanical properties of composites were improved at higher fibre contents (wt%), with composites made of MPN and MPF fibres exhibit increased mechanical properties compared to the composites consisting of IN and IF fibres. Overall, MPN composites had the highest tensile and flexural properties compared to the rest of the injection-moulded composites. **Moisture absorption**: composites with higher fibre content absorbed higher rates (Δm%) of moisture, resulting to greater reduction on the composites' tensile and flexural properties.
6: 3D printed composites	Floreon MPN, MPF, IN, and IF composites	**Mechanical properties:** the 3D printed composites showed greater tensile and flexural properties compared to the respective injection-moulded composites.
7: LCA	MPN, MPF, IN and IF fibres Floreon MPN, MPF, IN, and IF composites	**Supply chain:** the CO_2 emissions of flax and nettle fibres were strongly connected with the agricultural operations, applied fertilisers and the selected fibre preparation methods. The energy and material requirements for the composites manufacturing were depended on the selected manufacturing process, with the injection moulding having higher requirements compared to 3D printing.

REFERENCES

[1] S. Dixit, R. Goel, A. Dubey, P. R. Shivhare, and T. Bhalavi, "Natural Fibre Reinforced Polymer Composite Materials - A Review," *Polym. from Renew. Resour.*, vol. 8, no. 2, pp. 71–78, 2017.

[2] K. L. Pickering, M. G. A. Efendy, and T. M. Le, "A review of recent developments in natural fibre composites and their mechanical performance," *Compos. Part A Appl. Sci. Manuf.*, vol. 83, pp. 98–112, 2016.

[3] P. P. Adrian and B. M. Gheorghe, "Manufacturing Process and Applications of Composite Materials," *Ann. ORADEA Univ. Fascicle Manag. Technol. Eng.*, vol. XIX (IX), no. 2, pp. 3–8, 2010.

[4] J. Canning, S. Bandyopadhyay, P. Biswas, and M. Aslund, "Introduction of Fibre-Reinforced Polymers – Polymers and Composites: Concepts, Properties and Processes," in *Fiber Reinforced Polymers - The Technology Applied for Concrete Repair*, 2013, p. Chapter 1.

[5] O. Faruk, A. K. Bledzki, H. P. Fink, and M. Sain, "Biocomposites reinforced with natural fibers: 2000-2010," *Prog. Polym. Sci.*, vol. 37, no. 11, pp. 1552–1596, 2012.

[6] Department for Environment-Food & Rural Affairs, "Waste legislation and regulations." [Online]. Available: https://www.gov.uk/guidance/waste-legislation-and-regulations#eu-waste-framework-directive.

[7] International Organization for Standardization, "Greenhouse gases — Carbon footprint of products — Requirements and guidelines for quantification and communication (PD CEN ISO/TS 14067:2014)," 2014.

[8] A. Le Duigou, P. Davies, and C. Baley, "Environmental impact analysis of the production of flax fibres to be used as composite material reinforcement," *J. Biobased Mater. Bioenergy*, vol. 5, no. 1, pp. 153–165, 2011.

[9] B. Guinée, *Handbook on life cycle assessment. Operational guide to the ISO standards.* Centre of Environmental Science, Leiden University (CML), 2002.

[10] P. Pawelzik *et al.*, "Critical aspects in the life cycle assessment (LCA) of bio-

based materials – Reviewing methodologies and deriving recommendations.," *Resour. Recycl.*, vol. 73, pp. 211–228, 2013.

[11] J. Rybicka, A. Tiwari, and G. A. Leeke, "Technology readiness level assessment of composites recycling technologies," *J. Clean. Prod.*, vol. 112, pp. 1001–1012, 2016.

[12] "European Commission." [Online]. Available: http://ec.europa.eu/environment/index_en.htm.

[13] "European Commision-European strategy for plastics," 2016. [Online]. Available: http://ec.europa.eu/environment/waste/plastic_waste.htm.

[14] Y. Deng, *Life Cycle Assessment of biobased fibre-reinforced polymer composites*, no. June 2014. .

[15] Y. Li, "Textile Composites based on Natural Fibers," in *From Macro to Nanoscale*, S. and P. Thomas, Ed. L. A. Philadelphia, USA. Old City Publishing., 2009, pp. 202–227.

[16] A. K. Mohanty, L. T. Drzal, and F. Group, *Natural Fibers, Biopolymers, and Biocomposites*. Taylor&Francis, 2005.

[17] C. Baley, "Analysis of the flax fibres tensile behaviour and analysis of the tensile stiffness increase," *Compos. Part A Appl. Sci. Manuf.*, vol. 33, no. 7, pp. 939–948, Jul. 2002.

[18] X. Zeng, S. J. Mooney, and C. J. Sturrock, "Assessing the effect of fibre extraction processes on the strength of flax fibre reinforcement," *Compos. Part A Appl. Sci. Manuf.*, vol. 70, pp. 1–7, 2015.

[19] Floreon-Transforming Packaging Limited, "Floreon." [Online]. Available: http://floreon.com/about-floreon/what-is-floreon.

[20] M. D. Tabone, J. J. Cregg, E. J. Beckman, and A. M. Y. E. Landis, "Sustainability Metrics: Life Cycle Assessment and Green Design in Polymers," *Environ. Sci. Technol.*, vol. 44, no. 21, pp. 8264–8269, 2010.

[21] "PLA Plasicts." [Online]. Available: www.lca.plasticseurope.org.

[22] D. Garlotta, “A Literature Review of Poly (Lactic Acid),” *J. Polym. Environ.*, vol. 9, no. 2, pp. 63–84, 2002.

[23] E. T. H. Vink, K. R. Rábago, D. Glassner, and P. R. Gruber, “The Sustainability of NatureWorksTM Polylactide Polymers and IngeoTM Polylactide Fibers :an Update of the Future,” in *1st International Conference on Bio-based Polymers (ICBP 2003)*, 2003, pp. 551–564.

[24] P. Calvert, T. L. Lin, and H. Martin, “Extrusion freeform fabrication of chopped-fibre reinforced composites,” *High Perform. Polym.*, vol. 9, no. 4, pp. 449–456, 1997.

[25] A. K. Bledzki and J. Gassan, “Composites reinforced with cellulose based fibres,” *Prog. Polym. Sci.*, vol. 24, no. 2, pp. 221–274, 1999.

[26] A. K. Mohanty, M. Misra, and G. Hinrichsen, “Biofibres, biodegradable polymers and biocomposites: An overview.,” *Macromol. Mater. Eng.*, vol. 276, no. 3–4, pp. 1–24, 2000.

[27] A. K. Bledzki, V. E. Sperber, and O. Faruk, *Natural and wood fibre reiforcement in polymers*. Rapra Technology Ltd., 2002.

[28] S. Thomas, S. A. Paul, L. A. Pothan, and B. Deepa, “Cellulose Fibers: Bio- and Nano-Polymer Composites,” in *Natural Fibres: Structure, Properties and Applications*, S. K. S. K. Kaur, Ed. Springer Link, 2011, p. 3.42.

[29] D. Ray and S. Sain, “Plant fibre reinforcements,” in *Biocomposites for high-performance applications: Current barriers and future needs towards industrial development*, D. Ray, Ed. Woodhead publishing, 2017.

[30] P. H. F. Pereira *et al.*, “Vegetal fibers in polymeric composites: a review,” *Polímeros*, vol. 25, no. 1, pp. 9–22, 2015.

[31] M. L. T. Cossio, L. F. Giesen, G. Araya, and Et.al, *Bast and other plant fibres*, vol. XXXIII, no. 2. 2012.

[32] L. J. Gibson, “The hierarchical structure and mechanics of plant materials,” *J. R. Soc. interface*, vol. 9, no. 76, pp. 2749–2766, 2012.

[33] B. Madsen and E. K. Gamstedt, “Wood versus Plant Fibers: Similarities and

differences in composite applications.," *Adv. Mater. Sci. Eng.*, vol. 2013, pp. 1–14, 2013.

[34] J. Holbery and D. Houston, "Natural-fibre-reinforced polymer composites in automotive applications," *J. Miner. Met. Mater. Soc.*, vol. 58, no. 11, pp. 80–86, 2006.

[35] G. Siqueira, J. Bras, and A. Dufresne, "Cellulosic Bionanocomposites: A Review of Preparation, Properties and Applications," *Polymers (Basel).*, vol. 2, no. 4, pp. 728–765, 2010.

[36] H. Chen, "Chemical Composition and Structure of Natural Lignocellulose," in *Biotechnology of Lignocellulose: Theory and Practice*, 2014, pp. 25–71.

[37] A. Thygesen, J. Oddershede, H. Lilholt, A. B. Thomsen, and K. Ståhl, "On the determination of crystallinity and cellulose content in plant fibres," *Cellulose*, vol. 12, no. 6, pp. 563–576, 2005.

[38] D. P. Delmer and Y. Amor, "Cellulose Biosynthesis," *Plant Cell*, vol. 7, no. 7, pp. 987–1000, 1995.

[39] F. J. Kolpak and J. Blackwell, "Determination of the Structure of Cellulose II," *Macromolecules*, vol. 9, no. 2, pp. 273–278, 1976.

[40] K. H. Gardner and J. Blackwell, "The hydrogen bonding in native cellulose," *Biochim. Biophys. Acta*, vol. 343, no. 1, pp. 232–237, 1974.

[41] G. Chinga-Carrasco, "Cellulose fibres, nanofibrils and microfibrils: The morphological sequence of MFC components from a plant physiology and fibre technology point of view," *Nanoscale Res. Lett.*, vol. 6, no. 1, p. 417, 2011.

[42] H. O'Neil *et al.*, "Dynamics of water bound to crystalline cellulose," *Sci. Rep.*, vol. 7, 2017.

[43] R. A. Shanks, "Chemistry and structure of cellulosic fibres as reinforcements in natural fibre composites R.," in *Natural fibre composites*, A. H. and R. Shanks, Ed. Woodhead publishing, 2014, pp. 66–83.

[44] M. P. Ansell and L. Y. Mwaikambo, *Handbook of Textile Fibre Structure: Natural, Regenerated, Inorganic and Specialist Fibres*. Woodhead publishing

series in textiles, 2009.

[45] A. Gallos, G. Paes, F. Allais, and J. Beaugrand, “Lignocellulosic fibers: a critical review of the extrusion process for enhancement of the properties of natural fiber composites,” *RSC Adv.*, vol. 7, no. 55, pp. 34638–34654, 2017.

[46] R. A. Young, *Cellulose chemistry and its applications*. Elsevier science publishers B.V, 1985.

[47] Z. Persin, K. Stana-Kleinschek, and T. Kreze, “Hydrophilic/hydrophobic characteristics of different cellulose fibres monitored by tensiometry,” *Croat. Chem. Acta*, vol. 75, no. 1, pp. 271–280, 2002.

[48] A. Komuraiah, N. S. Kumar, and B. D. Prasad, “Chemical Composition of Natural Fibers and its Influence on their Mechanical Properties,” *Mech. Compos. Mater.*, vol. 50, no. 3, pp. 359–376, 2014.

[49] R. Joseph, F. R. Toledo, D. Romildo, B. James, S. Thomas, and L. H. De Carvalho, “A review on sisal fiber reinforced polymer composites,” *Rev. Bras. Eng. Agrícola e Ambient.*, vol. 3, no. 3, pp. 367–379, 1999.

[50] V. K. Kaushik, A. Kumar, and S. Kalia, “Effect of Mercerization and Benzoyl Peroxide Treatment on Morphology, Thermal Stability and Crystallinity of Sisal Fibers,” *Int. J. Text. Sci.*, vol. 1, no. 6, pp. 101–105, 2013.

[51] S. Jose, S. Rajna, and P. Ghosh, “Ramie Fibre Processing and Value Addition,” *Asian J. Text.*, vol. 7, no. 1, pp. 1–9, 2016.

[52] H. P. Fink, E. Walenta, and J. Kunze, “The structure of natural cellulosic fibres - Part 2. The supermolecular structure of bast fibres and their changes by mercerization as revealed by X-ray diffraction and C-13-NMR-spectroscopy,” *PAPIER*, vol. 53, no. 9, pp. 534–542, 1999.

[53] W. Hamad, *Cellulosic Materials: Fibers, Networks, and Composites*. Kluwer Academic Publishers., 2002.

[54] A. Thygesen, J. Oddershede, H. Lilholt, A. B. Thomsen, and K. Ståhl, “On the determination of crystallinity and cellulose content in plant fibres.,” *Cellulose*, vol. 12, no. 6, pp. 563–576, 2005.

[55] J. D. Mauseth, *Botany: An introduction to plant biology*, 5th ed. Jones & Barlett Learning, 2012.

[56] D. Sadava, H. C. Heller, G. H. Orians, W. K. Purves, and D. M. Hillis, *Life: The Science of Biology*, vol. 2. 2006.

[57] B. Ghanbarzadeh and H. Almasi, "Plant Fibres for Textile and Technical Applications," in *Advances in Agrophysical Research*, 2013, pp. 75–100.

[58] H. L. Bos, J. Müssig, and M. J. A. Van den Oever, "Mechanical properties of short-flax-fibre reinforced compounds," *Compos. Part A Appl. Sci. Manuf.*, vol. 37, no. 10, pp. 1591–1604, 2006.

[59] P. M. Tahir, A. B. Ahmed, S. Saifulazry, and Z. Ahmed, "Retting process of some bast plant fibres and its effect on fibre quality: A review," *Bioresources,* vol. 6, no. 4, pp. 5260–5281, 2011.

[60] K. Charlet, C. Baley, C. Morvan, J. P. Jernot, M. Gomina, and J. Bréard, "Characteristics of Hermès flax fibres as a function of their location in the stem and properties of the derived unidirectional composites," *Compos. Part A Appl. Sci. Manuf.*, vol. 38, no. 8, pp. 1912–1921, 2007.

[61] C. Zweben, "Composite materials," in *Mechanical Engineers*, 4rth Editi., M. Kutz, Ed. John Wiley & Sons Inc, 2015, pp. 1–36.

[62] P. Ouagne, B. Barthod-Malat, P. Evon, L. Labonne, and V. Placet, "Fibre Extraction from Oleaginous Flax for Technical Textile Applications: Influence of Pre-processing parameters on Fibre Extraction Yield, Size Distribution and Mechanical Properties," *Procedia Eng.*, vol. 200, pp. 213–220, 2017.

[63] L. Yan, N. Chouw, and K. Jayaraman, "Flax fibre and its composites - A review," *Compos. Part B Eng.*, vol. 56, pp. 296–317, 2014.

[64] S. J. Bennett, D. Wright, and G. Edwards-Jones, "The importance of time of spraying, desiccant type and harvest time on industrial fibre production from stand-retted fibre flax (Linum usitatissimum)," *J. Agric. Sci.*, vol. 145, no. 6, pp. 565–576, 2007.

[65] H. S. S. Sharma and C. F. Van Sumere, *The biology and processing of flax*.

Belfast: M Publications., 1992.

[66] P. Georgiopoulos, A. Christopoulos, S. Koutsoumpis, and E. Kontou, “The effect of surface treatment on the performance of flax/biodegradable composites,” *Compos. Part B Eng.*, vol. 106, pp. 88–98, 2016.

[67] S. Mishra, S. S. Tripathy, M. Misra, A. K. Mohanty, and S. K. Nayak, “Novel eco-friendly biocomposites:Biofibre reinroced biodegradable polyester amide composites-Fabrication and properties evaliation,” *J. Reinf. Plast.*, vol. 21, no. 1, pp. 55–70, 2002.

[68] L. Mohammed, M. N. M. Ansari, G. Pua, M. Jawaid, and M. S. Islam, “A Review on Natural Fiber Reinforced Polymer Composite and Its Applications,” *Int. J. Polym. Sci.*, vol. 2015, pp. 1–15, 2015.

[69] L. Y. Mwaikambo and M. P. Ansell, “Mechanical properties of alkali treated plant fibres and their potential as reinforcement materials. I. hemp fibres,” *J. Mater. Sci.*, vol. 41, no. 8, pp. 2483–2496, 2006.

[70] M. Y. Hashim, M. N. Roslan, A. M. Amin, A. Mujahid, A. Zaidi, and A. Ariffin, “Mercerization treatment parameter effect on natural fiber reinforced polymer matrix composite: A brief review,” *Int. J. Mater. Metall. Eng.*, vol. 6, no. 8, pp. 778–784, 2012.

[71] C. Baillie, *Green Composites: polymer composites and the environment,*. Woodhead Publishing Limited, Cambridge, 2004.

[72] J. Zhu *et al.*, “Effects of chemical treatments on physical properties of flax fibres,” in *5th International Seminar on Modern Polymeric Materials for Environmental Applications,* 2013, no. 1–9.

[73] C. Baley, “Influence of kink bands on the tensile strength of flax fibers,” *J. Mater. Sci.*, vol. 39, no. 1, pp. 331–334, 2004.

[74] T. Bayerl, M. Geith, A. A. Somashekar, and D. Bhattacharyya, “Influence of fibre architecture on the biodegradability of FLAX/PLA composites,” *Int. Biodeterior. Biodegrad.*, vol. 96, pp. 18–25, 2014.

[75] T. Nilsson and P. J. Gustafsson, “Influence of dislocations and plasticity on the

tensile behaviour of flax and hemp fibres," *Compos. Part A Appl. Sci. Manuf.*, vol. 38, no. 7, pp. 1722–1728, 2007.

[76] S. Kalia, B. S. Kaith, and I. Kaur, "Pretreatments of Natural Fibers and their Application as Reinforcing Material in Polymer Composites—A Review," *Polym. Eng. Sci.*, pp. 1253–1272, 2009.

[77] Y. Li, Q. Li, and H. Ma, "The voids formation mechanisms and their effects on the mechanical properties of flax fiber reinforced epoxy composites," *Compos. Part A Appl. Sci. Manuf.*, vol. 72, pp. 40–48, 2015.

[78] N. Stevulova, L. Kidalova, and J. Cigasova, "Lightweight Composites Based on Cellulosic Material," *Int. J. Mod. Manuf. Technol.*, vol. 5, no. 2, pp. 75–82, 2013.

[79] P. K. Ilankeeran, P. M. Mohite, and S. Kamle, "Axial Tensile Testing of Single Fibres," *Mod. Mech. Eng.*, vol. 02, no. 04, pp. 151–156, 2012.

[80] International Organization for Standardization, "Carbon fibre - Determination of the tensile properties of single-filament specimens (BS ISO 11566: 1996)," 1996.

[81] International Organization for Standardization, "Determination of the tensile properties of single-filament specimens (BS ISO 11566:1996)," 1996.

[82] R. Sengupta *et al.*, "An Improved Method for Single Fiber Tensile Test of Natural Fibers Wei," *Polym. Eng. Sci.*, vol. 47, pp. 819–825, 2007.

[83] N. E. Zafeiropoulos, G. G. Dijon, and C. A. Baillie, "A study of the effect of surface treatments on the tensile strength of flax fibres: Part I. Application of Gaussian statistics," *Compos. Part A Appl. Sci. Manuf.*, vol. 38, no. 2, pp. 621–628, 2007.

[84] H. Krässig and W. Kitchen, "Factors influencing tensile properties of cellulose fibers," *J. Polym. Sci.*, vol. 51, no. 1, pp. 123–172, 1961.

[85] B. Madsen, A. Thygesen, and H. Lilholt, "Plant fibre composites - porosity and stiffness," *Compos. Sci. Technol.*, vol. 69, no. 7–8, pp. 1057–1069, 2009.

[86] M. Aslan, "Characterisation of flax fibers and flax fiber composites. Being cellulose based sources of materials," 2012.

[87] N. Virgilio, E. G. Papazoglou, Z. Jankauskiene, S. D. Lonardo, M. Praczyk, and K. Wielgusz, “The potential of stinging nettle (Urtica dioica L.) as a crop with multiple uses,” *Ind. Crops Prod.*, vol. 68, pp. 42–49, 2015.

[88] A. K. Bledzki, V. E. Sperber, and O. Faruk, *Natural and Wood Fibre Reinforcement in Polymers*, vol. 13, no. 8. 2002.

[89] N. M. Van Der Velden, M. K. Patel, and J. G. Vogtländer, “LCA benchmarking study on textiles made of cotton, polyester, nylon, acryl, or elastane,” *Int. J. Life Cycle Assess.*, vol. 19, no. 2, pp. 331–356, 2014.

[90] M. Brebu and C. Vasile, “Thermal degradation of lignin—a review,” *Cellul. Chem. Technol.*, vol. 44, no. 9, pp. 353–363, 2010.

[91] M. J. A. Van den Oever and J. Beck, B; Mussig, “Agrofibre reinforced poly(lactic acid) composites: Effect of moisture on degradation and mechanical properties.,” *Compos. Part A*, vol. 41, pp. 1628 – 1635, 2010.

[92] K. Oksman, M. Skrifvars, and J. F. Selin, “Natural fibres as reinforcement in polylactic acid (PLA) composites,” *Compos. Sci. Technol.*, vol. 63, no. 9, pp. 1317–1324, 2003.

[93] J. Gassan and A. K. Bledzki, “Thermal degradation of flax and jute fibers,” *J. Appl. Polym. Sci.*, vol. 82, no. 6, pp. 1417–1422, 2001.

[94] H. Yang, R. Yan, H. Chen, D. H. Lee, and C. Zheng, “Characteristics of hemicellulose, cellulose and lignin pyrolysis,” *Fuel*, vol. 86, no. 12–13, pp. 1781–1788, 2007.

[95] L. Gao-jin, S. Wu, and R. Lou, “Kinetic Study of the Thermal Decomposition of Hemicellulose Isolated From Corn Stalk,” *BioResources*, vol. 5, no. 2, pp. 1281–1291, 2010.

[96] D. Shen, R. Xiao, S. Gu, and H. Zhang, “The Overview of Thermal Decomposition of Cellulose in Lignocellulosic Biomass,” in *Cellulose - Biomass Conversion*, 2013, pp. 193–226.

[97] K. Van De Velde and E. Baetens, “Thermal and mechanical properties of flax fibres as potential composite reinforcement,” *Macromol. Mater. Eng.*, vol.

286, no. 6, pp. 342–349, 2001.

[98] S. Yano, H. Hatakeyama, and T. Hatakeyama, “Effect of hydrogen bond formation on dynamic mechanical properties of amorphous cellulose,” *J. Appl. Polym. Sci.*, vol. 20, no. 12, pp. 3221–3231, 1976.

[99] C. A. S. Hill, A. J. Norton, and G. Newman, “The water vapour sorption properties of Sitka spruce determined using dynamic vapour sorption apparatus,” *Wood sci Technol*, vol. 44, pp. 497–514, 2010.

[100] L. Rautkari, C. A. S. Hill, S. Curling, Z. Jalaludin, and G. Ormondroyd, “What is the role of the accessibility of wood hydroxyl groups in controlling moisture content,” *J. Mater. Sci.*, 2013.

[101] C. Hill and M. Hudges, “Natural fibre reinfirced composites opportuinities and challenges,” *J. Biobased Mater. Bioenergy*, vol. 4, pp. 148–158, 2010.

[102] P. Wambua, J. Ivens, and I. Verpoest, “Natural fibres: can they replace glass in fibre reinforced plastics?,” *Compos. Sci. Technol.*, vol. 63, no. 9, pp. 1259–1264, Jul. 2003.

[103] J. Giridhar, R. Kishore, and R. M. V. G. K. Rao, “Moisture Absorption Characteristics of Natural Fibre Composites,” *Compos. Part B Eng.*, vol. 56, no. 11, pp. 979–984, 1980.

[104] C. M. Popescu, C. A. S. Hill, R. Anthony, G. Ormondroyd, and S. Curling, “Equilibrium and dynamic vapour water sorption properties of biochar derived from apple wood,” *Polym. Degrad. Stabilityp*, vol. 111, pp. 263–268, 2015.

[105] R. T. D. Prabhakaran, T. L. Andersen, and A. Lystrup, “Influence of moisture absorption on properties of fiber reinforced polyamide 6 composites,” *Proc. 26th Annu. Tech. Conf. Am. Soc. Compos. 2011 2nd Jt. Us-canada Conf. Compos.*, 2011.

[106] A. Pandian, M. Vairavan, J. J. T. Winowlin, and M. Uthayakumar, “Effect of Moisture Absorption Behavior on Mechanical Properties of Basalt Fibre Reinforced Polymer Matrix Composites,” *J. Compos.*, vol. 2014, pp. 1–8, 2014.

[107] N. Jauhari, R. Mishra, and H. Thakur, “Failure Analysis of Fibre-Reinforced Composite Laminates,” in *Materials Today: Proceedings*, 2017, vol. 4, no. 2, pp. 2851–2860.

[108] S. Ghahri and B. Mohebby, “Soybean as adhesive for wood composites: applications and properties,” 2017.

[109] M. Guo and G. Wanf, “Milk Protein Polymer and Its Application in Environmentally Safe Adhesives,” *Polymers (Basel).*, vol. 8, no. 324, 2016.

[110] T. J. Reinhart, “Overview of composite,” in *Handbook of Composites*, 2nd etidio., S. T. Peters, Ed. Chapman & Hall, 1998.

[111] J. M. Hodgkinson, *Mechanical testing of advanced fibre composites.* Woodhead puvlished limited.

[112] S. Maity, D. P. Gon, and P. Paul, “A Review of Flax Nonwovens: Manufacturing, Properties, and Applications,” *J. Nat. Fibers*, vol. 11, no. 4, pp. 365–390, 2014.

[113] J. L. Throne, “Processing Thermoplastic Composites,” in *Handbook of Composites*, 1998, pp. 1–9.

[114] I. Y. Chang and J. K. Lees, “Recent Development in Thermoplastic Composites: A Review of Matrix Systems and Processing Methods,” *J. Thermoplast. Compos. Mater.*, vol. 1, no. 3, pp. 277–296, 1988.

[115] J. Zhu, H. Zhu, J. Njuguna, and H. Abhyankar, “Recent development of flax fibres and their reinforced composites based on different polymeric matrices,” *Materials (Basel).*, vol. 6, no. 11, pp. 5171–5198, 2013.

[116] R. S. Bauer, S. L. Stewart, and H. D. Stenzenberger, “Composite Materials, Thermoset Polymer-Matrix,” in *Kirk-Othmer Encyclopedia of Chemical Technology*, John Wiley & Sons, Inc., 2000.

[117] A. Haque and S. Jeelani, “Environmental effects on the compressive properties : Thermosetting vs . thermoplastic vomposites,” *J. rei*, vol. 11, pp. 146–157, 1992.

[118] S. Y. Fu, X. Q. Feng, B. Lauke, and Y. W. Mai, “Effects of particle size, particle/matrix interface adhesion and particle loading on mechanical

properties of particulate–polymer composites," *Compos. Part B-Engineering*, vol. 39, no. 6, pp. 933–961, 2008.

[119] B. Lauke, "On the effect of particle size on fracture toughness of polymer composites," *Compos. Sci. Technol.*, vol. 68, no. 15–16, pp. 3365–3372, 2008.

[120] G. H. Staab, *Laminar composites*. Butterworth-Heinemann., 1999.

[121] S. Prashanth, K. M. Subbaya, K. Nithin, and S. Sachhidananda, "Fiber Reinforced Composites - A Review," *J. Mater. Sci. Eng.*, vol. 06, no. 03, pp. 2–6, 2017.

[122] D. U. Shah, "Natural fibre composites: Comprehensive Ashby-type materials selection charts," *Mater. Des.*, vol. 62, pp. 21–31, 2014.

[123] M. Ashby, "The CES EduPack database of natural and man-made materials," *Cambridge University and Granta Design*, 2008. .

[124] Y. Shao, S. Marikunte, and S. P. Shah, "Extruded fiber-reinforced composites," *Concr. Int.*, vol. 17, no. 4, pp. 48–52, 1995.

[125] F. Henson, *Plastic Extrusion Technology,* 2nd ed. New York. NY: Hanser Publishers, 1997.

[126] A. N. Gent, "Extruder," *Encyclopedia Britannica*. 1997.

[127] D. V Rosato and G. M. Rosato, *Injection Moulding Handbook*, 3rd ed. Norwell, MA: Kluwer Academic Publishers.

[128] S. G. Advani and E. M. Sozer, "Process Modeling in Composites Manufacturing," *Assem. Autom.*, vol. 24, no. 3, pp. 324–325, Sep. 2004.

[129] D. M. Bryce, "Plastic Injection Molding manufacturing startup and management," *Manuf. Process Fundam.*, vol. 4, 1999.

[130] H. Peltola, B. Madsen, R. Joffe, and N. Kalle, "Experimental Study of Fiber Length and Orientation in Injection Molded Natural Fiber / Starch Acetate Composites," *Adv. Mater. Sci. Eng.*, vol. 2011, pp. 1–7, 2011.

[131] J. Butler, *Compression and transfer moulding of plastics.* Interscience, 1959.

[132] D. M. Corbridge, L. T. Harper, D. S. A. De Focatiis, and N. A. Warrior,

"Compression moulding of composites with hybrid fibre architectures," *Compos. Part A Appl. Sci. Manuf.*, vol. 95, pp. 87–99, 2017.

[133] I. Tharazi *et al.*, "Optimization of Hot Press Parameters on Tensile Strength for Unidirectional Long Kenaf Fiber Reinforced Polylactic-Acid Composite," *Procedia Eng.*, vol. 184, pp. 478–485, 2017.

[134] M. I. M. Kandar and H. M. Akil, "Application of Design of Experiment (DoE) for Parameters Optimization in Compression Moulding for Flax Reinforced Biocomposites," *Procedia Chem.*, vol. 19, pp. 433–440, 2016.

[135] N. Birgitha, "Natural fiber composites optimization of microstructure and processing parameters.," 2007.

[136] C. Quijano-Solis, N. Yan, and S. Y. Zhang, "Effect of mixing conditions and initial fiber morphology on fiber dimensions after processing," *Compos. Part A Appl. Sci. Manuf.*, vol. 40, no. 4, pp. 351–358, 2009.

[137] K. Charlet, S. Eve, J. P. Jernot, M. Gomina, and J. Breard, "Tensile deformation of a flax fiber," *Procedia Eng.*, vol. 1, no. 1, pp. 233–236, 2009.

[138] A. Arbelaiz, B. Fernández, J. A. Ramos, A. Retegi, R. Llano-Ponte, and I. Mondragon, "Mechanical properties of short flax fibre bundle/polypropylene composites: Influence of matrix/fibre modification, fibre content, water uptake and recycling," *Compos. Sci. Technol.*, vol. 65, no. 10, pp. 1582–1592, Aug. 2005.

[139] R. Muthuraj, M. Misra, F. Defersha, and A. K. Mohanty, "Influence of processing parameters on the impact strength of biocomposites: A statistical approach," *Compos. Part A Appl. Sci. Manuf.*, vol. 83, pp. 120–129, 2016.

[140] B. Madsen, A. Thygesen, and H. Lilholt, "Plant fibre composites - porosity and volumetric interaction," *Compos. Sci. Technol.*, vol. 67, no. 7–8, pp. 1584–1600, 2007.

[141] M. Miao and M. Shan, "Highly aligned flax/polypropylene nonwoven preforms for thermoplastic composites.," *Compos. Sci. Technol.*, vol. 71, no. 15, pp. 713–1718, 2011.

[142] B. Lamy and C. Baley, “Stiffness prediction of flax fibers-epoxy composite materials.,” *J. Mater. Sci. Lett.*, vol. 19, no. 11, pp. 979–980, 2000.

[143] N. Graupner, J. Rößler, G. Ziegmann, and J. Müssig, “Fibre/matrix adhesion of cellulose fibres in PLA, PP and MAPP: A critical review of pull-out test, microbond test and single fibre fragmentation test results,” *Compos. Part A Appl. Sci. Manuf.*, vol. 63, pp. 133–148, 2014.

[144] J. E. Little, X. Yuan, and M. I. Jones, “Characterisation of voids in fibre reinforced composite materials,” *NDT E Int.*, vol. 46, pp. 122–127, 2012.

[145] S. W. Freiman and J. J. Mecholsky, “Microstructural effects,” in *The Fracture of brittle materials: Testing and analysis*, 1rst ed., J. Freiman, SW;Mecholsky, Ed. John Wiley & Sons Inc, 2012, pp. 131–144.

[146] D. R. Kaplan, “The science of plant morphology: definition, history, and role in modern biology,” *Am. J. Bot.*, vol. 88, no. 10, pp. 1711–1741, 2001.

[147] S. Alimuzzaman, “Nonwoven Flax Fibre Reinforced PLA Biodegradable Composites,” University of Manchester, 2013.

[148] A. Célino, S. Fréour, F. Jacquemin, and P. Casari, “The hygroscopic behavior of plant fibers: a review,” *Front. Chem.*, vol. 1, no. Januar, pp. 1–12, 2014.

[149] O. I. Okoli and G. F. Smith, “Failure modes of fibre reinforced composites: The effects of strain rate and fibre content,” *J. Mater. Sci.*, vol. 33, no. 22, pp. 5415–5422, 1998.

[150] International Organization for Standardization, “Plastics — Determination of tensile properties Part 4:Test conditions for isotropic and othotropic fibre-reinforced plastic composites (BS EN ISO 527-4:1997 BS 2782-3: Method 326F:1997),” 1997.

[151] International Organization for Standardization, “Plastics — Determination of tensile properties(BS EN ISO 527-2:1996 BS 2782-3: Method 322: 1994),” 1996.

[152] L. Yang, Y. Yan, Y. Liu, and Z. Ran, “Microscopic failure mechanisms of fiber-reinforced polymer composites under transverse tension and compression,” *Compos. Sci. Technol.*, vol. 72, no. 15, pp. 1818–1825, 2012.

[153] A. G. Evans, M. Y. He, and J. W. Hutchinson, “Interface Debonding and Fiber Cracking in Brittle Matrix Composites,” *Journal of the American Ceramic Society*, vol. 72, no. 12. pp. 2300–2303, 1989.

[154] V. Arumugam, S. V Karthikeyan, B. T. N. Sridhar, and A. J. Stanley, “Characterization of Failure Modes in Composite Laminates Under Flexural Loading Using Time-Frequency Analysis,” *Arab. J. Sci. Eng.*, vol. 38, no. 6, pp. 1471–1480, 2013.

[155] International Organization for Standardization, “Fibre-reinforced plastic composites — Determination of flexural properties(BS EN ISO 14125:1998+A1:2011),” 2012.

[156] J. M. Hodgkinson, *Mechanical Testing of Advanced Fibre Composites*. 2000.

[157] K. P. Mieck, T. Reussmann, and C. Hauspurg, “Correlations for the fracture work and falling weight impact properties of thermoplastic natural/long fibre composites,” *Mater. Sci. Eng. today*, vol. 31(2), pp. 169–174, 2000.

[158] S. Siengchin, “Reinforced Flax mat/modified Polylactide (PLA) Composites: Impact, Thermal, and Mechanical Properties,” *Mech. Compos. Mater.*, vol. 50, no. 2, pp. 257–266, 2014.

[159] N. Kuppusamy and R. A. Tomlinson, “RepeaTable pre-cracking preparation for fracture testing of polymeric materials,” *Eng. Fract. Mech.*, vol. 152, pp. 81–87, 2016.

[160] B. Budiansky and N. A. Flieck, “Compressive failure of fibre composites,” *Mech.Phy.Solids*, vol. 41, no. 1, pp. 118–211, 1993.

[161] M. Bayart, F. Gauvin, M. R. Foruzanmehr, S. Elkoun, and M. Robert, “Mechanical and moisture absorption characterization of PLA composites reinforced with nano-coated flax fibers,” *Fibers Polym.*, vol. 18, no. 7, pp. 1288–1295, 2017.

[162] A. C. Johnson, S. A. Hayes, and F. R. Jones, “The role of matrix cracks and fibre/matrix debonding on the stress transfer between fibre and matrix in a single fibre fragmentation test,” *Compos. Part A Appl. Sci. Manuf.*, vol. 43, no.

1, pp. 65–72, 2012.

[163] X. Xia, X. Shi, W. Liu, H. Zhao, and H. Li, “Effect of flax fiber content on polylactic acid (PLA) crystallization in PLA / flax fiber composites,” *Iran. Polym. J.*, vol. 26, no. 9, pp. 693–702, 2017.

[164] L. Monette, M. P. Anderson, and G. S. Grest, “The meaning of the critical length concept in composites: Study of matrix viscosity and strain rate on the average fiber fragmentation length in short-fiber polymer composites,” *Polym. Sci.*, vol. 14, no. 2, pp. 101–115, 1993.

[165] D. U. Shah, P. J. Schubel, P. Licence, and M. J. Clifford, “Determining the minimum, critical and maximum fibre content for twisted yarn reinforced plant fibre composites,” *Compos. Sci. Technol.*, vol. 72, no. 15, pp. 1909–1917, 2012.

[166] G. Lubin and S. T. Peters, *Handbook of composites*. Chapman & Hall., 1998.

[167] R. Z. Khoo, H. Ismail, and W. S. Chow, “Thermal and Morphological Properties of Poly (Lactic Acid)/Nanocellulose Nanocomposites,” *Procedia Chem.*, vol. 19, pp. 788–794, 2016.

[168] L. Běhálek, M. Maršálková, P. Lenfeld, J. Habr, J. Bobek, and M. Seidl, “Study of Crystallization of Polylactic Acid Composites and Nanocomposites With Natural Fibres By DSC Method,” pp. 1–6, 2013.

[169] A. Komesu, P. F. Martins Martinez, B. H. Lunelli, J. Oliveira, M. R. Wolf Maclel, and R. Maclel Filho, “Study of lactic acid thermal behavior using thermoanalytical techniques,” *J. Chem.*, vol. 2017, 2017.

[170] TA Instruments, “Thermal Analysis Investigation of a Poly (Lactic Acid) Biodegradable Plastic,” 2007.

[171] J. Walshaw *et al.*, “Characterization of forages by differential scanning calorimetry and prediction of their chemical composition and nutritive value,” *Anim. Feed Sci. Technol.*, vol. 71, no. 3–4, pp. 309–323, 1998.

[172] I. Sakurada, K. Kaji, K. Nakamae, and S. Wadano, “Experimental Determination of the elastic moduli of polymer crystalline regions in oriented polymers,”

vol. XXXIII, no. 2, pp. 81–87, 2012.

[173] A. Gregorov, “Application of Differential Scanning Calorimetry to the Characterization of Biopolymers,” in *Applications of Calorimetry in a Wide Context - Differential Scanning Calorimetry, Isothermal Titration Calorimetry and Microcalorimetry*, A. A. Elkord, Ed. 2013.

[174] N. Saba, M. Jawald, A. O. Alothman, and P. M. Tahir, “A Review on Dynamic mechanical analysis of natural fibre reinforced polymer composites,” *Constr. Build. Mater.*, vol. 106, 2015.

[175] A. Leal-Junior *et al.*, “Dynamic mechanical characterization with respect to temperature, humidity, frequency and strain in mPOFs made of different materials,” *Opt. Mater. Express*, vol. 8, no. 4, pp. 804–815, 2018.

[176] M. Avella, A. Buzarovska, M. E. Errico, G. Gentile, and A. Grozdanov, “Eco-challenges of bio-based polymer composites,” *Materials (Basel).*, vol. 2, no. 3, pp. 911–925, 2009.

[177] European Commision, “Commission proposals on financing sustainable growth- Low carbon and positive Crbon impact benchmarks,” 2018.

[178] Terrachoice, “Greenwashing report,” 2009.

[179] F. M. Belz and K. Peattie, *Sustainability marketing: A global perspective*. John Wiley & Sons Inc, 2012.

[180] International Organization for Standardization, “Biomimetics — Biomimetic materials , structures and components (BS ISO 18457:2016),” 2016.

[181] “European bioplastics.” [Online]. Available: http://www.european-bioplastics.org/.

[182] D. Rudi, K. Myrtha, A. Subyakto, A. Sulaeman, D. Dede Hermawan, and A. Hadiyane, “Agricultural waste fibers towards sustainability and advanced utilization: A review,” *Asian J. Plant Sci.*, vol. 15, no. 1–2, pp. 45–55, 2016.

[183] Y. Wang, “Fiber and Textile Waste Utilization,” *Waste and biomass valorization*, vol. 1, no. 1, pp. 135–143, 2010.

[184] “U.S. Environmental Protection Agency: Municipal Solid Waste in the United States: 2007 Facts and Figures, EPA530-R-08-010,” 2008. .

[185] R. G. Allaby, G. W. Peterson, D. A. Merriwether, and Y. B. Fu, “Evidence of the domestication history of flax (Linum usitatissimum L.) from genetic diversity of the sad2 locus,” *Theor. Appl. Genet.*, vol. 112, no. 1, pp. 58–65, 2005.

[186] M. Laux, “Agricultural marketing resource center,” *2017*. .

[187] “Natural fibre composite.” [Online]. Available: http://www.agrofibrecomposites.com/process.htm.

[188] H. L. Bos, *The potential of flax fibres as reinforcement for composite materials*. 2004.

[189] I. Baltina, L. Lapsa, Z. Jankauskiene, and E. Gruzdeviene, “Nettle Fibers as a Potential Natural Raw Material for Textile in Latvia,” pp. 3–4, 2012.

[190] E. Bodros and C. Baley, “Investigation of the use of stinging nettle fibres (Urtica Dioica) for polymer reinforcement : Study of single fibre tensile properties .,” pp. 10–11.

[191] DEFRA, “Sustainable technology in nettle growing - STING,” 2004. [Online]. Available: http://sciencesearch.defra.gov.uk/Default.aspx?Menu=Menu&Module=More&Location=None&Completed=0&ProjectID=12327.

[192] H. Fischer, E. Werwein, and N. Graupner, “Nettle fibre (Urtica dioica L.) reinforced poly(lactic acid): A first approach,” *J. Compos. Mater.*, vol. 46, no. 24, pp. 3077–3087, 2012.

[193] E. T. H. Vink, K. R. Rábago, D. Glassner, and P. R. Gruber, “Applications of life cycle assessment to NatureWorks™ polylactide (PLA) production,” *Polym. Degrad. Stab.*, vol. 80, no. 3, pp. 403–419, 2003.

[194] O. Avinc and A. Khoddami, “Overview of Poly(lactic acid) (PLA) Fibre,” *Fibre Chem.*, vol. 41, no. 6, pp. 391–401, 2010.

[195] S. Inkinen, M. Hakkarainen, A. C. Albertsson, and A. Södergård, “From lactic acid to poly(lactic acid) (PLA): Characterization and analysis of PLA and Its

precursors," *Biomacromolecules*, vol. 12, no. 3, pp. 523–532, 2011.

[196] "MakeitFrom." [Online]. Available: https://www.makeitfrom.com/material-group/Thermoplastic.

[197] S. Farah, G. D. Andersin, and R. Langer, "Physical and mechanical properties of PLA, and their functions in widespread applications — A comprehensive review," *Adv. Drug Deliv. Rev.*, vol. 107, pp. 367–392, 2016.

[198] D. Garlotta, "A Literature Review of Poly (Lactic Acid)," *J. Polym. Environ.*, vol. 9, no. 2, pp. 63–84, 2002.

[199] M. Kowalczyk, E. Piorkowska, P. Kulpinski, and M. Pracella, "Mechanical and thermal properties of PLA composites with cellulose nanofibers and standard size fibers," *Compos. Part A Appl. Sci. Manuf.*, vol. 42, no. 10, pp. 1509–1514, 2011.

[200] Y. Chen, L. M. Geever, J. A. Killion, J. G. Lyons, C. L. Higginbotham, and D. M. Devine, "Review of Multifarious Applications of Poly (Lactic Acid)," *Polym. - Plast. Technol. Eng.*, vol. 55, no. 10, pp. 1057–1075, 2016.

[201] T. A. Hottle, M. M. Bilec, and A. E. Landis, "Biopolymer production and end of life comparisons using life cycle assessment," *Resour. Conserv. Recycl.*, vol. 122, pp. 295–306, 2017.

[202] T. Ohkita and S. H. Lee, "Thermal degradation and biodegradability of poly (lactic acid)/corn starch biocomposites," *J. Appl. Polym. Sci.*, vol. 100, no. 4, pp. 3009–3017, 2006.

[203] C. Boonmee, C. Kositanont, and T. Leejarkpai, "Degradation of Poly(lactic acid) under Simulated Landfill Conditions," *Environ. Nat. Resour.*, vol. 14, no. 2, pp. 1–9, 2016.

[204] I. Spiridon, R. G. Ursu, and I. A. C. Spiridon, "New Polylactic Acid Composites for Packaging Applications: Mechanical Properties, Thermal Behavior, and Antimicrobial Activity," *Int. J. Polym. Anal. Charact.*, vol. 20, no. 8, pp. 681–692, 2015.

[205] A. M. Coltelli, N. Mallegni, S. Rizzo, P. Cinelli, and A. Lazzeri, "Improved Impact

Properties in Poly(lactic acid) (PLA) Blends Containing Cellulose Acetate (CA) Prepared by Reactive Extrusion," *Mater.*, vol. 12, no. 2, 2019.

[206] T. V Phuong, M. B. Coltelli, P. Cinelli, M. Cifelli, S. Verstichel, and A. Lazzeri, "Compatibilization and property enhancement of poly(lactic acid)/polycarbonate blends through triacetin-mediated interchange reactions in the melt," *Polymer (Guildf).*, vol. 55, pp. 4498–4513, 2014.

[207] C. H. Lee, S. M. Sapuan, and M. R. Hassan, "Thermal analysis of kenaf fiber reinforced floreon biocomposites with magnesium hydroxide flame retardant filler," *Polym. Compos.*, vol. 39, no. 3, pp. 869–875, 2016.

[208] M. S. Huda, L. T. Drzal, M. Misra, A. K. Mohanty, K. Williams, and D. F. Mielewski, "A study of 'Green' composites from recycled newspaper fibre reinforced poly(lactic acid).," *J. Ind. Eng. Chem. Res.*, vol. 44, pp. 5593 – 5601, 2005.

[209] R. H. Hu, J. K. Lim, C. I. Kim, and H. C. Yoon, "Biodegradable composites based on polylactic acid(PLA) and China jute fiber.," *Key Eng. Mater.*, vol. 353–358, pp. 1302–1305, 2007.

[210] D. K. Debeli, Z. Qin, and J. Guo, "Study on the Pre-Treatment , Physical and Chemical Properties of Ramie Fibers Reinforced Poly (Lactic Acid) (PLA) Biocomposite," *J. Nat. Fibers*, vol. 00, no. 00, pp. 1–15, 2017.

[211] S. M. Huda, L. T. Drzal, A. K. Mohanty, and M. Misra, "Chopped glass and recycled newspaper as reinforcement fibers in injection molded poly(lactic acid) (PLA) composites: A comparative study," *Compos. Sci. Technol.*, vol. 66, no. 11–12, pp. 1813–1824, 2006.

[212] A. Naceri, "An analysis of moisture diffusion according to fick's law and the tensile mechanical behavior of a glass fabric-reinforced composite," vol. 45, no. 3, pp. 331–336, 2009.

[213] M. Assarar, D. Scida, A. E. Mahi, C. Poilane, and R. Ayad, "Influence of water ageing on mechanical properties and damage events of two reinforced composite materials: Flax-fibres and glass-fibres," *Mater. Des.*, vol. 32, no. 2,

pp. 788–795, 2011.

[214] R. H. A. Haq, M. N. A. Rahman, A. M. T. Ariffin, M. F. Hassan, M. Z. Yunos, and S. Adzila, "Characterization and Mechanical Analysis of PCL/PLA composites for FDM feedstock filament," *IOP Conf. Ser. Mater. Sci. Eng.*, vol. 226, no. 1, 2017.

[215] F. Cerdas, M. Juraschek, S. Thiede, and C. Herrmann, "Life Cycle Assessment of 3D Printed Products in a Distributed Manufacturing System," *J. Ind. Ecol.*, vol. 21, 2017.

[216] A. Gilmour, A. M. F. Latif, and R. G. Piffer, "3D Printing of Functional Parts and their Structural Integrity," 2016.

[217] J. Gardan, "Additive manufacturing technologies: State of the art and trends," *Int. J. Prod. Res.*, vol. 54, no. 10, pp. 3118–3132, 2016.

[218] D. S. Engstrom, B. Porter, M. Pacios, and H. Bhaskaran, "Additive nanomanufacturing – A review," *J. Mater. Res.*, vol. 29, no. 17, pp. 1792–1816, 2014.

[219] "3D printer power." [Online]. Available: http://3dprinterpower.com/3d-printer-anatomy/.

[220] O. S. Es-Said, J. Foyos, R. Noorani, M. Mendelson, R. Marloth, and B. A. Pregger, "Effect of Layer Orientation on Mechanical Properties of Rapid Prototyped Samples," *Mater. Manuf. Process.*, vol. 15, no. 1, pp. 107–122, 2000.

[221] D. G. Schniederjans, "Adoption of 3D-printing technologies in manufacturing: A survey analysis," *Int. J. Prod. Econ.*, vol. 183, pp. 287–298, 2017.

[222] B. Zhang, B. Seong, V. Nguyen, and D. Byun, "3D printing of high-resolution PLA-based structures by hybrid electrohydrodynamic and fused deposition modeling techniques," *J. Micromechanics Microengineering*, vol. 26, no. 2, p. 025015, 2016.

[223] S. Hwang, E. I. Reyes, K. S. Moon, R. C. Rumpf, and N. S. Kim, "Thermo-mechanical Characterization of Metal/Polymer Composite Filaments and Printing Parameter Study for Fused Deposition Modeling in the 3D Printing Process," *J. Electron. Mater.*, vol. 44, no. 3, pp. 771–777, 2015.

[224] N. Mohan, P. Senthil, S. Vinodh, and N. Jayanth, “A review on composite materials and process parameters optimisation for the fused deposition modelling process,” *Virtual Phys. Prototyp.*, vol. 12, no. 1, pp. 47–59, 2017.

[225] M. Fernandez-Vicente, W. Calle, F. Santiago, and A. Conejero, “Effect of Infill Parameters on Tensile Mechanical Behavior in Desktop 3D Printing,” *3D Print. Addit. Manuf.*, vol. 3, no. 3, pp. 183–192, 2016.

[226] A. Farzadi, M. Solati-Hashjin, M. Asadi-Eydivand, and N. A. A. Osman, “Effect of layer thickness and printing orientation on mechanical properties and dimensional accuracy of 3D printed porous samples for bone tissue engineering,” *PLoS One*, vol. 9, pp. 1–14, 2014.

[227] B. M. Tymrak, M. Kreiger, and J. M. Pearce, “Mechanical properties of components fabricated with open-source 3-D printers under realistic environmental conditions,” *Mater. Des.*, vol. 58, pp. 242–246, 2014.

[228] A. W. Fatimatuzahraa, B. Farahaina, and W. A. Y. Yusoff, “The effect of employing different raster orientations on the mechanical properties and microstructure of Fused Deposition Modeling parts,” *ISBEIA 2011 - 2011 IEEE Symp. Business, Eng. Ind. Appl.*, pp. 22–27, 2011.

[229] “3D Matter.” [Online]. Available: http://my3dmatter.com/influence-infill-layer-height-pattern/.

[230] A. Le Duigou, M. Castro, R. Bevan, and N. Martin, “3D printing of wood fibre biocomposites: From mechanical to actuation functionality,” *Mater. Des.*, vol. 96, pp. 106–114, 2016.

[231] M. Kreiger and J. M. Pearce, “Environmental Life Cycle Analysis of distributed three-dimensional printing and conventional manufacturing of polymer products,” *Acs Sustain. Chem. Eng.*, vol. 1, no. 12, pp. 1511–1519, 2013.

[232] International Organization for Standardization, “Environmental management — Life cycle assessment — Requirements and guidelines(ISO 14044:2006),” 2006.

[233] International Organization for Standardization, “Environment managment-

Life cycle assesment(ISO/TS 14046:2002)," 2002.

[234] T. A. Hottle, M. M. Bilec, and A. E. Landis, "Sustainability assessments of bio-based polymers," *Polym. Degrad. Stab.*, vol. 98, no. 9, pp. 1898–1907, 2013.

[235] International Organization for Standardization, "Environmental Management - Life Cycle Assessment - Principles and Framework (ISO 14040:2006)," 2006.

[236] International Organization for Standardization, "Environmental management — Life cycle assessment — Examples of application of ISO 14041 to goal and scope definition and inventory analysis (ISO/TR 14049:2000(E))," vol. 2000, p. 43, 2000.

[237] International Organization for Standardization, "Greenhouse gases — Carbon footprint of products — Requirements and guidelines for quantification Gaz (ISO/DIS 14067)," 2017.

[238] Pr. Consultants, "SimaPro," 2011. .

[239] Chalmers, "Swedish life cycle center." [Online]. Available: http://lifecyclecenter.se/.

[240] Swiss centre for life cycle Inventories, "Ecoinvent Centre," *2010*. .

[241] N. P. J. Dissanayake, "Life cycle assesment of flax for the reinforcement of polymer matrix composites," 2012.

[242] L. Turunen and H. M. G. Van der Werf, "Life Cycle Analysis of Hemp Textile Yarn, Comparison of three hemp fibre processing scenarios and a flax scenario.," *French Natl. Inst. Agron. Res.*, 2006.

[243] M. L. M. Broeren, S. N. C. Dellaert, B. Cok, M. P. Patel, E. Worrell, and L. Shen, "Life cycle assessment of sisal fibre – Exploring how local practices can influence environmental performance.," *J. Clean. Prod.*, vol. 149, pp. 818–827, 2017.

[244] DEFRA, "Government review of waste policy in england 2011. Ref: PB13540," 2011.

[245] Greenhouse gas protocol, “Product life accounting and reporting standard.,” 2011.

[246] N. S. Bolan, D. C. Adriano, and D. Curtin, “Soil acidification and liming interactions with nutrient and heavy metal transformation and bioavailability,” *Adv. Agron.*, vol. 78, pp. 215–272, 2003.

[247] S. Sarkar, “Determination of optimum fertilizer and spacing requirement for sustaining higher growth and fibre yield of Indian ramie,” *Indian J. Agron.*, vol. 50, pp. 80–82, 2005.

[248] M. A. J. Huijbregts and J. Seppälä, “Life Cycle Impact assessment of pollutants causing aquatic eutrophication,” *Int. J. Life Cycle Assess.*, vol. 6, no. 339, 2001.

[249] L. Zampori, G. Dotelli, and V. Vernelli, “Life Cycle Assessment of Hemp Cultivation and Use of Hemp-Based Thermal Insulator Materials in Buildings.,” *Environ. Sci. Technol.*, vol. 47, p. 7413–7420, 2013.

[250] A. J. Norton, “The Life Cycle Assessment and Moisture Sorption Characteristics of Natural Fibre Thermal Insulation Materials.”

[251] H. J. Althaus, F. Werner, C. Stettler, and F. Dinkel, “Life Cycle Inventories of Renewable Materials,” Dübendorf, Switzerland, 2007.

[252] D. Kellenberger, H. Althaus, T. Künniger, M. Lehmann, N. Jungbluth, and P. Thalmann, “Life Cycle Inventories of Building Products,” Dübendorf, Switzerland, 2007.

[253] “Sustainable Intersification.” [Online]. Available: http://www.siplatform.org.uk/.

[254] M. S. Mudahar and T. P. Hignett, “Energy efficiency in nitrogen fertilizer production.,” *Energy Agric.*, vol. 4, pp. 159–177, 1985.

[255] A. Centre for Sustainable Crop Management, “UK Flax and Hemp production: The impact of changes in support measures on the competitiveness and future potential of UK fibre production and industrial use,” 2005.

[256] G. Henfaes Research Centre University of Wales:Bangor, “Guidelines for growing flax, in Flax and Hemp Project.,” 2004.

[257] European fertilizer manufacturers association, “Harvesting energy with Fertilizers,” 2009.

[258] C. Holzapfel, “Optimal nitrogen, phosporus and sulphur fertility in flax,” 2016.

[259] A. D. La Rosa, G. Cozzo, A. Latteri, G. Mancini, A. Recca, and G. Cicala, “A comparative life cycle assessment of a composite component for automotive,” *Chem. Eng. Trans.*, vol. 32, pp. 1723–1728, 2013.

[260] J. Bare, G. Norris, D. Pennington, and T. McKone, “The tool for the reduction and assessment of chemical and other environmental impacts.,” *J.Ind.Ecol.*, vol. 6, no. 3–4, pp. 49–78, 2002.

[261] M. A. J. Huijbregts *et al.*, “Is Cumulative fossil energy demand a useful indicator for the environmental performance of products?,” *Environ.Sci.Techonogy*, vol. 40, no. 3, pp. 641–648, 2005.

[262] National Research Council, *Carbon Management: Implications for R&D in the Chemical Sciences and Technology (A Workshop Report to the Chemical Sciences RoundTable)*. Washington, DC: The National Academies Press, 2001.

[263] Y. Yang, R. Boom, B. Irion, D. J. Van Heerden, P. Kuiper, and H. De Wit, “Recycling of composite materials,” *Chem. Eng. Process. Process Intensif.*, vol. 51, pp. 53–68, 2012.

[264] W. Kaminsky, “Recycling of polymers by pyrolysis,” *J. Phys. IV Colloq.*, vol. 3, pp. C7-1543-C7-1552, 1993.

[265] A. C. Hetherington, A. L. Borrion, O. G. Griffiths, and M. C. McManus, “Use of LCA as a development tool within early research: challenges and issues across different sectors,” *Int. J. Life Cycle Assess.*, vol. 19, no. 1, pp. 130–143, 2014.

[266] International Organization for Standardization, “Environmental management — Life cycle impact assessment — Examples of application of ISO 14042 (ISO 14047),” 2003.

[267] D. Minist, “Composite Materials Drive and Innovation,” pp. 2002–2005, 2002.

[268] M. Barth and M. Carus, “Carbon Footprint and sustainability of different

natural fibres for biocomposites and insulation material," 2015.

[269] L. Turunen and H. M. G. Van der Werf, "The environmental impacts of the production of hemp and flax textile yarn," *Ind. Crops Prod.*, vol. 27, no. 1, pp. 1–10, 2008.

[270] E. Bodros and C. Baley, "Study of the tensile properties of stinging nettle fibres (Urtica dioica)," *Mater. Lett.*, vol. 62, no. 14, pp. 2147–2149, 2008.

[271] International Organization for Standardization, "Carbon fibre — Determination of filament diameter and cross-sectional area (BS ISO 11567:1995)," 1995.

[272] International Organization for Standardization, "Textiles — Woven fabrics — Construction — Methods of analysis. Determination of crimp of yarn in fabric (BS ISO 7211-3:1984)," 1984.

[273] M. Aslan, G. Chinga-Carrasco, B. F. Sørensen, and B. Madsen, "Strength variability of single flax fibres," *J. Mater. Sci.*, vol. 46, no. 19, pp. 6344–6354, 2011.

[274] International Organization for Standardization, "Textiles — Yarns from packages — Method of test for breaking strength of yarn by the skein method (BS ISO 6939:1988)," 1988.

[275] A. A. A. Nasir, A. I. Azmi, and A. N. M. Khalil, "Parametric Study on the Residual Tensile Strength of Flax Natural Fibre Composites after Drilling Operation," *Procedia Manuf.*, vol. 2, no. February, pp. 97–101, 2015.

[276] M. A. Fuqua, S. Huo, and C. A. Ulven, "Natural fiber reinforced composites," *Polym. Rev.*, vol. 52, no. 3–4, pp. 259–320, 2012.

[277] Y. Zhou, Y. Wang, Y. Xia, and S. Jeelani, "Tensile behavior of carbon fiber bundles at different strain rates," *Mater. Lett.*, vol. 64, no. 3, pp. 246–248, 2010.

[278] E. Muñoz and J. A. Garcia-Manrique, "Water Absorption Behaviour and Its Effect on the Mechanical Properties of Flax Fibre Reinforced Bioepoxy Composites," *Int. J. Polym. Sci.*, vol. 2015, pp. 1–10, 2015.

[279] T. P. Nevell and S. Haig, “Cellulose chemistry and its applications,” in *Cellulose chemisty*, vol. 142, 1985, pp. 1–2.

[280] W. D. R. Brouwer, “Natural Fibre Composites in Structural Components : Alternative Applications for Sisal?,” pp. 2–7, 2005.

[281] D. M. Bruce and G. C. Davies, “Effect of Environmental Relative Humidity and Damag on Tensile Properties of Flax and Nettle Fibres,” *Text. Res. J.*, vol. 68, no. 9, pp. 623–629, 1998.

[282] American standards for testing materials, “Standard Test Method for Moisture Absorption Properties and Equilibrium Conditioning of Polymer Matrix Composite Materials (ASTM D5229),” Jan-2012.

[283] F. Xu, J. Yu, T. Tesso, F. Dowell, and D. Wang, “Qualitative and quantitative analysis of lignocellulosic biomass using infrared techniques: A mini-review,” *Appl. Energy*, vol. 104, pp. 801–809, 2013.

[284] V. Titok, V. Leontiev, S. Yurenkova, T. Nikitinskaya, T. Barannikova, and L. Khotyleva, “Infrared spectroscopy of fiber flax,” *J. Nat. Fibers*, vol. 7, no. 1, pp. 61–69, 2010.

[285] P. Garside and P. Wyeth, “Identification of Cellulosic Fibres by FTIR Spectroscopy - Thread and Single Fibre Analysis by Attenuated Total Reflectance,” *Stud. Conserv.*, vol. 48, no. 4, pp. 269–275, Dec. 2003.

[286] T. Kondo, “The assignment of IR absorption bands due to free hydroxyl groups in cellulose,” *Cellulose*, vol. 4, no. 4, pp. 281–292, 1997.

[287] T. Kondo and C. Sawatari, “A Fourier transform infra-red spectroscopic analysis of the character of hydrogen bonds in amorphous cellulose,” *Polymer (Guildf).*, vol. 37, no. 3, pp. 393–399, Feb. 1996.

[288] A. G. Vereshchagin and G. V Novitskaya, “The triglyceride composition of linseed oil,” *J. Am. Oil Chem. Soc.*, vol. 42, no. 11, pp. 970–974, 1965.

[289] T. Mukherjee and N. Kao, “PLA Based Biopolymer Reinforced with Natural Fibre: A Review,” *J. Polym. Environ.*, vol. 19, no. 714, 2011.

[290] C. H. Lee, S. M. Sapuan, J. H. Lee, and M. R. Hassan, “Mechanical properties of

kenaf fibre reinforced floreon biocomposites with magnesium hydroxide filler," *J. Mech. Eng. Sci.*, vol. 10, no. 3, pp. 2234–2248, 2016.

[291] R. Kumar, M. K. Yakubu, and R. D. Anandjiwala, "Biodegradation of flax fiber reinforced poly lactic acid," *Express Polym. Lett.*, vol. 4, no. 7, pp. 423–430, 2010.

[292] Y. Yuan, M. Guo, and Y. Wang, "Flax Fibers as Reinforcement in Poly (Lactic Acid) Biodegradable Composites," in *Intelligent Computing and Information Science: International Conference, ICICIS 2011, Chongqing, China, January 8-9, 2011. Proceedings, Part I*, R. Chen, Ed. Berlin, Heidelberg: Springer Berlin Heidelberg, 2011, pp. 547–553.

[293] International Organization for Standardization, "Methods for determining the density of non-cellular plantics Part 3: Gas pyknometer method (BS EN ISO 1183-1:2004)," 2004.

[294] International Organization for Standardization, "Fibre-reinforced plastic composites — Determination of flexural properties(EN ISO 14125:1998+A1:2011)," 2011.

[295] L. T. Drzal and M. Madhukar, "Fiber-matrix adhseion and its relationship to composite mechanical properties," *J. Mater. Sci.*, vol. 28, pp. 569–610, 1993.

[296] A. Kelly and W. R. Tyson, "Tensile properties of fibre-reinforced metals: Copper/tungsten and copper/molybdenum," *J. Mech. Phys. Solids*, vol. 13, no. 6, pp. 329–350, 1965.

[297] M. Bulota and T. Budtova, "Highly porous and light-weight flax / PLA composites," *Ind. Crop. Prod.*, vol. 74, pp. 132–138, 2015.

[298] M. Ho, H. Wang, J. H. Lee, C. Ho, and K. Lai, "Critical factors on manufacturing processes of natural fibre composites," *Compos. Part M*, vol. 43, pp. 3549–3562, 2012.

[299] A. G. Evans and F. W. Zok, "The physics and mechanics of fibre-reinforced brittle matrix composites," *J. Mater. Sci.*, vol. 29, no. 15, pp. 3857–3896, 1994.

[300] C. J. Shimaala and J. C. Whitwell, "Thermomechanical Behaviour of

Nonwovens. Part1: Response to Changes in Processing and Post-Bonding Variables," *Text. Res. J.*, vol. 46, pp. 405 – 417., 1976.

[301] E. Nassiopoulos, H. Abhyankar, and J. Niuguna, "Structural flax/PLA biocomposites: understanding of their thermomechanical behaviour," 2013.

[302] B. Benjamin and J. Müssig, "Impact and tensile properties of PLA/Cordenka and PLA/flax composites," *Compos. Sci. Technol.*, vol. 6, no. 7–8, pp. 1601–1607, 2008.

[303] P. K. Bajpai, I. Singh, and M. Jitendra, "Comparative studies of mechanical and morphological properties of polylactic acid and polypropylene based natural fiber composites," *J. Reinf. Plast. Compos.*, vol. 31, no. 24, pp. 1712–1724, 2012.

[304] N. Graupner and J. Müssig, "A comparison of the mechanical characteristics of kenaf and lyocell fibre reinforced poly(lactic acid) (PLA) and poly(3-hydroxybutyrate) (PHB) composites," *Compos. Part A Appl. Sci. Manuf.*, vol. 42, no. 12, pp. 2010–2019, 2011.

[305] A. M. Wass, "Compressive failure of fiber reinforced composites," 2003.

[306] E. Nassiopoulos, "Localised low velocity impact performance of FLAX/PLA biocomposites," Cranfield, 2015.

[307] X. Xia, W. Liu, L. Zhou, Z. Hua, H. Liu, and S. He, "Modification of flax fiber surface and its compatibilization in polylactic acid/flax composites," *Iran. Polym. J.*, vol. 25, no. 1, pp. 25–35, 2016.

[308] W. Tian, L. Qi, J. Zhou, and J. Guan, "Effects of the fiber orientation and fiber aspect ratio on the tensile strength of C sf / Mg composites," *Comput. Mater. Sci.*, vol. 89, pp. 6–11, 2014.

[309] D. Romanzini, A. Lavoratti, H. L. Ornaghi Jr, S. C. Amico, and A. J. Zattera, "Influence of fiber content on the mechanical and dynamic mechanical properties of glass/ramie polymer composites," *Mater. Des.*, vol. 47, pp. 9–15, 2013.

[310] F. M. Margem, S. N. Monteiro, J. B. Neto, R. J. S. Rodriguez, and B. G. Soares, "The dynamic-mechanical behavior of epoxy matrix composites reinforced

with ramie fibers," *Matéria*, vol. 5, no. 2, 2010.

[311] L. A. Pothan, Z. Oommen, and S. Thomas, "Dynamic mechanical analysis of banana fiber reinforced polyester composites," *Compos. Sci. Technol.*, vol. 63, pp. 283–93, 2003.

[312] M. Pyda, R. C. Bopp, and B. Wunderlich, "Heat capacity of poly(lactic acid)," *J. Chem. Thermodyn.*, vol. 36, no. 9, pp. 731–742, Sep. 2004.

[313] O. Martin and L. Averous, "Plasticization and properties of biodegradable multiphase systems polymer," *Poly(lactic acid)*, vol. 42, pp. 6209–6219, 2001.

[314] D. Y. Liu, X. W. Yuan, D. Bhattacharyya, and A. J. Easteal, "Characterisation of solution cast cellulose nanofibre – reinforced poly (lactic acid)," vol. 4, no. 1, pp. 26–31, 2010.

[315] V. S. G. Silverajah, N. A. Ibrahim, N. Zainuddin, W. M. Z. W. Yunus, and H. A. Hassan, "Mechanical, Thermal and Morphological Properties of Poly(lactic acid)/Epoxidized Palm Olein Blend," *Molecules*, vol. 17, pp. 11729–11747, 2012.

[316] A. Choudhury, "Isothermal crystallization and mechanical behavior of ionomer treated sisal/HDPE composites," *Mater. Sci. Eng. A*, vol. 4911–4912, pp. 492–500, 2008.

[317] D. Li *et al.*, "Preparation of plasticized poly (lactic acid) and its influence on the properties of composite materials," *PLoS One*, vol. 13, no. 3, pp. 1–15, 2018.

[318] A. Orue, A. Eceiza, C. Pena-Rodriguez, and A. Arbelaiz, "Water Uptake Behavior and Young Modulus Prediction of Composites Based on Treated Sisal and Poly(Lactic Acid)," *Materials (Basel).*, vol. 9, no. 400, pp. 1–15, 2016.

[319] G. H. Yew, A. M. M. Yusof, Z. A. M. Ishak, and U. S. Ishiaku, "Water absorption and enzymatic degradation of poly (lactic acid)/ rice starch composites," *Polym. Degrad. Stab.*, vol. 90, pp. 488–500, 2005.

[320] T. Alomayri, H. Assaedi, F. U. A. Skaikh, and I. M. Low, "Effect of water absorption on the mechanical properties of cotton fabric-reinforced geopolymer composites," *J. Asian Ceram. Soc.*, vol. 2, no. 3, pp. 223–230, 2014.

[321] C. Chow, X. Xing, and R. Li, “Moisture absorption studies of sisal fibre reinforced polypropylene composites,” *Compos. Sci. Technol.*, vol. 67, no. 2, pp. 306–313, Feb. 2007.

[322] LUZBOT Aleph Objects Inc, *TAZ 3.0 User Manual*. .

[323] Ultimaker B. V, “Ultimaker software-Cura.” .

[324] T. Letcher and M. Waytashek, “Material Property Testing of 3D-Printed Specimen in PLA on an Entry-Level 3D Printer,” in *Volume 2A: Advanced Manufacturing*, 2014, no. Volume 2.

[325] Q. Sun, G. M. Rizvi, C. T. Bellehumeur, and P. Gu, “Effect of processing conditions on the bonding quality of FDM polymer filaments,” *Rapid Prototyp. J.*, vol. 14, no. 2, pp. 72–80, 2008.

[326] R. Anitha, S. Arunachalam, and P. Radhakrishnan, “Critical parameters influencing the quality of prototypes in fused deposition modelling,” *J. Mater. Process. Technol.*, vol. 118, no. 1–3, pp. 385–388, 2001.

[327] J. T. Belter and A. M. Dollar, “Strengthening of 3D printed fused deposition manufactured parts using the fill compositing technique,” *PLoS One*, vol. 10, no. 4, pp. 1–19, 2015.

[328] F. Ning, W. Cong, Y. Hu, and H. Wang, “Additive manufacturing of carbon fiber-reinforced plastic composites using fused deposition modeling: Effects of process parameters on tensile properties,” *J. Compos. Mater.*, vol. 51, no. 4, pp. 451–462, 2017.

[329] X. Li *et al.*, “Measuring Mechanical Properties of the 3D Carbon/Carbon Composite Using Automated Grid Method,” *J. Test. Eval.*, vol. 41, no. 1, p. 20120006, 2013.

[330] M. Domingo-Espin, J. M. Puigoriol-Forcada, A. A. Garcia-Granada, J. Llumà, S. Borros, and G. Reyes, “Mechanical property characterization and simulation of fused deposition modeling Polycarbonate parts,” *Mater. Des.*, vol. 83, pp. 670–677, 2015.

[331] W. Wu, P. Geng, G. Li, D. Zhao, H. Zhang, and J. Zhao, “Influence of layer

thickness and raster angle on the mechanical properties of 3D-printed PEEK and a comparative mechanical study between PEEK and ABS," *Materials (Basel).*, vol. 8, pp. 5834–5846, 2015.

[332] S. N. Monteiro, V. Calado, R. J. S. Rodriguez, and F. M. Margem, "Thermogravimetric stability of polymer composites reinforced with less common lignocellulosic fibers - An overview," *J. Mater. Res. Technol.*, vol. 1, no. 2, pp. 117–126, 2012.

[333] H. Kim, E. Park, S. Kim, B. Park, N. Kim, and S. Lee, "Experimental Study on Mechanical Properties of Single- and Dual-material 3D Printed Products," *Procedia Manuf.*, vol. 10, pp. 887–897, 2017.

[334] V. E. Kuznetsov, A. N. Solonin, O. D. Urzhumtsev, R. Schilling, and A. G. Tavitov, "Strength of PLA Components Fabricated with Fused Deposition Technology Using a Desktop 3D Printer as a Function of Geometrical Parameters of the Process," *Polymers (Basel).*, vol. 10, no. 313, pp. 1–11, 2018.

[335] J. M. Chacón, M. A. Caminero, E. García-Plaza, and P. J. Núñez, "Additive manufacturing of PLA structures using fused deposition modelling: Effect of process parameters on mechanical properties and their optimal selection.," *Mater. Des.*, vol. 124, pp. 143–157, 2017.

[336] A. Arbelaiz, B. Fernández, J. A. Ramos, and I. Mondragon, "Thermal and crystallization studies of short flax fibre reinforced polypropylene matrix composites: Effect of treatments," *Thermochim. Acta*, vol. 440, no. 2, pp. 111–121, 2006.

[337] J. Torres, M. Cole, A. Owji, Z. DeMastry, and P. Gordon, A, "An approach for mechanical property optimization of Fused Deposition Modelling with Polylactic Acid via design of experiments," *Rapid Prototyp. J.*, vol. 22, no. 2, pp. 387–404, 2016.

[338] K. Chin Ang, K. Fai Leong, C. Kai Chua, and M. Chandrasekaran, "Investigation of the mechanical properties and porosity relationships in fused deposition modelling-fabricated porous structures," *Rapid Prototyp. J.*, vol. 12, no. 2, pp. 100–105, 2006.

[339] D. Pollard, C. Ward, G. Herrmann, and J. Etches, “The manufacture of honeycomb cores using Fused Deposition Modeling,” *Adv. Manuf. Polym. Compos. Sci.*, vol. 3, no. 1, pp. 21–31, 2017.

[340] K. Pitt, O. Lopez-Botello, A. D. Lafferty, I. Todd, and K. Mumtaz, “Investigation into the material properties of wooden composite structures with in-situ fibre reinforcement using additive manufacturing,” *Compos. Sci. Technol.*, vol. 138, pp. 32–39, 2017.

[341] H. N. Dhakal, Z. Y. Zwang, and W. M. O. Richardson, “Effect of water absorption on the mechanical properties of hemp fibre reinforced unsaturated polyester composites,” *Compos. Sci. Technol.*, vol. 67, no. 7–8, pp. 1674–1683, 2007.

[342] F. H. Froes, R. Boyer, and B. Dutta, “Additive manufacturing for aerospace applications-part I,” *Adv. Mater. Process.*, vol. 175, no. 5, pp. 36–40, 2017.

[343] V. Venkatesh, J. Thong, and X. Xu, “Consumer acceptance and user of information technology: Extending the unified theory of acceptance and use of technology,” *MIS Q.*, vol. 36, no. 1, pp. 157–178, 2012.

[344] S. J. Leigh, R. J. Bradley, C. P. Purssell, D. R. Billson, and D. A. Hutchins, “A Simple, Low-Cost Conductive Composite Material for 3D Printing of Electronic Sensors,” *PLoS One*, vol. 7, no. 11, pp. 1–6, 2012.

[345] V. Goodship, Ed., *Management, recycling and reuse of waste composites*, 1st ed. Woodhead Publishing Limited, 2010.

[346] SCEnAT, “scenat.” [Online]. Available: http://www.scenat.com/.

[347] A. H. Stromman, G. P. Peters, and E. G. Hertwich, “Approaches to correct for double counting in tiered hybrid life cycle inventories,” *J. Clean. Prod.*, vol. 17, no. 2, pp. 248–254, 2009.

[348] “Farmers weekly.” [Online]. Available: http://www.fwi.co.uk/.

[349] T. Nektalova, *Energy Density of Diesel Fuel.The Physics Factbook*. 2008.

[350] Ö. Tatar, E. Ilker, F. A. Tonk, H. Aygün, and Ö. Çaylak, “Impact of different nitrogen and potassium application on yield and fiber quality of ramie

(Boehmeria nivea).," *Int. J. Agric. Biol.*, vol. 12, pp. 369–372, 2010.

[351] J. Seiko, S. Rajna, and P. Ghosh, "Ramie fibre processing and value addition," *Asian J. Text.*, vol. 7, pp. 1–9, 2017.

[352] D. P. Singh, "Ramie (Boehmeria nivea)," 2009.

[353] E. G. Hertwich, S. F. Mateles, W. S. Pease, and T. E. McKone, "Human toxicity potentials for life-cycle assessment and toxics release inventory risk screening.," *Env. Toxicol Chem.*, vol. 20, no. 4, pp. 928–939, 2001.

[354] DG Research of the European Commission, "Interactive European Network for Industrial Crops and their Applications." .

[355] "NatureWorks." [Online]. Available: https://www.natureworksllc.com/.

[356] M. F. Cosate de Andrade, P. M. S. Souza, O. Cavalett, and A. P. Morales, "Life cycle assessment of poly(Lactic Acid) (PLA): Comparison between chemical recycling, mechanical recycling and composting," *J. Polym. Environ.*, vol. 24, no. 2, pp. 372–384, 2016.

[357] V. Piemonte, S. Sabatini, and F. Gironi, "Chemical recycling of PLA: A great opportunity towards the sustainable development?," *J. Polym. Environ.*, vol. 21, no. 3, pp. 640–647, 2013.

[358] "PAS 2050." [Online]. Available: http://shop.bsigroup.com/en/Browse-bySector/Energy–Utilities/Pas-2050/.

[359] "Rondol." [Online]. Available: http://rondol.com/en.

[360] S. Halliwell and NetComposites, "End of life option for composite waste," 2006.

APPENDIX

Appendix A-AVOVA for tensile strength of injection moulded and 3D printed composites

Table A-1 MPF (30/70)%

Anova: Single Factor

SUMMARY

Groups	*Count*	*Sum*	*Average*	*Variance*
Column 1	50	3416	68.32	1.418
Column 2	10	753.889	75.389	19.825

ANOVA

Source of Variation	*SS*	*df*	*MS*	*F*	*P-value*	*F crit*
Between Groups	416.410	1	416.410	97.418	$5.029E^{-14}$	4.007
Within Groups	247.918	58	4.275			
Total	664.328	59				

Table A-2 MPN (30/70)%

Anova: Single Factor

SUMMARY

Groups	*Count*	*Sum*	*Average*	*Variance*
Column 1	50	3831.714	76.634	3.226
Column 2	10	808.518	80.852	1.693

ANOVA

Source of Variation	*SS*	*df*	*MS*	*F*	*P-value*	*F crit*
Between Groups	148.232	1	148.232	49.602	2.483E-09	4.007
Within Groups	173.328	58	2.989			
Total	321.560	59				

Appendix B-AVOVA for flexural strength of injection moulded and 3D printed composites

Table B-1 MPF (30/70)%

Anova: Single Factor

SUMMARY

Groups	*Count*	*Sum*	*Average*	*Variance*
Column 1	50	5443.9	108.878	6.664
Column 2	10	1155	115.5	8.167

ANOVA

Source of Variation	*SS*	*df*	*MS*	*F*	*P-value*	*F crit*
Between Groups	365.424	1	365.424	52.980	9.967E-10	4.007
Within Groups	400.045	58	6.897			
Total	765.470	59				

Table B-2 MPN (30/70)%

Anova: Single Factor

SUMMARY

Groups	*Count*	*Sum*	*Average*	*Variance*
Column 1	50	5527.2	110.544	58.736
Column 2	10	1376.2	137.62	2.635

ANOVA

Source of Variation	*SS*	*df*	*MS*	*F*	*P-value*	*F crit*
Between Groups	6109.248	1	6109.248	122.109	6.734E-16	4.007
Within Groups	2901.819	58	50.031			
Total	9011.067	59				